

Faculdade de Engenharia da Universidade do Porto
Departamento de Engenharia Mecânica e Gestão Industrial

EFFICIENCY OF A GEARBOX
LUBRICATED WITH WINDMILL GEAR
OILS

David Emanuel Pimentel Gonçalves

Dissertação de Mestrado apresentada à
Faculdade de Engenharia da Universidade do Porto

Supervisor

Doutor Jorge Humberto O. Seabra
Professor Associado da FEUP

Co-supervisor

Doutor Ramiro Carneiro Martins
Investigador Auxiliar do INEGI

Porto, Julho 2011

Acknowledgments

I would like to acknowledge and give my sincere thanks to a few people without whom this work could not have been accomplished:

First of all, a special thanks to my parents and sister for the trust and uninterrupted incentive, not only during this work, but also in all these years of college education.

Secondly, to Professor Jorge Seabra, for the time, orientation and knowledge supplied.

I would also like to express my gratitude to Professor Ramiro Martins for the guidance and tireless support.

I wish to thank my fellow colleagues at CETRIB (Tribology, Vibrations and Industrial Maintenance Unity) for all the help, friendship and incentive transmitted during the moments shared at CETRIB: Albano Marinho, Beatriz Graça, Carlos Fernandes, Tiago Cousseau, Luís Magalhães, José Brandão, Armando Campos and Jorge Castro.

I also wish to acknowledge my friend and brother-in-law for his remarkable help and companionship given during all this years of education at FEUP.

Finally, I would like to express my gratitude to the Faculty of Engineering of the University of Porto (FEUP), by having made possible the attendance of this Mechanical Engineering Master's Degree Course and also for the resources provided.

to my family

Abstract

Ever since gears were first used there has been a constant demand for increasing power capacity in gear transmissions, to reduce the power losses, to increase the life time and also to decrease their weight. Therefore, in order to satisfy these increasing properties, new solutions have been researched and developed, such as the use of new materials, the application of surface coatings, improved surface finishing, different hardening treatments, improved geometry and the use of new lubricants.

Nowadays some of the main concerns in gear applications are scuffing failures, micropitting fatigue damage and of course, the power loss.

There is also a growing environmental concern that leads to an increasing interest in the reduction of power loss and the use of biodegradable non-toxic oils to reduce the environmental impact. Of course, higher performance in what concerns friction, wear, lifetime, etc. has also major impact in the environmental compatibility, because premature wear, high energy needs and low lifetime are also harmful.

As usual, any new solution presented must prove its technical performance and benefits proved in dedicated tests prior to its industrial application.

The major focus of this work was the study of the lubricant's influence in the power loss or efficiency of a gearbox using Windmill gear oils.

Five Windmill oils were tested in this work, based in the following base oils: Mineral, Polyalphaolefin (PAO), Polyalkylene glycol (PAG) and highly saturated synthetic Esters. Two of the five oils are Ester based and both are environmentally friendly lubricants, blended for industrial gear applications, and they are biodegradable and non-toxic.

The overall performance of the lubricants was assessed and their tribological performance has been evaluated for the transfer gearbox. This work pretends to provide an overview of the range of tribological systems where these oils could be used and also to allow the relative rating of their performance.

A numerical model for the energetic balance of the Transfer gearbox has been developed for the purpose of analysing the lubricant influence on the efficiency, integrating the mechanisms of power loss and heat evacuation. The model calculates the influence of each gearbox's component in the overall power loss, providing a better understanding of the churning and friction losses variation and its influence in the total power loss, using the experimentally obtained equilibrium temperature. The influence of the lubricant in the calculation of the average friction coefficient between gear teeth is also discussed in this work, mainly in what concerns the gear efficiency at low speed and high torque operating conditions, as it happens in the windmill gearboxes.

Of all the five oils, the PAG based was the one who achieved lower stabilization temperatures while also inducing less wear. Both the esters and the PAO based oils presented a similar performance, while the mineral based oil presented the worst performance, achieving the highest stabilization temperatures and the highest wear indexes.

Resumo

Desde a primeira vez que as transmissões por engrenagens foram utilizadas numa determinada aplicação, tem havido uma procura crescente de novas soluções que permitam maiores capacidades de carga, menores perdas de potência, maior tempo de vida e redução de peso dos componentes. Assim sendo, no sentido de satisfazer estes requisitos crescentes, novas soluções têm sido investigadas e desenvolvidas, como sendo o uso de novos materiais, diferentes tratamentos térmicos, melhores revestimentos, acabamentos superficiais e geometrias optimizadas, assim como também novos lubrificantes.

Nos dias de hoje, algumas das maiores preocupações na aplicação deste tipo de engrenagens são as perdas de potência e as avarias por *scuffing*, *pitting* e *micropitting*.

Acompanhando esta crescente evolução, tem também aumentado a preocupação ambiental que conduz a um interesse crescente na redução das perdas de potência e no uso de novos lubrificantes biodegradáveis e não tóxicos. Claro que, a elevada performance de um lubrificante no que diz respeito a atrito, desgaste e tempo de vida, tem grande importância para o meio ambiente, visto que grandes necessidades energéticas, desgaste prematuro e tempo de vida reduzido são também prejudiciais.

Assim, qualquer solução apresentada deve possuir uma eficiência comprovada em testes dedicados a fim de ser viável para a aplicação a que se destina.

O objectivo principal deste trabalho é o estudo da influência de cada lubrificante na eficiência de uma caixa de velocidades.

Foram testados cinco lubrificantes para caixas de velocidades de turbinas eólicas, cujos óleo base são: mineral, poli-alfa-olefina (PAO), poli-alcalino-glicol (PAG) e dois ésteres sobre-saturados. À excepção do óleo base mineral, todos os outros óleos são sintéticos, sendo que os dois ésteres são também biodegradáveis.

A eficiência geral dos lubrificantes foi testada, procurando-se avaliar a sua performance tribológica relativa a uma caixa de velocidades Transfer. Procurou-se também classificar relativamente cada um dos óleos base.

Foi também desenvolvido um modelo numérico que descreve o equilíbrio energético da caixa de velocidades com o propósito de analisar a influência do lubrificante na eficiência, através da modelização dos mecanismos de perda de potência e transferência de calor. O modelo procura descrever a influência de cada componente singular nas perdas de potência globais da caixa de velocidades, permitindo perceber a variação das perdas por atrito e chapinagem com a carga e velocidade de rotação. A influência do lubrificante no cálculo do coeficiente de atrito entre os dentes das engrenagens é também discutida, sobretudo no que diz respeito à eficiência da engrenagem a baixas velocidades e elevados binários, característicos das caixas de

velocidades de turbinas eólicas.

Dos cinco óleos testados, o PAGD apresentou as menores temperaturas de estabilização, induzindo também menor desgaste. Ambos os ésteres e o PAOR apresentaram performances semelhantes. Por outro lado, o MINR apresentou não só as temperaturas mais elevadas como também os mais elevados índices de desgaste, com consequência para a sua eficiência.

Keywords

Transfer Gearbox
Gearbox Test Rig
Gears
Scuffing
Pitting
Micropitting
Power losses
Friction coefficient
Biodegradable oils
Windmill oils
Non-toxic lubricants
Lubricants influence on efficiency

Palavras chave

Caixa de velocidades Transfer
Banco de ensaios de caixas de velocidade
Engrenagens
Gripagem
Pitting
Micropitting
Perda de potência
Coeficiente de atrito
Óleo biodegradável
Óleos para caixas de velocidades de turbinas eólicas
Óleos não tóxicos
Influência do lubrificante na eficiência

Contents

Acknowledgments	iii
Abstract	vii
Resumo	ix
Keywords	xi
List of Contents	xiii
List of Figures	xv
List of Tables	xix
Nomenclature	xxi
1. Introduction	1
1.1. Aim and thesis outline	1
2. Lubrication and Lubricants	3
2.1. Introduction	3
2.2. Lubricant Types	4
2.2.1. Lubricant oil	4
2.2.2. Greases	5
2.2.3. Solid Lubricants	6
2.2.4. Gaseous Lubricants	6
2.3. Physical properties of lubricating oils	7
2.3.1. Viscosity	7
2.3.2. Density	12
2.3.3. Other properties	12
2.3.4. Glass transition temperature	13
2.3.5. Environmental Specifications	13
2.4. Additives	14
2.5. Windmill gear oils	16
2.5.1. Oil properties measurement	19
3. Gearbox Test Rig and Transfer Gearbox	23
3.1. Test Rig	23

3.2. Transfer Gearbox	27
3.2.1. Multiplier Gearbox	29
3.2.2. Gear geometry and material	30
3.2.3. Shafts	33
3.2.4. Rolling Bearings	35
3.2.5. Lubrication	36
4. Experimental evaluation of the transfer gearbox performance	37
4.1. Introduction	37
4.2. Test Procedure	37
4.2.1. Oil analysis procedure	40
4.3. Relative performance of the windmill oils	43
4.3.1. Heat transfer analysis	46
4.3.2. Oil samples analysis	51
5. Power loss in Gearboxes	55
5.1. Introduction	55
5.2. Energetic flows	55
5.2.1. Introduction	55
5.2.2. Energy dissipation mechanisms	57
5.2.3. Heat transfer mechanisms	61
5.2.4. Energy balance	62
5.3. Transfer Gearbox Modelling	64
5.3.1. Friction coefficient optimization for gears and rolling bearings	67
5.3.2. Optimized model	80
6. Conclusions and future work	83
6.1. Experimental results	83
6.2. Model evaluation	84
6.3. Future works	85
Bibliography	87
A. Appendix	89
A.1. Test Reports	89
A.2. Gearbox simulation - KissSys	141

List of Figures

2.1. Laminar flow of a fluid.	7
2.2. Representation of the viscosity variation with the temperature for a Paraffinic mineral oil (ISO VG 32).	8
2.3. SAE J300 Classification [1].	11
2.4. SAE J306 Classification [1].	11
2.5. ISO classification [1].	12
2.6. Green certification symbols	13
2.7. Engler Viscometer	19
2.8. Densimeter.	20
3.1. Gearbox test rig.	23
3.2. Hydraulic oil supply station.	24
3.3. Gear set.	25
3.4. Static torque application mechanism resulting from hydraulic cylinder axial movement.	25
3.5. AC electrical motor.	26
3.6. Transfer Gearbox vehicle application.	27
3.7. Cross section of the transfer gearbox and 3D model view.	27
3.8. Gearbox schematic representation and speed map.	28
3.9. Fork and toothed ring mechanism.	28
3.10. Gearbox speed map, when working as a multiplier.	29
3.11. Contact in helical gears.	31
3.12. Gear 1-2 meshing and tooth form.	32
3.13. Gear 3-5 meshing and tooth form.	32
3.14. Input shaft displacements.	33
3.15. Input shaft stress.	33
3.16. Intermediate shaft displacements.	34
3.17. Intermediate shaft stress.	34
3.18. Output shaft displacements.	34
3.19. Output shaft stress.	34
3.20. Bearings numbering	36

List of Figures

4.1. Transfer gearbox.	38
4.2. Oil samples.	39
4.3. Vacuum pump.	39
4.4. Direct Reading Ferrografer.	41
4.5. Ferrogram scheme.	42
4.6. Analytic Ferrographer.	42
4.7. Bi-chromatic microscope.	42
4.8. Stabilization temperature for each input torque at 135rpm	43
4.9. Stabilization temperature for each input torque at 235rpm	44
4.10. Test gearbox wall stabilization temperature for each input torque at 135rpm	45
4.11. Test gearbox wall stabilization temperature for each input torque at 235rpm	45
4.12. Heat transfer coefficient linear regression and heat based power losses at 135rpm	46
4.13. Heat transfer coefficient linear regression and heat based power losses at 235rpm	47
4.14. Torque loss for each oil tested at 135rpm	47
4.15. Torque loss for each oil tested at 235rpm	48
4.16. Gearbox efficiency at 135rpm	49
4.17. Gearbox efficiency at 235rpm	49
4.18. Particles size Index for each tested oil. *- undiluted sample	52
4.19. Wear particles concentration (CPUC) and wear severity index (ISUC) for each tested oil	52
4.20. Oil: MINR, ampliatiion:x200, dilution:0,1	53
4.21. Oil: PAOR, ampliatiion:x200, dilution:0,1	53
4.22. Oil: ESTF, ampliatiion:x200, dilution:0,1	53
4.23. Oil: PAGD, ampliatiion:x200, dilution:1	53
4.24. Oil: MINR, ampliatiion:x1000, dilution:0,1.	54
4.25. Oil: PAOR, ampliatiion:x1000, dilution:0,1.	54
4.26. Oil: ESTF, ampliatiion:x1000, dilution:0,1.	54
4.27. Oil: PAGR, ampliatiion:x1000, dilution:1.	54
5.1. Elasto-Hydrodynamic regimes of lubrication	56
5.2. Stribeck curve.	58
5.3. Power losses and heat removal diagram example for a FZG gearbox. .	63
5.4. Model behaviour for the MINR oil, without coefficients optimization.	65
5.5. Model behaviour for the PAOR oil, without coefficients optimization.	65

5.6. Model behaviour for the ESTF oil, without coefficients optimization.	66
5.7. Model behaviour for the PAGD oil, without coefficients optimization.	66
5.8. Model optimized for the MINR oil (Lubricant factor X_{L1}).	69
5.9. Model optimized for the PAOR oil (Lubricant factor X_{L1}).	69
5.10. Model optimized for the ESTF oil (Lubricant factor X_{L1}).	70
5.11. Model optimized for the PAGD oil (Lubricant factor X_{L1}).	70
5.12. Lubricant film thickness.	72
5.13. Specific Lubricant film thickness.	72
5.14. Mean coefficient of friction between gear teeth, along the meshing line.	73
5.15. Coefficient of friction comparison for MIN-R oil.	74
5.16. Coefficient of friction comparison for PAO-R oil.	74
5.17. Coefficient of friction comparison for EST-F oil.	75
5.18. Coefficient of friction comparison for PAG-D oil.	75
5.19. Model optimized for the MINR oil (Lubricant factor X_{L2}).	78
5.20. Model optimized for the PAOR oil (Lubricant factor X_{L2}).	78
5.21. Model optimized for the ESTF oil (Lubricant factor X_{L2}).	79
5.22. Model optimized for the PAGD oil (Lubricant factor X_{L2}).	79
5.23. Comparison of the coefficient of friction obtained for each oil tested considering each X_L factor.	80
5.24. Power loss distribution for the MINR oil (Lubricant factor X_{L2}).	81
5.25. Power loss distribution for the PAOR oil (Lubricant factor X_{L2}).	81
5.26. Power loss distribution for the ESTF oil (Lubricant factor X_{L2}).	82
5.27. Power loss distribution for the PAGD oil (Lubricant factor X_{L2}).	82

List of Tables

2.1. Lubricant piezoviscosity dependent constants s and t [2]	10
2.2. Tested lubricants properties.	17
2.3. MINR, PAOR and ESTR oils quality level.	18
2.4. PAGD and ESTF oils quality level.	18
2.5. Constants values for the conversion.	20
2.6. Tested lubricants measured properties.	21
3.1. AC Motor technical features.	25
3.2. Gears geometry on the Transfer Gearbox.	30
3.3. Mechanical properties of the steel DIN 15CrNi6 after heat treatment.	31
3.4. Gear loads and resistance for $n_1 = 235\text{rpm}$ and $T_1 = 1000\text{Nm}$	32
3.5. Mechanical properties of the steel DIN 15CrNi6 used in the shaft.	33
3.6. Resistance of the shafts and minimum rolling bearing life.	34
3.7. Gearbox bearings	35
3.8. Rolling Bearings service life factors.	36
4.1. Operating conditions in gear efficiency tests.	38
4.2. Stabilization temperature values	43
4.3. Ferrometry analysis results	51
5.1. Optimized coefficients.	68
5.2. Optimized coefficients.	77
5.3. Average reductions in the friction coefficient.	80

Nomenclature

Symbol	Units	Designation
A	[m ²]	Immersed area
A_{cn}	[m ²]	Base support area
A_{cv}	[m ²]	Gearbox case exterior area - convection
A_{rad}	[m ²]	Gearbox case exterior area - radiation
b	[m]	Teeth width
CPUC	[/]	Concentration of particles ferrometric index
d	[m]	Gear pitch diameter
d	[/]	Dilution factor
d_a	[m]	Addendum diameter
d_b	[m]	Base diameter
d_m	[m]	Bearing mean diameter
d_s	[m]	Shaft diameter
E	[Pa]	Young modulus
E^*	[Pa]	Equivalent Young modulus
Fa	[N]	Axial load
f_0	[/]	Coefficient for churning bearing losses
f_1	[/]	Coefficient for friction bearing losses
F_{bt}	[N]	Tooth normal force, transversal section
Fr	[/]	Froude Number
Fr	[N]	Radial load
g	[m/s ²]	Aceleration of gravity
h	[m]	Gear immersion length
h_0	[m]	Lubricant film thickness
h_a	[m]	Addendum height
Hv	[/]	Geometric power loss factor
ISUC	[/]	Wear severity index
l_{min}	[m]	Minimal length of contact line
n	[rpm]	Rotational speed
P_{fr}	[W]	Gear friction losses
P_{in}	[W]	Input power
P_{M0}	[W]	Bearing no-load dependent losses
P_{M1}	[W]	Bearing load dependent losses
P_{sl}	[W]	Seal losses
P_{spl}	[W]	Gear churning losses

Symbol	Units	Designation
Q_{cn}	[W]	Heat removal by conduction
Q_{ncv}	[W]	Heat removal by convection
Q_{rad}	[W]	Heat removal by radiation
r	[m]	Pitch radius
Ra	$[\mu m]$	Roughness average
Re	[/]	Reynolds number
R_{eq}	[mm]	Equivalent curvature radius
t	[m]	Gearbox wall thickness
u	[/]	Gear ratio
$v_{\Sigma c}$	[m/s]	Sum velocity at pitch point
V_{oil}	$[m^3]$	Gearbox oil volume
XL	[/]	Lubricant factor
z	[/]	Gear number of teeth
α	[rad]	Pressure angle
α_{cn}	[/]	Conduction heat transfer coefficient
α_{ncv}	[/]	Convection heat transfer coefficient
α_{rad}	[/]	Radiation heat transfer coefficient
α_{piezo}	$[Pa^1]$	Piezoviscosity coefficient
Δ	[/]	Specific film thickness
Δ_{Pexp}	[W]	Experimentally obtained power loss
Δ_{Pnum}	[W]	Numerically obtained power loss
ϵ	[/]	Case surface emissivity
ϵ_i	[/]	Addendum contact ratio
ϵ_α	[/]	Transverse contact ratio
η_{oil}	[mPa.s]	Lubricant dynamic viscosity
θ_∞	$[^\circ C]$	Room temperature
θ_m	$[^\circ C]$	Base support average temperature
θ_{oil}	$[^\circ C]$	Oil bath temperature
θ_w	$[^\circ C]$	Gearbox wall temperature
ν	[cSt]	Lubricant kinematic viscosity
ν	[/]	Poisson's coefficient
ρ	$[Kg/m^3]$	Specific weight
ρ_c	[m]	Equivalent curvature radius at pitch point
σ_i	$[\mu m]$	Gear flank roughness
μ_1	[/]	Bearing friction coefficient
μ_{mz}	[/]	Mean Friction coefficient

1. Introduction

Bearing in mind the gearbox's expected life and energy efficiency, there has been many research on different areas of development over the years regarding gearboxes, such as thermal and mechanical treatment of the components, surface coatings, improved geometry and lubricants formulation.

Following this growth in gearboxes research, there is also a growing environmental awareness which leads to an increasing interest not only in biodegradable low toxicity oils but also the search for lubricants with higher performance. The aim is then to decrease the environmental impact while trying to find out technical advantages. In fact, the environmental performance of lubricants can also be measured in terms of friction, wear, lifetime and efficiency, since premature wear or high energy needs are also harmful to the environment.

The load carrying capacity of lubricants and their thermal behaviour are of greater importance in what concerns oil aging, wear, scuffing, micro-pitting and pitting. Therefore, the major concern in the modern gearboxes is to reach lower operating temperatures, in order to achieve higher efficiencies.

On the other hand, while the rheologic models can describe the physical behaviour of the lubricant in the most diversified conditions, they can not however, predict the influence of the additive package. Thus, only through dedicated experimental testing one can evaluate the energetic performance of the lubricant.

1.1. Aim and thesis outline

The thesis here reported is result of the experimental and numerical work accomplished for the course of Mechanical Engineering Master's Degree under the branch of Project and Mechanical Construction. This work was realized at CETRIB (Tribology, Industrial Maintenance and Vibrations Unit of INEGI).

The primary objective of this work is to experimentally evaluate the energetic behaviour of a Transfer Gearbox lubricated Windmill Gear oils. Furthermore, the development of a numerical model, aiming to simulate the gearbox's behaviour and

1. Introduction

its efficiency, was also a goal.

This thesis is composed by six chapters, including this introductory chapter, explaining the need to search for new solutions for lubricants in gear applications.

This thesis resulted from a large amount of experimental work using different Lubricants, thus chapter 2 is dedicated to present the different kind of lubricants, their tribological properties and the most important kinds of additive packages used to improve each base oil. Each one of the gear oils tested is presented according to their manufacturer catalog and also according to the physical properties measured in this work.

The Third Chapter is focused in the detailed explanation of the gearbox test rig used as well as in the Transfer gearbox tested.

The Fourth Chapter is dedicated to introduce and explain the objectives of a new type of gearbox tests, with the purpose of studying the efficiency of a Transfer Gearbox using Windmill Gear Oils. In this chapter all the test sequences performed are explained and the results are presented in terms of oil temperature evolution and torque loss.

The Chapter Five is dedicated to introduce the different mechanisms of energy dissipation within the Transfer gearbox and also the model developed for the studying of the energetic balance and power loss of the same gearbox. Also in this chapter, the correlation between the model developed and the experimental results obtained from the test rig is analysed, attending to the importance of the lubricant's factor in the calculation of the friction coefficient between gear teeth. The chapter intends to validate the model developed for the transfer gearbox.

The final chapter is dedicated to present this work's conclusions and suggest future works.

2. Lubrication and Lubricants

2.1. Introduction

The main purpose of using a lubricant is to reduce friction and wear between two surfaces in relative motion. In principle, any substance - solid, liquid or gas - interposed between two surfaces, making easier their relative slip, is a potential lubricant. However, other features are often required from the lubricants, the most important being a good separation of the surfaces and a good evacuation of the heat generated in the contact. Some of these characteristics are inherent, such as a low shear strength and good thermal conductivity, while others are related with surfaces, ie, give them a good protection against corrosion and wear, even in the absence of movement [3].

The need to fulfill these basic requirements restricts the ability to choose efficient lubricants to a limited number of base materials either animal, vegetable, mineral or synthetic. Another factor that has been growing significantly in recent years and that further restricts the choice of a lubricant is the environmental concern, which is leading to the development of new environmentally friendly lubricants.

Moreover, in elastohydrodynamic contacts, the lubricant flows through the contact in a very short period of time of about 1 ms , suffering a shock pressure of about 1 GPa or higher, being submitted to deformation rates that can reach 10^{-7} s^{-1} , and temperature rises above 100 K [1].

These conditions, characterized by high and fast variations in pressure and temperature, can be satisfied by the surfaces in contact and the lubricating film that separates them, justifying the change of the lubricant properties, which are observed experimentally and theoretically determined [1]. Thereby warranting the difficulties in characterizing the physical, chemical, rheological and tribological behaviour of a lubricant within the contact.

This chapter is intended to make a brief description of the main characteristics and properties of lubricants as well as the description of the specific gear oils used in this work.

2.2. Lubricant Types

2.2.1. Lubricant oil

The base oils can be classified according to their origin:

Vegetable and animal oils

The vegetable and animal oils were certainly the first lubricants to be used by man. These lubricants have several advantages over mineral oils, eg, the high viscosity, low evaporation rate and rapid biodegradability, this last aspect being maybe the most important. Unfortunately, these vegetable oils oxidize quickly, having low resistance to high temperatures. So with the increase in requirements to which the lubricants were progressively submitted, their use has been largely replaced by synthetic made and petroleum based products.

Mineral oils

Obtained from the distillation of crude petroleum, these oils are complex mixtures of organic and inorganic compounds and can be distinguished by their chemical composition [4]. These oils can be paraffinic, naphthenic and aromatic. The aromatic fraction is usually undesirable and can be found in small proportions. Therefore, these are least used in the lubrication, while the paraffinic and naphthenic based oils are widely used due to their low cost and reasonable performance.

- Paraffinic: Characterized by its high-level fluidity point, high viscosity index, good oxidation resistance, good oiliness and high amount of carbon residue;
- Naphthenic: Opposed to the paraffinic, these oils present low level fluidity point, low viscosity index, low oxidation resistance, large oiliness and low amount of carbon residue;
- Mixed: Manufactured using paraffinic and naphathenic base oils, these are widely used, exhibiting a large range of viscosity grades, low volatility, resistance to deterioration and also protection against corrosion [4].

Synthetic oils

Synthetic lubricants are obtained by synthesis of light hydrocarbons with the inclusion of some non-petroleum organic elements. These lubricants have some benefits, such as increased oil longevity, better heat resistance and can be environmentally friendly [5]. They have, however, a higher cost. Even so, these oils have been widely used in aviation and industrial application for many years now.

These oils are generally obtained starting with a synthetic base obtained from petroleum and then other compounds are added to match the desired viscosity and other required properties. This way, they become more expensive but present better performance than the mineral oils, being specific to the application in hand [5].

Synthetic oils can be grouped in the following categories [6], [5]:

- Polyalphaolefins (PAO) - are the most common synthetics base lubricants. Although they are bad additive solvents, they have a low fluidity point, good thermal stability and a high viscosity index;
- Polyglycols (between which the Polyalkalineglycol - PAG) - characterized by their low friction coefficient, they are ideal for high sliding applications where the friction is very strong;
- Esters - are a wide class of lubricants. Each ester has several different properties as the good behaviour at low temperatures, the high thermal resistance and the fact that most of them are biodegradable, making its class of vital importance for many gear oil formulations aiming to be classified as biodegradable.

Some chemical agents, commonly called additives, are often added to these base oils, which give them certain properties after finished. Some additives provide them useful new properties, that do not exist originally while others can only improve their natural properties (view section 2.4).

2.2.2. Greases

A grease is defined as the "dispersion of a thickening agent in a lubricating oil" [3]. The thickening agents can be of two types:

Soaps - Aluminum, Barium, Calcium, Lithium, Sodium and Strontium.

No soap - Organic clays, Polyureas, Inorganic compounds.

2.2.3. Solid Lubricants

A solid lubricant is a film of solid material composed of organic or inorganic compounds that is interposed between the surfaces to be lubricated [3].

Inorganic solid lubricants

Solid gelatinous;

Mixtures of soft solids;

Coverings and chemical reaction with the surface.

Organic solid lubricants

Soaps, waxes and fats;

Polymer films.

2.2.4. Gaseous Lubricants

The lubrication with gas is analogous in many aspects to lubrication with liquid, so the same principles of hydrodynamic lubrication film might be applied.

Although both gases and liquids are viscous fluids, they differ in two very important properties: the viscosity of gases is much smaller and the compressibility is much higher than those of liquids. Thus, the load carrying capacity and film thickness in the contact are much lower when using a gaseous lubricant.

The gaseous lubricants used for this purpose are air, steam, industrial gases, etc.

2.3. Physical properties of lubricating oils

2.3.1. Viscosity

To accurately describe the behaviour of a lubricating oil, their physical and rheological characteristics should be well known. Probably the most important property of a lubricant oil is its viscosity. This property reflects the degree of internal friction or the resistance which a fluid offers to slip, thus becoming a dominant factor in power losses of mechanical components as bearings and gears.

By definition the viscosity of the fluid is the resistance imposed by its molecules to the inside slip over each other.

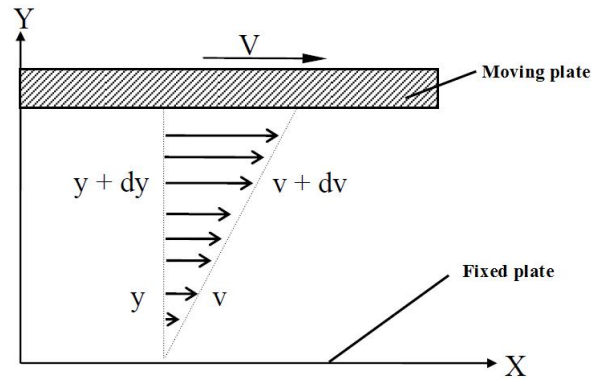


Figure 2.1.: Laminar flow of a fluid.

Newton's law of viscous flow establishes that the linear shear stress within a fluid is proportional to the variation of the fluid speed with the height between the plates surface (figure 2.1).

$$\tau = \sigma_{xy} = \eta \frac{dv}{dy} \quad (2.1)$$

In the equation 2.1, η is a proportionality constant known as dynamic viscosity. The derivative $\frac{dv}{dy}$ is the variation of the fluid speed with the fluid height and can be referred to as shear rate or speed gradient. Assuming that the shear rate is constant, the result can be simplified according to the equation 2.2:

$$\frac{dv}{dy} = \frac{U}{h} \quad (2.2)$$

which leads to the equation 2.3.

$$\tau = \sigma_{xy} = \eta \frac{U}{h} \quad (2.3)$$

2. Lubrication and Lubricants

The unit of dynamic viscosity, also called absolute viscosity, is measured in Pascal Second (Pa.s) in the International System and is equivalent to $N.s/m^2$.

The kinematic viscosity (ν), which is inversely proportional to the density of the fluid (ρ), is obtained when the flow of fluid is caused by the gravity. Thus, the expression $\nu = \frac{\eta}{\rho}$ gives the kinematic viscosity in m^2/s , being common to represent the result in mm^2/s or cSt (centiStokes), which is the unit most commonly used.

To better understand the above and check the remaining properties of a lubricating oil see references [1,3].

2.3.1.1. Termoviscosity

Represents the variation of viscosity with temperature and can be described by the following laws:

- **Law of Cameron** (Cameron's equation is simple but is only valid for small variations in temperature);
- **ASTM D314 Standard**;
- **Vogel's Law**.

The viscosity of the most usual mineral and synthetic oils decreases when the temperature increases.

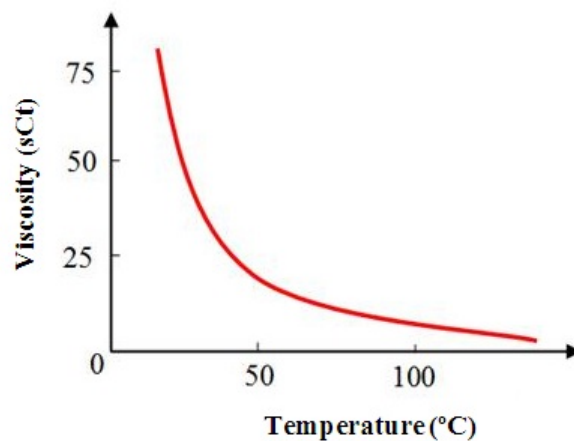


Figure 2.2.: Representation of the viscosity variation with the temperature for a Paraffinic mineral oil (ISO VG 32).

As an example, in the proximity of 20 ° C the viscosity decreases about:

- 2,5% for water;
- 10% to 15% for oil.

The method used in this work to determine the numerical viscosity of the oils to be tested was the **ASTM D314 Standard**:

$$\log(\log(\nu + c)) = n - m \cdot \log(\theta) \quad (2.4)$$

where θ represent the temperature in Kelvin and $c = 0,7cSt$.

The parameters m and n are lubricant dependent and given by equations 2.5 and 2.6:

$$m = \frac{\log\left(\frac{\log(\nu_{40}+c)}{\log(\nu_{100}+c)}\right)}{\log\left(\frac{\log(100+273.15)}{\log(40+273.15)}\right)} \quad (2.5)$$

$$n = \log(\log(\nu_{100} + c)) + m \cdot \log(100) \quad (2.6)$$

where, ν_{40} and ν_{100} represent the lubricant's viscosity, respectively at the reference temperature of 40°C and 100°C , between which the ASTM D341 Standard can be applied.

2.3.1.2. Piezoviscosity

Represents the variation of viscosity with pressure. The lubricant viscosity rises considerably with the increase of pressure. This is a very important property since the lubricants can be submitted to very high contact pressures as it happens in rolling bearings and gears.

Barus [7] propose the following law, valid for a certain reference temperature:

$$\eta_s = \eta_0 \cdot e^{\alpha \cdot p}. \quad (2.7)$$

In equation 2.7, η_s represents the lubricants viscosity at the pressure p , η_0 represents the viscosity at atmospheric pressure and reference temperature θ_0 and α represents the piezoviscosity coefficient, characteristic of each lubricant.

This coefficient can be related to the kinematic viscosity using the Law of Gold:

$$\alpha = s \cdot \nu^t \times 10^{-9} \quad (2.8)$$

in which s and t are lubricant dependent constants [2] (see table 2.1).

Table 2.1.: Lubricant piezoviscosity dependent constants s and t [2]

Pressure	Base Oil	Mineral	PAO	Ester	PAG
0.2 GPa	s	9.904	7.382	6.605	5.489
	t	0.1390	0.1335	0.1360	0.1485
0.6 GPa	s	8.097	7.008	5.897	-
	t	0.1534	0.0984	0.1173	-

2.3.1.3. Viscosity Index

The viscosity index represents the need to specify how the various classes of oils react to temperature variation. The method most used was proposed by Dan and Davis in 1929. These authors classified all known oils at that time in different categories according to the value of its kinematic viscosity (SUS) at 210 °F (98.8 °C). Among all the oils with the same viscosity at 210 °F they have retained the two oils that had the lowest and highest viscosity at 100 °F (37.8 °C) .

2.3.1.4. Viscosity Grades

When choosing a lubricant the main concern is its viscosity. The need to have a sufficient lubricating film compels the use of a high viscosity oil. However the viscosity can not be very high because it will cause excessive flow friction losses. Therefore several classification methods have been developed. Nowadays, there are three viscosity numbering systems: two methods for automotive lubricants and another for the industrial ones [5].

The two classifications for automotive lubricants are from Society of Automotive Engineers: SAE J300 (figures 2.3) and SAE J306 (figure 2.4). The first one classifies the oils according to their viscosity, evaluated at low shear rates and high temperatures (100°C), at high shear rates and for high temperatures (150°C) and also in a combination of both (high and low) shear rates and low temperatures (-5°C to -40°C).

The SAE J306 viscosity grade is classified according to the maximum temperature achieved when the viscosity reaches 150 Pa.s, and then the oil is cooled and the viscosity is measured at 100°C in accordance to ASTM Standard D2983. The suffix

SAE viscosity grade	Low temperature viscosity		High temperature viscosity		
	Low temperature cranking viscosity cP, °C ¹	Low temperature pumping viscosity cP, °C ²	Kinematic viscosity cSt at 100°C (low speed deformation) ³		Minimum viscosity cP at 150°C (high speed deformation) ⁴
			min	max	
0W	6200 a -35	60,000 a -40	3.8	—	—
5W	6600 a -30	60,000 a -35	3.8	—	—
10W	7000 a -25	60,000 a -30	4.1	—	—
15W	7000 a -20	60,000 a -25	5.6	-	—
20W	9500 a -15	60,000 a -20	5.6	—	—
25W	13,000 a -10	60,000 a -15	9.3	—	—
20	—	—	5.6	<9.3	2.6
30	—	—	9.3	<12.5	2.9
40	—	—	12.5	<16.3	2.9 (0W-40, 5W-40, 10W-40)
40	—	—	12.5	<16.3	3.7 (15W-40, 20W-40, 25W-40, 40)
50	—	—	16.3	<21.9	3.7
60	—	—	21.9	<26.1	3.7

¹ ASTM D 5293, ² ASTM D 4684, ³ ASTM D 445, ⁴ ASTM D 4683, ASTM D 4741
1cP = 1mPa s; 1 cSt = 1mm²/S

Figure 2.3.: SAE J300 Classification [1].

SAE viscosity grade	Maximum temperature for a dynamic viscosity of 150,000 cP, °C	Kinematic viscosity cSt @ 100°C	
		Min	Max
70W	-55	4.1	-
75W	-40	4.1	-
80W	-26	7.0	-
85W	-22	11.0	-
80	-	7.0	<11.0
85	-	11.0	<13.5
90	-	13.5	<24.0
140	-	24.0	<41.0
250	-	41.0	-

Figure 2.4.: SAE J306 Classification [1].

letter W present in some of the SAE grades refers to the word "winter" and designates the use of the lubricant at low ambient temperatures and the grades without the suffix are referred to oils developed for more warmer environments.

On the other hand, the classification for the industrial lubricants have been developed by the American Society for Testing Materials (ASTM) and by the Society of Tribologists and Lubrication Engineers (STLE). This classification came to allow the specification of multigrade oils which are very common in industrial lubricants. The oil viscosity is measured at 40°C according to standards ASTM D2422, ISO 3228 and DIN N°51519.

2. Lubrication and Lubricants

ISO Standard 3448 ASTM D-2422	Midpoint viscosity [cSt (mm ² /s)] at 40.0°C	Kinematic viscosity limits [cSt (mm ² /s)] at 40.0°C	
		Minimum	Maximum
ISO VG 2	2.2	1.98	2.42
ISO VG 3	3.3	2.88	3.52
ISO VG 5	4.6	4.14	5.06
ISO VG 7	6.8	6.12	7.48
ISO VG 10	10	9.00	11.0
ISO VG 15	15	13.5	16.5
ISO VG 22	22	19.8	24.2
ISO VG 32	32	28.8	35.2
ISO VG 46	46	41.4	50.6
ISO VG 68	68	61.2	74.8
ISO VG 100	100	90.0	110
ISO VG 150	150	135	165
ISO VG 220	220	198	242
ISO VG 320	320	288	352
ISO VG 460	460	414	506
ISO VG 680	680	612	748
ISO VG 1000	1000	900	1100
ISO VG 1500	1500	1350	1650

Figure 2.5.: ISO classification [1].

2.3.2. Density

Density (Kg/m^3) is the ratio between the mass and the volume of a body. Usually its variation with the temperature is not relevant, however the variation with the pressure might be more important as the lubricant film thickness is highly influenced by the contact pressure.

2.3.3. Other properties

- **Specific Heat ($J/Kg.K$):** is the amount of heat which is necessary to transfer to a body of unitary mass to increase its temperature of one Kelvin degree;
- **Thermal Conductivity ($W/m.K$):** is the heat flow transferred due to a unitary temperature gradient per unit of time in a normal direction to a surface of unitary area;
- **Thermal Diffusivity (m^2/s):** property which describes the temperature propagation within a substance and is defined by the ratio between the thermal conductivity and the product between the density and the specific heat.

2.3.4. Glass transition temperature

When a lubricant is cooled at constant pressure, its viscosity increases continuously until it reaches values of about 10^{12} Pa.s. From a certain temperature, the lubricant exhibits a behaviour similar to that of an amorphous or glassy solid, this temperature being called "glass transition temperature" [1].

This transformation also occurs at constant temperature, if the pressure at which the lubricant is submitted continually increases. The pressures and temperatures involved in the operation of an elastohydrodynamic contact are sufficient for such lubricant transformation to occur or at least to achieve extremely high viscosities.

2.3.5. Environmental Specifications

Following the increasing environmental concerns, it became necessary to create certification systems so it became possible to stimulate and promote the recycling, biodegradability and resources preservation concepts in order to greatly reduce the pollution. This way the producers are stimulated to produce environmental friendly oils. As an example the two following environmental certificates are applicable to oils: GreenMark whose symbol is represented in the left of figure 2.6 and Blauer Engel which is represented in the right. The GreenMark is Chinese (Taiwan) while the Blauer Engel is a German certificate. Both symbols however represent the green certification, ie, the low toxicity behaviour of the lubricant to the environment and nature [8].

Green certification



Symbol GreenMark
Taiwan



Symbol Blue Angel
Germany

Figure 2.6.: Green certification symbols

2.4. Additives

Additives are agents which, when added to the base lubricant, improve their properties so to suit specific application requirements. The amount of additive used varies from a few hundredths up to 30%. The additives, improving the characteristics of lubricating oils, have largely contributed to the progress of the primitive internal combustion engines and all industrial machinery [1].

In addition to the properties of each additive, all of them must be soluble in the base oil product and insoluble in aqueous solutions. Furthermore, the additives can be classified in two groups:

1. Those which modify the physical characteristics (fluidity, foam formation, viscosity index, etc);
2. Those that affect the chemical nature of the base oil (oxidation inhibitors, detergents, extreme pressure agents).

The variety of lubricant additives is very large and their effect on the base oil is not the scope of this work. Still, the most common additives which have a specific purpose are shown below:

- **Additives that improve the viscosity index:** are used to increase the viscosity of the base oil at high temperature and/or decrease it at lower temperatures. These additives are usually polymers;
- **Anti-wear (AW):** reinforce the anti-wear properties of the lubricants, by creating a protective film from the reaction with the surfaces in contact;
- **Extreme-pressure (EP):** avoiding the adhesion between the metallic surfaces in relative slip at extreme pressure conditions, these additives react chemically with the surfaces in contact, creating a film which avoids the micro-welding of the roughness tips and its consequent fracture, and the micropitting, which deteriorates the surfaces;
- **Antioxidants:** additives that interrupt the chemical reaction between the oxygen and the hydrocarbons, decreasing the lubricants oxidation ageing. These additives increase the resistance to high temperatures allowing to increase the lubricant service life;
- **Dispersing additive - detergents:** those which clean the lubricated surfaces;
- **Corrosion inhibitors:** protect against chemical attack on metal surfaces;

- **Oxidation/Rust inhibitors:** Increase oil and machine life while decreasing the varnish and the sludge on metal parts;
- **Foam inhibitors or anti-foaming additives:** prevent the foam formation;
- **Pourpoint depressants:** Decrease the temperature at which the oil can be pumped;
- **pH modifiers:** Allow the control of the pH of the oil;

Unfortunately there is still no way to predict exactly the effect of mixing some chemicals in base oils, since they are mutually affected. Therefore, some properties of the lubricant can only be obtained by experimental testing or even by trial and error [9].

2.5. Windmill gear oils

Some of the most common windmill turbines failures are due to the poor lubrication of the gearbox gears and rolling bearings. Especially when the winds are light, the gearbox components are submitted to high loads and very low speeds. This severe conditions cause frequently the rupture of the lubricant film leading to the structure's overheating and sometimes the collapse. Therefore, there is a high need for lubricants which can overcome these severe conditions and ensure the mechanism's stability. The windmill gear oils have high viscosity grades and also have extreme pressure and anti-wear additives, in order to resist these severe operating conditions.

Five windmill gear oils were tested in this work. They all have a viscosity grade ISO VG 320 at 40°C but their base oils are different:

- MINR - Mineral based;
- PAOR - Polyalphaolephine based;
- ESTF - Highly saturated Ester based;
- PAGD - Polyalkalineglycol based;
- ESTR - Highly saturated Ester based;

The most significant properties of the five lubricants are shown in the Table 2.2, according with the informations given by the manufacturers.

Table 2.2.: Tested lubricants properties.

Parameter	Units	Reference					
		MINR	PAOR	ESTR	PAGD	ESTF	ESTR
Base oil		Mineral	PAO	Ester	PAG	PAG	Ester
Measurement Method							
Physical Properties							
Density @ 15°C	g/cm^3	ASTM D4052	0.899	<i>n/a</i>	<i>n/a</i>	1.051	<i>n/a</i>
Viscosity @ 40°C	<i>cSt</i>	ASTM D445/DIN 51562 – 1	320	320	320	320	320
Viscosity @ 100°C	<i>cSt</i>	ASTM D445/DIN 51562 – 1	24.03	35.5	<i>n/a</i>	54	36
Viscosity Index	/	ASTM D2270/DIN ISO2909	95	158	<i>n/a</i>	237	160
Inflammability Point	°C	ASTM D92/DIN ISO2592	210	210	<i>n/a</i>	<i>n/a</i>	270
Pour Point	°C	ASTM D97/DIN ISO3016	-9	-42	<i>n/a</i>	-39	-45
Corrosion Resistance Properties							
Copper corrosion, 3h at 100°C	/	ASTM D130	1a	<i>n/a</i>	<i>n/a</i>	Pass	<i>n/a</i>
Rust, method A	/	ASTM D665	Pass	Pass	<i>n/a</i>	Pass	<i>n/a</i>
Rust, method B	/	ASTM D665	Pass	<i>n/a</i>	<i>n/a</i>	Pass	<i>n/a</i>
Wear Properties							
FAG FE-8 Roller wear	mg	DIN 51819-3	3	<i>n/a</i>	<i>n/a</i>	Pass	<i>n/a</i>
Micropitting Test	/	FVA 54/7	GF>10	<i>n/a</i>	<i>n/a</i>	<i>n/a</i>	GF>10
FZG A20/8,3/90°	/	DIN 51354	>12	>12	<i>n/a</i>	<i>n/a</i>	>12

2. Lubrication and Lubricants

The quality level was also obtained through the manufacturers catalogues and is presented in the Tables 2.3 and 2.4.

Table 2.3.: MINR, PAOR and ESTR oils quality level.

Reference	MINR	PAOR	ESTR
Quality level	Din 51517 Part 3 CLP Flender Industrial Gear ISO 12925-1 CKD	Din 51517 Part 3 CLP Flender Industrial Gear US Steel 224 AGMA 9005 – <i>E02EP</i> Cincinnati Lamb: P-35 (ISO 460), P-59 (ISO 320) P-76 (ISO 100), P-77 (ISO 150) P-74 (ISO 220)	<i>n/a</i>

Table 2.4.: PAGD and ESTF oils quality level.

Reference	PAGD	ESTF
Quality level	<i>n/a</i>	Din 51517 Part 3 CLP Biodegradability > 90% CEC L-33-A-93

2.5.1. Oil properties measurement

During this work, the tested Lubricants were also submitted to density and viscosity measurements to confirm the data provided from the manufacturers.

The viscosity can be measured according to different normalized methods. According to the standard ASTM D445, the viscosity of a lubricant can be determined by measuring the time, in seconds, needed for a fluid volume to flow through a calibrated capillary, at a controlled temperature. In this work, the viscosity was determined using an Engler's viscometer (2.7).



Figure 2.7.: Engler Viscometer

This viscometer (according to the IP 212/92 standard), is composed by a recipient where the lubricant sample is deposited. This recipient has a calibrated capillary in the bottom which allows the oil to flow. This capillary is closed until the oil is at the desired temperature. To perform the oil heating, this recipient is surrounded by another recipient which is filled with a fluid, heated by an electrical resistance. In this way it is easier to maintain a constant temperature within the fluid to measure the viscosity. There are two thermometer, one for each recipient.

2. Lubrication and Lubricants

This procedure was realized for three different temperatures: 40, 70 and 100°C . The measured flow time was then converted using the equation 2.9.

$$^{\circ}Engler = \frac{t_T}{t_{20^{\circ}C}} \quad (2.9)$$

In the equation 2.9, t_T represents the time needed for 200ml of lubricant to flow at the temperature T , while $t_{20^{\circ}C}$ represents the time needed for 200ml water to flow at 20°C . The calculated $^{\circ}Engler$ can then be converted to centistokes (cSt) using the following equation:

$$cSt = ^{\circ}Engler \cdot k_1 + \frac{k_2}{^{\circ}Engler + k_3} \quad (2.10)$$

The values of k_1 , k_2 and k_3 are given by:

Table 2.5.: Constants values for the conversion.

	k1	k2	k3
$^{\circ}Engler < 3$	14,867	75,568	-6,198
$^{\circ}Engler > 3$	7,624	-2,717	-1,522

The specific weight was measured using a densimeter (figure 2.8).



Figure 2.8.: Densimeter.

The measured properties values were slightly different from the catalogues but they all are within the admissible range of the ISO viscosity grade. The results are shown in the Table 2.6.

Table 2.6.: Tested lubricants measured properties.

Parameter	Units	Reference	MINR	PAOR	ESTR	PAGD	ESTF
		Base oil	Mineral	PAO	Ester	PAG	Ester
		Method					
Physical Properties							
Density @ 15°C	g/cm^3	/	0.902	0.892	0.915	1.059	0.957
Density @ 25°C	g/cm^3	/	0.896	0.886	0.907	1.052	0.950
Viscosity @ 40°C	cSt	ASTM D341	319.25	313.57	302.86	290.26	324.02
Viscosity @ 70°C	cSt	ASTM D341	65.87	85.41	77.48	102.33	88.09
Viscosity @ 100°C	cSt	ASTM D341	22.41	33.33	34.85	51.06	36.06
Viscosity Index	/	"based" on ASTM D341	85	150	162	241	159
Thermoviscosity @ 40°C	K^{-1}	"based" on ASTM D341	0.0639	0.0507	0.0491	0.0373	0.0499
Thermoviscosity @ 100°C	K^{-1}	"based" on ASTM D341	0.0301	0.0267	0.0262	0.0221	0.0262
Piezoviscosity @ 40°C	Pa^{-1}	"based" on ASTM D341	2.207E-08	1.590E-08	1.437E-08	1.278E-08	1.450E-08
Piezoviscosity @ 100°C	Pa^{-1}	"based" on ASTM D341	1.527E-08	1.182E-08	1.071E-08	9.884E-09	1.076E-08

3. Gearbox Test Rig and Transfer Gearbox

3.1. Test Rig

The gearbox tests were performed using a back-to-back test rig with re-circulating power. The test rig used was developed to test gearboxes with variable dimensions, thus there are two adjustable platforms for each gearbox (test and slave), connected by an output torque and speed sensor. According to the schematic view at Figure 3.1, the letters **a** and **b** represent flexible links which allow axial misalignments, while **Sen.1** and **Sen.2** represent the torque and speed sensors, to measure the input and output conditions of the tested gearbox, respectively. The sensor **Sen.2** is attached to a mobile platform which allows the adjustment of its height and depth, between the two gearboxes.

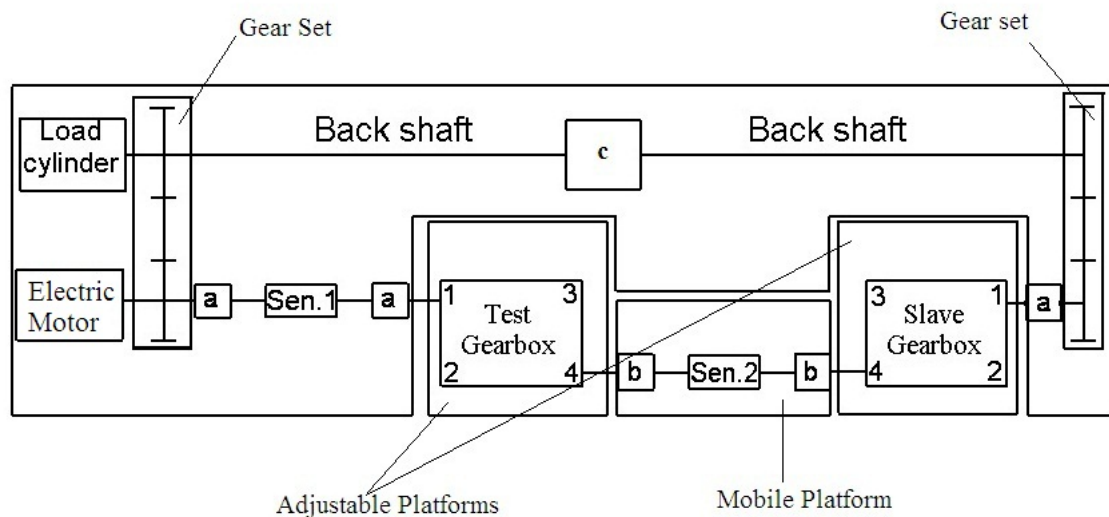


Figure 3.1.: Gearbox test rig.

3. Gearbox Test Rig and Transfer Gearbox

On the left side there is the driving electrical motor and the hydraulic cylinder responsible for the applied torque. Since the power is re-circulating, the motor only supplies the power needed to overcome the frictional and inertial losses at start and maintain the desired operating speed constant. In order to maintain this re-circulating power and close the loop, two sets of gears are necessary at each end, connected by a long rear shaft. This shaft is divided by a support box, which decreases the effective balancing length in order to reduce the vibrations (c). Each one of these gear sets is lubricated by oil injection in dry case, supplied by the hydraulic station shown in Figure 3.2.



Figure 3.2.: Hydraulic oil supply station.

These gear sets have two gears each, so that all the outside shafts run with the same sense (Figure 3.3). The left gear set box is connected to both the electrical motor and the hydraulic cylinder responsible for the application of the static torque to the whole system. This static torque results from the axial movement of the cylinder which pushes a helical gear to describe a linear movement over another fixed helical gear, leading to a relative spin between the two, which is dependent of the helix angle (Figure 3.4).



Figure 3.3.: Gear set.

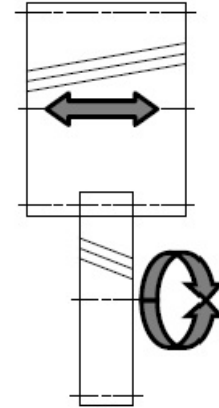


Figure 3.4.: Static torque application mechanism resulting from hydraulic cylinder axial movement.

The electrical motor is connected to the left gear set by two timing belts, as represented by the Figure 3.5 and its speed control is done through a variable-frequency drive, which allow the motor to achieve 4300rpm. The AC motor technical features are shown in Table 3.1.

Table 3.1.: AC Motor technical features.

Type PFMH-250M83		
Nominal speed	1480	rpm
Nominal power	55	kW
Frequency	50	Hz
Cos F	0.87	—
Voltage	220/380	V
Current intensity	181/104	A

3. Gearbox Test Rig and Transfer Gearbox



Figure 3.5.: AC electrical motor.

The test and slave gearboxes are equal and work back-to-back, allowing the speed at the test gearbox's entrance to be equal to the speed at the slave gearbox's exit, this meaning that the test gearbox will multiply the input speed, while the slave gearbox will reduce it or vice-versa. With this purpose, the test gearbox needs to be reversible, so it can work at both conditions.

3.2. Transfer Gearbox

The transfer gearbox is generally used at the exit of the main vehicle gearbox and allows the vehicle to have two drive shafts and an additional motion exit for an auxiliary mechanism, as is shown in Figure 3.6. The transfer gearbox, like the conventional vehicle gearboxes, is a reducer gearbox, which means that it increases the torque while it decreases the output speed.

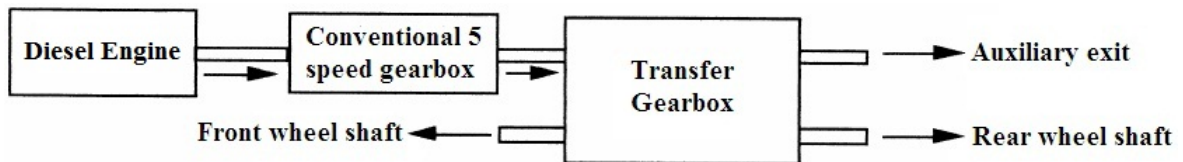


Figure 3.6.: Transfer Gearbox vehicle application.

The transfer gearbox that was tested has two speeds, doubling the cinematic relations from the main gearbox. That way, it allows 10 kinematic relations when used at the exit of a conventional 5 speed gearbox. The cross section view of the transfer gearbox is shown at Figure 3.7.

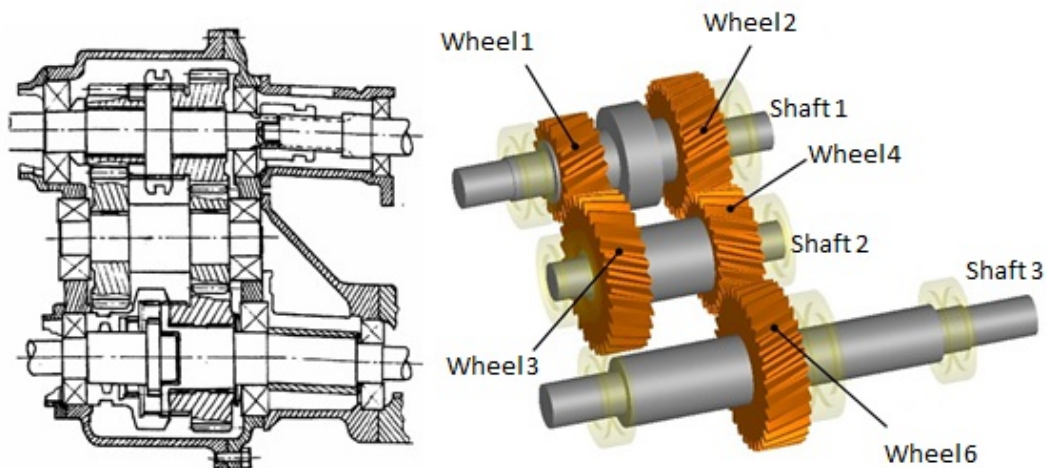


Figure 3.7.: Cross section of the transfer gearbox and 3D model view.

As it is possible to see in Figure 3.7, the Transfer Gearbox consists in three shafts where five wheels are mounted. The wheels at the intermediate shaft(2) are keyed, while the wheels at the input(1) and output(3) shafts are mounted in needle bearings, running loose. All the shafts are supported by roller and ball bearings. As

3. Gearbox Test Rig and Transfer Gearbox

it was already said, the Transfer Gearbox allows two different speeds at the output shaft. The first speed is obtained when the wheels 1-3 and 4-6 are geared and the wheel 2 is running loose. When this speed is geared the 4x4 traction is activated and both the front and rear wheel shafts are active. On the other hand, the second speed is obtained when the wheels 2-4-6 are geared and the wheels 1-3 are running loose. The gearbox speed map is shown in the Figure 3.8 as well as the schematic representation of the shafts and gears.

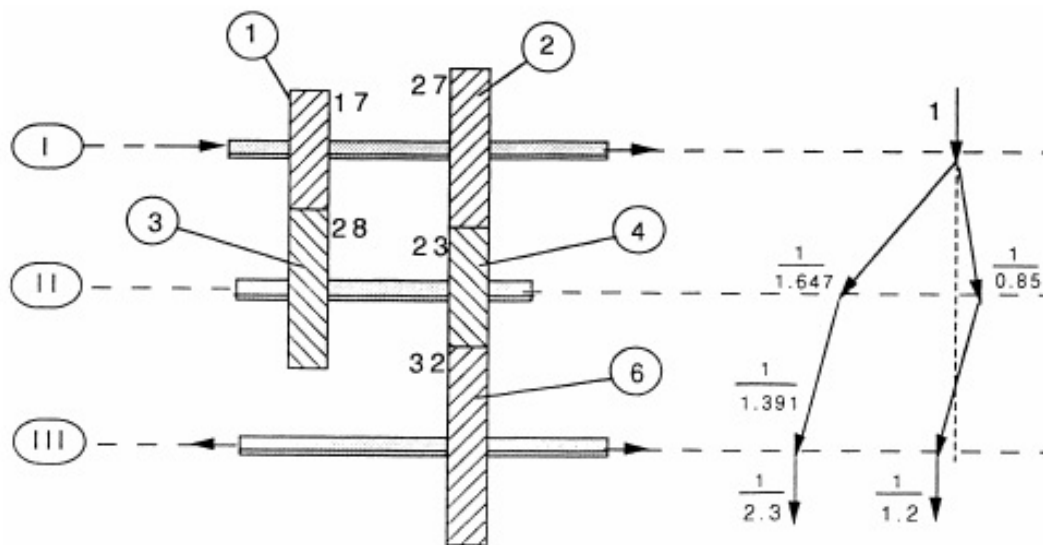


Figure 3.8.: Gearbox schematic representation and speed map.

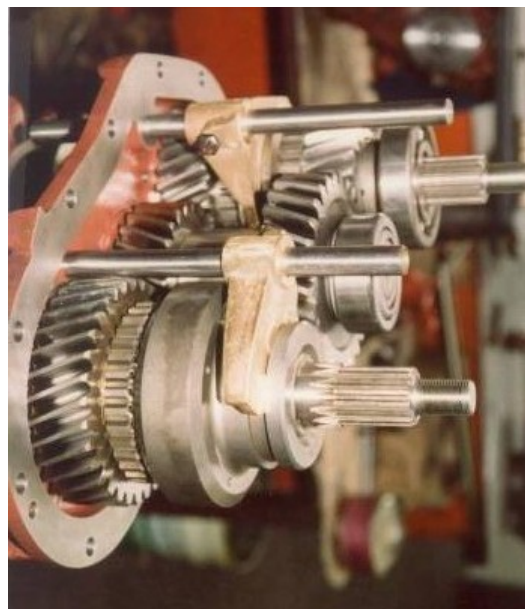


Figure 3.9.: Fork and toothed ring mechanism.

The gear selection is realized through a fork and toothed ring mechanism (Figure 3.9). There are two of these mechanisms, one allowing the speed shift and the other allowing the selection of the additional traction to the front vehicle wheels. The speed shift is performed when the fork and ring mechanism selects the first or second wheel, which starts to run together with the first shaft. This constructive solution forces the wheels 1 and 2 to be permanently running which causes an increased power loss through churning and also more noise at work.

3.2.1. Multiplier Gearbox

The main objective of this study was to evaluate the energetic efficiency of the wind mill gear oils presented in chapter 2. In order to simulate these oils usual operating conditions, some work parameters were changed to test the gearbox efficiency at low speeds and high torques. With this in mind, the gearbox was used as a multiplier gearbox instead of a reducer gearbox and the electric motor was connected to the rear wheel shaft of the gearbox. In the tests performed, only the first gear was considered and the transfer gearbox was used as a multiplier, as it is the case of all windmill gearboxes. The new speed map for the multiplier gearbox is presented in Figure 3.10.

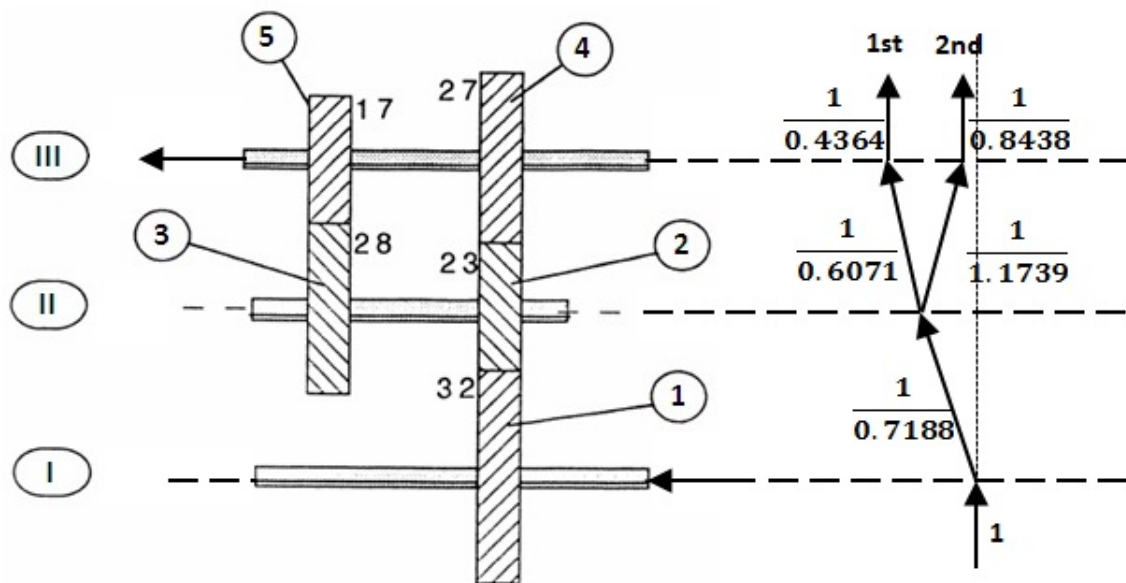


Figure 3.10.: Gearbox speed map, when working as a multiplier.

3.2.2. Gear geometry and material

The gear ratio is dependent of the wheels teeth number and the gears geometry are presented in Table 3.2.

Table 3.2.: Gears geometry on the Transfer Gearbox.

Wheel Number	1	2	4	3	5	Units
Module (m)	3.5	3.5	3.5	4	4	mm
Number of teeth (z)	32	23	27	28	17	–
Addendum modification (x)	0.381	0.415	0.161	-0.24	0.051	–
Face width (b)	35	35	35	33.5	35	mm
Pressure angle (α)	20	20	20	20	20	$^\circ$
Helix angle (β)	20	20	20	20	20	$^\circ$
Number of teeth for dimensional control (k)	5	4	4	4	3	–
Maximum Teeth thickness (Ek)	49.25	38.46	38.092	30.75	30.75	mm
Minimum Teeth thickness (Ek)	49.212	38.43	38.062	30.72	30.72	mm
Outside radius w. long addendum	128.6	95.3	108.4	125.2	80.7	mm
Outside radius w. short addendum	128.2	95.15	108.25	125	80.6	mm
Centre distance (a)	105H7		95H7			mm
		95H7				mm
Gear ratio ($i = z_2/z_1$)	0.7188		0.6071			–
		1.1739				–

In the first speed, the transmission ratio is $i = 0.4364$, meaning that the input speed will be multiplied 2.3 times, through gears 1-2 and 3-5, while the wheel 4 is running loose:

$$i = \frac{z_2}{z_1} \cdot \frac{z_5}{z_3} = 0.7188 \cdot 0.6071 \simeq 0.4364. \quad (3.1)$$

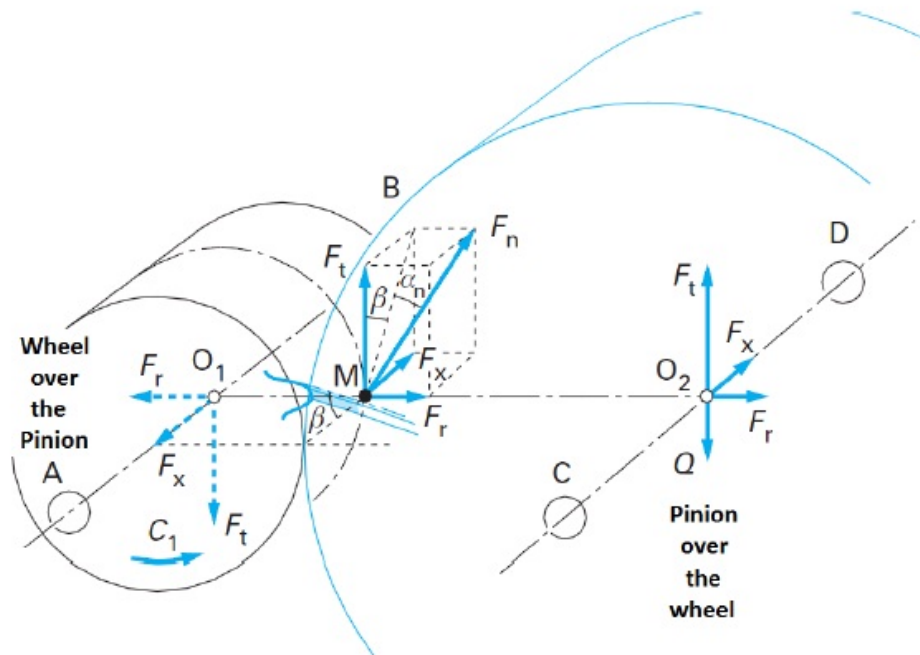
The gears were made with carburized steel DIN 15CrNi6 (Table 3.3) and after the teeth were carved, it was applied the following heat treatment:

- Hardening under controlled atmosphere;
- Diffusion;
- Quenching in oil;
- Annealing.

Table 3.3.: Mechanical properties of the steel DIN 15CrNi6 after heat treatment.

Property	Value	Units
Flexural Tensile Strength (σ_{FE})	620	MPa
Fatigue Strength (σ_{Hlim})	1300	MPa
Poisson Coefficient (ν)	0.3	
Specific Weight (ρ)	7850	Kg/m^3
Young's Modulus (E)	210	GPa
Hardness	58-62	HRC
Heat treatment depth	0.8	μm

The gears safety factors for the most severe operating conditions, where determined with the software KissSoft[®]. These safety factors were calculated according to the loads applied in each pinion as is represented in Figure 3.11. There were only considered the loaded gears 1-2 and 3-5, as the wheel 4 was running loose. The results are shown in Table 3.4 for Mineral based oil ISO VG 320. For more detailed information about this calculation, see appendix A.2.

**Figure 3.11.:** Contact in helical gears.

3. Gearbox Test Rig and Transfer Gearbox

Table 3.4.: Gear loads and resistance for $n_1 = 235\text{rpm}$ and $T_1 = 1000\text{Nm}$.

	Units	z1	z2	z3	z5
Oil bath temperature	[°C]	102			
Speed	[rpm]	235	327	327	538.5
Torque	[Nm]	1000	718.8	718.8	436.4
Tangential force	[N]	16780.2		12159.5	
Axial Force	[N]	6107.5		4389.8	
Radial force	[N]	6499.5		4671.5	
Tooth normal force, transverse section	[N]	19003.2		13658.2	
Tooth Root Safety	[/]	2.3565	2.4004	3.3337	3.5782
Tooth Flank Safety against pitting	[/]	1.2879	1.2879	1.2881	1.2815
Safety against scuffing (integral temperature)	[/]	2.5223		2.1428	
Safety against scuffing (flash temperature)	[/]	3.9291		1.8959	

The gears meshing and tooth form are represented in Figures 3.12 and 3.13.

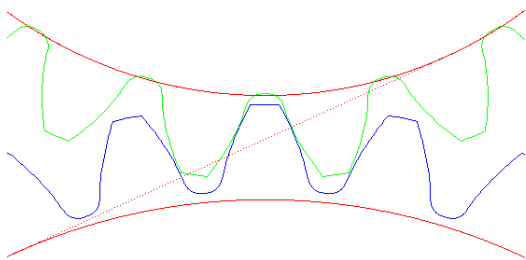


Figure 3.12.: Gear 1-2 meshing and tooth form.

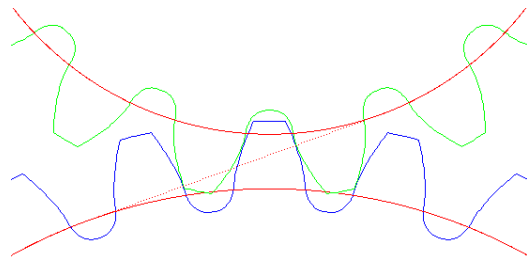


Figure 3.13.: Gear 3-5 meshing and tooth form.

3.2.3. Shafts

The gearbox shafts were made from the same steel used for the gears, hardened and quenched. The properties are shown below in the Table 3.5.

Table 3.5.: Mechanical properties of the steel DIN 15CrNi6 used in the shaft.

Property	Value	Units
Tensile Strength (σ_r)	900	MPa
Yield Stress (σ_y)	650	MPa
Maximum alternating normal stress (σ_W)	400	MPa
Flexural Tensile Strength (σ_{bF})	750	MPa
Maximum alternating bending stress (σ_{bW})	450	MPa
Torsional limit stress (τ_{tF})	390	MPa
Maximum Torsional alternating stress (τ_W)	270	MPa
Poisson Coefficient (ν)	0.3	
Specific Weight (ρ)	7850	Kg/m^3
Young's Modulus (E)	210	GPa
Hardness	58-62	HRC

The shafts maximum deflection and maximum principal stress for $n_1 = 235\text{rpm}$ and $T_1 = 1000\text{Nm}$, where simulated using again the Software KissSoft®. The results are shown in the Table 3.6 and in Figures 3.14 to 3.19. For more detailed information about this calculation, see appendix A.2.

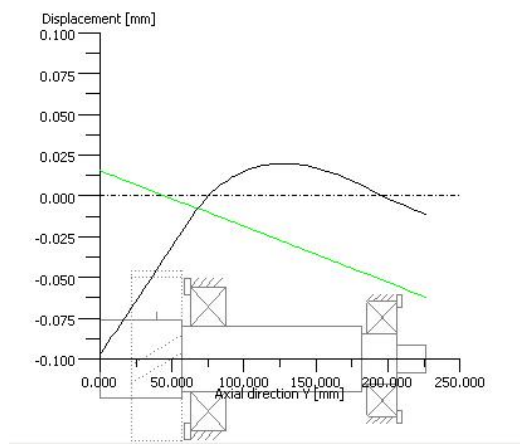


Figure 3.14.: Input shaft displacements.

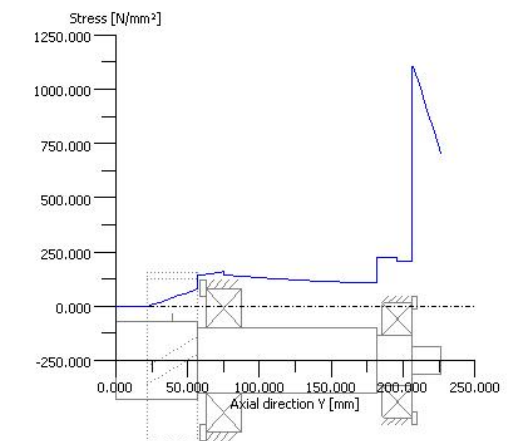


Figure 3.15.: Input shaft stress.

3. Gearbox Test Rig and Transfer Gearbox

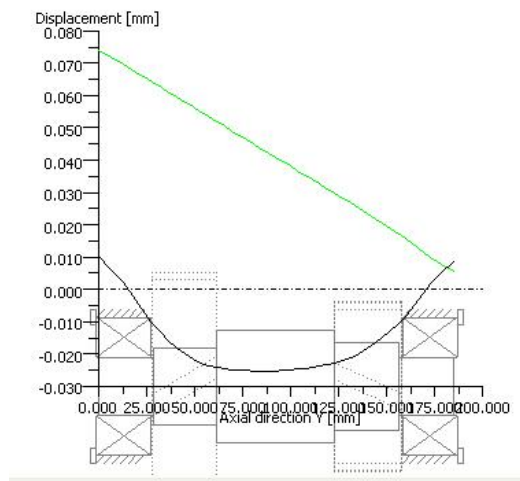


Figure 3.16.: Intermediate shaft displacements.

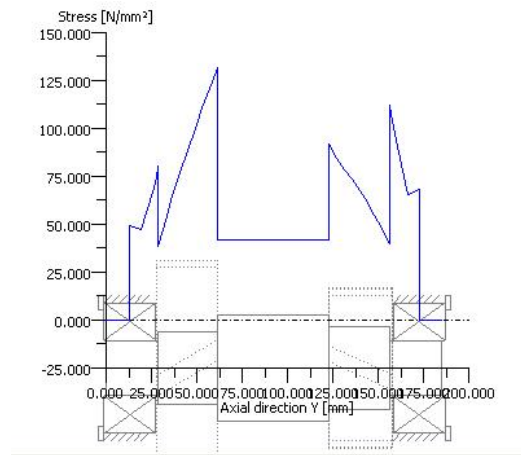


Figure 3.17.: Intermediate shaft stress.

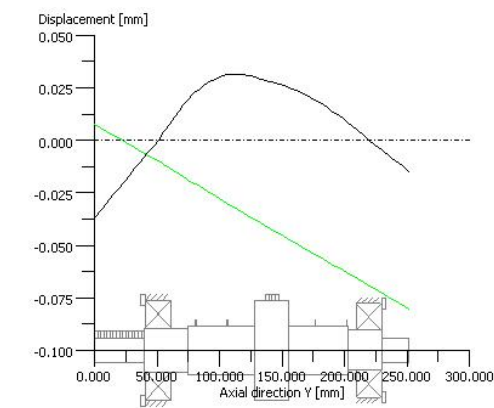


Figure 3.18.: Output shaft displacements.

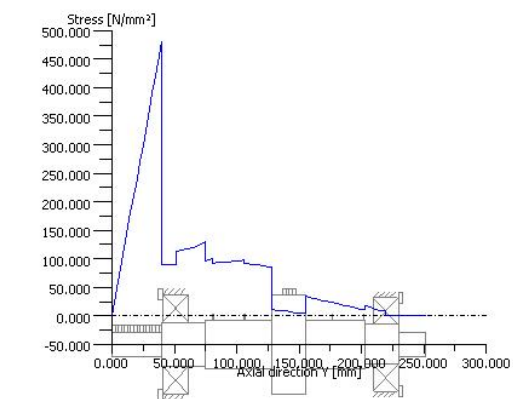


Figure 3.19.: Output shaft stress.

Table 3.6.: Resistance of the shafts and minimum rolling bearing life.

Shaft	1	2	3
Max. Deflection [mm]	0.09721	0.02523	0.03701
Max. principal stress [N/mm ²]	1102.66	131.73	481.19
Min. bearing service life [h]	8449.42	830.48	223.32
Min. static bearing safety	2.66	3.6	1.9

3.2.4. Rolling Bearings

The gearbox uses four different types of rolling bearings. Its complete version has a total of 17 bearings, however, the tested gearbox is not equipped with the auxiliary exit, so the number is reduced to 15. The four constructive types are:

- Deep groove ball bearings;
- Cylindrical roller bearings;
- Tapered roller bearings;
- Needle roller bearings.

The transfer gearbox cross section and the rolling bearings numbering are shown below in the Figure 3.20. The rolling bearings characteristics are presented in Table 3.7, according to that numbering.

Table 3.7.: Gearbox bearings

Number	Rolling Bearing Type	Reference	C [N]	C_0 [N]	d [mm]	D [mm]	Max. Speed [rpm]
1	Ball	RMS 11	31500	22000	35	89	9000
2	Ball	RMS 10	23500	16100	32	79	10500
3, 4	Tapered roller	32306	67000	53000	30	72	6500
5	Cylindrical roller	NJ309E	91500	62000	45	100	6700
6, 7	Ball	6307	26000	18300	35	80	9000
8 to 12	Needle roller	K 38x43x27 F	30500	68000	38	43	11000
13 to 15	Needle roller	K 14x18x13	9150	12500	14	18	26000

3. Gearbox Test Rig and Transfer Gearbox

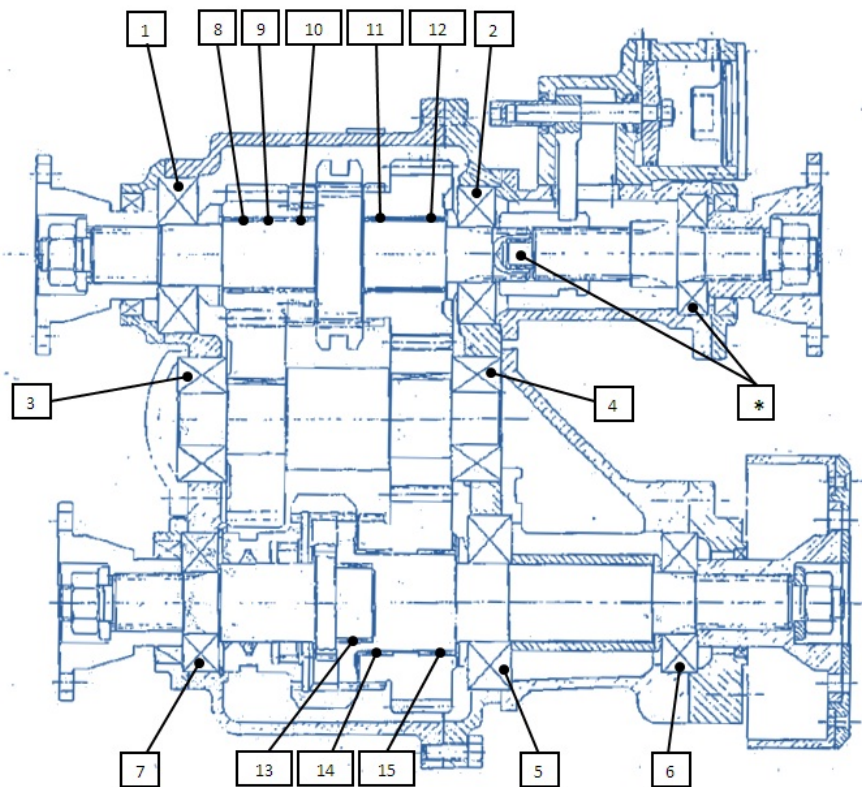


Figure 3.20.: Bearings numbering

The rolling bearings service life for the most severe conditions was also calculated with KissSoft[®]. The results for the rolling bearings supporting the shafts are presented in Table 3.8. For more detailed information about this calculation, see appendix A.2.

Table 3.8.: Rolling Bearings service life factors.

Rolling bearing	1	2	3	4	5	6
Static service factor - S0	1.9	5.33	6.43	3.6	4.05	2.66
Service life - Lnh [h]	1042	29993	17754	830	8813	8449

3.2.5. Lubrication

The lubrication of the gearbox is performed by churning in oil bath, where the nominal volume used is 2.85 liters. The manufacturer recommends the use of an SAE 80W90 oil.

In the tests, the gearbox was lubricated with 5 different windmill gear oils, already described in section 2.5.

4. Experimental evaluation of the transfer gearbox performance

4.1. Introduction

The experimental evaluation of the transfer gearbox energetic efficiency was performed in the gearbox test rig presented in the previous chapter. Since the lubricants to be tested were developed for windmill turbines gearboxes, the transfer gearbox usual test procedure was modified so high torques and low speeds could be tested.

Two sets of trials were realized, each one at a fixed speed and increasing torques. Each trial performed with the five windmill gear oils, will be analysed attending to the following relevant aspects:

- Oil bath temperature evolution;
- Torque Loss;
- Global energetic efficiency.

4.2. Test Procedure

The operating conditions established for each oil to be tested were: two levels of input speed and three levels of torque. For each speed level, three levels of torque were tested - Table 4.1.

4. Experimental evaluation of the transfer gearbox performance

Table 4.1.: Operating conditions in gear efficiency tests.

Test Sequence [/]	Input speed [rpm]	Input torque [Nm]	Input Power [kW]	Total test time [h]
1	235	500	13.090	6
2		750	19.635	6
3		1000	26.180	6
4	135	500	7.854	6
5		750	11.781	6
6		1000	15.708	6

Since there were five wind mill oils to be tested, six trials were realized for each oil leading to a total of thirty tests.

The trials were conducted only at transfer's gearbox first gear in which the total gear ratio was higher, and thus the speed at the input shaft was multiplied through gears 1-2 and 3-5. The stabilization temperature is reached after an estimated time of 6 hours and all the tests were performed after a run-in period of 15 minutes at 250rpm and 300Nm after which the oil temperature was about 25 to 35°C . After the run-in, the slave gearbox was disengaged so there was absolutely no torque applied and then the test rig workbench was re-calibrated. The temperature variation is free, ie, the test rig does not allow the oil bath temperature control.

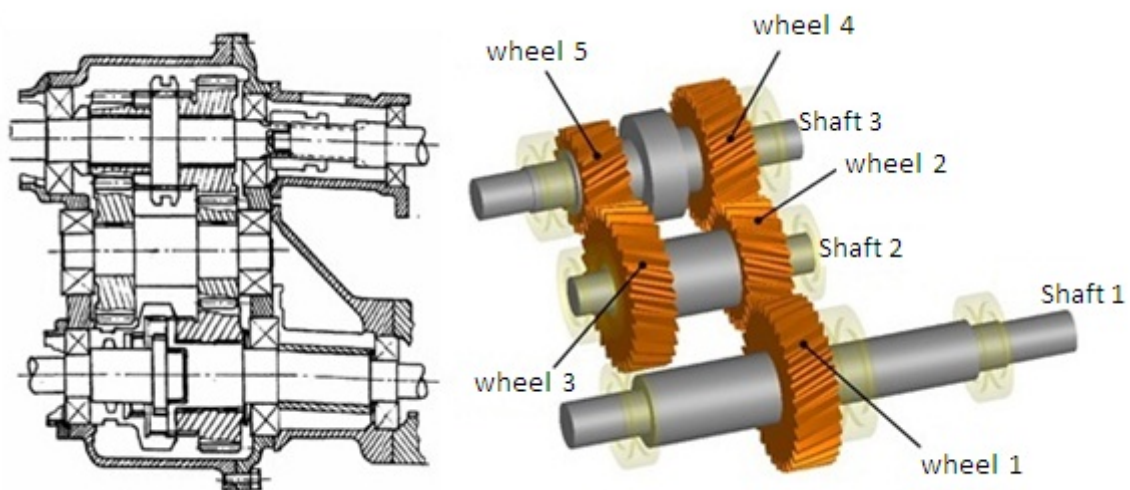


Figure 4.1.: Transfer gearbox.

After each oil has been submitted to six different and successful trials, a lubricant sample was collected (figure 4.2) with an appropriated vacuum pump (figure 4.3) so it could be analysed through Direct Reading Ferrometry (DR III) and also Analytic Ferrography (FM III), both techniques described in the next section. The transfer gearbox was then cleaned up and the oil changed.

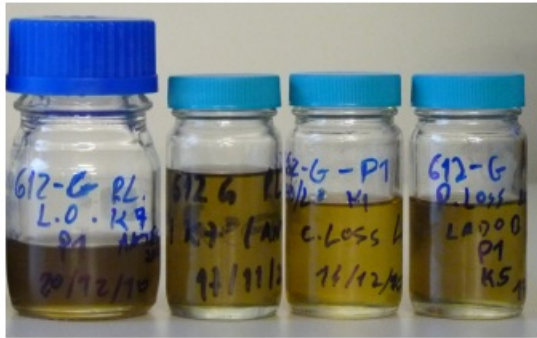


Figure 4.2.: Oil samples.



Figure 4.3.: Vacuum pump.

For each trial four different temperatures have been measured using thermocouples: test gearbox oil temperature, test gearbox wall temperature, slave gearbox wall temperature and room temperature. The input and output speeds and also the input torque were measured. The output torque was not able to be measured correctly since the sensor (**Sen.2**) was not working properly.

The oil volume used in the master gearbox was only 2,0l instead of the 2,85l recommended by the manufacturer, in order to reduce the churning losses and helping in a better understanding of the influence of gear oil formulation on the friction losses.

The slave gearbox was running using a different oil, ie, a PAO based oil with an ISO VG 150 viscosity grade. Therefore, is expected a different behaviour between the test and the slave gearbox.

4.2.1. Oil analysis procedure

The analysis of particles contained in lubricant samples give a quite good indication about the wear of the lubricated gearbox components, since the gearbox is closed and the particles presented in the sample can only be generated from the contacting surfaces.

The Direct Reading Ferrometry and the Analytic Ferrography techniques, allow the identification and characterization of the wear particles present in the oil samples generated during the tests performed in the gearbox. The characterization of the wear particles is based on the size, shape and number of wear particles.

Generally, this allows the comparison of the lubricants and materials tested, but in the present work this analysis will serve only to search for a similar tendency between the temperature stabilization results and the wear particles obtained. This is due to the fact that the gears were not changed between each set of trials causing each oil sample to have less wear particles than the previous oil sample tested, not only because of the polishing and accommodation of the roughness tips but also because of the accumulation of each oil additive package in the gears surface.

4.2.1.1. Direct Reading Ferrometry: equipment and procedure

The direct reading ferrografer measures quantitatively the ferrous particles concentration contained in the lubricant (figure 4.4). The technique consists in forcing 1ml of lubricant sample to pass through a capillary which is submitted to a strong magnetic field and two light beams while a optical system performs opacity measurements, quantifying the light intensity which is directly proportional to the density of the deposited particles. These particles are deposited by the magnetic field action.

The ferrographer measures two indexes:

- large particles index D_L , for particles with size greater than $5\mu\text{m}$;
- small particles index D_S , for particles with size smaller than $5\mu\text{m}$



Figure 4.4.: Direct Reading Ferrografer.

From the knowledge of these two indexes it is possible to calculate the wear particle concentration index CPUC, which grows when the sum of large and small particles increases, and the wear severity index ISUC, which grows when the number of large particles is bigger than the number of small particles. These indexes are present in equations 4.1 and 4.2:

$$CPUC = \frac{D_L + D_S}{d} \quad (4.1)$$

$$ISUC = \frac{(D_L)^2 - (D_S)^2}{d^2} \quad (4.2)$$

where **d** refers to the sample dilution factor in cases of excessive contamination.

4. Experimental evaluation of the transfer gearbox performance

4.2.1.2. Analytic Ferrography: equipment and procedure

This technique is used to obtain more detailed information of the lubricant particles and is performed on a diluted oil sample which is passed through a glass slide (Figure 4.5) while submitted to a magnetic field, being the the wear particles deposited along the slide according to their magnetic sensibility and size. The larger particles are the first to be deposited at the beginning of the ferrogram, and their size will progressively decrease in size along the length of the ferrogram. Some of the non metallic particles also deposit by gravity at the end of the ferrogram.

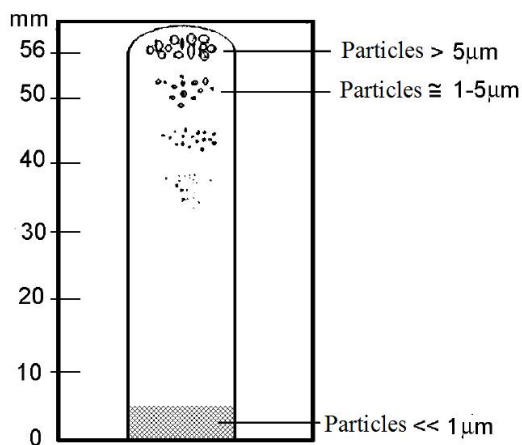


Figure 4.5.: Ferrogram scheme.

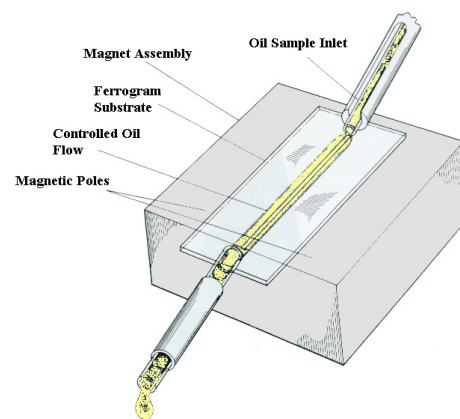


Figure 4.6.: Analytic Ferrographer.

The ferrogram obtained is then observed on a bi-chromatic light microscope (figure 4.7) and visually analysed. This analysis provides information concerning the size of the particles, their morphologies, concentration and the type of wear that originates them, as well as the component of their origin.



Figure 4.7.: Bi-chromatic microscope.

4.3. Relative performance of the windmill oils

The table 4.2 shows the stabilization temperature values measured for all the trials performed. The stabilization temperature is defined in equation 4.3.

$$\Delta\theta = \theta_{oil} - \theta_{room} \quad (4.3)$$

Table 4.2.: Stabilization temperature values

	Speed	135rpm			235rpm			Units
		Torque	500Nm	750Nm	1000Nm	500Nm	750Nm	
1	MINR	26,1	35,98	52,18*	43,92	59,11	77,08	°C
2	PAOR	24,17	30,33	38,32	37,02	50,83	63,41	
3	ESTF	22,32	30,3	39,2	38,31	49,79	63,23	
4	PAGD	19,92	27,12	33,74	34,58	44,93	55,55	
5	ESTR	—	—	—	37,74	49,52	68,92**	

*- trial performed at 155rpm; **- trial performed at 267rpm

The following figures 4.8 and 4.9 show the stabilization temperature of the gearbox oil, for each tested oil and for the three considered torques:

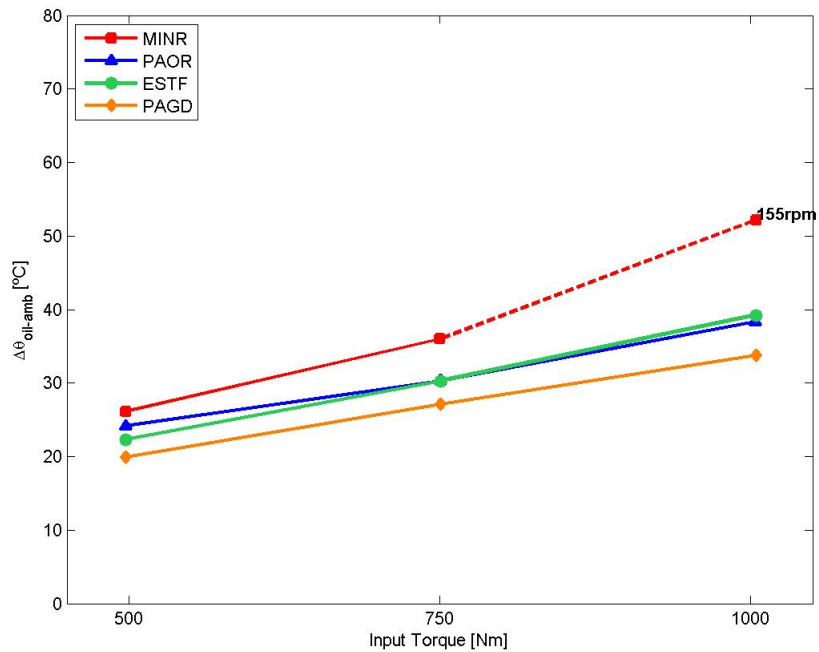


Figure 4.8.: Stabilization temperature for each input torque at 135rpm

4. Experimental evaluation of the transfer gearbox performance

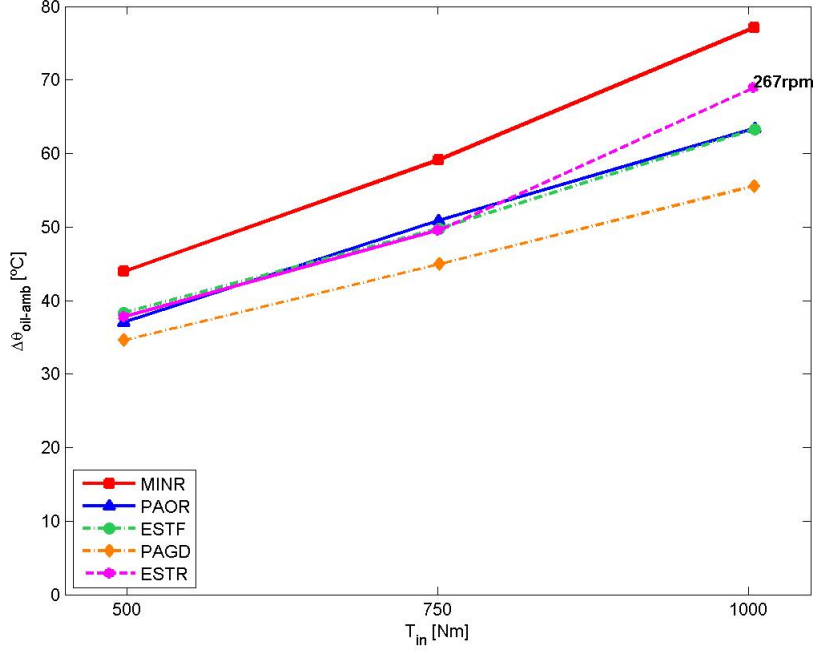


Figure 4.9.: Stabilization temperature for each input torque at 235rpm

Independently of the applied torque, the PAGD oil always presented the lower stabilization temperatures while the MINR always presented the higher. As the previous figures show, the ESTR was only tested at the speed of 235rpm since the gearbox test rig broke down and could not be fixed in time to finish the tests at 135rpm. Still, its behaviour was very similar to the ESTF, but this last one achieved slightly higher temperatures with consequence to its efficiency. The PAOR oil on the other hand, performed the same way that both the Esters while also achieving slightly higher stabilization temperatures.

Analysing the figures 4.8 and 4.9 it can be noticed that the stabilization temperature rises with the increase of the applied torque, suggesting as expected that the friction rises with the load, generating an increase of temperature. This is due to the increase of the coefficient of friction with the load as described by Höhn et al. [10] in the expression 4.4.

$$\mu_{mz} = 0.048 \cdot \left(\frac{F_{bt}}{b} \right)^{0.2} \cdot (\eta_{oil})^{-0.05} \cdot (R_a)^{0.25} \cdot X_L \quad (4.4)$$

On the other hand, the speed rise generates more heat leading also to higher oil temperature, even though the friction coefficient should be decreasing with the speed. This is probably due to the increase of churning inside the gearbox.

4.3. Relative performance of the windmill oils

The figures 4.10 and 4.11 show the evolution of the tested gearbox wall temperature with the load applied. As expected, the wall temperature behaviour confirms the oil bath stabilization temperature results as their behaviour is very similar.

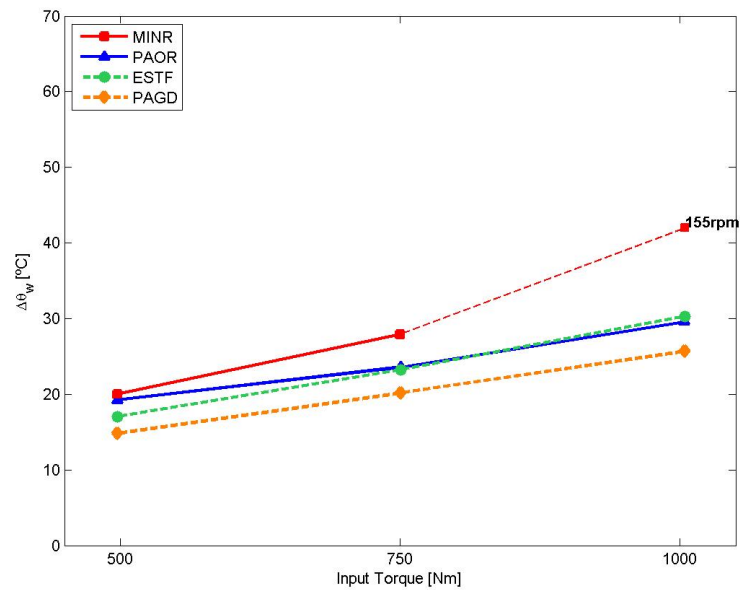


Figure 4.10.: Test gearbox wall stabilization temperature for each input torque at 135rpm

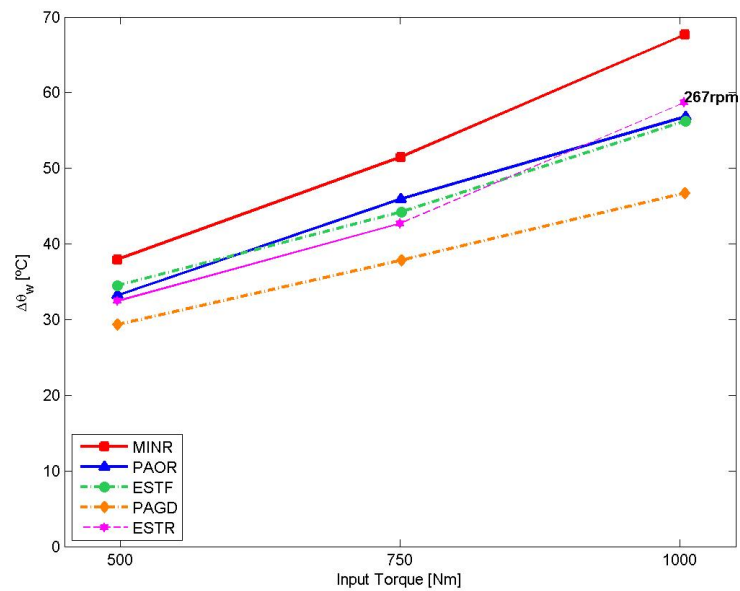


Figure 4.11.: Test gearbox wall stabilization temperature for each input torque at 235rpm

4. Experimental evaluation of the transfer gearbox performance

Whatever the input speed and torque, the stabilization temperatures of the oil bath and the gearbox wall, follow the same trend:

$$\Delta\theta^{PAGD} < \Delta\theta^{ESTR} \simeq \Delta\theta^{ESTF} \simeq \Delta\theta^{PAOR} < \Delta\theta^{MINR}. \quad (4.5)$$

4.3.1. Heat transfer analysis

Since it was not always possible to measure the output torque, the heat transfer coefficient of the gearbox was calculated using the results available, and then generalized for the three heat evacuation mechanisms (conduction, convection and radiation). This coefficient was approximated using a linear regression through the experimental results for the wall stabilization temperatures obtained for the mineral based oil at 235rpm (first set of trials), when the output torque sensor was working properly. The following expression for the heat transfer coefficient was determined:

$$\alpha = 0.2031 \cdot \Delta\theta_{wall-room} + 8.5367. \quad (4.6)$$

Applying that regression to the other wall temperatures obtained for the different oils at 235rpm and 135rpm, allowed to calculate the heat based power losses presented in Figures 4.12 and 4.13.

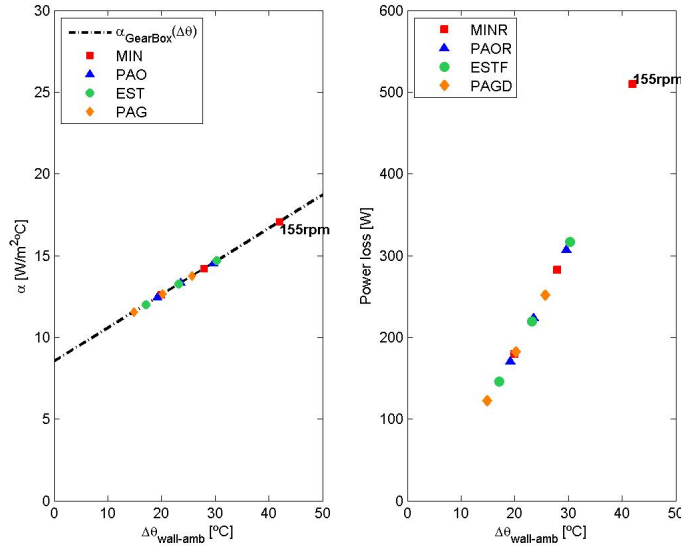


Figure 4.12.: Heat transfer coefficient linear regression and heat based power losses at 135rpm

4.3. Relative performance of the windmill oils

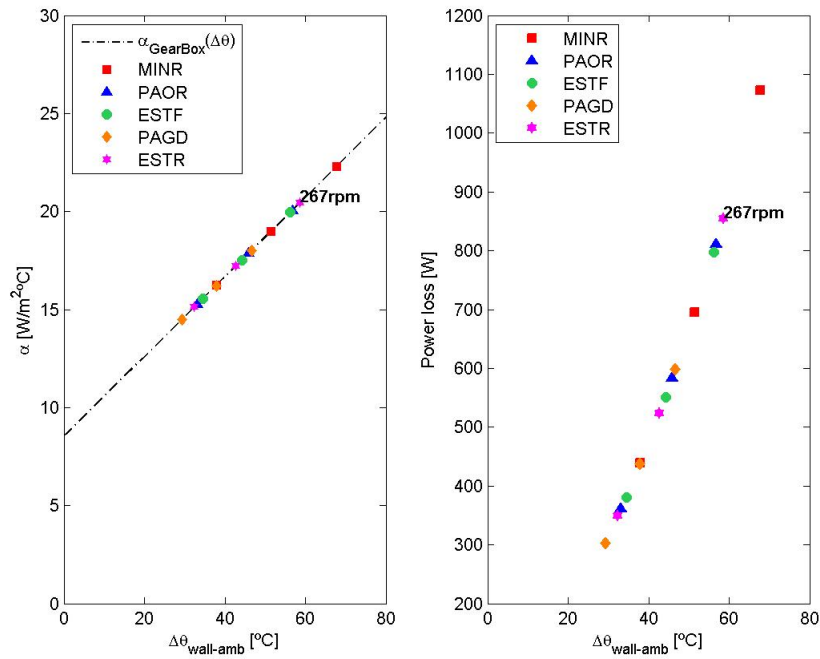


Figure 4.13.: Heat transfer coefficient linear regression and heat based power losses at 235rpm

In order to exclude the influence of the input speed, the gearbox torque loss was determined through the heat based power loss, as presented in Figures 4.14 and 4.15.

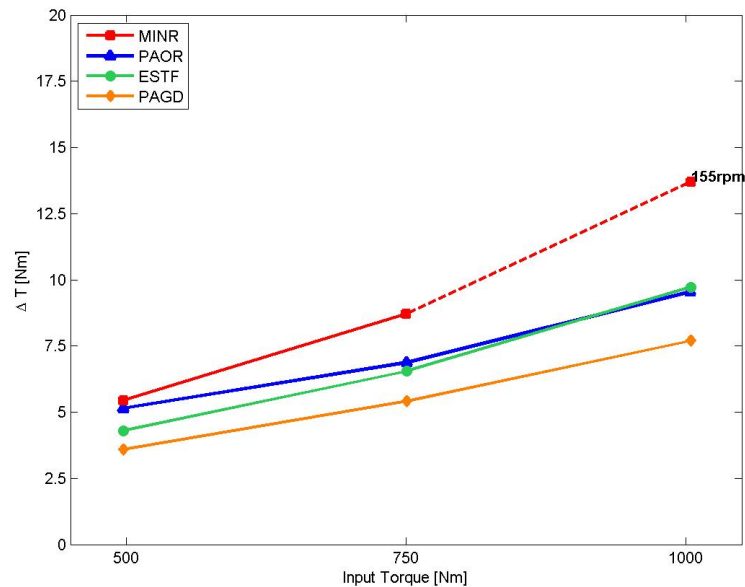


Figure 4.14.: Torque loss for each oil tested at 135rpm

4. Experimental evaluation of the transfer gearbox performance

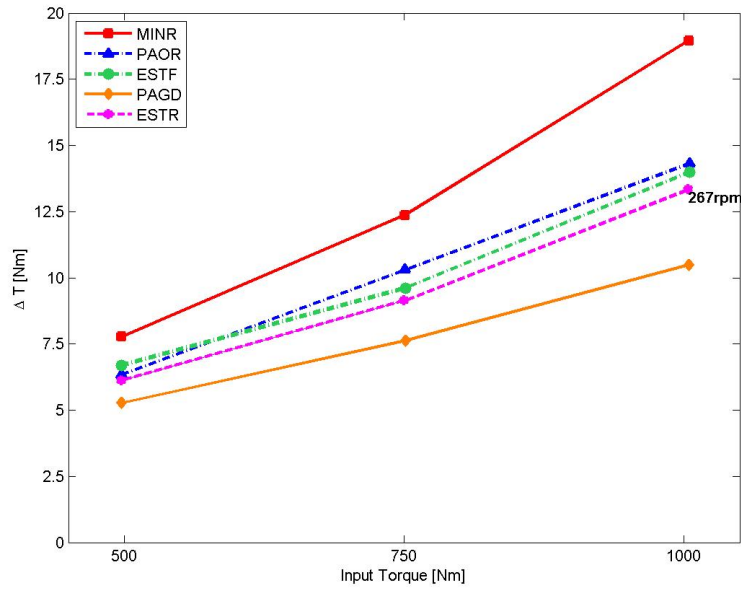


Figure 4.15.: Torque loss for each oil tested at 235rpm

Whatever the input speed and torque, the torque loss inside the gearbox follow always the same trend:

$$\Delta T^{PAGD} < \Delta T^{ESTR} \simeq \Delta T^{ESTF} \simeq \Delta T^{PAOR} < \Delta T^{MINR}. \quad (4.7)$$

For an input speed of 135rpm and an input torque of 1000Nm, the following torque losses were observed:

$$\Delta T^{PAGD} \simeq 7.5Nm; \quad (4.8)$$

$$\Delta T^{ESTF} \simeq \Delta T^{PAOR} \simeq 9.5Nm; \quad (4.9)$$

$$\Delta T^{MINR} \simeq 13Nm. \quad (4.10)$$

4.3. Relative performance of the windmill oils

The values of the gearbox torque loss obtained from the heat transfer analysis allow the calculation of the gearbox efficiency as represented in the figures 4.16 and 4.16.

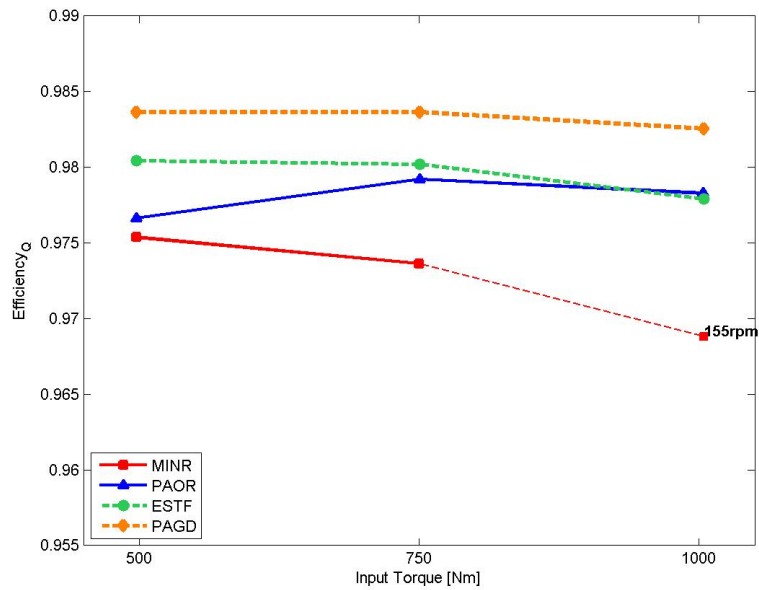


Figure 4.16.: Gearbox efficiency at 135rpm

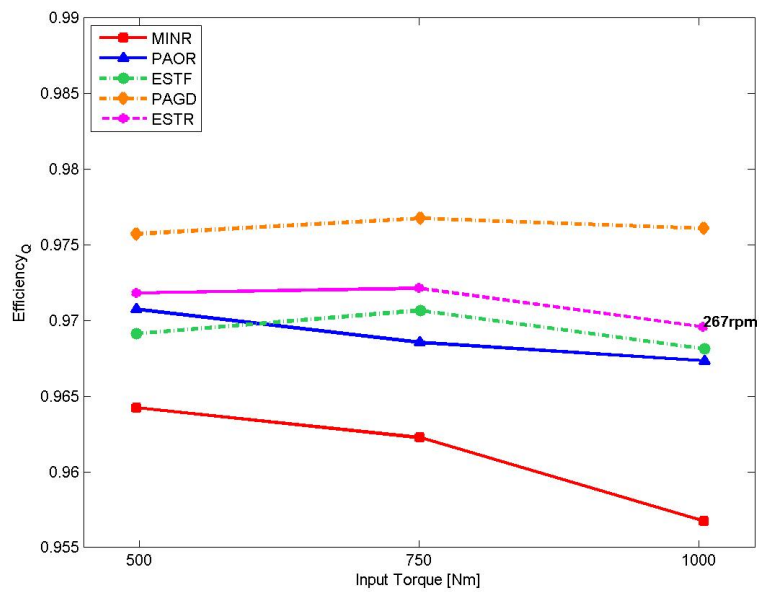


Figure 4.17.: Gearbox efficiency at 235rpm

4. Experimental evaluation of the transfer gearbox performance

These results show that whatever the input speed and torque, the gearbox efficiency (ε_Q) always follow the same trend:

$$\varepsilon_Q^{PAGD} > \varepsilon_Q^{ESTR} \simeq \varepsilon_Q^{ESTF} \simeq \varepsilon_Q^{PAOR} > \varepsilon_Q^{MINR}. \quad (4.11)$$

For an input speed of 235rpm and an input torque of 750Nm, the following gearbox efficiencies were calculated:

$$\varepsilon_Q^{PAGD} \simeq 97.7\%; \quad (4.12)$$

$$\varepsilon_Q^{ESTR} \simeq 97.2\%; \quad (4.13)$$

$$\varepsilon_Q^{ESTF} \simeq 97.1\%; \quad (4.14)$$

$$\varepsilon_Q^{PAOR} \simeq 96.9\%; \quad (4.15)$$

$$\varepsilon_Q^{MINR} \simeq 96.3\%; \quad (4.16)$$

The figures 4.16 and 4.17 show that the gearbox efficiency is almost independent of the applied torque, decreasing very slightly with it for every oil, being the mineral oil the most affected. Still, comparing both figures, it can be concluded that the efficiency decreases with the input speed, suggesting the increase of the churning losses even though the friction losses are lower.

4.3.2. Oil samples analysis

The results obtained from the Direct Ferrometry are shown in the Table 4.3. The samples were taken after each set of trials without exchanging any of the gears of the gearbox. This way, it is expected that the wear severity decreases with each new oil set of trials since the gears have more running cycles and the roughness peaks are now accommodated. Therefore, the samples will be analysed searching for similarities with the experimental performances determined in the previous section, even though these oil samples do not have the same initial conditions.

Table 4.3.: Ferrometry analysis results

Test order	Oil sample	DL	DS	CPUC	ISUC	Sample dilution
1	MINR	38.8	12.4	512	1.40E+05	0.1
2	PAOR	17.8	5.1	229	2.90E+04	0.1
3	ESTF	20	5.8	258	3.70E+04	0.1
4	PAGD	24.2*	5*	29.2	5.60E+02	1

*- Indexes without sample dilution

Despite these results cannot be compared directly for the reason above explained, they allowed to confirm some of the efficiency conclusions withdrawn from the experimental temperatures and heat transfer analysis. The PAGD oil sample presented fewer wear particles than any other oil samples, while the mineral based oil presented the highest amount of wear particles and also the bigger ones. In fact, the PAGD results are two orders of magnitude lower than the previous oils tested confirming its good relative performance. Comparing the PAOR and ESTF based oils, the best performance is from the PAOR oil since the ESTF presented more wear particles even though its set of trials was realized after the PAOR tests. Figures 4.18 and 4.19 demonstrate these results.

4. Experimental evaluation of the transfer gearbox performance

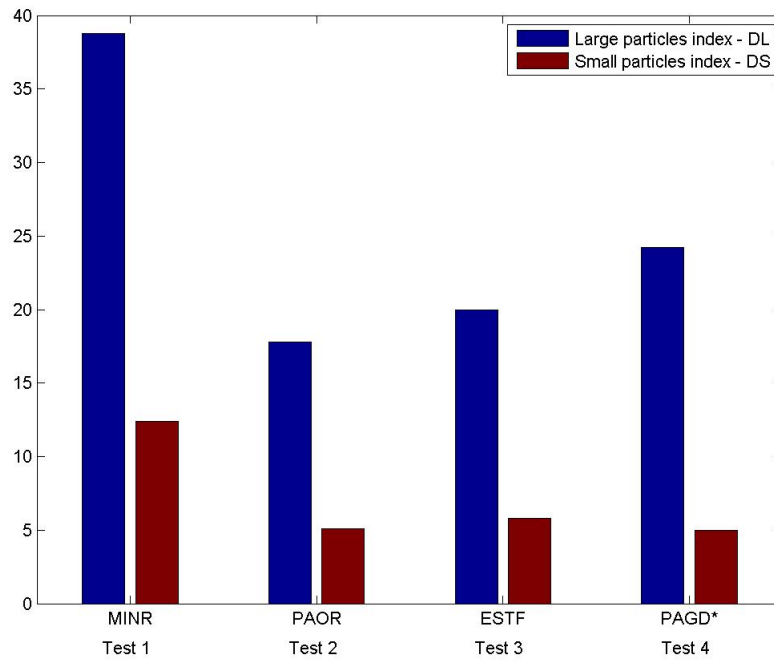


Figure 4.18.: Particles size Index for each tested oil. *- undiluted sample

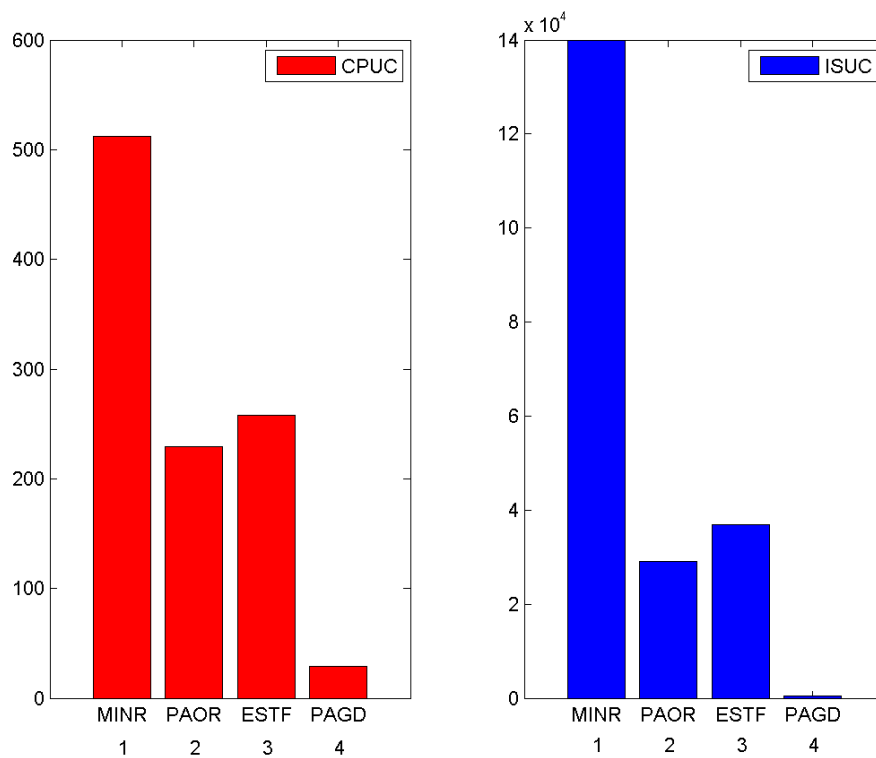


Figure 4.19.: Wear particles concentration (CPUC) and wear severity index (ISUC) for each tested oil

4.3. Relative performance of the windmill oils

Figures 4.20 to 4.23, present pictures of the ferrograms obtained by analytic Ferrography of each gear oil sample, showing once again, the relative evaluation of the lubricant performance according to the wear particles present in each sample.

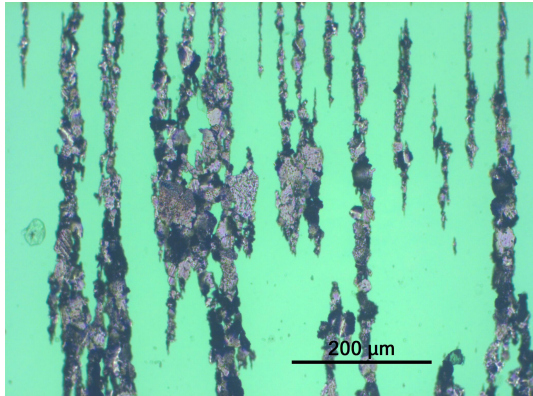


Figure 4.20.: Oil: MINR, ampliation:x200, dilution:0,1

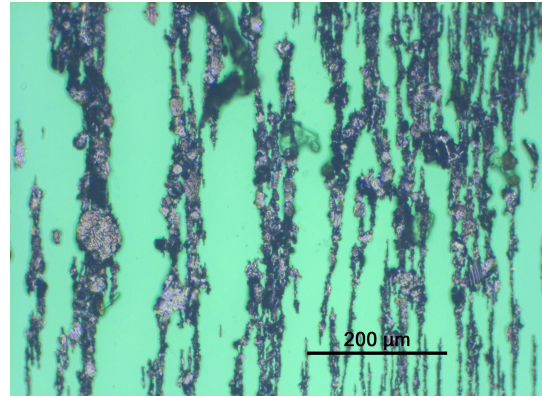


Figure 4.21.: Oil: PAOR, ampliation:x200, dilution:0,1

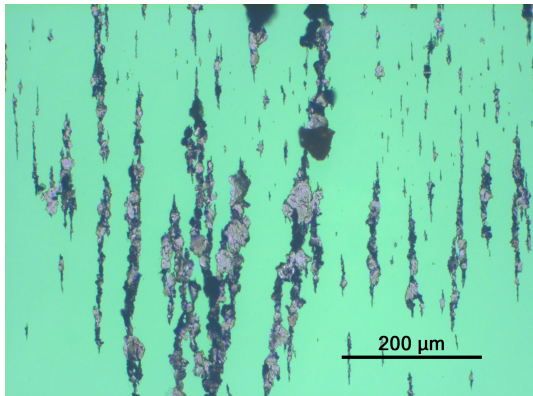


Figure 4.22.: Oil: ESTF, ampliation:x200, dilution:0,1

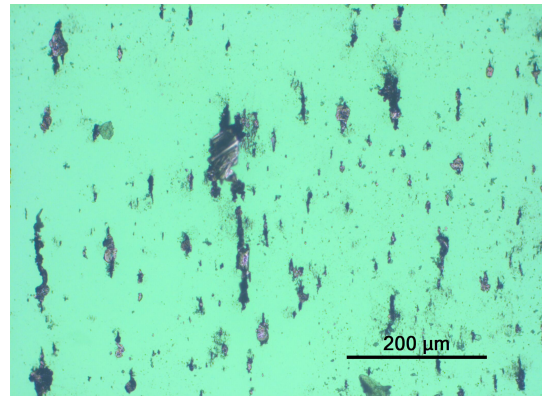


Figure 4.23.: Oil: PAGD, ampliation:x200, dilution:1

As it can be noticed, the PAGD sample (figure 4.23) presents fewer particles than any of the other oils for the same ampliation and without dilution, suggesting once again the best wear performance of this oil.

4. Experimental evaluation of the transfer gearbox performance

In a general way, all the oils presented the same type of ferrous wear particles, due to contact fatigue and combined wear. Some particles showed thermal oxidation probably resulting from re-entering the contact.

As expected from the direct ferrometry results, the MINR sample presented very large wear particles resultant from contact fatigue, some of them extremely oxidized. The PAOR, on the other hand, presented smaller wear particles which result from combined wear (both contact fatigue and sliding).

The ESTF oil sample, presented typical contact fatigue wear particles of small and medium size. The PAGD based oil sample was the one which presented the smaller wear ferrous particles also due to contact fatigue. In this last sample there were also present various friction polymers.

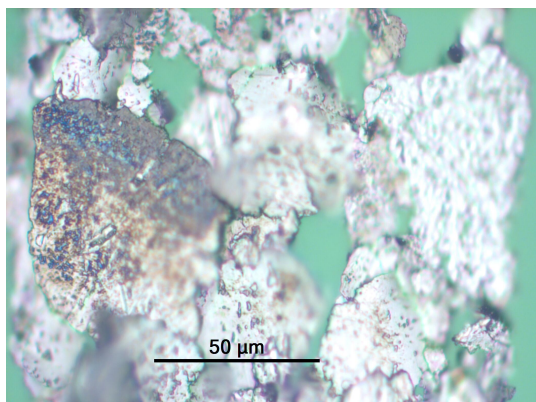


Figure 4.24.: Oil: MINR, ampliation:x1000, dilution:0,1.

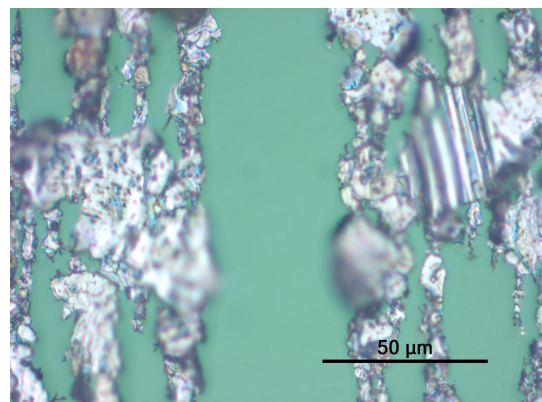


Figure 4.25.: Oil: PAOR, ampliation:x1000, dilution:0,1.

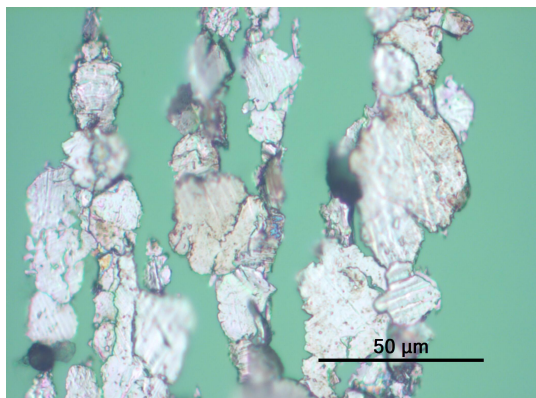


Figure 4.26.: Oil: ESTF, ampliation:x1000, dilution:0,1.

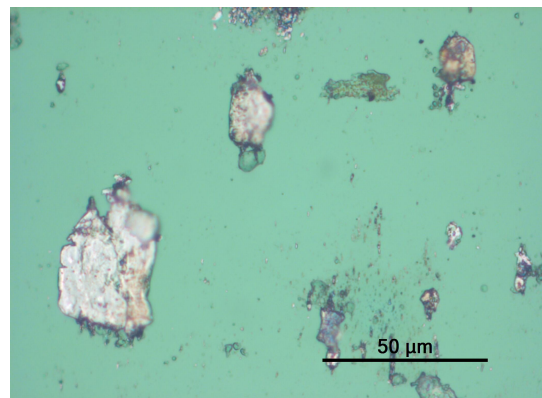


Figure 4.27.: Oil: PAGR, ampliation:x1000, dilution:1.

5. Power loss in Gearboxes

5.1. Introduction

This chapter presents the modelling and simulation of the energetic behaviour of a gearbox. The various energetic flows present inside a gearbox are analysed. These flows are classified and separated in two types: dissipated energy and energy evacuation. The first is referred to all the energy generated within the gearbox, as the energy dissipation at the teeth's contact and the gear's churning losses. On the other hand, the energy evacuation concerns the several forms of heat transfer as the radiation, convection and conduction. In the last part of this chapter the energetic behaviour of a Transfer Gearbox is simulated and the most important parameters for the correct modelling are analysed attending to the influence of the lubricant in the calculation of the coefficient of friction.

5.2. Energetic flows

5.2.1. Introduction

The maximum power that can be transferred through a mechanical transmission is limited both by the maximum load supported by the mechanical components of the gearbox and also by the maximum temperature which the lubricant can achieve. The lubricant operating temperature is defined by the thermal balance between the heat generated inside the gearbox and the heat evacuated through the gearbox case. High oil operating temperature, decreases the wear, scuffing, micropitting and pitting load capacity of the gears, as well as the lubricant service life (oxidation) [10].

There are several energetic dissipation mechanisms in a mechanical transmission. The knowledge of these mechanisms is extremely important to the mechanic systems efficiency and the power consumption. The factors which influence the energetic performance (power save) of the mechanical transmissions are the following [11]:

5. Power loss in Gearboxes

- Load dependent losses - accounting for the tooth friction power losses, which are due to the sliding of the gear tooth and to the friction coefficient between the contacting surfaces, and also for the friction between rolling bearing elements.
- No-load dependent losses - this type of power losses, also called churning power losses, are referred to the viscous friction between all mechanical rolling elements and the fluid where they are immersed. It happens for both the gears and bearings.
- Transmission ratio and its control;
- Mass and inertia of the components of the transmission.

This work will focus only in the first two factors even though the large importance of the others to the gearbox manufacturing.

The gear friction power losses and the churning losses are the most significant forms of dissipation in which the lubricant has an important role. In the load dependent power losses the lubricant is very important since it defines the friction coefficient which depends on the Elastohydrodynamic regime of lubrication present in the contact:

- **Full film lubrication:** refers to a total separation of surfaces by a lubricant film thickness ($\Lambda > 2$);
- **Mixed film lubrication:** refers to a partial film thickness, where part of the load is carried by the fluid and some of it is carried by the gear surface roughness peaks ($0.7 < \Lambda < 2$);
- **Boundary film lubrication:** refers to the most severe mixed lubrication situation, where there is almost no lubricant film between the surfaces and the metal-metal surface contact occurs ($\Lambda < 0.7$). The normal load is supported by the roughness tips.

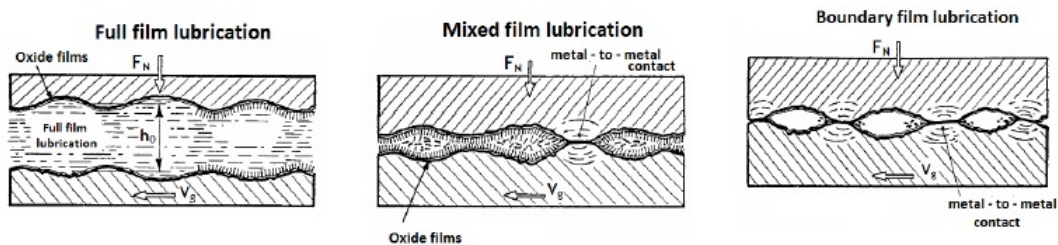


Figure 5.1.: Elasto-Hydrodynamic regimes of lubrication

5.2.2. Energy dissipation mechanisms

5.2.2.1. Load dependent power loss

- Gear mesh power loss

The gear meshing power loss only depends of the transmitted power, the geometry factor \mathbf{H}_v and the mean value of the friction coefficient along the meshing line μ_{mz} . Höhn et al. [10], propose the following equation 5.1 for the friction power loss:

$$P_{fr} = P_{in} \cdot \mu_{mz} \cdot H_v \quad (5.1)$$

where \mathbf{H}_v is given by equation 5.2.

$$H_v = \frac{\pi \cdot (u + 1)}{z_1 \cdot u \cdot \cos \beta_b} [1 - \varepsilon_\alpha + (\varepsilon_1)^2 + (\varepsilon_2)^2] \quad (5.2)$$

Friction between gear teeth is very important since it will define the heat generation. The coefficient of friction μ is defined as the relation between the normal load (F_N) and the tangential load (F_T):

$$\mu = \frac{F_T}{F_N} \quad (5.3)$$

Höhn et al. [10] suggest the following expression for the mean friction coefficient along the meshing line, which results from several trials performed in disc machines and FZG test rigs:

$$\mu_{mz} = 0.048 \cdot \left(\frac{F_{bt}}{l_{min}} \right)^{0.2} \cdot (\eta_{oil})^{-0.05} \cdot (R_a)^{0.25} \cdot X_L \quad (5.4)$$

where F_{bt} represents the normal force at teeth in the transversal section, l_{min} represents the average meshing line length for helical gears and R_a is set as the composite roughness of gears tooth flanks, given by [12]:

$$R_a = 3.8 \cdot \sqrt[4]{0.5 \cdot (\sigma_1 + \sigma_2)} \quad (5.5)$$

5. Power loss in Gearboxes

On the other hand, \mathbf{X}_L represents a lubricant dependent factor [10, 13], which can be optimized for each lubricant, correlating the model to the experimental results:

$$X_L = \frac{a}{(var_1)^{b1} \dots (var_n)^{bn}} \quad (5.6)$$

As said, the coefficient of friction is related to the specific lubricant film thickness and this relation is usually represented by the Stribeck curve (figure 5.2):

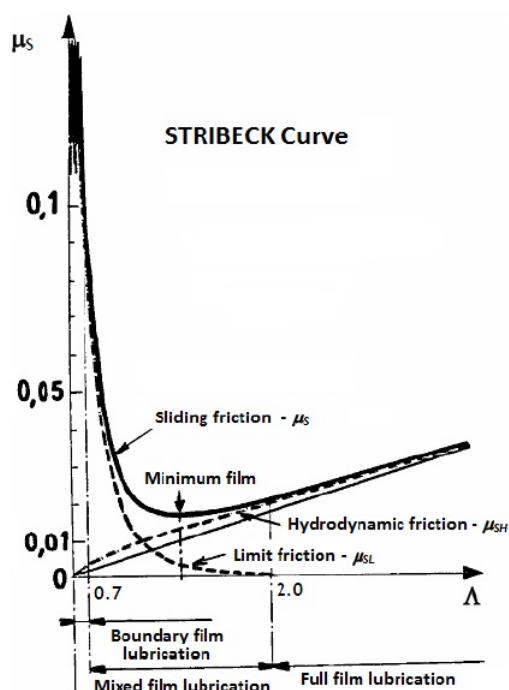


Figure 5.2.: Stribeck curve.

- Friction power loss in the rolling bearings

The load dependent power loss in rolling bearings is dependent of the speed, the load on the bearing, the friction coefficient (μ_1) and the type and dimensions of the bearing:

$$P_{M1} = \mu_1 \cdot f_1 \cdot F \cdot \frac{d_m}{2} \cdot \frac{\pi}{30} \quad (5.7)$$

The values μ_1 and f_1 are related to each rolling bearing, and are obtained from

the manufacturers catalogues. On the other hand, \mathbf{F} represents the load applied on the rolling bearing, given by the equation 5.8.

$$F = \sqrt{F_a^2 + F_r^2} \quad (5.8)$$

In the equation 5.8, \mathbf{F}_a represents the axial load while \mathbf{F}_r , represents the radial load on the bearing.

5.2.2.2. No-Load dependent power loss

- Shafts and Gears churning power loss

The friction resulting from the contact of a moving object partially immersed within a fluid is called churning. In a gearbox we have both churning from gears and shafts within the oil, the air or within the mixture air/oil and also from the churning effect that occurs at the entrance of the contact between gear tooth. The parameters which influence the power loss by churning are the gears geometry, speed, the immersion depth and the gear wet surface as well as the oil viscosity and density at the work temperature. The inner configuration of the gearbox case has also a major influence. According to Changenet et al. [14–16], these gear power losses from churning result in the expression:

$$P_{spl} = \frac{\rho A}{2} \cdot \left(\frac{\pi \cdot n}{30}\right)^3 \cdot \left(\frac{d}{2}\right)^3 \cdot \left(\frac{2 \cdot h}{d}\right)^{0.45} \cdot \left(\frac{V_{oil}}{d}\right)^{0.1} \cdot (F_R)^{-0.6} \cdot (Re)^{-0.21} \quad (5.9)$$

where ρ designates the oil density, \mathbf{A} represents each wheel submersed area, \mathbf{V}_{oil} the oil volume, \mathbf{h} the wheel immersed length and \mathbf{d} is referred to the pitch diameter of each wheel. The Froude and Reynolds numbers are calculated through the expressions 5.10 and 5.11.

$$F_R = \left(\frac{n\pi}{30} \cdot \frac{d}{2}\right)^2 (g \cdot \pi d)^{-1} \quad (5.10)$$

$$Re = \frac{n \cdot \pi}{30} \cdot \left(\frac{d}{2}\right)^2 \cdot (\nu \cdot 10^{-6})^{-1} \quad (5.11)$$

5. Power loss in Gearboxes

The dragging effect that occurs due to the shafts rotation and its associated power loss can be evaluated by the same procedure used for the churning power loss of gears.

- Seals power loss

Again according to Höhn et al. [10], the power loss at the seals can be estimated through the expression:

$$P_{sl} = 7.69 \cdot 10^{-6} \cdot d_s^2 \cdot n \quad (5.12)$$

These power losses are usually very low, especially at low speeds, which is the case. Therefore, these power losses will not be considered in the model.

- No-load dependent power loss in rolling bearings

This kind of power loss depends on the speed, on the type of lubricant and its viscosity at work temperature and also on the rolling bearing dimensions and constructive type. This type of power loss are calculated according to the following expression [14,17]:

$$P_{M0} = f_0 \cdot 10^{-7} \cdot (\nu \cdot n)^{\frac{2}{3}} \cdot d_m^3 \cdot \frac{\pi \cdot n}{30} \quad (5.13)$$

5.2.3. Heat transfer mechanisms

In the general gearboxes, lubricated by churning in oil bath, the primary mechanisms of heat transfer to the surrounding environment are the convection and radiation through the gearbox case surface. There is also a small fraction of heat evacuated by conduction through the shafts and couplings but not usually accounted for.

The determination of the heat flows by convection and also radiation requires the knowledge of the gearbox case temperature. Winter et al. [12], have done measurements of the temperature distribution of the oil case and found that the maximum variation was smaller than 5°K, so the oil case mean temperature can be used without significant error.

5.2.3.1. Radiation

According to the Stefan Boltzman Law, the radiation heat flow can be calculated using the expression 5.14, [12].

$$Q_{rad} = \alpha_{rad} \cdot (\theta_w - \theta_\infty) \cdot A_{rad} \quad (5.14)$$

The radiation coefficient α_{rad} is determined according to the expression 5.15.

$$\alpha_{rad} = 0.23 \cdot 10^{-6} \cdot \varepsilon \cdot \left(\frac{\theta_w + \theta_\infty}{2} \right)^3 \quad (5.15)$$

Where θ_w represents the oil case mean temperature and θ_∞ the test rig room temperature.

5.2.3.2. Convection

There are two forms of convection:

- Natural;
- Forced.

However, the pure natural convection never occurs alone once there is always some forced convection. This forced air flow comes generally from refrigeration fans

5. Power loss in Gearboxes

and the convection heat flow can be determined according to expression 5.16, combining the forced and natural convection coefficients:

$$Q_{ncv} = \alpha_{cv} \cdot (\theta_w - \theta_\infty) \cdot A_{cv} \quad (5.16)$$

5.2.3.3. Conduction

Although this form of heat transfer might be of smaller importance, has to be taken into account for a rigorous calculation. However, to simplify the calculations involved in the determination of the equipment temperature coupled with the gearbox and its evolution, the evacuated heat flow in stationary regime can be defined by:

$$Q_{cn} = \alpha_{cn} \cdot A_{cn} \cdot \left(\frac{\theta_w - \theta_m}{t} \right) \quad (5.17)$$

Where θ_w represents the gearbox case temperature, θ_m the gearbox case base temperature and t the thickness between the points at the given temperatures.

5.2.4. Energy balance

The thermal equilibrium of a gearbox is reached when the operating temperature stabilizes, i.e. when the power dissipated inside the gearbox is equal to the heat evacuated from the gearbox to the surrounding environment. The highest the equilibrium temperature, the higher will be the power losses, resulting in lower efficiency, higher oil oxidation and shorter oil life [13]. The equation of thermal balance is represented by the equation 5.18.

$$P_{fr} + P_{spl} + P_{sl} + P_{M1} + P_{M0} = Q_{rad} + Q_{ncv} + Q_{cn} \quad (5.18)$$

The sum of the heat flows can also be simplified, considering a coefficient which represents the three forms of heat transfer, as it is shown below:

$$Q_{rad} + Q_{ncv} + Q_{cn} = Q_{total} = \alpha \cdot A_t \cdot (T_w - T_\infty) \quad (5.19)$$

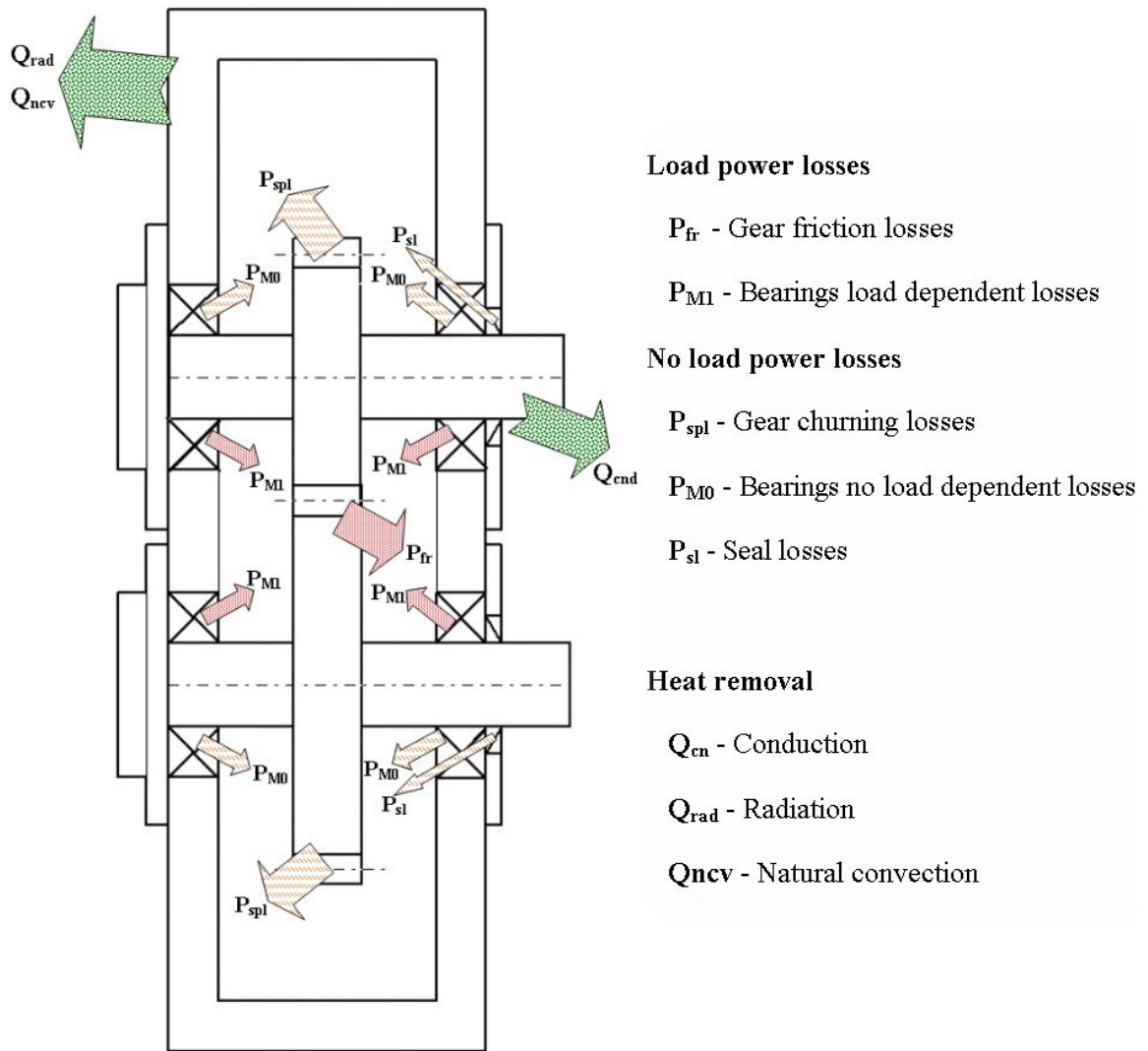


Figure 5.3.: Power losses and heat removal diagram example for a FZG gearbox.

5.3. Transfer Gearbox Modelling

The simulation model was realized using the Software MATLAB[®]. This analytic model pretends to simulate the different oil, speed and torque conditions used in the laboratory tests. It is also verified the agreement between the experimental and numerical results.

The total power loss was obtained by adding all the singular component's power losses previously described. The analytic model created has some limitations since it only describes the specific transfer gearbox used and does not account for the following factors:

- Multiplier gears instead of reducer;
- The influence of gears sense of rotation to the oil flow;
- The influence of each rolling component in the churning power losses of the other components;
- The influence of gearbox case shape and housings on the churning losses.

The theories presented in the previous section result from several experimental tests performed in FZG and disc test machines. However, any gearbox with more than one gear is much more complex since it introduces more intervening components. In fact, the transfer gearbox tested has at least fifteen active bearings while three gears are running, two of them loaded, which makes it very different from the FZG tests. Furthermore, the trials here performed were realized at very high torques and very low speeds which leads us close to boundary friction conditions where some of the models can not be applied. The oil bath temperature was free, ie, the oil bath temperature was not controlled or fixed which also differs from some of the tests to which the equations were established. Therefore, and since the friction and churning theories presented in the previous section were implemented considering only the singular power loss of each component, it was necessary to rearrange some coefficients in order to better correlate the results.

Figures 5.4 to 5.7 demonstrate how the model behaves before the coefficients were optimized. The first three data points are referred to the trials at 135rpm while the last three are referred to the trials at 235rpm. The numbers over the data points represent the percentage of error between the numerical and experimental results (respectively, the blue and red curves).

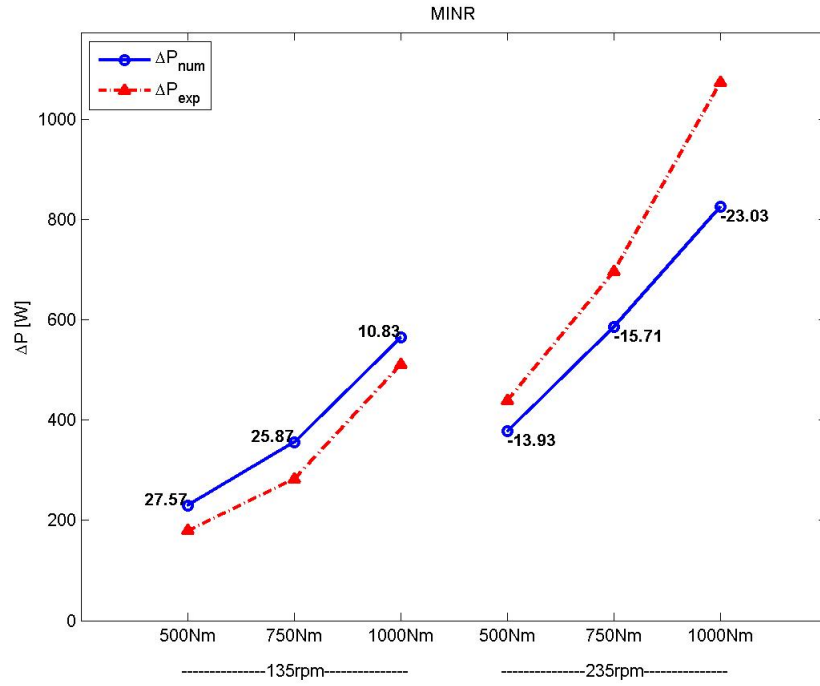


Figure 5.4.: Model behaviour for the MINR oil, without coefficients optimization.

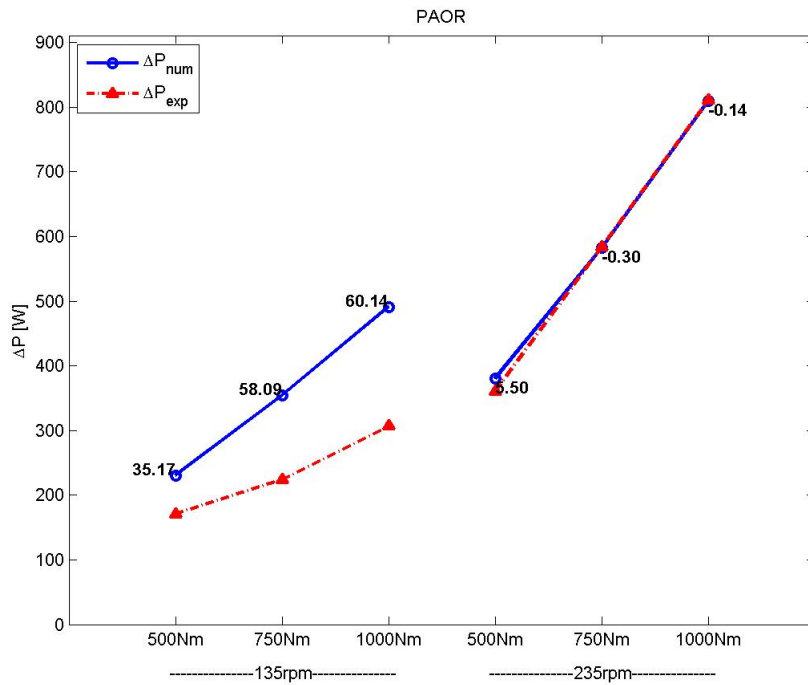


Figure 5.5.: Model behaviour for the PAOR oil, without coefficients optimization.

5. Power loss in Gearboxes

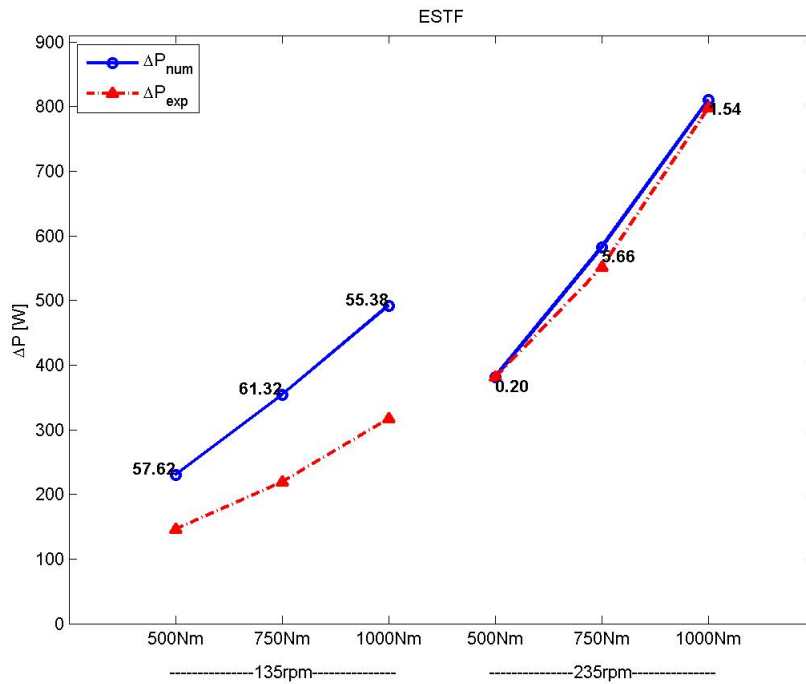


Figure 5.6.: Model behaviour for the ESTF oil, without coefficients optimization.

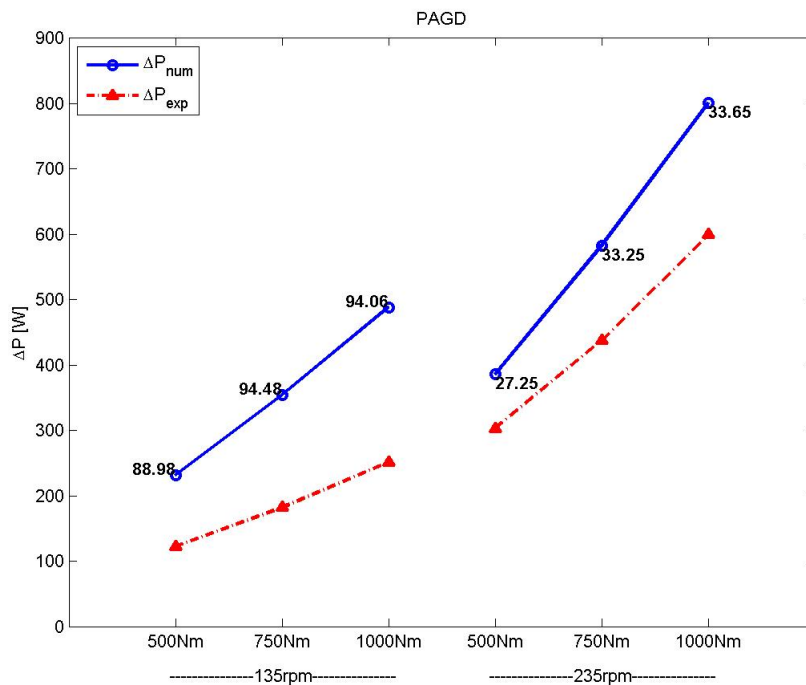


Figure 5.7.: Model behaviour for the PAGD oil, without coefficients optimization.

From the previous figures, it can be concluded that the model approximates better the results for the 235rpm tests than those at 135rpm. This comes to confirm, as expected, that the models used were developed for higher speeds, with coefficient of friction far from the boundary friction. Another conclusion that can be withdrawn is that the correlation for the Mineral based oil (MINR) presents an overall error smaller than those for the synthetic oils, which is predicted by Höhn et al. [10] when they defined the X_L factor to be equal to one for non aditivated mineral based oils.

5.3.1. Friction coefficient optimization for gears and rolling bearings

5.3.1.1. Optimization considering single load dependent coefficient

For the first iteration process three coefficients were defined, that should be optimized, correlating numerical and experimental values. The lubricant factor \mathbf{X}_L from equation (5.6) was defined as function of a_1 , b_1 and b_2 as displayed in equation 5.20. A speed coefficient will not be considered at this time since the difference between the two speed levels of the tests is not very large.

$$X_{L1} = a_1 \cdot \left(\frac{F_{bt}}{l_{min}} \right)^{-b_1} \cdot (\eta_{oil})^{b_2} \quad (5.20)$$

The average friction coefficient μ_{mz} of the gears is now given by equation 5.21.

$$\mu_{mz} = \mathbf{a}_1 \cdot 0.048 \cdot \frac{\left(\frac{F_{bt}}{l_{min}} \right)^{0.2-b_1}}{\rho_c^{0.2} \cdot (\nu_{\Sigma c})^{0.2}} \cdot (\eta_{oil})^{b_2-0.05} \cdot (R_a)^{0.25} \quad (5.21)$$

Accompanying this change, the bearings friction coefficient was also amended to match the alteration produced by the X_L in the average coefficient of friction of the gears (5.21). Therefore the rolling bearings friction power losses are dependent of the coefficient a_2 , as represented in equation 5.22.

$$P_{rf} = \mathbf{a}_2 \cdot \mu_1 \cdot f_1 \cdot F \cdot \frac{d_m}{2} \cdot \frac{\pi}{30} \quad (5.22)$$

In order to obtain the best numeric and simultaneously physical optimized solution, it was used the non-linear least squares method from the built-in MATLAB[®] toolbox. The function to optimize was defined as sum of the relative error between the

5. Power loss in Gearboxes

numeric determined power losses and those obtained from the heat transfer analysis of the experimental results, as displayed in equation 5.23.

$$func = \sum_1^6 \frac{\Delta P_{num} - \Delta P_{exp}}{\Delta P_{exp}} \quad (5.23)$$

The optimized coefficient values are presented in the following table 5.1:

Table 5.1.: Optimized coefficients.

Oil reference	a ₁	b ₁	b ₂	a ₂
MINR	≈ 1	0.0039	≈ 0	0.98
PAOR	≈ 1	0.05	≈ 0	0.76
ESTF	≈ 1	0.06	≈ 0	0.74
PAGD	≈ 1	0.10	≈ 0	0.56

Figures 5.8, 5.9, 5.10 and 5.11 display the comparison between the numerical and experimental results for this first optimization approach. These results show a much better correlation between the experimental and numerical results, while the model behaviour is now very similar to every oil. However, there is still a very different behaviour between the results at different speeds. The model seems to approach the experimental curves by excess at 135rpm and by default at higher speed (235rpm). This seems to confirm what was mentioned previously that the speed might present a different influence to the friction coefficient at low speeds, than it was predicted by the model used. In fact, at the speed of 135rpm each gear has a tangential speed under 1m/s. This might indicate that the tests were performed very close to boundary friction, i.e., to the very left of the Stribeck curve (figure 5.2) where the model should not be applied, because it was not developed for these operating conditions.

During this optimization process has also become evident that the viscosity coefficient **b**₂ always leaned to the initial iteration value of zero, showing that the optimization process was not dependent on the oil viscosity.

Although the correlation has improved, the overall error is still quite large ($\varepsilon \simeq 25\%$). Therefore, a new approach was sought in the next section.

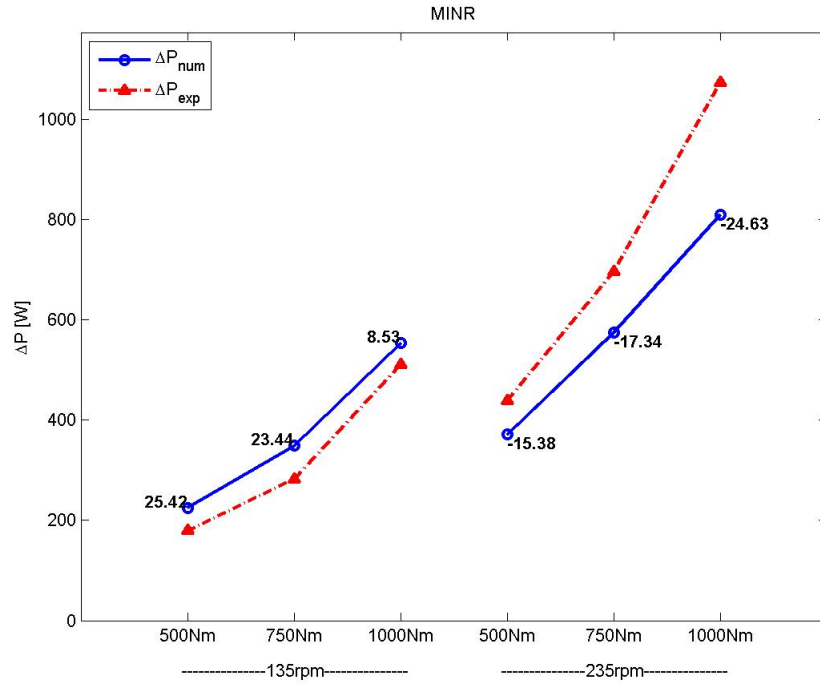


Figure 5.8.: Model optimized for the MINR oil (Lubricant factor X_{L1}).

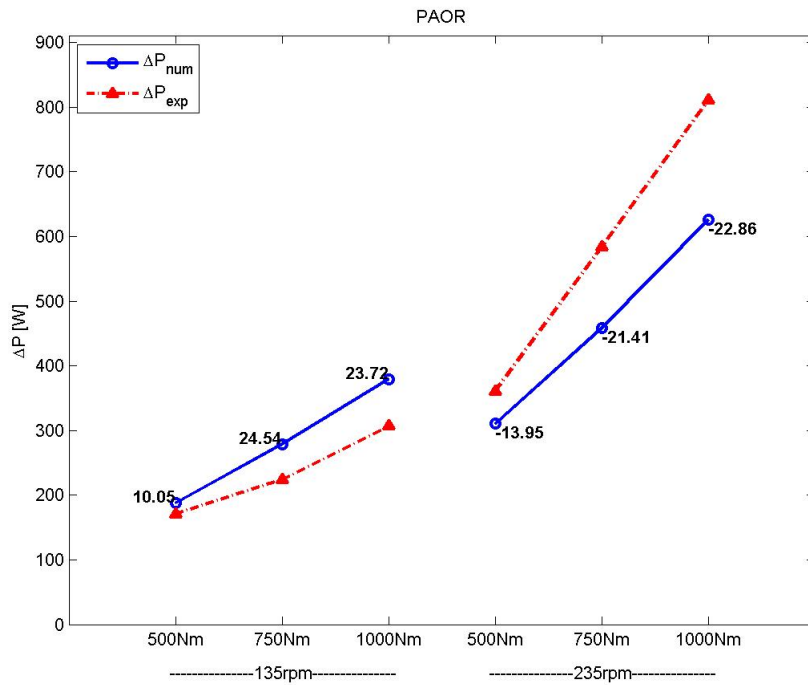


Figure 5.9.: Model optimized for the PAOR oil (Lubricant factor X_{L1}).

5. Power loss in Gearboxes

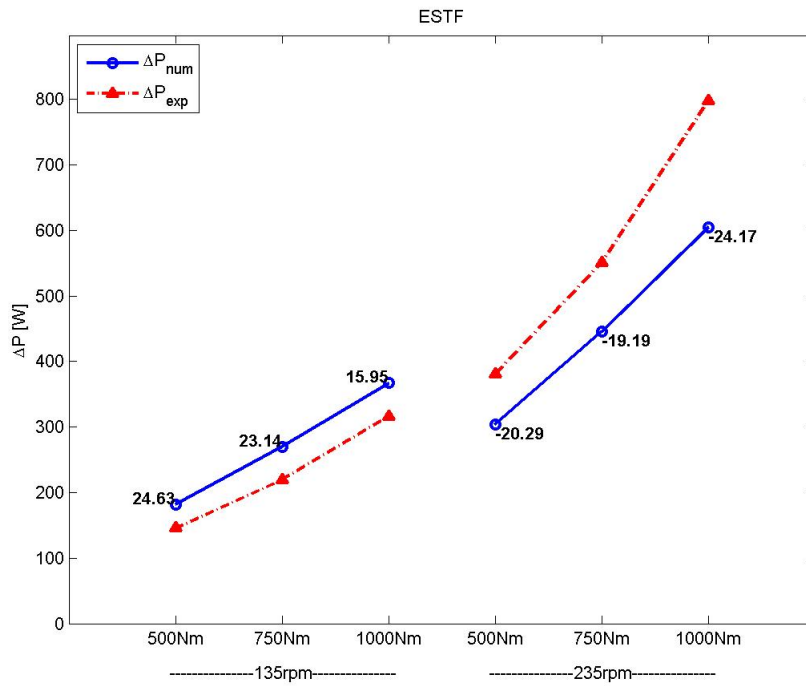


Figure 5.10.: Model optimized for the ESTF oil (Lubricant factor X_{L1}).

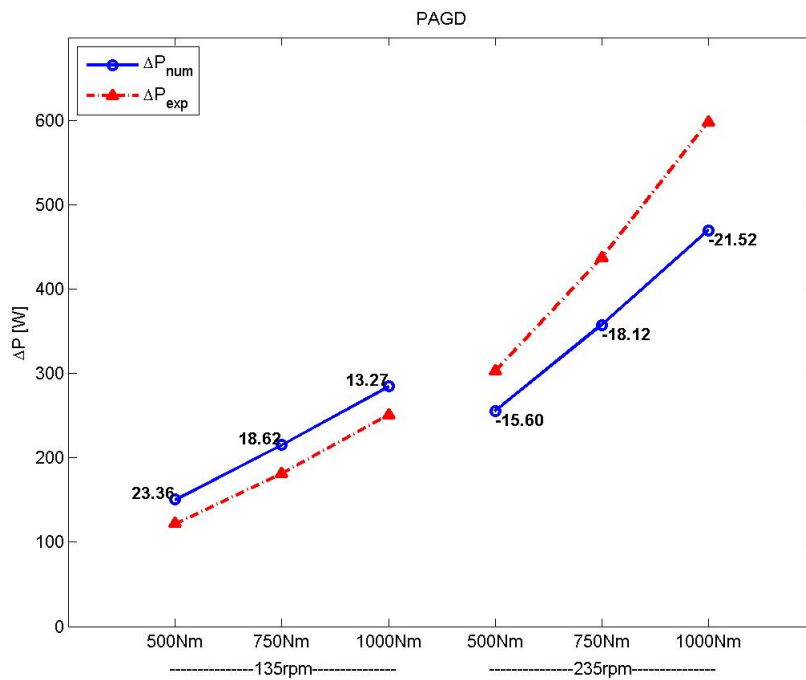


Figure 5.11.: Model optimized for the PAGD oil (Lubricant factor X_{L1}).

The lubricant film thickness was also calculated in order to verify if the test conditions were in fact near to boundary film lubrication and boundary friction. The Dowson's expression [18] for the centre film thickness was used, given by equation 5.24.

$$h_0 = 0.975 \cdot R_{eq} \cdot U^{0.727} \cdot G^{0.727} \cdot W^{-0.091} \quad (5.24)$$

The factors **U**, **G** and **W** represent the speed, material and load influence and are defined in equations 5.25, 5.26 and 5.27, respectively.

$$U = \eta_{oil} \cdot \frac{U_1 + U_2}{2 \cdot R_{eq} \cdot E^*} \quad (5.25)$$

$$G = 2 \cdot \alpha_{piezo} \cdot E^* \quad (5.26)$$

$$W = \frac{F_{bt}/l_{min}}{R_{eq} \cdot E^*} \quad (5.27)$$

where the R_{eq} parameter stands for the equivalent radius of curvature, U_i represents the tangential speed of each gear and E^* represents the equivalent Young Modulus, calculated according to equation 5.28.

$$E^* = \frac{1}{\left(\frac{1-\nu_1^2}{E_1} + \frac{1-\nu_2^2}{E_2}\right)} \quad (5.28)$$

The results of the film thickness calculation for the most loaded gear (z1-z2, see figure 4.1), operating with each oil tested, are displayed in figure 5.12.

The specific film thickness, given by the equation 5.29, was also determined:

$$\Delta = \frac{h_0}{\sqrt{(\sigma_1)^2 + (\sigma_2)^2}} \quad (5.29)$$

In the equation 5.29, σ_1 and σ_2 represent the tooth roughness of each individual pinion and wheel.

5. Power loss in Gearboxes

The calculated specific film thickness is represented in the figure 5.13. All the values are very low, within the range $[0.07 - 0.32]$, showing as expected, that the tests were performed within the boundary lubrication regime ($\Lambda < 0.7$).

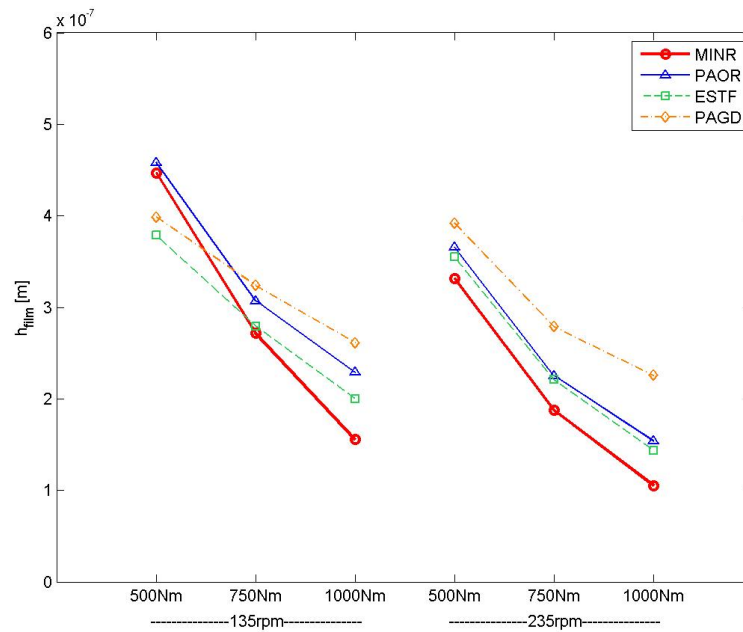


Figure 5.12.: Lubricant film thickness.

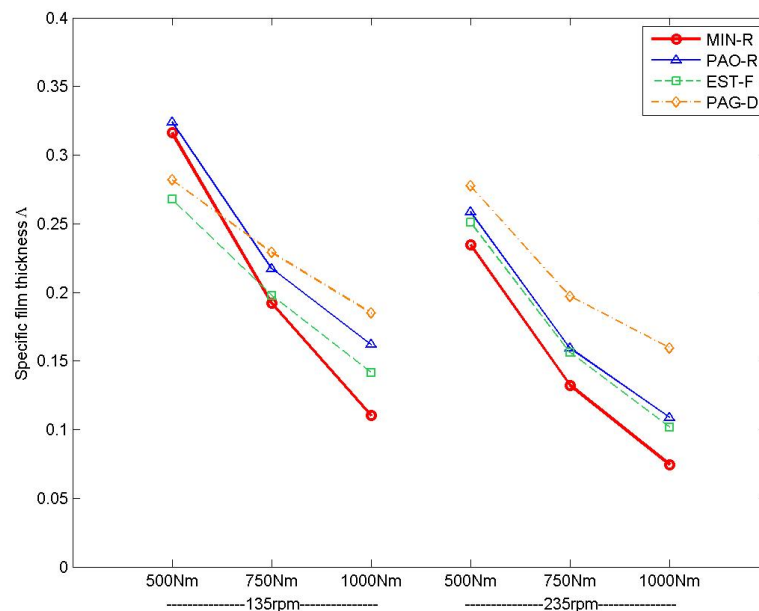


Figure 5.13.: Specific Lubricant film thickness.

This also seems to be indicated by the calculated gear friction coefficient without any optimized coefficient ($X_L = 1$), which is very high. In fact, not only is high as it is very similar for all the oils - figure 5.14.

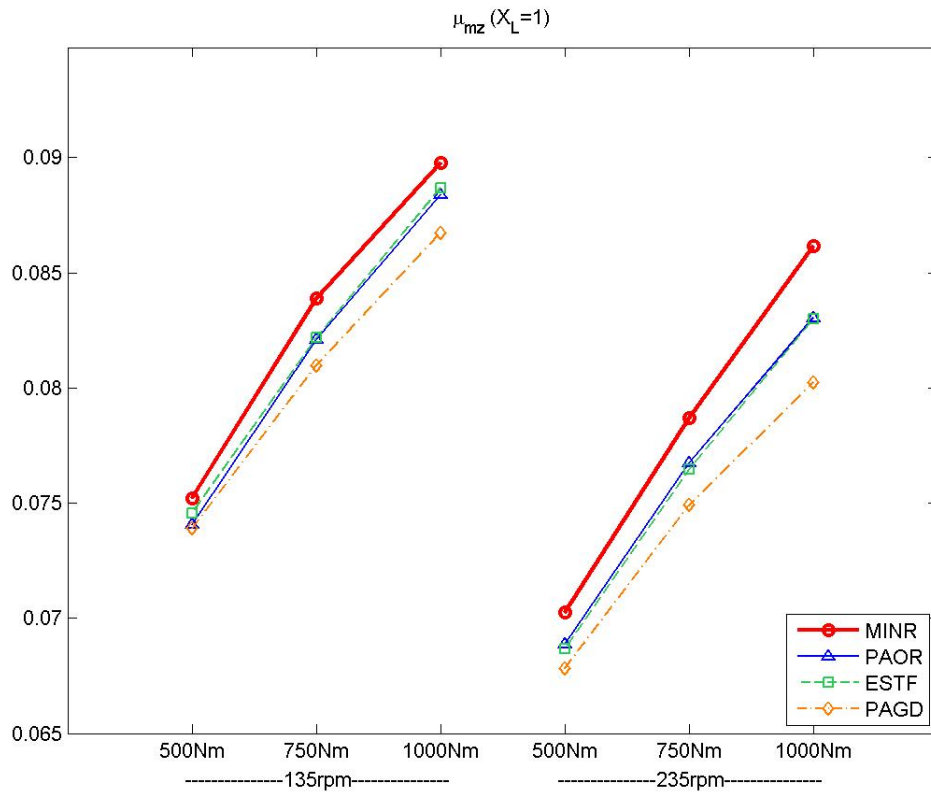


Figure 5.14.: Mean coefficient of friction between gear teeth, along the meshing line.

5. Power loss in Gearboxes

These results might be compared with those obtained using the software KissSoft®. Although the calculation method is different, the results seem to be very close (see figures from 5.15 to 5.18). Even so, both approaches for the friction coefficient do not explain the large differences between each oil, obtained for the experimental results.

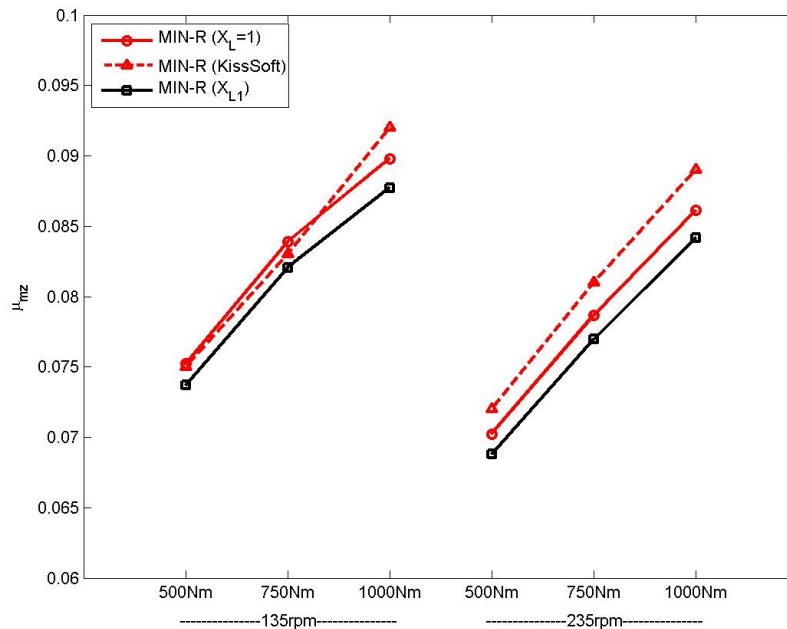


Figure 5.15.: Coefficient of friction comparison for MIN-R oil.

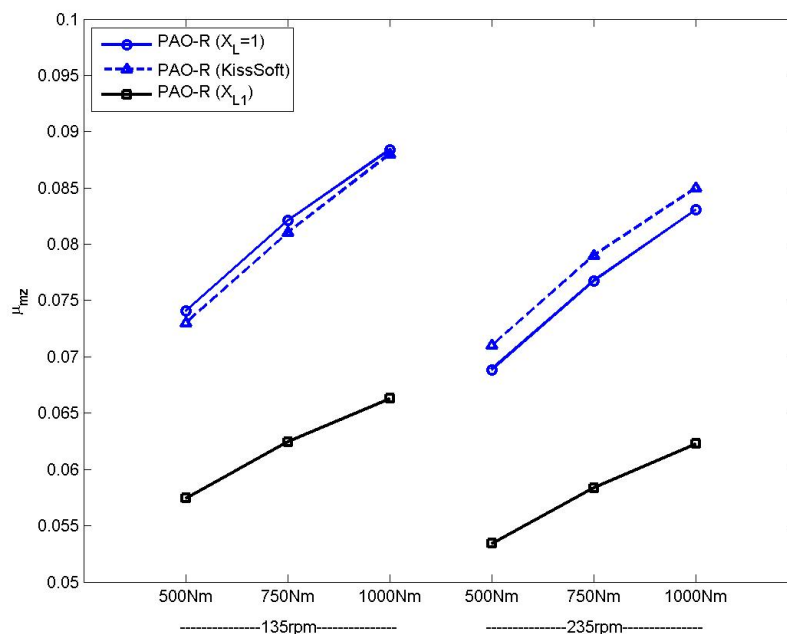


Figure 5.16.: Coefficient of friction comparison for PAO-R oil.

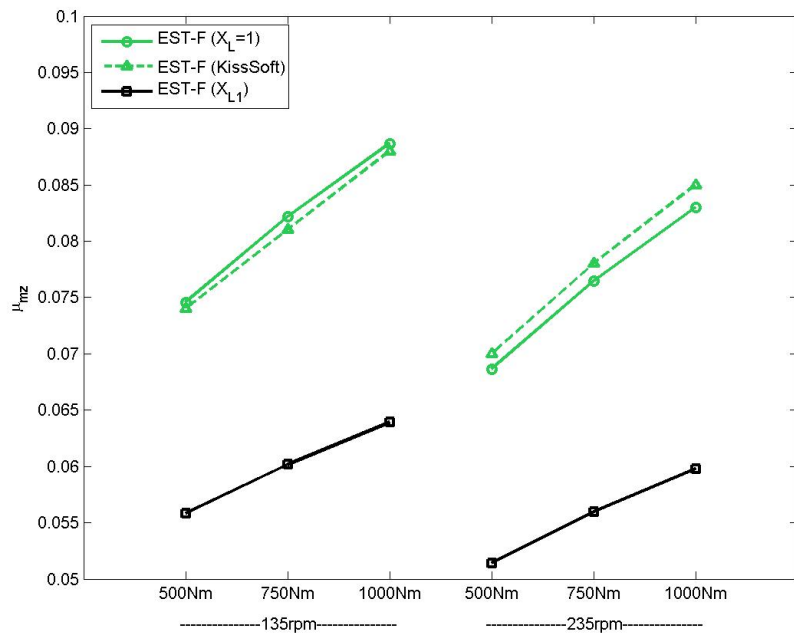


Figure 5.17.: Coefficient of friction comparison for EST-F oil.

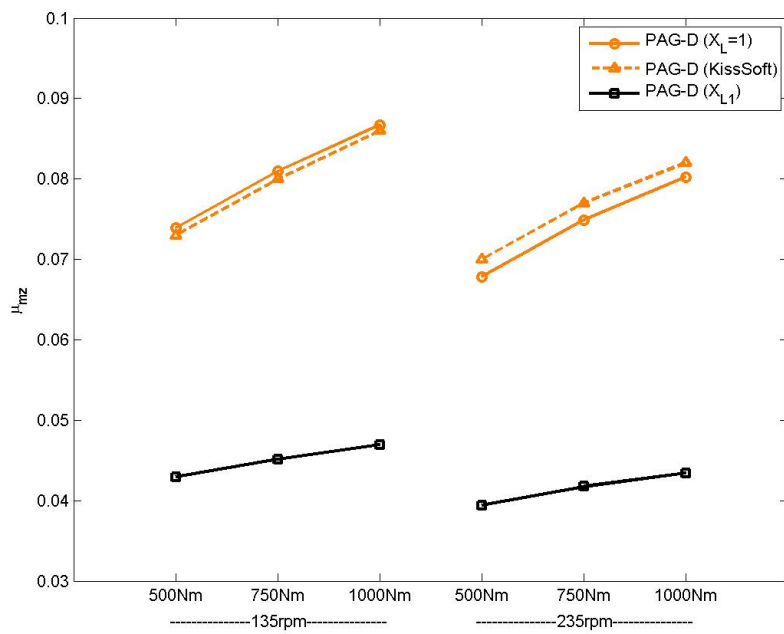


Figure 5.18.: Coefficient of friction comparison for PAG-D oil.

5.3.1.2. Optimization considering both load and speed dependent coefficients

This new optimization process intends to decrease the friction coefficient at 135rpm while increasing it to 235rpm, in an effort of better correlate the results, optimizing them for each tested oil. Although the speed difference between 135 and 235rpm is not very large, it seems to be conditioning the optimization results. Given the tests proximity to the boundary friction and since the speed proved to have a major influence in the coefficient of friction, the load factor X_L was modified to take into account the influence of speed. Therefore, the new X_L factor is given by the equation 5.30, where the optimization coefficients are again a_1 , b_1 and b_2 .

$$X_{L2} = a_1 \cdot \frac{\left(\frac{F_{bt}}{l_{min}}\right)^{-b_1}}{(\nu_{\Sigma c})^{-b_2}} \quad (5.30)$$

The average friction coefficient μ_{mz} of the gears is now given by equation 5.31. The power loss model of the rolling bearings was kept the same (equation 5.22).

$$\mu_{mz} = \mathbf{a}_1 \cdot 0.048 \cdot \frac{\left(\frac{F_{bt}}{l_{min}}\right)^{0.2-b_1}}{\rho_c^{0.2} \cdot (\nu_{\Sigma c})^{0.2-b_2}} \cdot (\eta_{oil})^{-0.05} \cdot (R_a)^{0.25} \quad (5.31)$$

Accompanying this modification, the optimization function was now defined only as the relative error between the numeric obtained power losses and those obtained from the heat transfer analysis of the experimental results, as displayed in equation 5.32.

$$func = \frac{\Delta P_{num} - \Delta P_{exp}}{\Delta P_{exp}} \quad (5.32)$$

Initially, it was imposed a limit range considered acceptable to each coefficient, so the optimization process would reach faster a solution. However, this also proved not to be the ideal approach since the speed coefficient b_2 was always tending towards the upper range limit. The next step was to set free all the coefficients, not imposing any condition to their evolution in the optimization process.

The coefficients were then optimized by the same non-linear least squares method, leading to a quite good correlation. The results are presented in the table 5.2.

Table 5.2.: Optimized coefficients.

Oil reference	a1	b1	b2	a2
MINR	0.47	-0.14	0.95	$\simeq 1$
PAOR	0.98	0.04	0.93	0.75
ESTF	0.59	-0.05	$\simeq 1$	0.74
PAGD	0.46	-0.05	0.92	0.57

Figures 5.19, 5.20, 5.21 and 5.22 show the comparison between the numerical and experimental results for this second iteration optimization approach.

This second optimization lead to a very good numerical solution, with significantly lower overall error. However, although this could be an interesting approach to the speed dependency on the friction coefficient, a conclusion from this numerical solution can not be withdrawn completely since there were only tested two speed levels, which might not be sufficient to allow the definition of a new friction coefficient law valid at low speeds and very low specific lubricant film thickness. Furthermore, the oil bath temperature was free, allowing the increase of speed to increase the oil temperature and therefore, to decrease the oil viscosity which makes it even harder to understand the effect of speed. This clearly states that a more complex behaviour is happening in the tests than the one described within this model. Therefore, also a more complex model should be implemented in following works and a larger number of speed values should be tested.

5. Power loss in Gearboxes

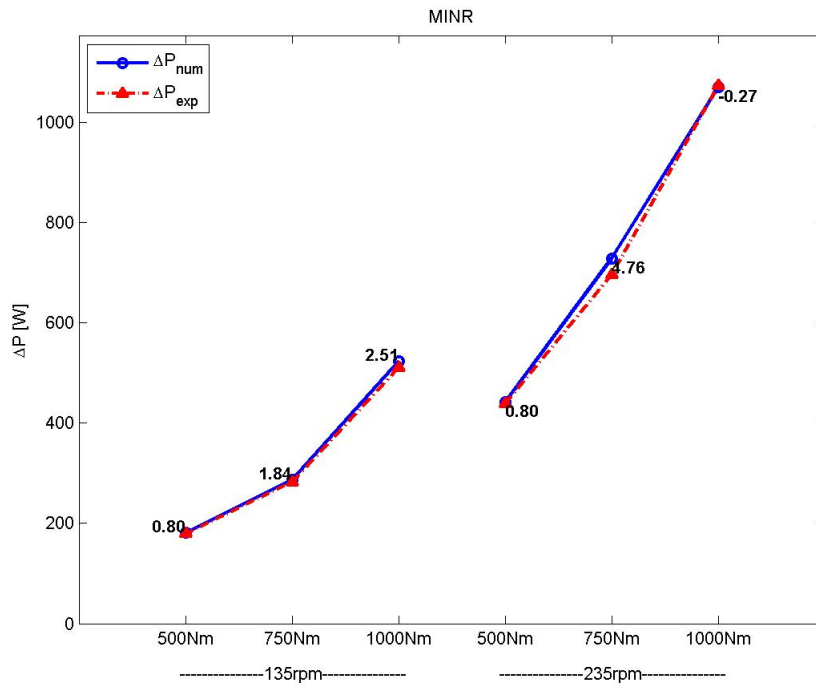


Figure 5.19.: Model optimized for the MINR oil (Lubricant factor X_{L2}).

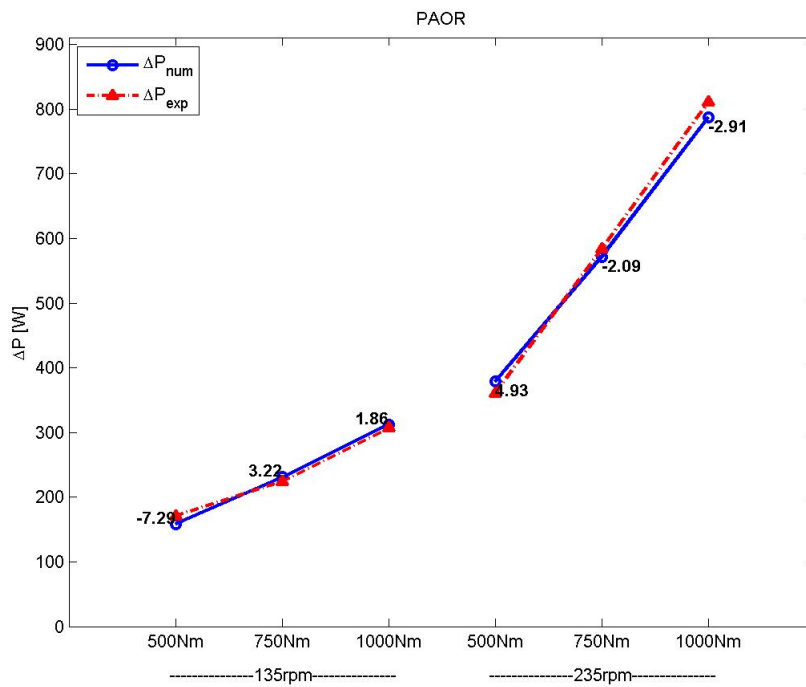


Figure 5.20.: Model optimized for the PAOR oil (Lubricant factor X_{L2}).

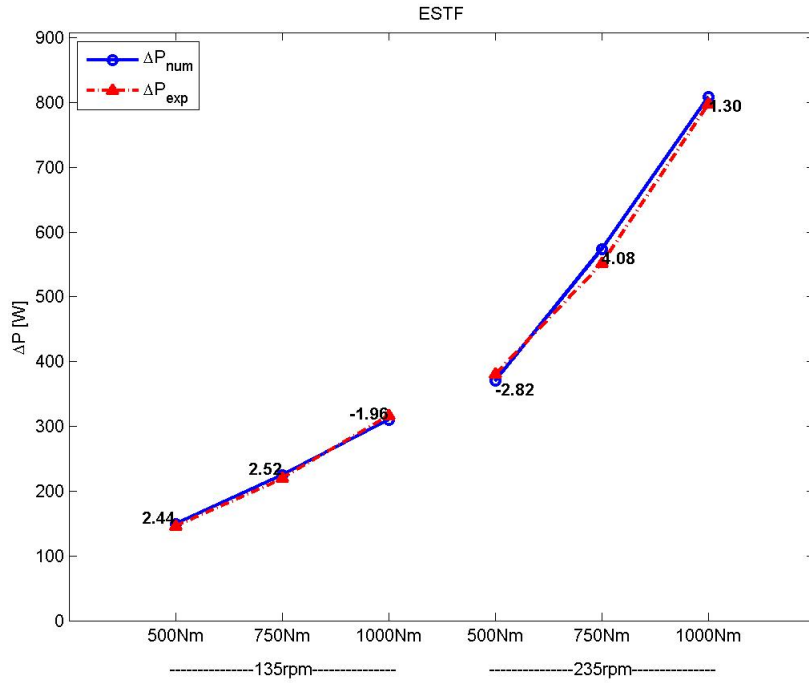


Figure 5.21.: Model optimized for the ESTF oil (Lubricant factor X_{L2}).

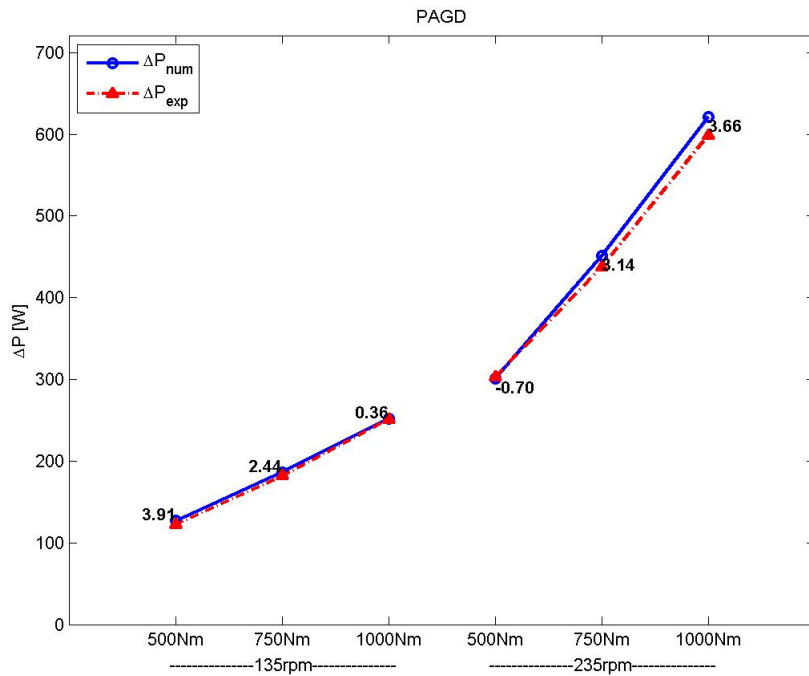


Figure 5.22.: Model optimized for the PAGD oil (Lubricant factor X_{L2}).

5.3.2. Optimized model

This last optimization gives place to the new values of the coefficient of friction between gear teeth. It's now clear the difference between oils and the way they influence the coefficient of friction. In the table 5.3 are shown the average reductions of this coefficient for the last optimization process, when compared to the non-optimized values (see figure 5.14).

The figure 5.23 shows the new coefficient of friction for each oil. It can be observed that the friction coefficient not only increases significantly with the load, as expected, but it also increases with the speed. The increase of friction coefficient with speed contradicts the initial model used, although the operating conditions are in the zone of boundary film lubrication. Once, with the increase of speed, the temperature rises and the viscosity decreases and it seems correct to consider that the friction coefficient will also rise because the contact becomes more severe.

Table 5.3.: Average reductions in the friction coefficient.

Oil reference	MINR	PAOR	ESTF	PAGD
Average reduction	$\simeq 0\%$	25%	26%	43%

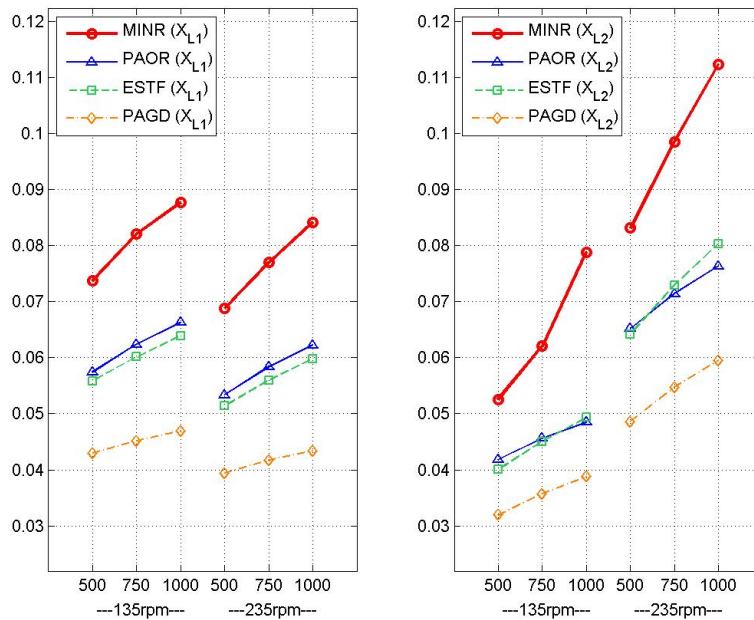


Figure 5.23.: Comparison of the coefficient of friction obtained for each oil tested considering each X_L factor.

Figures 5.24 to 5.27, show the power loss and its distribution for all the oils tested. The new friction coefficient influences the power loss of the gears (P_{fg}) and also the one of the bearings (P_{M1}). These power losses become reduced for the trials at 135rpm and increased for the trials at 235rpm in comparison to the original model. This behaviour seems quite logical, once for the higher velocity the trials are closer to the boundary friction due to the thinner film thickness, thus the friction should be higher and lead to higher energy dissipation.

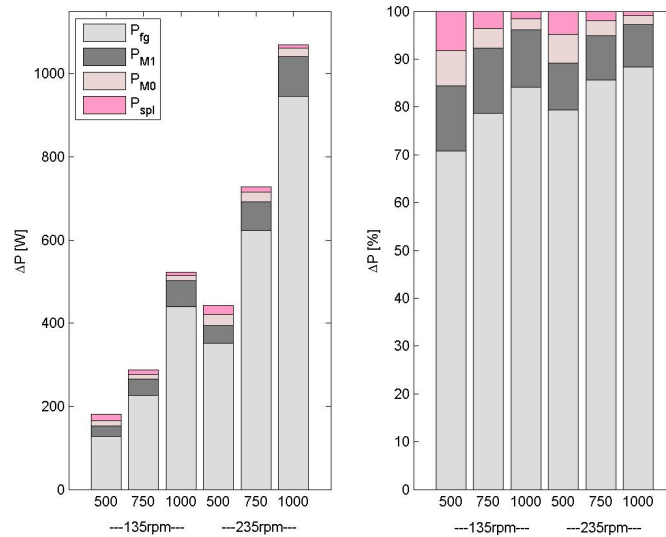


Figure 5.24.: Power loss distribution for the MINR oil (Lubricant factor X_{L2}).

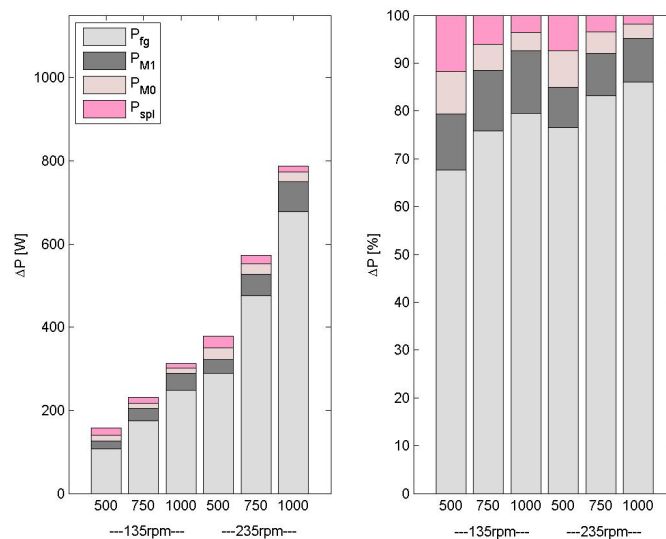


Figure 5.25.: Power loss distribution for the PAOR oil (Lubricant factor X_{L2}).

5. Power loss in Gearboxes

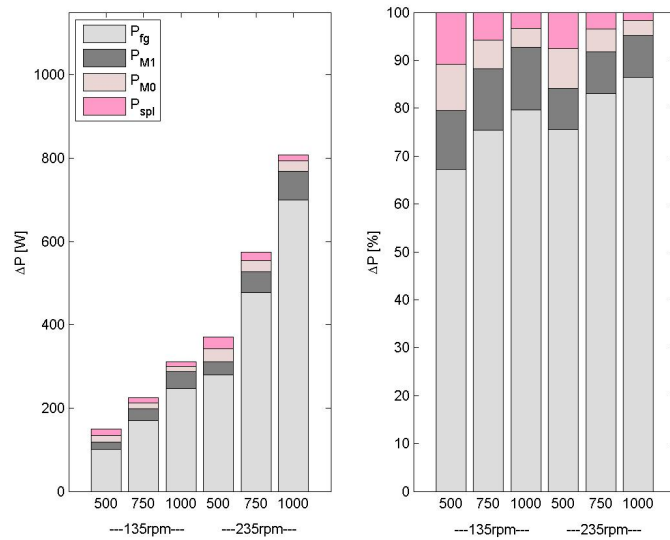


Figure 5.26.: Power loss distribution for the ESTF oil (Lubricant factor X_{L2}).

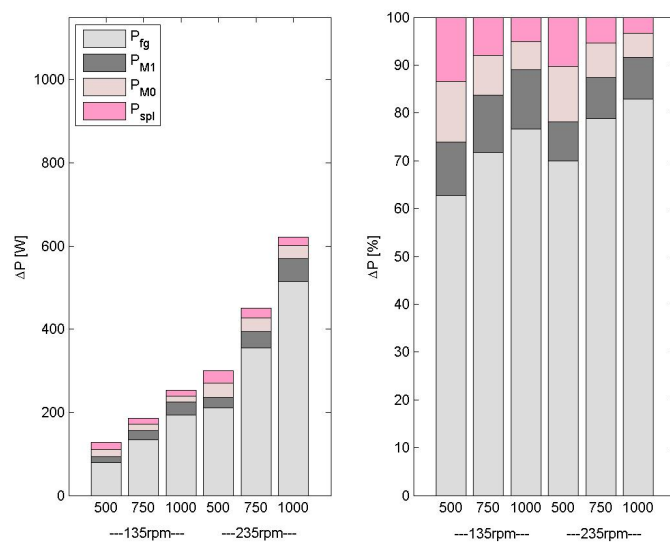


Figure 5.27.: Power loss distribution for the PAGD oil (Lubricant factor X_{L2}).

These figures show that the total power loss increases not only with the speed but also with the torque applied. This power loss increase is due mainly to the gears friction rise. In the rolling bearings, this increase of the friction power loss is not so clear and it represents always less than 15% of the total power losses.

The churning power losses of the gears decrease with both the torque and the speed increase, because the viscosity decreases in both situations. The churning losses of the gears decrease faster than the bearings churning losses.

6. Conclusions and future work

6.1. Experimental results

Analysing the experimentally obtained stabilization temperatures, several conclusions might be withdrawn. Furthermore, the correlation of these results and those obtained from the heat transfer analysis allows the relative comparison between the tested oils, while also attending to the direct reading ferrometry and analytic ferrography results. The following conclusions are appointed:

- I) The gearbox's efficiency decreases with the input speed while it is almost independent on the input load applied, decreasing very slightly with it.
- II) The PAGD oil performance was the best of all the five oils. Not only the gearbox achieved lower stabilization temperatures but also the CPUC and ISUC values were much lower than for any other oil.
- III) The MINR oil presented the worst results. This oil's sample presented high values of CPUC and ISUC, and while running this oil, the gearbox achieved the highest temperatures. This oil is also the most affected by the applied torque since its efficiency decreased greatly with it.
- IV) Both the esters tested and the PAOR oil, have a similar performance achieving approximately the same stabilization temperatures. The PAOR achieved slightly higher temperatures with result to its efficiency.
- V) Comparing the PAOR and the ESTF oils, the ferrometry and ferrography results are worse for the ESTF sample even though this oil was tested after the PAOR. This might indicate that the PAOR oil is better against wear.

6.2. Model evaluation

Regarding the simulation model implemented for the transfer gearbox, some conclusions might be taken:

- I) The churning losses both at bearings and gears proved not to be very intervening in the power losses at lower speeds, as expected;
- II) The model implemented for the friction coefficient without any optimized parameters, presented better results for higher speeds than for lower;
- III) The $X_L = 1$ factor for mineral oils which was predicted in the model [10], was verified since it lead to lower errors without any optimization.
- IV) The optimization considering only a load dependent coefficient showed a good correlation. However, the overall error was still large.
- V) The optimization considering not only a load dependent coefficient but also a speed dependent coefficient, proved to lead to a much better correlation, while the overall error obtained was very small. The new formulation for the friction coefficient is highly dependent on the speed, which might be valid to low speeds and high torque conditions. Since for these conditions the film thickness is very low, the speed increase leads to boundary friction and consequently, to higher energy dissipation.
- VI) The optimization resulted in lower and very distinct friction coefficients between different base oils. Although the model might need additional study to correctly describe the real energetic behaviour of the gearbox, it showed already that at lower speeds the coefficient of friction is highly influenced by the rotational speed.

6.3. Future works

Continuing this work, additional research could be done, for example:

- I) The ESTR trials should be finished allowing to compare both ester biodegradable oils.
- II) One or more different speed levels should be experimentally tested for the same three torque levels. This way, the new formulation for the coefficient of friction could be confirmed to low speed and high torques (windmill operating conditions).
- III) Same input speed and torque tests should also be performed at FZG test rig, for the same reason of the previous point.
- IV) The trials should be repeated and between each trial set, the gears should be changed, in order to allow the ferrometry and ferrography results to be directly compared between oils and therefore, being able to rate their wear performance.
- V) A wider research should be performed, regarding the churning and friction losses dependency on the oil viscosity, the gearbox housing, gears sense of rotation and also the combined effect of several gears running inside the gearbox.

Bibliography

- [1] A. S. J.O. Seabra, A. Campos, “Lubrificação elastohidrodinâmica,” Porto, 2002.
- [2] J. W. Gold, A. Schmidt, H. Dicke, H. Loos, and C. Aßmann, “Viscosity-pressure-temperature behaviour of mineral and synthetic oils,” *Journal of Synthetic Lubrication*, vol. 18, no. 1, p. 51, 2001.
- [3] B. M. M. Graça, “Análise de lubrificantes,” Notas de Curso, 2002.
- [4] J. O’Connor, *Standard handbook of lubrication engineering*. McGraw Hill, 1968.
- [5] D. M. Pirro and A. A. Wessol, *Lubrication fundamentals*. Marcel Dekker, 2001.
- [6] R. P. Carreteiro and P. N. A. Belmiro, *Lubrificantes e lubrificação industrial*. Interciência, 2006.
- [7] R. Gohar, *Elastohydrodynamics*. Ellis Horwood L.td, 1988.
- [8] “The brochure environmental label german ”blue angel” product requirements,” June 2001. RAL German institute for quality assurance and indication.
- [9] J. S. F. Brandão, “Gear micropitting prediction using the dang van high-cycle fatigue criterion,” Tese Dissertação da Universidade do Porto, 2007.
- [10] B.-R. Höhn, K. Michaelis, and T. Vollmer, “Thermal rating of gear drives: Balance between power loss and heat dissipation,” *AGMA Technical Paper*, 1996.
- [11] D. Simner, *Quantifying the potencial fuel economy benefict of transmission lubricants*, vol. 2. Industrial and Automotive Lubrication, 1998.
- [12] H. Winter and K. Michaelis, “Investigations on the thermal balance of gear drives,” in *Fifth World Congress on Theory of Machines and Mechanisms*, American Society of Mechanical Engineers, 1979.
- [13] R. Martins, J. Seabra, A. Brito, C. Seyfert, and A. Luther, R.and Igartua, “Friction coefficient in fzg gears lubricated with industrial gear oils:biodegradable ester vs. mineral oil,” *Tribology International*, vol. 39, no. 6, pp. 512–521, 2006.

Bibliography

- [14] C. Changenet and M. Pasquier, “Power losses and heat exchange in reduction gears: Numerical and experimental results,” *VDI Berichte*, vol. 2, no. 1665, pp. 603–613, 2002.
- [15] C. Changenet and P. Velez, “A model for the prediction of churning losses in geared transmissions -preliminary results,” *Journal of Mechanical Design*, vol. 1, pp. 128–133, Jan 2007.
- [16] X.-M. Changenet C. and P. Velez, “Power loss predictions in geared transmissions using thermal networks-applications to a six-speed manual gearbox,” *Journal of Mechanical Design*, vol. Vol. 128, May 2006.
- [17] P. Eschmann, L. Hasbargen, U. Weigand, J. Brndlein, and F. K. G. S. KGaA., *Ball and roller bearings - Theory, design and applications*. 1985.
- [18] D. Dowson and G. Higginson, *Elastohydrodynamic lubrication*. S. I. Editon, Pergamon Press Ltd., 1977.

A. Appendix

A.1. Test Reports

Tests performed with MINR oil

Test Report
Transfer Gearbox Efficiency using "Wind Mill Gear Oils"

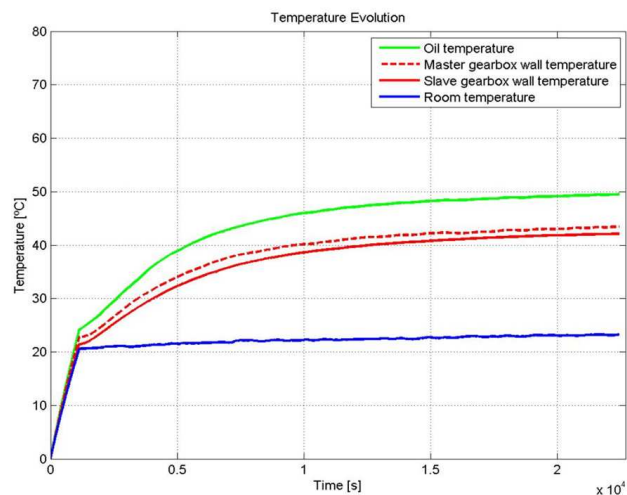
Researcher: David Gonçalves

Trial Parameters	Values	Units
Trial type:	Constant speed and torque	
Total trial duration	3600	min
Input speed:	135	rpm
Input torque:	500	Nm

Oil properties	Values	Units
ISO VG	320	
Base oil	Mineral (Repsol)	MINR
Cinematic viscosity @ 40°C	319.24	cSt
Cinematic viscosity @ 100°C	22.51	cSt
Density @ 15°C	0.902	g/cm ³

Average parameters for last hour of trial	Values	Units
Effective input speed (n_in)	139.9844	rpm
Effective input torque (T_in)	497.1559	Nm
Effective output speed (n_out)	315.0316	rpm
Theoretical Output torque (T_th_out)	220.9115	Nm

Average results for temperature stabilization after 6h	Values	Units
Oil temperature (θ_{oil})	49.24	°C
Room temperature (θ_{amb})	23.13	°C
Master gearbox wall temperature (θ_w)	43.15	°C
Slave gearbox wall temperature (θ_{ws})	41.90	°C
$\Delta\theta_{(oil-amb)}$	26.11	°C
$\Delta\theta_{(w-amb)}$	20.01	°C
$\Delta\theta_{(ws-amb)}$	18.77	°C



Test Report
 Transfer Gearbox Efficiency using "Wind Mill Gear Oils"

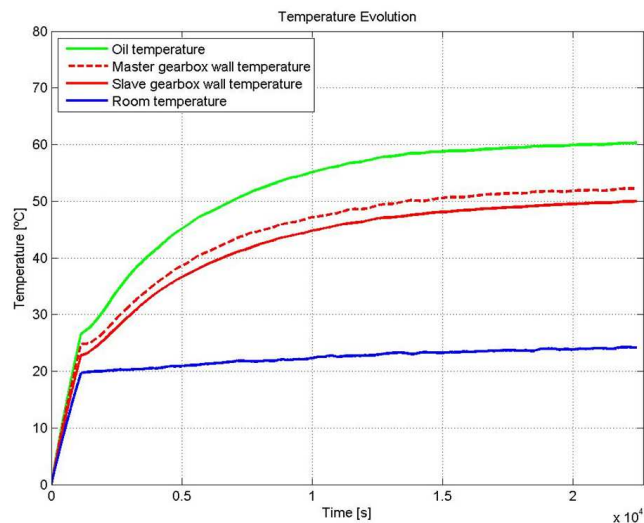
Researcher: David Gonçalves

Trial Parameters	Values	Units
Trial type:	Constant speed and torque	
Total trial duration	3600	min
Input speed:	135	rpm
Input torque:	750	Nm

Oil properties	Values	Units
ISO VG	320	
Base oil	Mineral (Repsol)	MINR
Cinematic viscosity @ 40°C	319.24	cSt
Cinematic viscosity @ 100°C	22.51	cSt
Density @ 15°C	0.902	g/cm ³

Average parameters for last hour of trial	Values	Units
Effective input speed (n _{in})	136.3626	rpm
Effective input torque (T _{in})	750.2872	Nm
Effective output speed (n _{out})	309.4797	rpm
Theoretical Output torque (T _{th_out})	330.5906	Nm

Average results for temperature stabilization after 6h	Values	Units
Oil temperature (θ _{oil})	59.98	°C
Room temperature (θ _{amb})	24.00	°C
Master gearbox wall temperature (θ _w)	51.92	°C
Slave gearbox wall temperature (θ _{ws})	49.62	°C
Δθ _(oil-amb)	35.98	°C
Δθ _(w-amb)	27.93	°C
Δθ _(ws-amb)	25.63	°C



Test Report
Transfer Gearbox Efficiency using "Wind Mill Gear Oils"

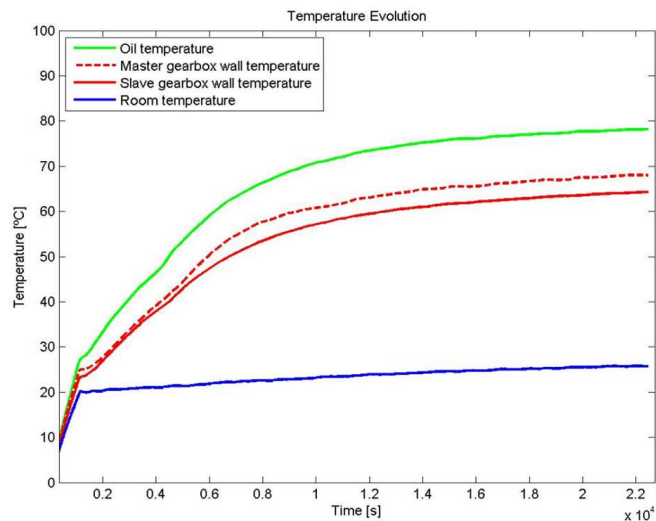
Researcher: David Gonçalves

Trial Parameters	Values	Units
Trial type:	Constant speed and torque	
Total trial duration	3600	min
Input speed:	135	rpm
Input torque:	1000	Nm

Oil properties	Values	Units
ISO VG	320	
Base oil	Mineral (Repsol)	MINR
Cinematic viscosity @ 40°C	319.24	cSt
Cinematic viscosity @ 100°C	22.51	cSt
Density @ 15°C	0.902	g/cm ³

Average parameters for last hour of trial	Values	Units
Effective input speed (n_in)	155.4627	rpm
Effective input torque (T_in)	1004.3000	Nm
Effective output speed (n_out)	355.2393	rpm
Theoretical Output torque (T_th_out)	439.5000	Nm

Average results for temperature stabilization after 6h	Values	Units
Oil temperature (θ_{oil})	77.76	°C
Room temperature (θ_{amb})	25.59	°C
Master gearbox wall temperature (θ_w)	67.57	°C
Slave gearbox wall temperature (θ_{ws})	63.80	°C
$\Delta\theta_{(oil-amb)}$	52.18	°C
$\Delta\theta_{(w-amb)}$	41.98	°C
$\Delta\theta_{(ws-amb)}$	38.21	°C



Test Report
Transfer Gearbox Efficiency using "Wind Mill Gear Oils"

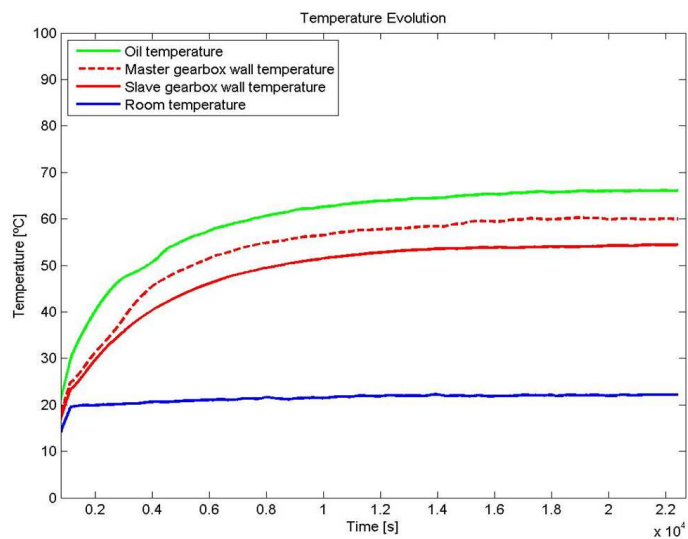
Researcher: David Gonçalves

Trial Parameters	Values	Units
Trial type:	Constant speed and torque	
Total trial duration	3600	min
Input speed:	235	rpm
Input torque:	500	Nm

Oil properties	Values	Units
ISO VG	320	
Base oil	Mineral (Repsol)	MINR
Cinematic viscosity @ 40°C	319.24	cSt
Cinematic viscosity @ 100°C	22.51	cSt
Density @ 15°C	0.902	g/cm ³

Average parameters for last hour of trial	Values	Units
Effective input speed (n_in)	235.4778	rpm
Effective input torque (T_in)	497.3674	Nm
Effective output speed (n_out)	539.2527	rpm
Theoretical Output torque (T_th_out)	210.1292	Nm

Average results for temperature stabilization after 6h	Values	Units
Oil temperature (θ_{oil})	66.03	°C
Room temperature (θ_{amb})	22.10	°C
Master gearbox wall temperature (θ_w)	60.04	°C
Slave gearbox wall temperature (θ_{ws})	54.25	°C
$\Delta\theta_{(oil-amb)}$	43.93	°C
$\Delta\theta_{(w-amb)}$	37.95	°C
$\Delta\theta_{(ws-amb)}$	32.15	°C



Test Report
Transfer Gearbox Efficiency using "Wind Mill Gear Oils"

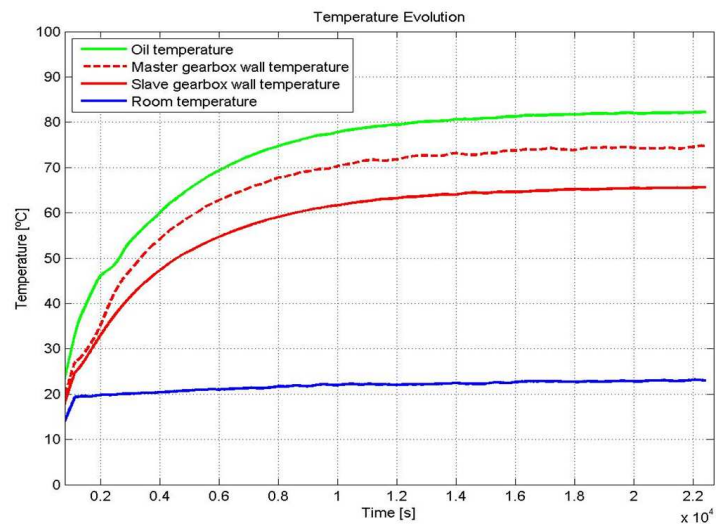
Researcher: David Gonçalves

Trial Parameters	Values	Units
Trial type:	Constant speed and torque	
Total trial duration	3600	min
Input speed:	235	rpm
Input torque:	750	Nm

Oil properties	Values	Units
ISO VG	320	
Base oil	Mineral (Repsol)	MINR
Cinematic viscosity @ 40°C	319.24	cSt
Cinematic viscosity @ 100°C	22.51	cSt
Density @ 15°C	0.902	g/cm ³

Average parameters for last hour of trial	Values	Units
Effective input speed (n_{in})	234.4463	rpm
Effective input torque (T_{in})	750.5282	Nm
Effective output speed (n_{out})	536.9889	rpm
Theoretical Output torque (T_{th_out})	327.6764	Nm

Average results for temperature stabilization after 6h	Values	Units
Oil temperature (θ_{oil})	82.04	°C
Room temperature (θ_{amb})	22.92	°C
Master gearbox wall temperature (θ_w)	74.38	°C
Slave gearbox wall temperature (θ_{ws})	65.44	°C
$\Delta\theta_{(oil-amb)}$	59.11	°C
$\Delta\theta_{(w-amb)}$	51.45	°C
$\Delta\theta_{(ws-amb)}$	42.52	°C



Test Report
Transfer Gearbox Efficiency using "Wind Mill Gear Oils"

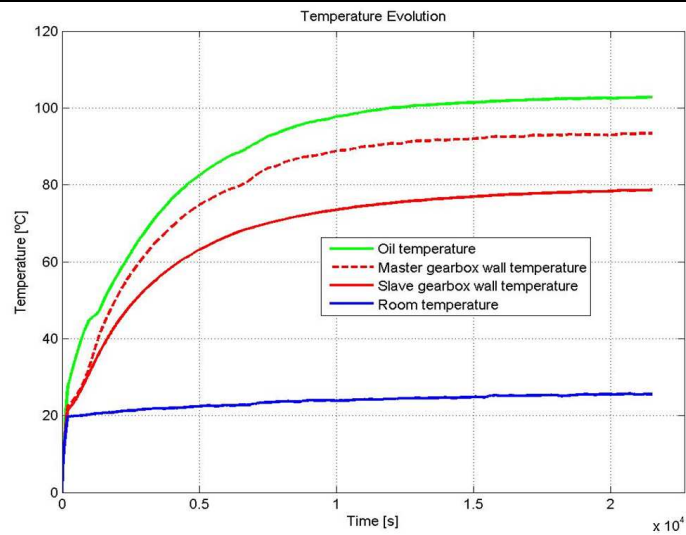
Researcher: David Gonçalves

Trial Parameters	Values	Units
Trial type:	Constant speed and torque	
Total trial duration	3600	min
Input speed:	235	rpm
Input torque:	1000	Nm

Oil properties	Values	Units
ISO VG	320	
Base oil	Mineral (Repsol)	MINR
Cinematic viscosity @ 40°C	319.24	cSt
Cinematic viscosity @ 100°C	22.51	cSt
Density @ 15°C	0.902	g/cm ³

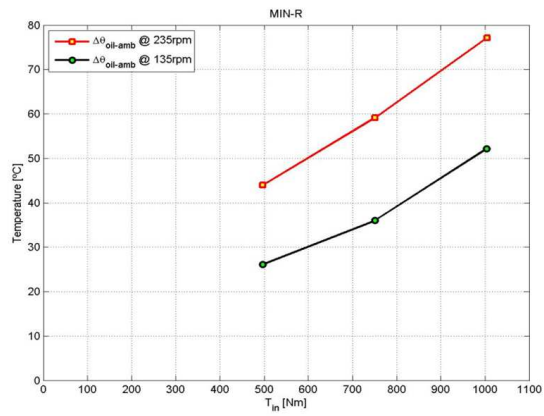
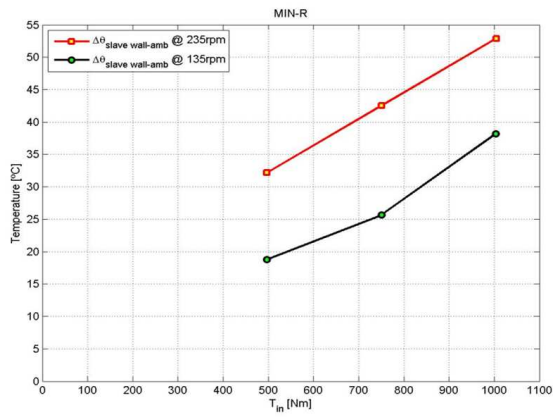
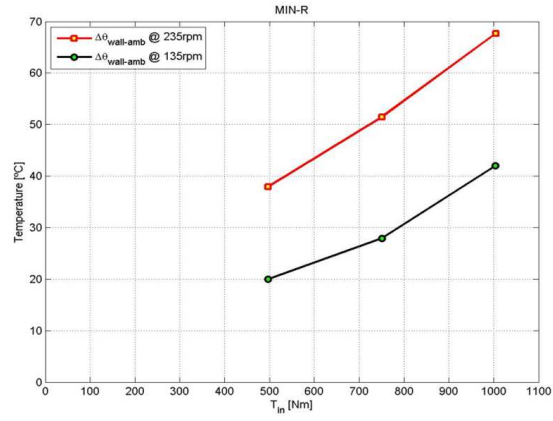
Average parameters for last hour of trial	Values	Units
Effective input speed (n_in)	235.7918	rpm
Effective input torque (T_in)	1004.3000	Nm
Effective output speed (n_out)	540.4022	rpm
Theoretical Output torque (T_th_out)	438.2046	Nm

Average results for temperature stabilization after 6h	Values	Units
Oil temperature (θ_{oil})	102.54	°C
Room temperature (θ_{amb})	25.45	°C
Master gearbox wall temperature (θ_w)	93.12	°C
Slave gearbox wall temperature (θ_{ws})	78.33	°C
$\Delta\theta_{(oil-amb)}$	77.08	°C
$\Delta\theta_{(w-amb)}$	67.66	°C
$\Delta\theta_{(ws-amb)}$	52.87	°C



Test Report
Transfer Gearbox Efficiency using "Wind Mill Gear Oils"

Stabilization Temperatures of the full trial set



Tests performed with PAOR oil

Test Report
Transfer Gearbox Efficiency using "Wind Mill Gear Oils"

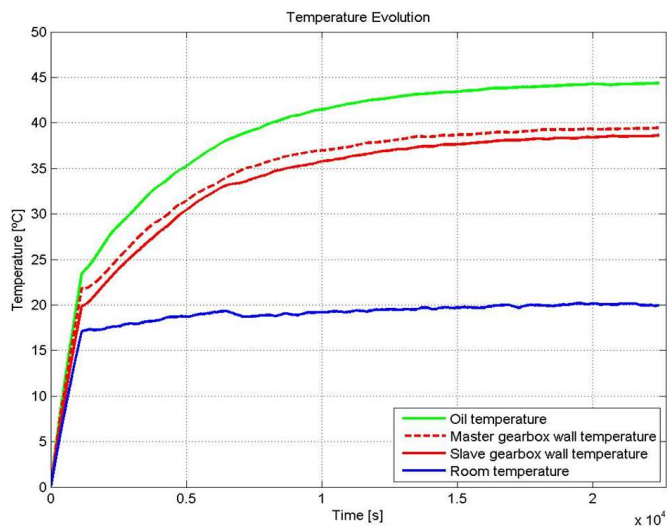
Researcher: David Gonçalves

Trial Parameters	Values	Units
Trial type:	Constant speed and torque	
Total trial duration	3600	min
Input speed:	135	rpm
Input torque:	500	Nm

Oil properties	Values	Units
ISO VG	320	
Base oil	PAO (Repsol)	PAOR
Cinematic viscosity @ 40°C	313.56	cSt
Cinematic viscosity @ 100°C	34.07	cSt
Density @ 15°C	0.892	g/cm ³

Average parameters for last hour of trial	Values	Units
Effective input speed (n_in)	140.2742	rpm
Effective input torque (T_in)	497.1222	Nm
Effective output speed (n_out)	317.0927	rpm
Theoretical Output torque (T_th_out)	219.9149	Nm

Average results for temperature stabilization after 6h	Values	Units
Oil temperature (θ_{oil})	44.24	°C
Room temperature (θ_{amb})	20.07	°C
Master gearbox wall temperature (θ_w)	39.33	°C
Slave gearbox wall temperature (θ_{ws})	38.47	°C
$\Delta\theta_{(oil-amb)}$	24.17	°C
$\Delta\theta_{(w-amb)}$	19.26	°C
$\Delta\theta_{(ws-amb)}$	18.40	°C



Test Report
 Transfer Gearbox Efficiency using "Wind Mill Gear Oils"

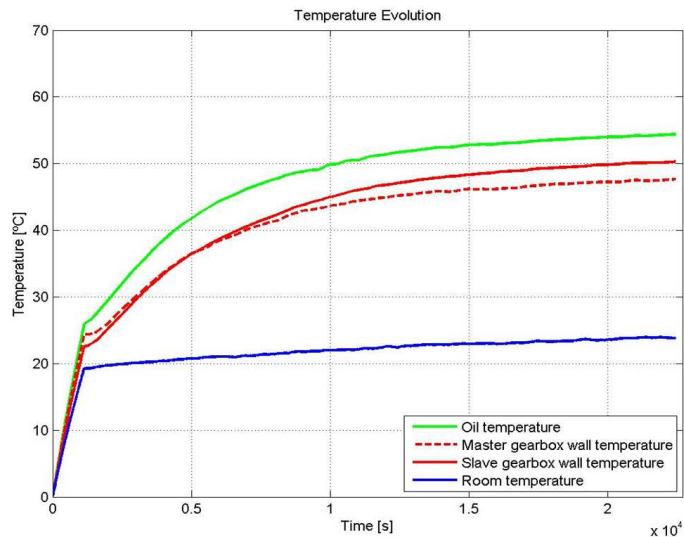
Researcher: David Gonçalves

Trial Parameters	Values	Units
Trial type:	Constant speed and torque	
Total trial duration	3600	min
Input speed:	135	rpm
Input torque:	750	Nm

Oil properties	Values	Units
ISO VG	320	
Base oil	PAO (Repsol)	PAOR
Cinematic viscosity @ 40°C	313.56	cSt
Cinematic viscosity @ 100°C	34.07	cSt
Density @ 15°C	0.892	g/cm ³

Average parameters for last hour of trial	Values	Units
Effective input speed (n_in)	137.0009	rpm
Effective input torque (T_in)	750.5328	Nm
Effective output speed (n_out)	310.8568	rpm
Theoretical Output torque (T_th_out)	330.7751	Nm

Average results for temperature stabilization after 6h	Values	Units
Oil temperature (θ_{oil})	54.07	°C
Room temperature (θ_{amb})	23.75	°C
Master gearbox wall temperature (θ_w)	47.34	°C
Slave gearbox wall temperature (θ_{ws})	49.95	°C
$\Delta\theta_{(oil-amb)}$	30.33	°C
$\Delta\theta_{(w-amb)}$	23.59	°C
$\Delta\theta_{(ws-amb)}$	26.21	°C



Test Report
Transfer Gearbox Efficiency using "Wind Mill Gear Oils"

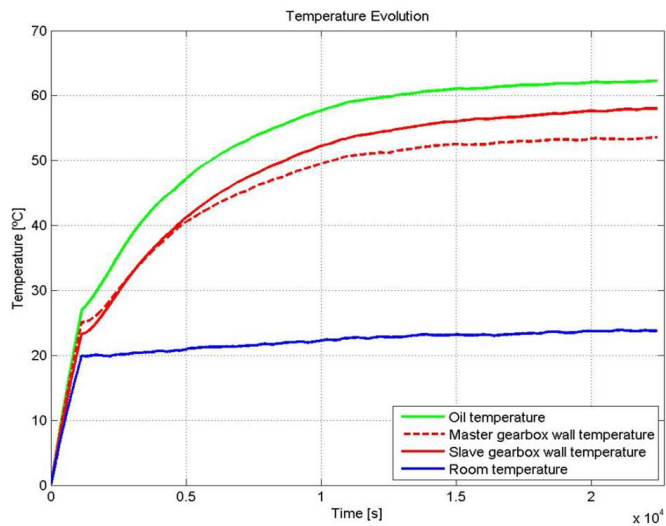
Researcher: David Gonçalves

Trial Parameters	Values	Units
Trial type:	Constant speed and torque	
Total trial duration	3600	min
Input speed:	135	rpm
Input torque:	1000	Nm

Oil properties	Values	Units
ISO VG	320	
Base oil	PAO (Repsol)	PAOR
Cinematic viscosity @ 40°C	313.56	cSt
Cinematic viscosity @ 100°C	34.07	cSt
Density @ 15°C	0.892	g/cm ³

Average parameters for last hour of trial	Values	Units
Effective input speed (n_in)	134.3166	rpm
Effective input torque (T_in)	1004.0000	Nm
Effective output speed (n_out)	306.8231	rpm
Theoretical Output torque (T_th_out)	439.5139	Nm

Average results for temperature stabilization after 6h	Values	Units
Oil temperature (θ_{oil})	62.04	°C
Room temperature (θ_{amb})	23.71	°C
Master gearbox wall temperature (θ_w)	53.32	°C
Slave gearbox wall temperature (θ_{ws})	57.69	°C
$\Delta\theta_{(oil-amb)}$	38.32	°C
$\Delta\theta_{(w-amb)}$	29.61	°C
$\Delta\theta_{(ws-amb)}$	33.97	°C



Test Report
Transfer Gearbox Efficiency using "Wind Mill Gear Oils"

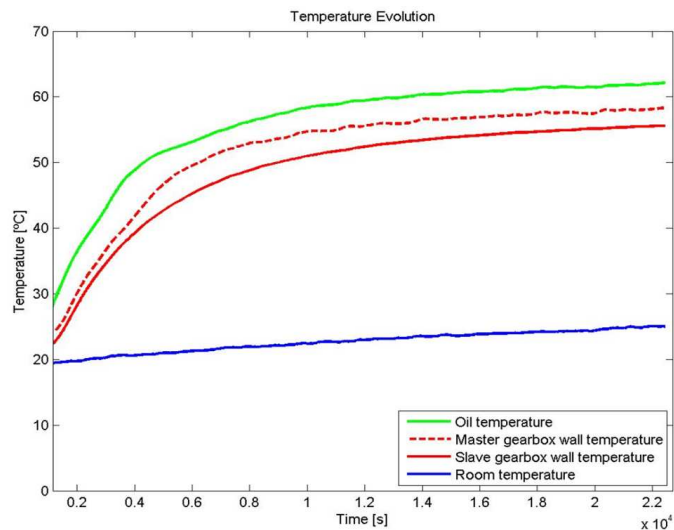
Researcher: David Gonçalves

Trial Parameters	Values	Units
Trial type:	Constant speed and torque	
Total trial duration	3600	min
Input speed:	235	rpm
Input torque:	500	Nm

Oil properties	Values	Units
ISO VG	320	
Base oil	PAO (Repsol)	PAOR
Cinematic viscosity @ 40°C	313.56	cSt
Cinematic viscosity @ 100°C	34.07	cSt
Density @ 15°C	0.892	g/cm ³

Average parameters for last hour of trial	Values	Units
Effective input speed (n_in)	236.8458	rpm
Effective input torque (T_in)	497.3823	Nm
Effective output speed (n_out)	542.8882	rpm
Theoretical Output torque (T_th_out)	216.9930	Nm

Average results for temperature stabilization after 6h	Values	Units
Oil temperature (θ_{oil})	61.70	°C
Room temperature (θ_{amb})	24.67	°C
Master gearbox wall temperature (θ_w)	57.87	°C
Slave gearbox wall temperature (θ_{ws})	55.27	°C
$\Delta\theta_{(oil-amb)}$	37.02	°C
$\Delta\theta_{(w-amb)}$	33.19	°C
$\Delta\theta_{(ws-amb)}$	30.60	°C



Test Report
Transfer Gearbox Efficiency using "Wind Mill Gear Oils"

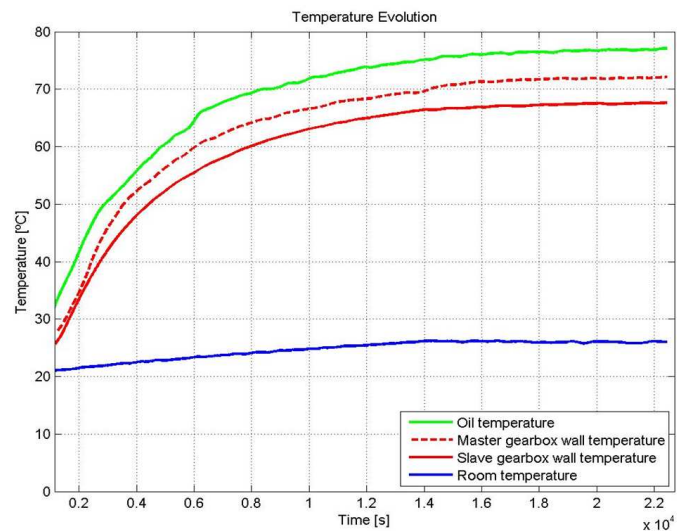
Researcher: David Gonçalves

Trial Parameters	Values	Units
Trial type:	Constant speed and torque	
Total trial duration	3600	min
Input speed:	235	rpm
Input torque:	750	Nm

Oil properties	Values	Units
ISO VG	320	
Base oil	PAO (Repsol)	PAOR
Cinematic viscosity @ 40°C	313.56	cSt
Cinematic viscosity @ 100°C	34.07	cSt
Density @ 15°C	0.892	g/cm ³

Average parameters for last hour of trial	Values	Units
Effective input speed (n_{in})	236.2062	rpm
Effective input torque (T_{in})	750.6541	Nm
Effective output speed (n_{out})	541.3473	rpm
Theoretical Output torque (T_{th_out})	327.5331	Nm

Average results for temperature stabilization after 6h	Values	Units
Oil temperature (θ_{oil})	76.80	°C
Room temperature (θ_{amb})	25.98	°C
Master gearbox wall temperature (θ_w)	71.91	°C
Slave gearbox wall temperature (θ_{ws})	67.49	°C
$\Delta\theta_{(oil-amb)}$	50.83	°C
$\Delta\theta_{(w-amb)}$	45.93	°C
$\Delta\theta_{(ws-amb)}$	41.52	°C



Test Report
Transfer Gearbox Efficiency using "Wind Mill Gear Oils"

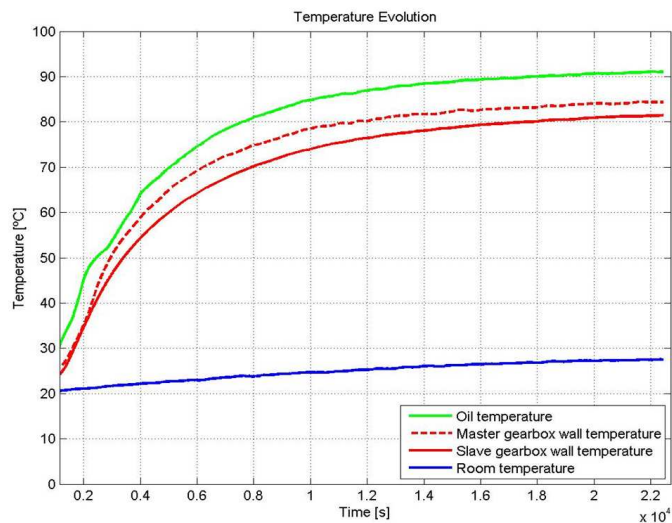
Researcher: David Gonçalves

Trial Parameters	Values	Units
Trial type:	Constant speed and torque	
Total trial duration	3600	min
Input speed:	235	rpm
Input torque:	1000	Nm

Oil properties	Values	Units
ISO VG	320	
Base oil	PAO (Repsol)	PAOR
Cinematic viscosity @ 40°C	313.56	cSt
Cinematic viscosity @ 100°C	34.07	cSt
Density @ 15°C	0.892	g/cm ³

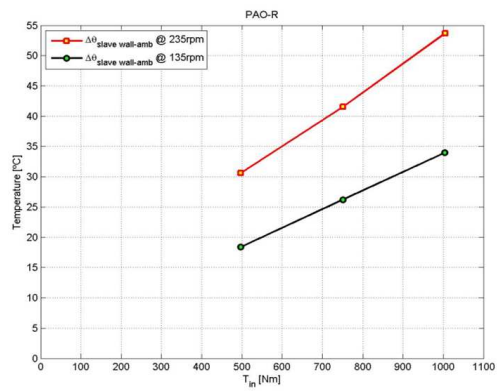
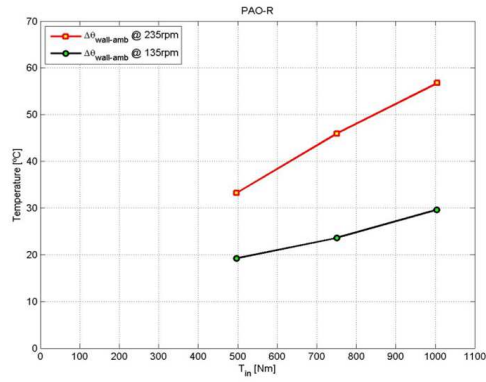
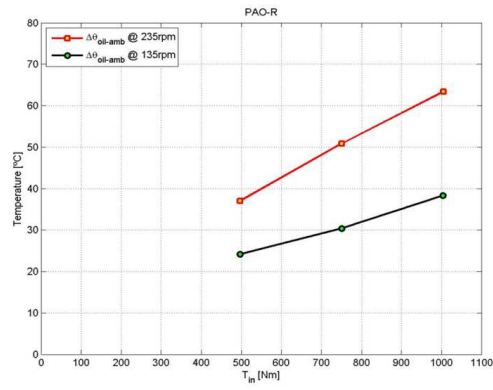
Average parameters for last hour of trial	Values	Units
Effective input speed (n_in)	235.9039	rpm
Effective input torque (T_in)	1005.0000	Nm
Effective output speed (n_out)	540.8631	rpm
Theoretical Output torque (T_th_out)	438.3335	Nm

Average results for temperature stabilization after 6h	Values	Units
Oil temperature (θ_{oil})	90.73	°C
Room temperature (θ_{amb})	27.32	°C
Master gearbox wall temperature (θ_w)	84.09	°C
Slave gearbox wall temperature (θ_{ws})	81.04	°C
$\Delta\theta_{(oil-amb)}$	63.41	°C
$\Delta\theta_{(w-amb)}$	56.77	°C
$\Delta\theta_{(ws-amb)}$	53.72	°C



Test Report
Transfer Gearbox Efficiency using "Wind Mill Gear Oils"

Stabilization Temperatures of the full trial set



Tests performed with ESTR oil

Test Report
 Transfer Gearbox Efficiency using "Wind Mill Gear Oils"

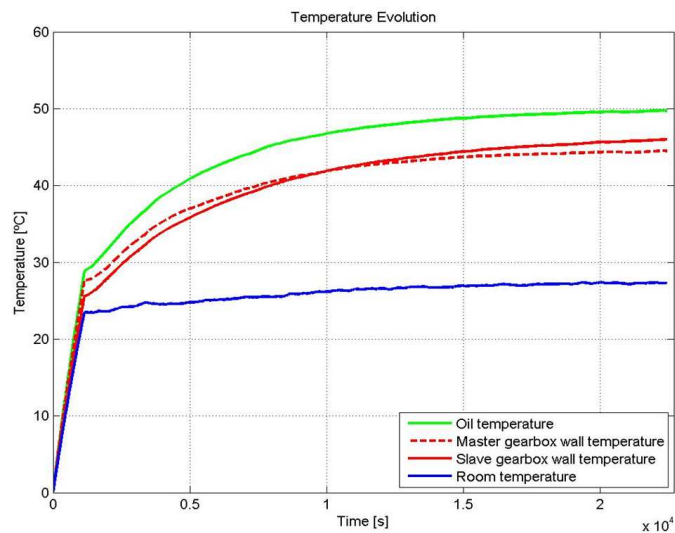
Researcher: David Gonçalves

Trial Parameters	Values	Units
Trial type:	Constant speed and torque	
Total trial duration	3600	min
Input speed:	135	rpm
Input torque:	500	Nm

Oil properties	Values	Units
ISO VG	320	
Base oil	Ester (Fuchs)	ESTF
Cinematic viscosity @ 40°C	324.03	cSt
Cinematic viscosity @ 100°C	36.07	cSt
Density @ 15°C	0.957	g/cm ³

Average parameters for last hour of trial	Values	Units
Effective input speed (n_in)	143.0178	rpm
Effective input torque (T_in)	497.2962	Nm
Effective output speed (n_out)	323.4957	rpm
Theoretical Output torque (T_th_out)	219.8552	Nm

Average results for temperature stabilization after 6h	Values	Units
Oil temperature (θ_{oil})	49.59	°C
Room temperature (θ_{amb})	27.28	°C
Master gearbox wall temperature (θ_w)	44.34	°C
Slave gearbox wall temperature (θ_{ws})	45.69	°C
$\Delta\theta_{(oil-amb)}$	22.31	°C
$\Delta\theta_{(w-amb)}$	17.07	°C
$\Delta\theta_{(ws-amb)}$	18.41	°C



Test Report
Transfer Gearbox Efficiency using "Wind Mill Gear Oils"

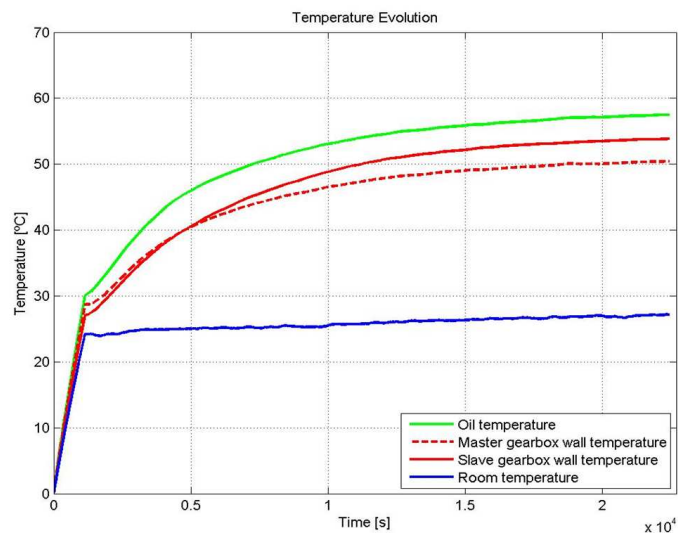
Researcher: David Gonçalves

Trial Parameters	Values	Units
Trial type:	Constant speed and torque	
Total trial duration	3600	min
Input speed:	135	rpm
Input torque:	750	Nm

Oil properties	Values	Units
ISO VG	320	
Base oil	Ester (Fuchs)	ESTF
Cinematic viscosity @ 40°C	324.03	cSt
Cinematic viscosity @ 100°C	36.07	cSt
Density @ 15°C	0.957	g/cm ³

Average parameters for last hour of trial	Values	Units
Effective input speed (n_in)	140.8882	rpm
Effective input torque (T_in)	750.9093	Nm
Effective output speed (n_out)	319.7749	rpm
Theoretical Output torque (T_th_out)	330.8397	Nm

Average results for temperature stabilization after 6h	Values	Units
Oil temperature (θ_{oil})	57.25	°C
Room temperature (θ_{amb})	26.95	°C
Master gearbox wall temperature (θ_w)	50.20	°C
Slave gearbox wall temperature (θ_{ws})	53.59	°C
$\Delta\theta_{(oil-amb)}$	30.30	°C
$\Delta\theta_{(w-amb)}$	23.25	°C
$\Delta\theta_{(ws-amb)}$	26.64	°C



Test Report
Transfer Gearbox Efficiency using "Wind Mill Gear Oils"

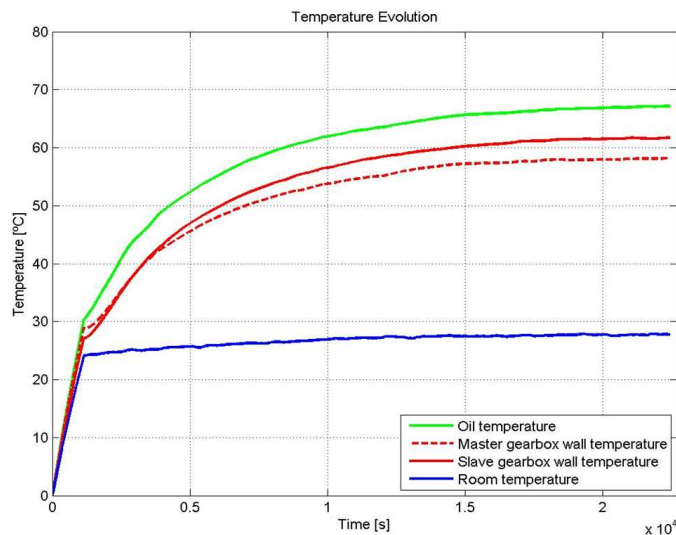
Researcher: David Gonçalves

Trial Parameters	Values	Units
Trial type:	Constant speed and torque	
Total trial duration	3600	min
Input speed:	135	rpm
Input torque:	1000	Nm

Oil properties	Values	Units
ISO VG	320	
Base oil	Ester (Fuchs)	ESTF
Cinematic viscosity @ 40°C	324.03	cSt
Cinematic viscosity @ 100°C	36.07	cSt
Density @ 15°C	0.957	g/cm ³

Average parameters for last hour of trial	Values	Units
Effective input speed (n_in)	136.3022	rpm
Effective input torque (T_in)	1004.5000	Nm
Effective output speed (n_out)	311.0404	rpm
Theoretical Output torque (T_th_out)	440.1785	Nm

Average results for temperature stabilization after 6h	Values	Units
Oil temperature (θ_{oil})	66.94	°C
Room temperature (θ_{amb})	27.73	°C
Master gearbox wall temperature (θ_w)	58.02	°C
Slave gearbox wall temperature (θ_{ws})	61.56	°C
$\Delta\theta_{(oil-amb)}$	39.20	°C
$\Delta\theta_{(w-amb)}$	30.28	°C
$\Delta\theta_{(ws-amb)}$	33.82	°C



Test Report
 Transfer Gearbox Efficiency using "Wind Mill Gear Oils"

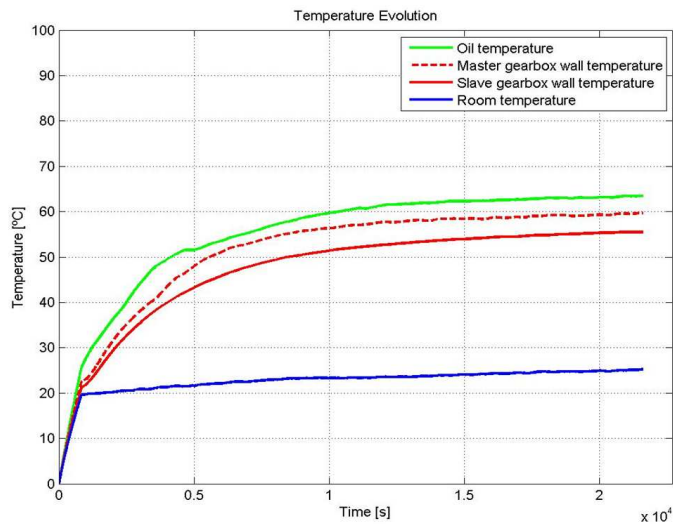
Researcher: David Gonçalves

Trial Parameters	Values	Units
Trial type:	Constant speed and torque	
Total trial duration	3600	min
Input speed:	235	rpm
Input torque:	500	Nm

Oil properties	Values	Units
ISO VG	320	
Base oil	Ester (Fuchs)	
Cinematic viscosity @ 40°C	324.03	cSt
Cinematic viscosity @ 100°C	36.07	cSt
Density @ 15°C	0.957	g/cm ³

Average parameters for last hour of trial	Values	Units
Effective input speed (n_in)	237.0012	rpm
Effective input torque (T_in)	497.4351	Nm
Effective output speed (n_out)	543.1641	rpm
Theoretical Output torque (T_th_out)	217.0481	Nm

Average results for temperature stabilization after 6h	Values	Units
Oil temperature (θ_{oil})	63.16	°C
Room temperature (θ_{amb})	24.85	°C
Master gearbox wall temperature (θ_w)	59.31	°C
Slave gearbox wall temperature (θ_{ws})	55.23	°C
$\Delta\theta_{(oil-amb)}$	38.31	°C
$\Delta\theta_{(w-amb)}$	34.46	°C
$\Delta\theta_{(ws-amb)}$	30.38	°C



Test Report
Transfer Gearbox Efficiency using "Wind Mill Gear Oils"

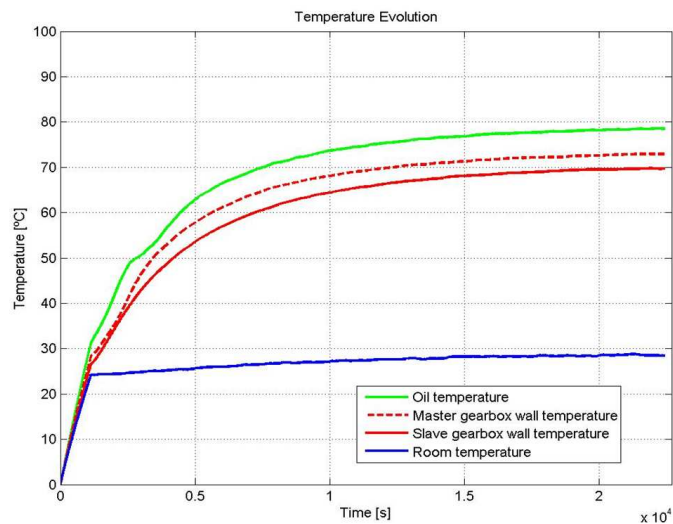
Researcher: David Gonçalves

Trial Parameters	Values	Units
Trial type:	Constant speed and torque	
Total trial duration	3600	min
Input speed:	235	rpm
Input torque:	750	Nm

Oil properties	Values	Units
ISO VG	320	
Base oil	Ester (Fuchs)	ESTF
Cinematic viscosity @ 40°C	324.03	cSt
Cinematic viscosity @ 100°C	36.07	cSt
Density @ 15°C	0.957	g/cm ³

Average parameters for last hour of trial	Values	Units
Effective input speed (n_in)	239.0463	rpm
Effective input torque (T_in)	751.0178	Nm
Effective output speed (n_out)	547.5634	rpm
Theoretical Output torque (T_th_out)	327.8672	Nm

Average results for temperature stabilization after 6h	Values	Units
Oil temperature (θ_{oil})	78.31	°C
Room temperature (θ_{amb})	28.52	°C
Master gearbox wall temperature (θ_w)	72.74	°C
Slave gearbox wall temperature (θ_{ws})	69.58	°C
$\Delta\theta_{(oil-amb)}$	49.79	°C
$\Delta\theta_{(w-amb)}$	44.22	°C
$\Delta\theta_{(ws-amb)}$	41.06	°C



Test Report
Transfer Gearbox Efficiency using "Wind Mill Gear Oils"

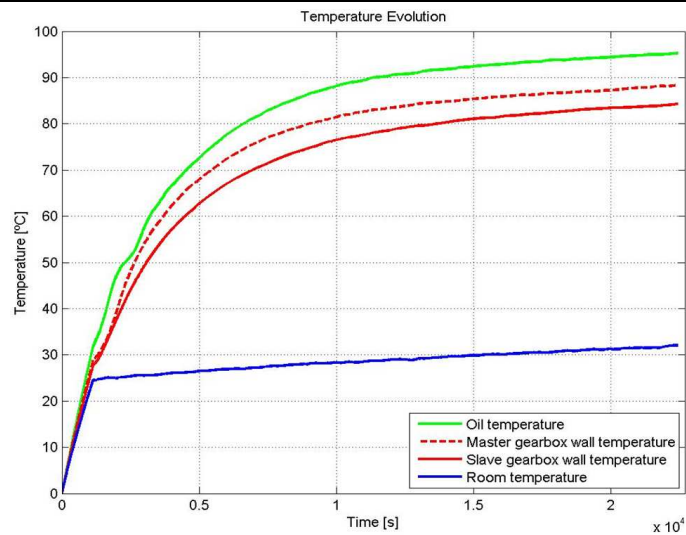
Researcher: David Gonçalves

Trial Parameters	Values	Units
Trial type:	Constant speed and torque	
Total trial duration	3600	min
Input speed:	235	rpm
Input torque:	1000	Nm

Oil properties	Values	Units
ISO VG	320	
Base oil	Ester (Fuchs)	ESTF
Cinematic viscosity @ 40°C	324.03	cSt
Cinematic viscosity @ 100°C	36.07	cSt
Density @ 15°C	0.957	g/cm ³

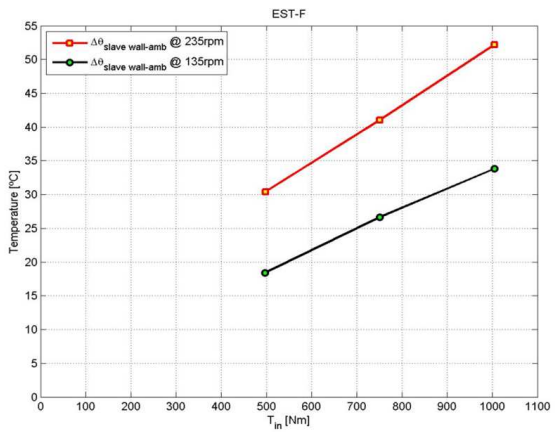
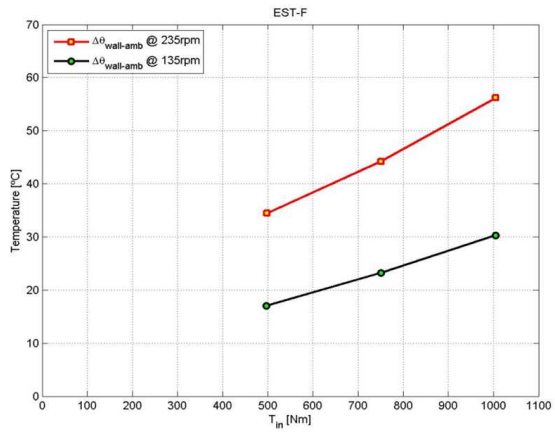
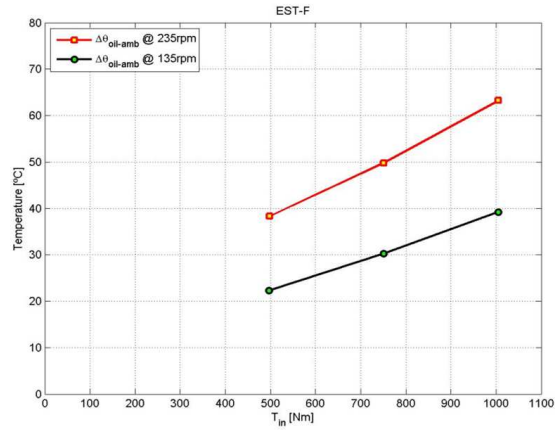
Average parameters for last hour of trial	Values	Units
Effective input speed (n_in)	237.7995	rpm
Effective input torque (T_in)	1004.9000	Nm
Effective output speed (n_out)	544.7900	rpm
Theoretical Output torque (T_th_out)	339.6841	Nm

Average results for temperature stabilization after 6h	Values	Units
Oil temperature (θ_{oil})	94.65	°C
Room temperature (θ_{amb})	31.41	°C
Master gearbox wall temperature (θ_w)	87.60	°C
Slave gearbox wall temperature (θ_{ws})	83.59	°C
$\Delta\theta_{(oil-amb)}$	63.23	°C
$\Delta\theta_{(w-amb)}$	56.19	°C
$\Delta\theta_{(ws-amb)}$	52.18	°C



Test Report
Transfer Gearbox Efficiency using "Wind Mill Gear Oils"

Stabilization Temperatures of the full trial set



Tests performed with PAGD oil

Test Report
 Transfer Gearbox Efficiency using "Wind Mill Gear Oils"

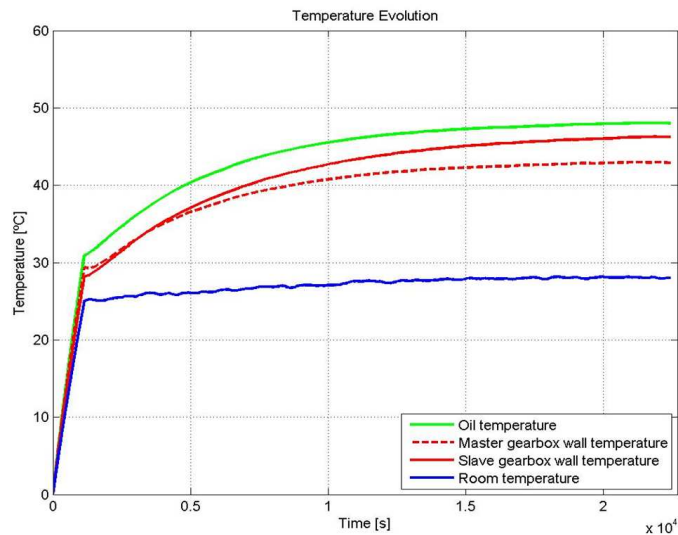
Researcher: David Gonçalves

Trial Parameters	Values	Units
Trial type:	Constant speed and torque	
Total trial duration	3600	min
Input speed:	135	rpm
Input torque:	500	Nm

Oil properties	Values	Units
ISO VG	320	
Base oil	PAG (Dow)	PAGD
Cinematic viscosity @ 40°C	290.26	cSt
Cinematic viscosity @ 100°C	51.06	cSt
Density @ 15°C	1.059	g/cm ³

Average parameters for last hour of trial	Values	Units
Effective input speed (n_in)	143.4118	rpm
Effective input torque (T_in)	497.4957	Nm
Effective output speed (n_out)	325.1914	rpm
Theoretical Output torque (T_th_out)	219.3992	Nm

Average results for temperature stabilization after 6h	Values	Units
Oil temperature (θ_{oil})	47.97	°C
Room temperature (θ_{amb})	28.05	°C
Master gearbox wall temperature (θ_w)	42.91	°C
Slave gearbox wall temperature (θ_{ws})	46.11	°C
$\Delta\theta_{(oil-amb)}$	19.92	°C
$\Delta\theta_{(w-amb)}$	14.86	°C
$\Delta\theta_{(ws-amb)}$	18.06	°C



Test Report
 Transfer Gearbox Efficiency using "Wind Mill Gear Oils"

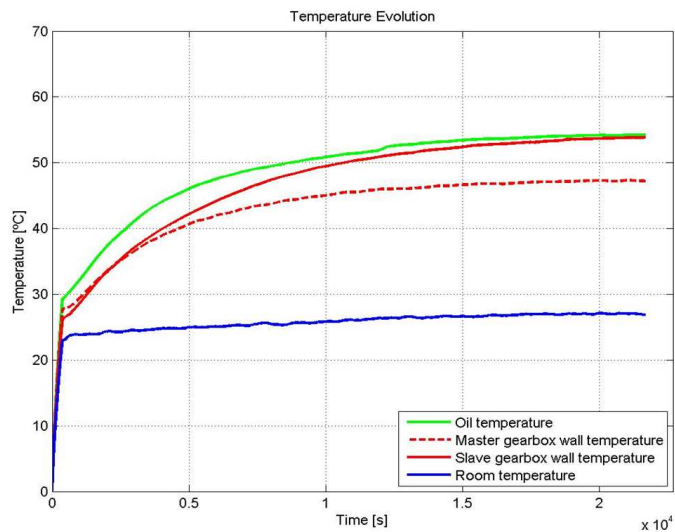
Researcher: David Gonçalves

Trial Parameters	Values	Units
Trial type:	Constant speed and torque	
Total trial duration	3600	min
Input speed:	135	rpm
Input torque:	750	Nm

Oil properties	Values	Units
ISO VG	320	
Base oil	PAG (Dow)	PAGD
Cinematic viscosity @ 40°C	290.26	cSt
Cinematic viscosity @ 100°C	51.06	cSt
Density @ 15°C	1.059	g/cm ³

Average parameters for last hour of trial	Values	Units
Effective input speed (n_in)	141.4202	rpm
Effective input torque (T_in)	750.8135	Nm
Effective output speed (n_out)	320.5319	rpm
Theoretical Output torque (T_th_out)	331.2625	Nm

Average results for temperature stabilization after 6h	Values	Units
Oil temperature (θ_{oil})	54.12	°C
Room temperature (θ_{amb})	27.00	°C
Master gearbox wall temperature (θ_w)	47.21	°C
Slave gearbox wall temperature (θ_{ws})	53.63	°C
$\Delta\theta_{(oil-amb)}$	27.12	°C
$\Delta\theta_{(w-amb)}$	20.21	°C
$\Delta\theta_{(ws-amb)}$	26.63	°C



Test Report
Transfer Gearbox Efficiency using "Wind Mill Gear Oils"

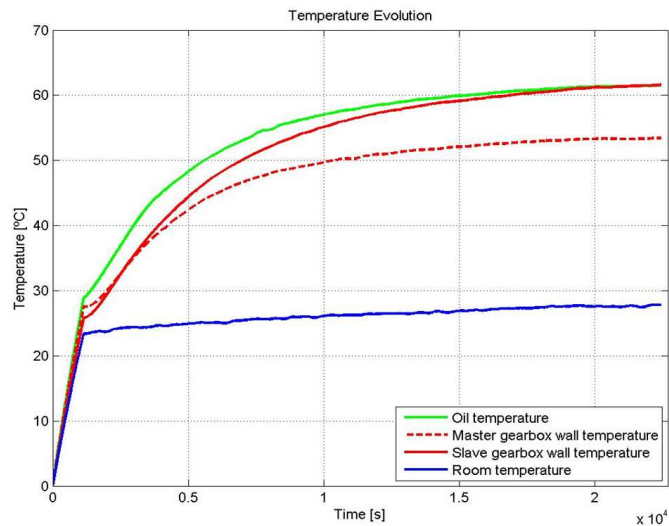
Researcher: David Gonçalves

Trial Parameters	Values	Units
Trial type:	Constant speed and torque	
Total trial duration	3600	min
Input speed:	135	rpm
Input torque:	1000	Nm

Oil properties	Values	Units
ISO VG	320	
Base oil	PAG (Dow)	PAGD
Cinematic viscosity @ 40°C	290.26	cSt
Cinematic viscosity @ 100°C	51.06	cSt
Density @ 15°C	1.059	g/cm ³

Average parameters for last hour of trial	Values	Units
Effective input speed (n_in)	137.0134	rpm
Effective input torque (T_in)	1004.5000	Nm
Effective output speed (n_out)	312.3777	rpm
Theoretical Output torque (T_th_out)	440.5910	Nm

Average results for temperature stabilization after 6h	Values	Units
Oil temperature (θ_{oil})	61.36	°C
Room temperature (θ_{amb})	27.62	°C
Master gearbox wall temperature (θ_w)	53.30	°C
Slave gearbox wall temperature (θ_{ws})	61.27	°C
$\Delta\theta_{(oil-amb)}$	33.74	°C
$\Delta\theta_{(w-amb)}$	25.68	°C
$\Delta\theta_{(ws-amb)}$	33.65	°C



Test Report
Transfer Gearbox Efficiency using "Wind Mill Gear Oils"

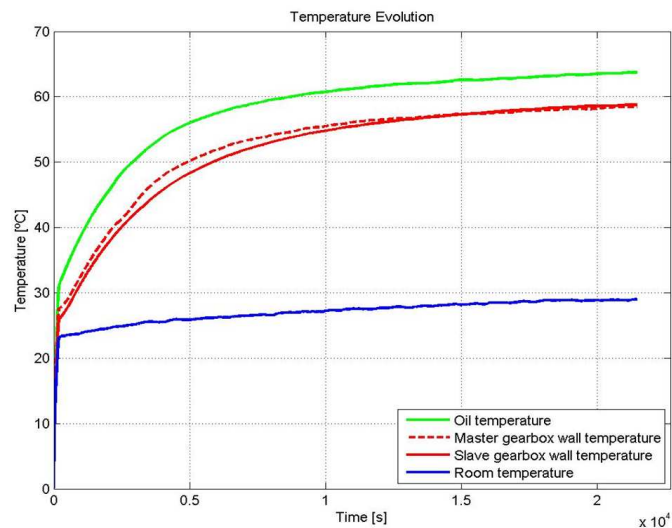
Researcher: David Gonçalves

Trial Parameters	Values	Units
Trial type:	Constant speed and torque	
Total trial duration	3600	min
Input speed:	235	rpm
Input torque:	500	Nm

Oil properties	Values	Units
ISO VG	320	
Base oil	PAG (Dow)	PAGD
Cinematic viscosity @ 40°C	290.26	cSt
Cinematic viscosity @ 100°C	51.06	cSt
Density @ 15°C	1.059	g/cm ³

Average parameters for last hour of trial	Values	Units
Effective input speed (n_in)	239.5157	rpm
Effective input torque (T_in)	497.5456	Nm
Effective output speed (n_out)	548.7939	rpm
Theoretical Output torque (T_th_out)	217.1489	Nm

Average results for temperature stabilization after 6h	Values	Units
Oil temperature (θ_{oil})	63.44	°C
Room temperature (θ_{amb})	28.86	°C
Master gearbox wall temperature (θ_w)	58.21	°C
Slave gearbox wall temperature (θ_{ws})	58.52	°C
$\Delta\theta_{(oil-amb)}$	34.58	°C
$\Delta\theta_{(w-amb)}$	29.35	°C
$\Delta\theta_{(ws-amb)}$	29.66	°C



Test Report
Transfer Gearbox Efficiency using "Wind Mill Gear Oils"

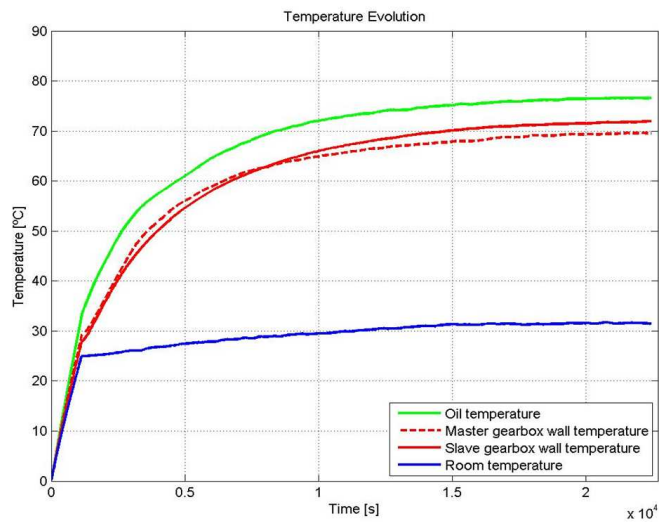
Researcher: David Gonçalves

Trial Parameters	Values	Units
Trial type:	Constant speed and torque	
Total trial duration	3600	min
Input speed:	235	rpm
Input torque:	750	Nm

Oil properties	Values	Units
ISO VG	320	
Base oil	PAG (Dow)	PAGD
Cinematic viscosity @ 40°C	290.26	cSt
Cinematic viscosity @ 100°C	51.06	cSt
Density @ 15°C	1.059	g/cm ³

Average parameters for last hour of trial	Values	Units
Effective input speed (n_in)	239.2103	rpm
Effective input torque (T_in)	751.2121	Nm
Effective output speed (n_out)	548.0350	rpm
Theoretical Output torque (T_th_out)	327.8946	Nm

Average results for temperature stabilization after 6h	Values	Units
Oil temperature (θ_{oil})	76.48	°C
Room temperature (θ_{amb})	31.55	°C
Master gearbox wall temperature (θ_w)	69.41	°C
Slave gearbox wall temperature (θ_{ws})	71.64	°C
$\Delta\theta_{(oil-amb)}$	44.93	°C
$\Delta\theta_{(w-amb)}$	37.86	°C
$\Delta\theta_{(ws-amb)}$	40.09	°C



Test Report
Transfer Gearbox Efficiency using "Wind Mill Gear Oils"

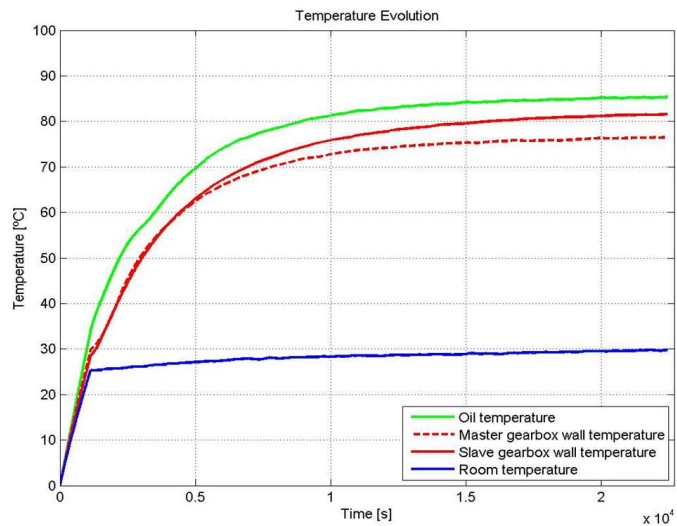
Researcher: David Gonçalves

Trial Parameters	Values	Units
Trial type:	Constant speed and torque	
Total trial duration	3600	min
Input speed:	235	rpm
Input torque:	1000	Nm

Oil properties	Values	Units
ISO VG	320	
Base oil	PAG (Dow)	PAGD
Cinematic viscosity @ 40°C	290.26	cSt
Cinematic viscosity @ 100°C	51.06	cSt
Density @ 15°C	1.059	g/cm ³

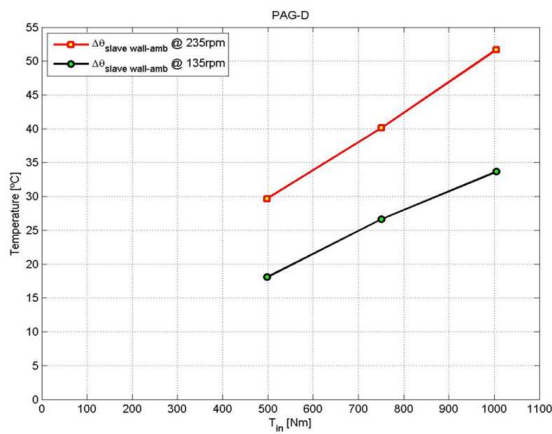
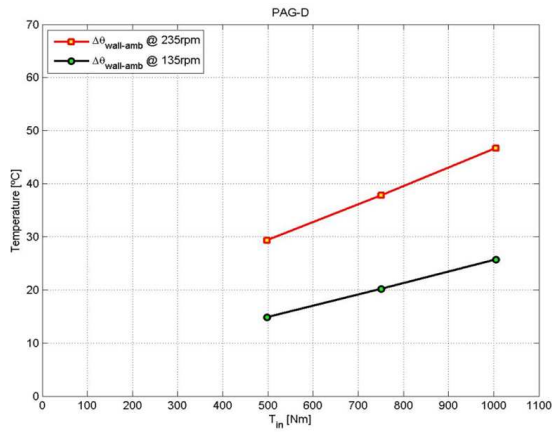
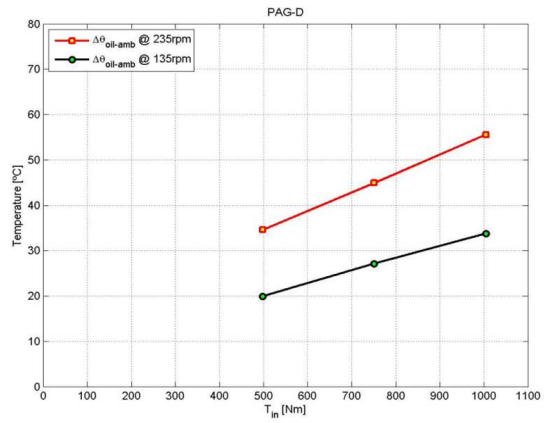
Average parameters for last hour of trial	Values	Units
Effective input speed (n_in)	238.1248	rpm
Effective input torque (T_in)	1004.5000	Nm
Effective output speed (n_out)	545.5815	rpm
Theoretical Output torque (T_th_out)	438.4356	Nm

Average results for temperature stabilization after 6h	Values	Units
Oil temperature (θ_{oil})	85.13	°C
Room temperature (θ_{amb})	29.58	°C
Master gearbox wall temperature (θ_w)	76.28	°C
Slave gearbox wall temperature (θ_{ws})	81.28	°C
$\Delta\theta_{(oil-amb)}$	55.55	°C
$\Delta\theta_{(w-amb)}$	46.70	°C
$\Delta\theta_{(ws-amb)}$	51.70	°C



Test Report
Transfer Gearbox Efficiency using "Wind Mill Gear Oils"



Stabilization Temperatures of the full trial set



Ferrometry and Ferrograhy results



Relatório de Análise de Lubrificantes

Análise nº:	59 - 62 / 11
Tipo de análise:	Ferrometria e Ferrografia Analítica
Confidencialidade:	1
Cliente:	INEGI - Cetrib
Morada:	Porto
Telefone / Fax:	
Equipamento:	BANCO de ENSAIOS (Power Loss)
Lubrificante:	WINDMILL LUBS
Dossier:	/
Nº de páginas:	7
Data:	08/06/11
Responsável:	Beatriz Graça – Jorge Seabra
Rúbrica:	 

OBJECTIVO

Análise de quatro amostras de óleos lubrificantes (ESTF, MINR, PAOR e PAG) resultantes de ensaios de Power Loss efectuados no Banco de Ensaios, para avaliação do desgaste presente.

As amostras analisadas foram as seguintes:

Amostra Nº	Factor Diluição	Análises efectuadas	
		Ferrometria	Ferrografia Analítica
ESTF	0,1	X	X
MINR	0,1	X	X
PAOR	0,1	X	X
PAG	1	X	X

RESULTADOS DAS ANÁLISES

Nas páginas seguintes são apresentados os resultados referentes às análises de Ferrometria (DR III) e Ferrografia Analítica (FM III).



CLIENTE: INEGI		MÁQUINA: Banco de Ensaios			
MORADA: Porto		Ref. ÓLEOS: WINDMILL LUBS			
DATA: 01/06/11		ENSAIOS - POWER LOSS			
IDENTIFICAÇÃO					
Amostra n°:	ESTF	MINR	PAOR	PAG	
Data amostra:	Abr-11	Abr-11	Abr-11	Abr-11	
Análise n°:	59/11	60/11	61/11	62/11	
Ciclos/Máquina:	-	-	-	-	
Ciclos/Óleo:	-	-	-	-	
FERROMETRIA					
d:	0,1	0,1	0,1	1	
DL:	20,0	38,8	17,8	24,2	
DS:	5,8	12,4	5,1	5,0	
CPUC:	258,0	512,0	229,0	29,2	
ISUC:	3,7E+04	1,4E+05	2,9E+04	5,6E+02	
FERROGRAFIA:					
Desgaste normal					
Desgaste severo					
Desgaste abrasão					
Desgaste combinado					
Desgaste fadiga					
Esferas Metálicas					
Ligas não ferrosas					
Óxidos de ferro					
Minerais/Orgânicos					
OILVIEW:					
Índice OilLife:					
Índice Oxidação:					
Índice Contaminação:					
Índice Ferromagnético:					
Grandes Contaminantes:					
Constante Dielétrica:					
FILTRAGEM					
(Nº Partículas/10 ml)					
5 - 15 µm					
15 - 25 µm					
25 - 50 µm					
50 - 100 µm					
> 100 µm					
VISCOSIDADE					
(cSt a 40° C):					
ACIDEZ (TAN)					
(mg KOH)					
P. INFLAMAÇÃO					
(° C)					
DIAGNÓSTICO:					
LEGENDA					
DL - Índice de partículas grandes					Não existe
DS - Índice de partículas pequenas				f	Fraco
CPUC - Concentração part. de desgaste				M	Médio
ISUC - Índice Severidade de Desgaste				F	Forte

Os resultados apresentados referem-se exclusivamente às amostras ensaiadas.

Este documento não pode ser reproduzido, total ou parcialmente, sem a autorização por escrito do INEGI.

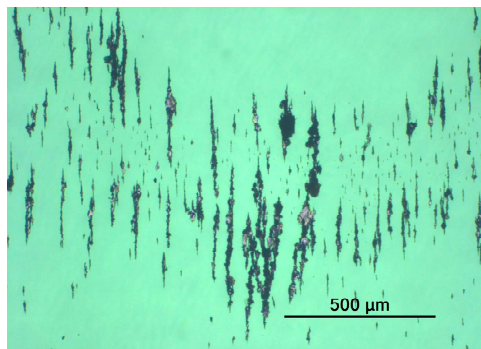
Pág. 3 / 7

Relatório Nº 62/11

MOD LAL-REL01

CLIENTE: INEGI	MÁQUINA: Banco de Ensaios
MORADA: Porto	Ref. ÓLEO: WINDMILL LUBS - ESTF
DATA: 01/06/11	ENSAIOS - Power Loss

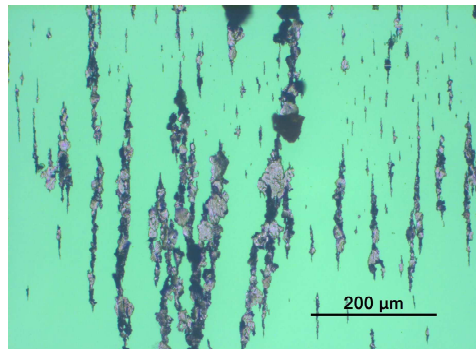
Fotografia 1



Ampliação: x 100 Diluição: 0,1
 Localização: Núcleo Luz: Branca / Verde

Observações: Presença de partículas ferrosas de pequenas dimensões e grandes dimensões.

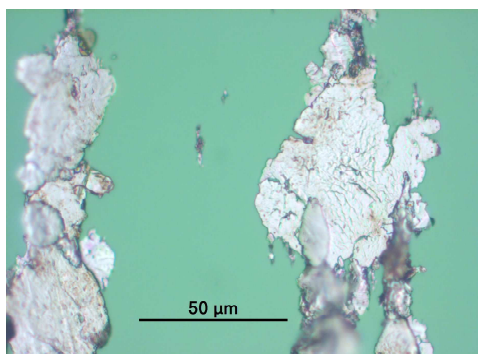
Fotografia 2



Ampliação: x 200 Diluição: 0,1
 Localização: Núcleo Luz: Branca / Verde

Observações: Ampliação da Fotografia 1. Presença de partículas ferrosas de pequenas e grandes dimensões.

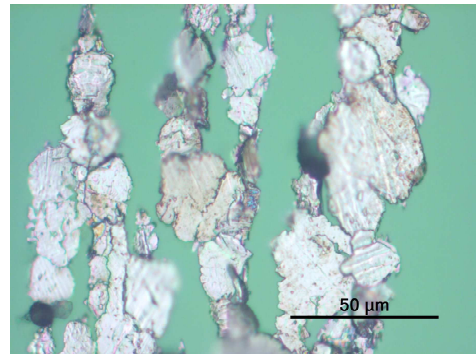
Fotografia 3



Ampliação: x 1000 Diluição: 0,1
 Localização: Núcleo Luz: Branca / Verde

Observações: Ampliação da Fotografia 2. Partículas ferrosas de desgaste de grandes dimensões, típicas de desgaste de fadiga e praticamente sem oxidação superficial.

Fotografia 4



Ampliação: x 1000 Diluição: 0,1
 Localização: Núcleo Luz: Branca / Verde

Observações: Ampliação da Fotografia 2. Partículas ferrosas de desgaste de grandes dimensões, típicas de desgaste de fadiga e praticamente sem oxidação superficial.

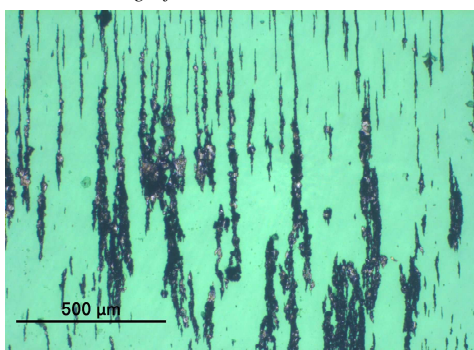
Os resultados apresentados referem-se exclusivamente às amostras ensaiadas.
 Este documento não pode ser reproduzido, total ou parcialmente, sem a autorização por escrito do INEGI.



CLIENTE: **INEGI**
MORADA: Porto
DATA: 01/06/11

MÁQUINA: Banco de Ensaios
Ref. ÓLEO: WINDMILL LUBS - MINR
ENSAIOS - Power Loss

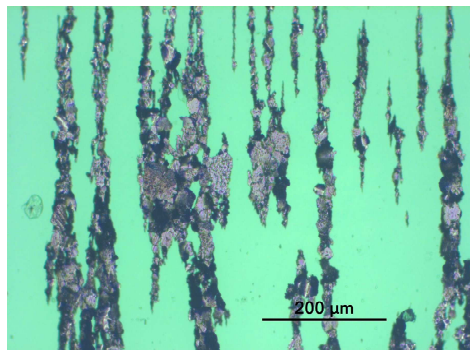
Fotografia 5



Ampliação: x 100 Diluição: 0,1
Localização: Núcleo Luz: Branca / Verde

Observações: Presença de partículas ferrosas de pequenas e grandes dimensões.

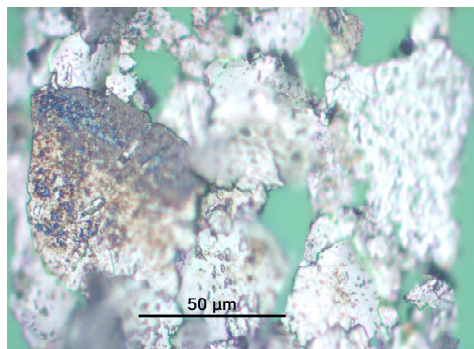
Fotografia 6



Ampliação: x 200 Diluição: 0,1
Localização: Núcleo Luz: Branca / Verde

Observações: Ampliação da Fotografia 5. Presença de partículas ferrosas de pequenas e grandes dimensões.

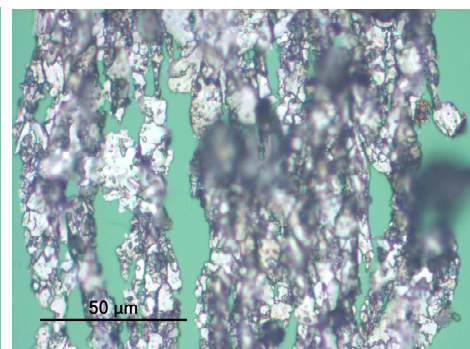
Fotografia 7



Ampliação: x 1000 Diluição: 0,1
Localização: Núcleo Luz: Branca / Verde

Observações: Ampliação da Fotografia 6. Partículas ferrosas de desgaste grandes dimensões, algumas severamente oxidadas.

Fotografia 8

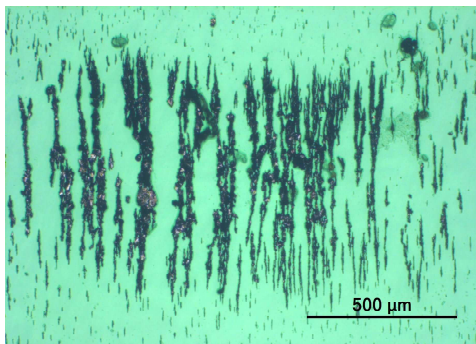


Ampliação: x 1000 Diluição: 0,1
Localização: Núcleo Luz: Branca / Verde

Observações: Ampliação da Fotografia 6. Partículas ferrosas de pequenas dimensões e médias dimensões. Presença de alguns óxidos termicos (partículas negras).

CLIENTE: INEGI MORADA: Porto DATA: 01/06/11	MÁQUINA: Banco de Ensaios Ref. ÓLEO: WINDMILL LUBS - PAOR ENSAIOS - Power Loss
--	--

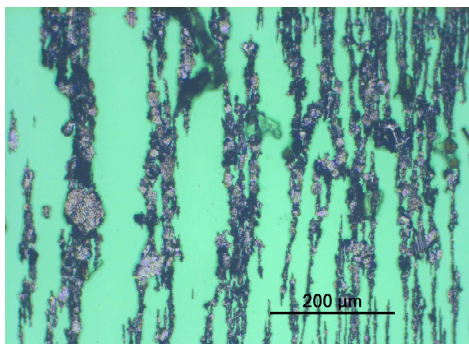
Fotografia 9



Ampliação: x 100 Diluição: 0,1
 Localização: Núcleo Luz: Branca / Verde

Observações: Presença de partículas ferrosas de pequenas dimensões e grandes dimensões.

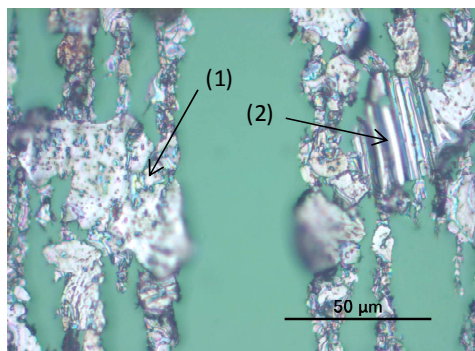
Fotografia 10



Ampliação: x 200 Diluição: 0,1
 Localização: Núcleo Luz: Branca / Verde

Observações: Ampliação da Fotografia 9. Presença de partículas ferrosas de pequenas e grandes dimensões.

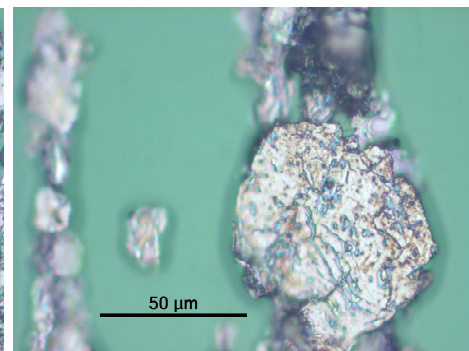
Fotografia 11



Ampliação: x 1000 Diluição: 0,1
 Localização: Núcleo Luz: Branca / Verde

Observações: Ampliação da Fotografia 10. Partículas ferrosas de desgaste de grandes e pequenas dimensões, algumas de desgaste de fadiga (1), outras de desgaste combinado (2).

Fotografia 12



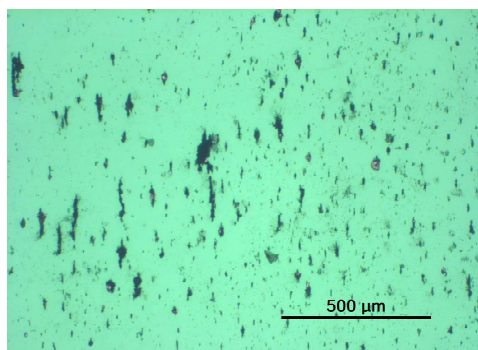
Ampliação: x 1000 Diluição: 0,1
 Localização: Núcleo Luz: Branca / Verde

Observações: Ampliação da Fotografia 10. Partícula ferrosa de grandes dimensões típica de desgaste de fadiga e com alguma oxidação termica.

Os resultados apresentados referem-se exclusivamente às amostras ensaiadas.
 Este documento não pode ser reproduzido, total ou parcialmente, sem a autorização por escrito do INEGI.

CLIENTE: INEGI MORADA: Porto DATA: 01/06/11	MÁQUINA: Banco de Ensaios Ref. ÓLEO: WINDMILL LUBS - PAG ENSAIOS - Power Loss
--	---

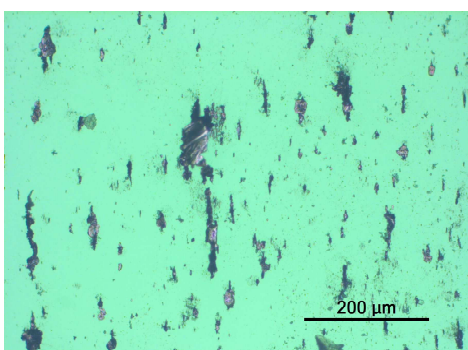
Fotografia 13



Ampliação: x 100 Diluição: 1
 Localização: Núcleo Luz: Branca / Verde

Observações: Presença de poucas partículas ferrosas de desgaste.

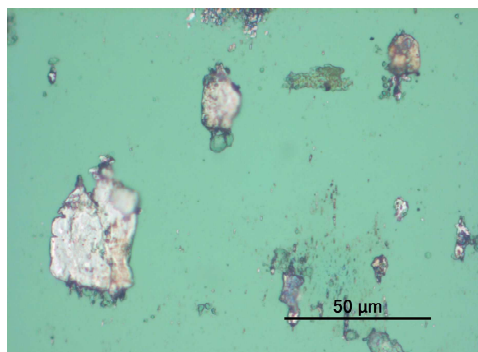
Fotografia 14



Ampliação: x 200 Diluição: 1
 Localização: Núcleo Luz: Branca / Verde

Observações: Ampliação da Fotografia 13. Presença de algumas partículas ferrosas de grandes dimensões.

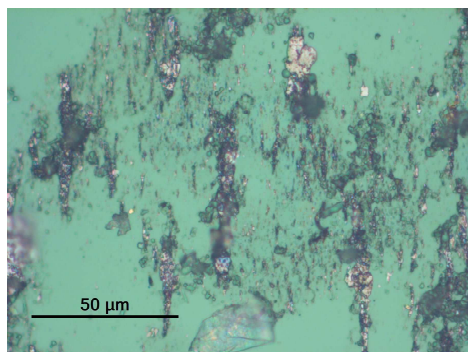
Fotografia 15



Ampliação: x 1000 Diluição: 1
 Localização: Núcleo Luz: Branca / Verde

Observações: Ampliação da Fotografia 14. Partículas ferrosas de desgaste de fadiga, algumas de grandes dimensões.

Fotografia 16

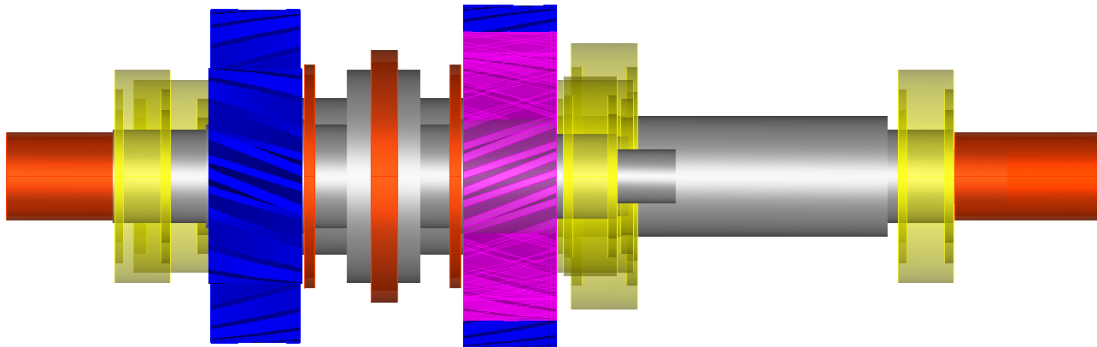
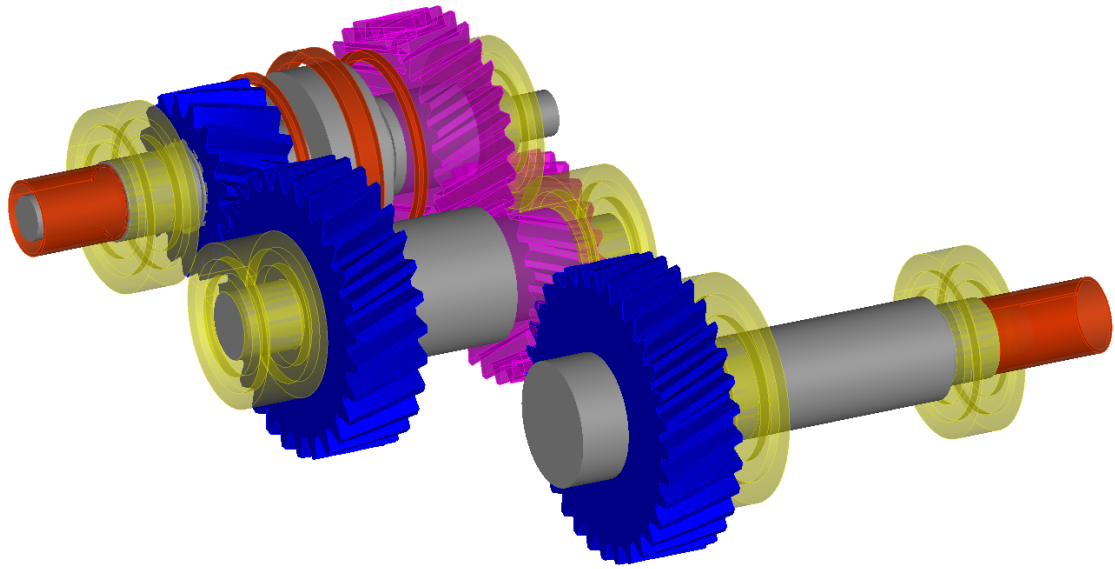


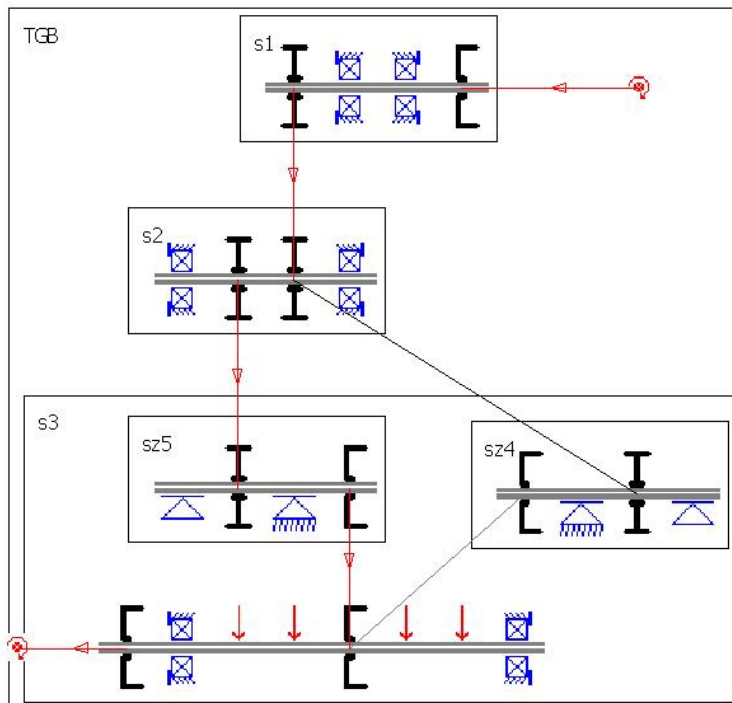
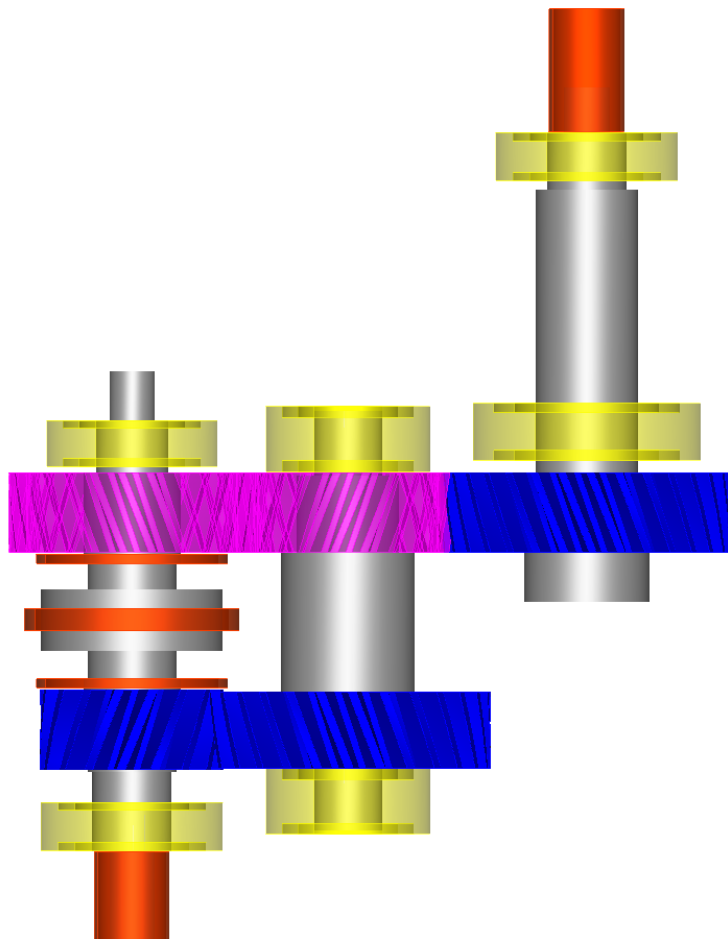
Ampliação: x 1000 Diluição: 1
 Localização: Núcleo Luz: Branca / Verde

Observações: Presença significativa de polímeros de atrito.

A.2. Gearbox simulation - KissSys

Transfer Gearbox 3D Model View





_O.System.TGB.gp1.GP1

KISSsoft - Release 04-2010E

KISSsoft evaluation

File

Name: 1st.gear_235rpm_1000Nm

Important hint: At least one warning has occurred during the calculation:

1-> Calculation according to DIN 3990, Part 41, for motor gear boxes requires a sensible tooth trace correction

Annotation:

Adjust tooth trace correction accordingly.

CALCULATION OF A HELICAL GEAR PAIR

Drawing or article number:

Gear 1: 0.000.0

Gear 2: 0.000.0

Calculation method DIN 3990 Part 41 (Vehicle gear box) Method B

Calculating according to DIN 3990, part 41

		----- GEAR 1 -----	----- GEAR 2 --
Power (kW)	[P]		24.609
Speed (1/min)	[n]	235.0	327.0
Torque (Nm)	[T]	1000.0	718.7
Application factor	[KAF, KAH]		1.00 1.00
Required service life	[H]		100000000.00
Gear driving (+) / driven (-)		+	-

1. TOOTH GEOMETRY AND MATERIAL

(Geometry calculation according to ISO 21771)

		----- GEAR 1 -----	----- GEAR 2 --
Center distance (mm)	[a]		105.011
Centre distance tolerance			ISO 286 Measure h7
Normal module (mm)	[mn]		3.5000
Pressure angle at normal section (°)	[alfn]		20.0000
Helix angle at reference circle (°)	[beta]		20.0000
Number of teeth	[z]	32	23
Facewidth (mm)	[b]	35.00	35.00
Hand of gear		left	right
Accuracy grade	[Q-ISO1328]	6	6
Inner diameter (mm)	[di]	0.00	0.00
Inside diameter of rim (mm)	[dbi]	0.00	0.00

Material

Gear 1: 15 CrNi 6, Case-carburized steel, case-hardened
ISO 6336-5 Figure 9/10 (MQ), core strength >=25HRC Jominy J=12mm<HRC28

Gear 2: 15 CrNi 6, Case-carburized steel, case-hardened
ISO 6336-5 Figure 9/10 (MQ), core strength >=25HRC Jominy J=12mm<HRC28

		----- GEAR 1 -----	----- GEAR 2 --
Surface hardness		HRC 60	HRC 60
Fatigue strength. tooth root stress (N/mm ²)			
	[sigFlim]	430.00	430.00
Fatigue strength for Hertzian pressure (N/mm ²)			
	[sigHlim]	1500.00	1500.00
Tensile strength (N/mm ²)	[Rm]	1000.00	1000.00
Yield point (N/mm ²)	[Rp]	685.00	685.00
Young's modulus (N/mm ²)	[E]	206000	206000
Poisson's ratio	[ny]	0.300	0.300
Average roughness, Ra, tooth flank (µm)	[RAH]	0.60	0.60
Mean roughness height, Rz, flank (µm)	[RZH]	4.80	4.80
Mean roughness height, Rz, root (µm)	[RZF]	20.00	20.00

Information on preliminary treatments

Tool or reference profile of gear 1 :

Reference profile 1.25 / 0.38 / 1.0 ISO 53.2 Profil A

Grinding allowance (mm)	[g]	0.000
Addendum coefficient	[haP*]	1.000
Dedendum coefficient	[hfP*]	1.250
Tip radius factor	[rhoaP*]	0.000
Root radius factor	[rhofP*]	0.380

Tip form height coefficient	[hFaP*]	0.000
Protuberance height factor	[hprP*]	0.000
Protuberance angle	[alfprP]	0.000
Ramp angle	[alfKP]	0.000

not topping

Tool or reference profile of gear 2 :

Reference profile 1.25 / 0.38 / 1.0 ISO 53.2 Profil A		
Grinding allowance (mm)	[g]	0.000
Addendum coefficient	[haP*]	1.000
Dedendum coefficient	[hfP*]	1.250
Tip radius factor	[rhoaP*]	0.000
Root radius factor	[rhoFP*]	0.380
Tip form height coefficient	[hFaP*]	0.000
Protuberance height factor	[hprP*]	0.000
Protuberance angle	[alfprP]	0.000
Ramp angle	[alfKP]	0.000

not topping

Information on final treatment

Dedendum reference profile (module)	[hfP*]	1.250	1.250
Tooth root radius Refer. profile (module)	[roFP*]	0.380	0.380
Addendum Reference profile (module)	[haP*]	1.000	1.000
Protuberance height (module)	[hprP*]	0.000	0.000
Protuberance angle (°)	[alfprP]	0.000	0.000
Buckling root flank height (module)	[hFaP*]	0.000	0.000
Buckling root flank angle (°)	[alfKP]	0.000	0.000

Type of profile modification:

Tip relief (µm)	[Ca]	No	2.00	2.00
-----------------	------	----	------	------

Lubrication type	oil bath lubrication	
Type of oil (Own input)	Oil: ISO-VG 320	
Lubricant base	Mineral-oil base	
Kinem. viscosity oil at 40 °C (mm ² /s)	[nu40]	320.00
Kinem. viscosity oil at 100 °C (mm ² /s)	[nu100]	22.51
FZG-Test A/8.3/90 (ISO 14635-1)	[FZGtestA]	12
Specific density at 15 °C (kg/dm ³)	[roOil]	0.902
Oil temperature (°C)	[TS]	102.000

Overall transmission ratio	[itot]	----- GEAR 1 -----	----- GEAR 2 --
Gear ratio	[u]	-0.719	
Transverse module (mm)	[mt]	1.391	
Pressure angle at Pitch circle (°)	[alfT]	3.725	
Working transverse pressure angle (°)	[alfwt]	21.173	
Working pressure angle at normal section (°) [alfwn]	[alfwt.e/i]	24.557	
Helix angle at operating pitch circle (°)	[alfwn]	24.557 / 24.515	
		23.176	
	[betaw]	20.463	
Base helix angle (°)	[betab]	18.747	
Reference centre distance (mm)	[ad]	102.427	
Sum of profile shift coefficients	[Summexi]	0.7960	
Profile shift coefficient	[x]	0.3810	0.4150
Tooth thickness (Arc) (module)	[sn*]	1.8481	1.8729
Tip alteration (mm)	[k]	-0.202	-0.202
Reference diameter (mm)	[d]	119.188	85.666
Base diameter (mm)	[dB]	111.142	79.883
Tip diameter (mm)	[da]	128.451	95.167
	[da.e/i]	128.451 / 128.441	95.167 / 95.157
Tip diameter allowances (mm)	[Ada.e/i]	0.000 / -0.010	0.000 / -0.010
Tip chamfer / tip rounding (mm)	[hK]	0.000	0.000
Tip form diameter (mm)	[dFa]	128.451	95.167
	[dFa.e/i]	128.451 / 128.441	95.167 / 95.157
Operating pitch diameter (mm)	[dw]	122.195	87.828
	[dw.e/i]	122.195 / 122.154	87.828 / 87.799
Root diameter (mm)	[df]	113.105	79.821
Generating Profile shift coefficient			
Information on preliminary treatments	[xE.e/i]	0.3575 / 0.3339	0.3915 / 0.3679
Information on final treatment	[xE.e/i]	0.3575 / 0.3339	0.3915 / 0.3679
Manufactured root diameter with xE (mm)	[df.e/i]	112.940 / 112.775	79.656 / 79.492
(calculated with preliminary treatment tool)			
Theoretical tip clearance (mm)	[c]	0.875	0.875
Effective tip clearance (mm)	[c.e/i]	1.045 / 0.923	1.045 / 0.923
Active root diameter (mm)	[dNf]	116.693	83.098
	[dNf.e/i]	116.698 / 116.641	83.103 / 83.052
Root form diameter (mm)	[dFf]	115.399	82.254

(mm)	[dFf.e/i]	115.277 / 115.156	82.146 / 82.041
(calculated with final machining tool)			
Reserve (dNf-dFf)/2 (mm)	[cF.e/i]	0.771 / 0.682	0.531 / 0.453
Addendum (mm)	[ha]	4.631	4.751
(mm)	[ha.e/i]	4.631 / 4.627	4.751 / 4.745
Dedendum (mm)	[hf]	3.041	2.922
(mm)	[hf.e/i]	3.124 / 3.206	3.005 / 3.087
Roll angle at dFa (°)	[xsi_dFa.e/i]	33.198 / 33.188	37.099 / 37.086
Roll angle to dNa (°)	[xsi_dNa.e/i]	33.198 / 33.188	37.099 / 37.086
Roll angle to dNf (°)	[xsi_dNf.e/i]	18.342 / 18.246	16.431 / 16.296
Roll angle at dFf (°)	[xsi_dFf.e/i]	15.773 / 15.538	13.734 / 13.406
Tooth height (mm)	[H]	7.673	7.673
Virtual gear no. of teeth	[zn]	37.976	27.296
Normal Tooth thickness at Tip cyl. (mm)	[san]	2.544	2.324
(mm)	[san.e/i]	2.486 / 2.416	2.264 / 2.192
Normal space width at tip cylinder (mm)	[efn]	2.654	0.000
(mm)	[efn.e/i]	2.679 / 2.705	0.000 / 0.000
Max. sliding velocity at tip (m/s)	[vga]	0.401	0.448
Specific sliding at the tip	[zetaa]	0.505	0.506
Specific sliding at the root	[zetaf]	-1.024	-1.022
Sliding factor on tip	[Kga]	0.266	0.298
Sliding factor on root	[Kgf]	-0.298	-0.266
Pitch on reference circle (mm)	[pt]		11.701
Base pitch (mm)	[pbt]		10.911
Transverse pitch on contact-path (mm)	[pet]		10.911
Lead height (mm)	[pz]	1028.765	739.425
Axial pitch (mm)	[px]		32.149
Length of path of contact (mm)	[ga, e/i]		14.418 (14.502 / 14.399)
Length T1-A, T2-A (mm)	[T1A, T2A]	17.781 (17.696/17.790)	25.862 (25.862/25.853)
Length T1-B (mm)	[T1B, T2B]	21.287 (21.287/21.278)	22.356 (22.271/22.366)
Length T1-C (mm)	[T1C, T2C]	25.392 (25.343/25.392)	18.251 (18.216/18.251)
Length T1-D (mm)	[T1D, T2D]	28.692 (28.608/28.701)	14.951 (14.951/14.942)
Length T1-E (mm)	[T1E, T2E]	32.199 (32.199/32.189)	11.444 (11.360/11.454)
Length T1-T2 (mm)	[T1T2]		43.643 (43.559 / 43.643)
Diameter of single contact point B (mm)	[d-B]	119.018 (119.018/119.011)	91.545 (91.463/91.555)
Diameter of single contact point D (mm)	[d-D]	125.082 (125.005/125.090)	85.297 (85.297/85.290)
Addendum contact ratio	[eps]	0.624 (0.628/ 0.623)	0.698 (0.701/ 0.697)
Minimal length of contact line (mm)	[Lmin]		47.872
Transverse contact ratio	[eps_a]		1.321
Transverse contact ratio with allowances	[eps_a.e/m/i]		1.329 / 1.324 / 1.320
Overlap ratio	[eps_b]		1.089
Total contact ratio	[eps_g]		2.410
Total contact ratio with allowances	[eps_g.e/m/i]		2.418 / 2.413 / 2.408

2. FACTORS OF GENERAL INFLUENCE

		----- GEAR 1 -----	GEAR 2 --
Nominal circum. force at pitch circle (N)	[Ft]		16780.2
Axial force (N)	[Fa]		6107.5
Radial force (N)	[Fr]		6499.5
Normal force (N)	[Fnorm]		19003.2
Tangent.load at p.c.d.per mm (N/mm) (N/mm)	[w]		479.43
Only as information: Forces at pitch circle:			
Nominal circumferential force (N)	[Ftw]		16367.3
Axial force (N)	[Faw]		6107.5
Radial force (N)	[Frw]		7478.8
Circumferential speed pitch d.. (m/sec)	[v]		1.47
Running-in value (µm)	[yp]		0.6
Running-in value (µm)	[yf]		0.6
Correction coefficient	[CM]		0.800
Gear body coefficient	[CR]		1.000
Reference profile coefficient	[CBS]		0.975
Material coefficient	[E/Est]		1.000
Singular tooth stiffness (N/mm/µm)	[c']		13.745
Meshing stiffness (N/mm/µm)	[cg]		17.058
Reduced mass (kg/mm)	[mRed]		0.01842
Resonance speed (min-1)	[nE1]		9082
Nominal speed (-)	[N]		0.026
Subcritical range			
Running-in value (µm)	[ya]		0.6
Bearing distance l of pinion shaft (mm)	[l]		70.000
Distance s of pinion shaft (mm)	[s]		7.000
Outside diameter of pinion shaft (mm)	[dsh]		35.000
Load according DIN 3990/1 Figure 6.8 (0:6.8a, 1:6.8b, 2:6.8c, 3:6.8d, 4:6.8e)	[-]		4

coefficient K' according to DIN 3990/1 diagram 6.8	[K']		-1.00
Without support effect			
Tooth trace deviation (active) (µm)	[Fby]		3.61
from deformation of shaft (µm)	[fsh*B1]		3.70
Tooth without tooth trace correction			
Position of Contact pattern: favorable			
from production tolerances (µm)	[fma*B2]		8.50
Tooth trace deviation, theoretical (µm)	[Fbx]		4.25
Running-in value (µm)	[yb]		0.6
Dynamic factor	[KV]		1.006
Width factor - flank	[KHb]		1.064
- Tooth root	[KFb]		1.050
- Scuffing	[KBb]		1.064
Transverse coefficient - flank	[KHα]		1.013
- Tooth root	[KFα]		1.013
- Scuffing	[KBα]		1.013
Helix angle coefficient scuffing	[Kbg]		1.206
Number of load changes (in mio.)	[NL]	141000.000	1961739.130

3. TOOTH ROOT STRENGTH

		----- GEAR 1 -----	GEAR 2 --
Calculation of Tooth form coefficients according method: B			
(Calculate tooth shape coefficient YF with addendum mod. x)			
Application factor	[KAF]	1.00	
Tooth form factor	[YF]	1.31	1.28
Stress correction factor	[YS]	2.18	2.19
Working angle (°)	[alfen]	23.03	23.77
Bending lever arm (mm)	[hF]	3.94	3.77
Tooth thickness at root (mm)	[sFn]	7.85	7.75
Tooth root radius (mm)	[roF]	1.52	1.53
(hF* = 1.124/1.077 sFn* = 2.243/2.214 roF* = 0.436/0.437 dsFn = 114.39/81.06 alfsFn = 30.00/30.00)			
Contact ratio factor	[Yeps]	1.000	
Helix angle factor	[Ybet]	0.833	
Effective facewidth (mm)	[beff]	35.00	35.00
Nominal shear stress at tooth root (N/mm²)			
	[sigF0]	326.50	320.40
Tooth root stress (N/mm²)	[sigF]	349.41	342.88
Permissible bending stress at root of Test-gear			
Support factor	[YdrelT]	1.001	1.000
Surface factor	[YRrelT]	0.957	0.957
Size coefficient (Tooth root)	[YX]	1.000	1.000
Finite life factor	[YNT]	1.000	1.000
	[YdrelT*YRrelT*YX*YNT]	0.957	0.957
Alternating bending coefficient	[YM]	1.000	1.000
Stress correction factor	[Yst]	2.00	
Limit strength tooth root (N/mm²)	[sigFG]	823.36	823.05
Permissible tooth root stress (N/mm²)			
	[sigFP=sigFG/SFmin]	588.12	587.89
Required safety	[SFmin]	1.40	1.40
Safety for Tooth root stress	[SF=sigFG/sigF]	2.36	2.40
Transmittable power (kW)	[kWRating]	41.42	42.19

4. SAFETY AGAINST PITTING (TOOTH FLANK)

		----- GEAR 1 -----	GEAR 2 --
Application factor	[KAH]	1.00	
Zone factor	[ZH]	2.183	
Elasticity coefficient (N ^{0.5} /mm)	[ZE]	189.812	
Contact ratio factor	[Zeps]	0.870	
Helix angle factor	[Zbet]	0.969	
Effective facewidth (mm)	[beff]	35.00	
Nominal flank pressure (N/mm²)	[sigH0]	1083.85	
Surface pressure at Operating pitch circle (N/mm²)			
	[sigHw]	1128.67	
Single tooth contact factor	[ZB, ZD]	1.00	1.00
Flank pressure (N/mm²)	[sigH]	1128.67	1128.67
Lubrication factor	[ZL]	1.047	1.047
Speed factor	[ZV]	0.959	0.959
Roughness factor	[ZR]	0.964	0.964

Material mating factor	[ZW]	1.000	1.000
Finite life factor	[ZNT]	1.000	1.000
	[ZL*ZV*ZR*ZNT]	0.969	0.969
Small amount of pitting permissible (0=no, 1=yes)		0	0
Size coefficient (flank)	[ZX]	1.000	1.000
Limit strength pitting (N/mm ²)	[sigHG]	1453.62	1453.62
Permissible surface pressure (N/mm ²) [sigHP=sigHG/SHmin]		1453.62	1453.62
Safety for surface pressure at pitch circle			
Required safety	[SHw]	1.29	1.29
Transmittable power (kW)	[SHmin]	1.00	1.00
Safety for stress at single tooth contact	[kWRating]	40.82	40.82
	[SHBD=sigHG/sigH]	1.29	1.29
(Safety regarding nominal torque)	[(SHBD)^2]	1.66	1.66

5. STRENGTH AGAINST SCUFFING

Calculation method according DIN3990

Application factor	[KA]	1.25	
Lubrication coefficient (for lubrication type)	[XS]	1.000	
Relative structure coefficient (Scoring)	[XWrelT]	1.000	
Thermal contact factor (N/mm/s ^{0.5} /K)	[BM]	13.795	13.795
Relevant tip relief (µm)	[Ca]	2.00	2.00
Optimal tip relief (µm)	[Ceff]	28.11	
Effective facewidth (mm)	[beff]	35.000	
Applicable circumferential force/tooth width (N/mm)	[wBt]	627.067	
Flash factor (°K*N ^{-0.75} *s ^{0.5} *m ^{-0.5} mm)	[XM]	50.002	
Pressure angle factor (eps1: 1.031, eps2: 0.624)	[Xalfbet]	0.698	
Flash temperature-criteria			
Tooth mass temperature (°C)	[theM-B]	126.54	
theM-B = theoil + XS*0.47*theflamax	[theflamax]	52.21	
Scuffing temperature (°C)	[theS]	403.59	
Coordinate gamma (point of highest temp.)	[Gamma]	0.225	
[Gamma.A]= -0.300 [Gamma.E]= 0.268			
Highest contact temp. (°C)	[theB]	178.75	
Geometry factor	[XB]	0.138	
Load sharing factor	[XGam]	1.000	
Dynamic viscosity (mPa*s)	[etaM]	9.35	
Coefficient of friction	[mym]	0.155	
Required safety	[SBmin]	2.000	
Safety factor for scuffing (flash-temp)	[SB]	3.929	
Integral temperature-criteria			
Tooth mass temperature (°C)	[theM-C]	120.46	
theM-C = theoil + XS*0.70*theflaint	[theflaint]	26.37	
Integral scuffing temperature (°C)	[theSint]	403.59	
Contact ratio factor	[Xeps]	0.315	
Dynamic viscosity (mPa*s)	[etaOil]	17.71	
Averaged coefficient of friction	[mym]	0.134	
Geometry factor	[XBE]	0.257	
Meshing factor	[XQ]	1.000	
Tip relief factor	[XCa]	1.007	
Integral tooth flank temperature (°C)	[theint]	160.01	
Required safety	[SSmin]	1.800	
Safety factor for scuffing (intg.-temp.)	[SSint]	2.522	
Safety referring to transferred torque	[SSL]	5.199	

6. MEASUREMENTS FOR TOOTH THICKNESS

	----- GEAR 1 -----	----- GEAR 2 --
Information on preliminary treatments		
Tooth thickness allowance (final treatment) (mm)		
	[As.e/i]	-0.060 / -0.120 -0.060 / -0.120
Grinding allowance (per flank) (mm)	[q]	0.000 0.000
Additional measure for preliminary treatment (mm)		
	[+Asp.e/i]	0.000 / 0.000 0.000 / 0.000
Actual base tangent length ('span') (mm)	[Wk.e/i]	49.225 / 49.168 38.447 / 38.390
Actual dimension over balls (mm)	[MdK.e/i]	131.314 / 131.183 97.565 / 97.442
Actual dimensions over 3 rolls (mm)	[Md3R.e/i]	0.000 / 0.000 97.777 / 97.654
Information on final treatment		
Tooth thickness deviation	DIN3967 d26	DIN3967 d26
Tooth thickness allowance (normal section) (mm)		
	[As.e/i]	-0.060 / -0.120 -0.060 / -0.120

Number of teeth spanned	[k]	5.000	4.000
Base tangent length (no backlash) (mm)	[Wk]	49.281	38.503
Actual base tangent length ('span') (mm)	[Wk.e/i]	49.225 / 49.168	38.447 / 38.390
Diameter of contact point (mm)	[dMWk.m]	120.511	87.777
Theoretical diameter of ball/pin (mm)	[DM]	6.263	6.492
Eff. Diameter of ball/pin (mm)	[DMeff]	6.500	6.500
Theor. dim. centre to ball (mm)	[MrK]	65.722	48.950
Actual dimension centre to ball (mm)	[MrK.e/i]	65.657 / 65.591	48.889 / 48.827
Diameter of contact point (mm)	[dMMr.m]	122.076	88.409
Diametral measurement over two balls without clearance (mm)	[MdK]	131.444	97.687
Actual dimension over balls (mm)	[MdK.e/i]	131.314 / 131.183	97.565 / 97.442
Theor. dimension over two pins (mm)	[MdR]	131.444	97.900
Actual dimension over rolls (mm)	[MdR.e/i]	131.314 / 131.183	97.777 / 97.654
Dimensions over 3 pins without clearance (mm)	[Md3R]	0.000	97.900
Actual dimensions over 3 rolls (mm)	[Md3R.e/i]	0.000 / 0.000	97.777 / 97.654
Chordal tooth thickness (no backlash) (mm)	['sn]	6.466	6.550
Actual chordal tooth thickness (mm)	['sn.e/i]	6.406 / 6.346	6.490 / 6.430
Reference chordal height from da.m (mm)	[ha]	4.706	4.859
Tooth thickness (Arc) (mm)	[sn]	6.468	6.555
(mm)	[sn.e/i]	6.408 / 6.348	6.495 / 6.435
Backlash free center distance (mm)	[aControl.e/i]	104.872	/104.732
Backlash free center distance, allowances (mm)	[jta]	-0.140	/ -0.279
Centre distance allowances (mm)	[Aa.e/i]	0.000	/ -0.035
Circumferential backlash from Aa (mm)	[jt_Aa.e/i]	0.000	/ -0.032
Radial clearance (mm)	[jx]	0.279	/ 0.105
Circumferential backlash (transverse section) (mm)	[jt]	0.262	/ 0.099
Torsional angle using fixed values gear 1 (°)		0.3503	/0.1323
Normal backlash (mm)	[jn]	0.231	/ 0.087

7. TOLERANCES

		----- GEAR 1 -----	GEAR 2 --
According ISO 1328:			
Accuracy grade	[Q-ISO1328]	6	6
Single normal pitch deviation (µm)	[fpt]	8.50	8.50
Base circle pitch deviation (µm)	[fpb]	7.50	7.50
Cumulative circular pitch deviation over z/8 pitches (µm)	[Fpz/8]	15.00	12.00
Profile deviation (µm)	[ffa]	8.50	8.50
Profile angular deviation (µm)	[fHa]	7.00	7.00
Profile total deviation (µm)	[Fa]	11.00	11.00
Helix form deviation (µm)	[fFb]	8.50	8.50
Helix slope deviation (µm)	[fHb]	8.50	8.50
Tooth helix deviation (µm)	[Fb]	12.00	12.00
Total cumulative pitch deviation (µm)	[Fp]	27.00	27.00
Runout tolerance (µm)	[Fr]	21.00	21.00
Total radial composite tolerance (µm)	[Fi"]	36.00	36.00
Tooth-to-tooth radial composite tolerance (µm)	[fi"]	14.00	14.00
Total tangential composite deviation (µm)	[Fi']	40.00	40.00
Tooth-to-tooth tangential composite deviation (µm)	[fi']	14.00	14.00
Tolerance for alignment of axes (recommendation acc. ISO/TR 10064, Quality 6)			
Maximum value for deviation error of axis (µm)	[fSigbet]	12.75	
Maximum value for inclination error of axes (µm)	[fSigdel]	25.51	

8. ADDITIONAL DATA

Torsional stiffness (MNm/rad)	[cr]	1.8	1.0
Mean coeff. of friction (acc. Niemann)	[mum]	0.089	
Wear sliding coef. by Niemann	[zetw]	0.668	
Power loss from gear load (kW)	[PVZ]	0.299	
(Meshing efficiency (%))	[etaz]	98.784)	
Weight - calculated with da (g)	[Mass]	3551.36	1949.37
Moment of inertia (System referenced to wheel 1): calculation without consideration of the exact tooth shape			
single gears ((da+df)/2...di) (kgm ²)	[TraeghMom]	0.00570	0.00157
System ((da+df)/2...di) (kgm ²)	[TraeghMom]	0.00874	

_O.System.TGB.gp2.GP2

KISSsoft - Release 04-2010E

KISSsoft evaluation

File

Name: 1st.gear_235rpm_1000Nm

Important hint: At least one warning has occurred during the calculation:

1-> Power or torque are too small.

The strength calculation does not run!

2-> Calculation according to DIN 3990, Part 41, for motor gear boxes requires a sensible tooth trace correction

Annotation:

Adjust tooth trace correction accordingly.

3-> Small line loads [w]:

The calculation of tooth contact stiffness [cg] is very uncertain.

It could result inaccurate, high values for dynamic coefficient [KV],

face load coefficient [KHb] and transverse coefficient [KH_a].

We recommend to enter these values directly

(for example KV=1.0, KHb=1.5, KH_a=1.0)

and to use a more accurate method for the calculation of cg

(see 'Tooth contact stiffness'in 'Details' of resistance window).

4-> Gear pair 1 - 2 :

The transverse coefficient, Kha, is very high

The formulae in the standard probably do not suit this case.

CALCULATION OF A HELICAL GEAR PAIR

Drawing or article number:

Gear 1: 0.000.0

Gear 2: 0.000.0

Calculation method DIN 3990 Part 41 (Vehicle gear box) Method B

Calculating according to DIN 3990, part 41

		----- GEAR 1 -----	GEAR 2 --
Power (W)	[P]	0.0000	
Speed (1/min)	[n]	327.0	278.5
Torque (Nm)	[T]	0.000	0.000
Application factor	[KAF, KAH]	1.00	1.00
Required service life	[H]	99999999.00	
Gear driving (+) / driven (-)		-	+

1. TOOTH GEOMETRY AND MATERIAL

(Geometry calculation according ISO 21771)

		----- GEAR 1 -----	GEAR 2 --
Center distance (mm)	[a]	95.011	
Centre distance tolerance		ISO 286 Measure h7	
Normal module (mm)	[mn]	3.5000	
Pressure angle at normal section (°)	[alfn]	20.0000	
Helix angle at reference circle (°)	[beta]	20.0000	
Number of teeth	[z]	23	27
Facewidth (mm)	[b]	35.00	35.00
Hand of gear		right	left
Accuracy grade	[Q-ISO1328]	6	6
Inner diameter (mm)	[di]	0.00	0.00
Inside diameter of rim (mm)	[dbi]	0.00	0.00

Material

Gear 1: 15 CrNi 6, Case-carburized steel, case-hardened

ISO 6336-5 Figure 9/10 (MQ), core strength >=25HRC Jominy J=12mm<HRC28

Gear 2: 15 CrNi 6, Case-carburized steel, case-hardened

ISO 6336-5 Figure 9/10 (MQ), core strength >=25HRC Jominy J=12mm<HRC28

		----- GEAR 1 -----	GEAR 2 --
Surface hardness		HRC 60	HRC 60
Fatigue strength. tooth root stress (N/mm ²)			
	[sigFlim]	430.00	430.00
Fatigue strength for Hertzian pressure (N/mm ²)			
	[sigHlim]	1500.00	1500.00
Tensile strength (N/mm ²)	[Rm]	1000.00	1000.00

7/47

Yield point (N/mm ²)	[Rp]	685.00	685.00
Young's modulus (N/mm ²)	[E]	206000	206000
Poisson's ratio	[ny]	0.300	0.300
Average roughness, Ra, tooth flank (µm)	[RAH]	0.60	0.60
Mean roughness height, Rz, flank (µm)	[RZH]	4.80	4.80
Mean roughness height, Rz, root (µm)	[RZF]	20.00	20.00

Information on preliminary treatments

Tool or reference profile of gear 1 :

Reference profile 1.25 / 0.38 / 1.0 ISO 53.2 Profil A			
Grinding allowance (mm)	[q]		0.000
Addendum coefficient	[haP*]		1.000
Dedendum coefficient	[hfP*]		1.250
Tip radius factor	[rhoaP*]		0.000
Root radius factor	[rhofP*]		0.380
Tip form height coefficient	[hFaP*]		0.000
Protuberance height factor	[hprP*]		0.000
Protuberance angle	[alfprP]		0.000
Ramp angle	[alfKP]		0.000

not topping

Tool or reference profile of gear 2 :

Reference profile 1.25 / 0.38 / 1.0 ISO 53.2 Profil A			
Grinding allowance (mm)	[q]		0.000
Addendum coefficient	[haP*]		1.000
Dedendum coefficient	[hfP*]		1.250
Tip radius factor	[rhoaP*]		0.000
Root radius factor	[rhofP*]		0.380
Tip form height coefficient	[hFaP*]		0.000
Protuberance height factor	[hprP*]		0.000
Protuberance angle	[alfprP]		0.000
Ramp angle	[alfKP]		0.000

not topping

Information on final treatment

Dedendum reference profile (module)	[hfP*]	1.250	1.250
Tooth root radius Refer. profile (module)	[rofP*]	0.380	0.380
Addendum Reference profile (module)	[haP*]	1.000	1.000
Protuberance height (module)	[hprP*]	0.000	0.000
Protuberance angle (°)	[alfprP]	0.000	0.000
Buckling root flank height (module)	[hFaP*]	0.000	0.000
Buckling root flank angle (°)	[alfKP]	0.000	0.000

Type of profile modification:

		No	
Tip relief (µm)	[Ca]	2.00	2.00

Lubrication type

Type of oil (Own input)		oil bath lubrication	
Lubricant base		Oil: ISO-VG 320	
		Mineral-oil base	
Kinem. viscosity oil at 40 °C (mm ² /s)	[nu40]		320.00
Kinem. viscosity oil at 100 °C (mm ² /s)	[nu100]		22.51
FZG-Test A/8.3/90 (ISO 14635-1)	[FZGtestA]		12
Specific density at 15 °C (kg/dm ³)	[roOil]		0.902
Oil temperature (°C)	[TS]		102.000

		----- GEAR 1 -----	GEAR 2 --
Overall transmission ratio	[itot]		-0.852
Gear ratio	[u]		1.174
Transverse module (mm)	[mt]		3.725
Pressure angle at Pitch circle (°)	[alft]		21.173
Working transverse pressure angle (°)	[alfwt]		23.951
	[alfwt.e/i]	23.951 / 23.903	
Working pressure angle at normal section (°)	[alfwn]		22.607
Helix angle at operating pitch circle (°)	[betaw]		20.374
	[betab]		18.747
Base helix angle (°)	[betaw]		20.374
Reference centre distance (mm)	[ad]		93.116
Sum of profile shift coefficients	[Summexi]		0.5760
Profile shift coefficient	[x]	0.4150	0.1610
Tooth thickness (Arc) (module)	[sn*]	1.8729	1.6880
Tip alteration (mm)	[k]	-0.121	-0.121
Reference diameter (mm)	[d]	85.666	100.565
Base diameter (mm)	[dB]	79.883	93.776
Tip diameter (mm)	[da]	95.329	108.450
	[da.e/i]	95.329 / 95.319	108.450 / 108.440
Tip diameter allowances (mm)	[Ada.e/i]	0.000 / -0.010	0.000 / -0.010

Tip chamfer / tip rounding (mm)	[hK]	0.000	0.000
Tip form diameter (mm)	[dFa]	95.329	108.450
(mm)	[dFa.e/i]	95.329 / 95.319	108.450 / 108.440
Operating pitch diameter (mm)	[dw]	87.410	102.612
(mm)	[dw.e/i]	87.410 / 87.378	102.612 / 102.574
Root diameter (mm)	[dF]	79.821	92.942
Generating Profile shift coefficient			
Information on preliminary treatments	[xE.e/i]	0.3915 / 0.3679	0.1375 / 0.1139
Information on final treatment	[xE.e/i]	0.3915 / 0.3679	0.1375 / 0.1139
Manufactured root diameter with xE (mm)	[dF.e/i]	79.656 / 79.492	92.777 / 92.612
(calculated with preliminary treatment tool)			
Theoretical tip clearance (mm)	[c]	0.875	0.875
Effective tip clearance (mm)	[c.e/i]	1.045 / 0.923	1.045 / 0.923
Active root diameter (mm)	[dNf]	83.037	97.082
(mm)	[dNf.e/i]	83.042 / 82.990	97.086 / 97.037
Root form diameter (mm)	[dFf]	82.254	95.898
(mm)	[dFf.e/i]	82.146 / 82.041	95.804 / 95.711
(calculated with final machining tool)			
Reserve (dNf-dFf)/2 (mm)	[cF.e/i]	0.501 / 0.422	0.687 / 0.617
Addendum (mm)	[ha]	4.831	3.943
(mm)	[ha.e/i]	4.831 / 4.826	3.943 / 3.938
Dedendum (mm)	[hf]	2.922	3.812
(mm)	[hf.e/i]	3.005 / 3.087	3.894 / 3.976
Roll angle at dFa (°)	[xi_dFa.e/i]	37.313 / 37.299	33.283 / 33.270
Roll angle to dNa (°)	[xi_dNa.e/i]	37.313 / 37.299	33.283 / 33.270
Roll angle to dNf (°)	[xi_dNf.e/i]	16.271 / 16.133	15.357 / 15.241
Roll angle at dFf (°)	[xi_dFf.e/i]	13.734 / 13.406	11.979 / 11.700
Tooth height (mm)	[H]	7.754	7.754
Virtual gear no. of teeth	[zn]	27.296	32.043
Normal Tooth thickness at Tip cyl. (mm)	[san]	2.230	2.592
(mm)	[san.e/i]	2.170 / 2.098	2.533 / 2.463
Normal space width at tip cylinder (mm)	[efn]	0.000	0.000
(mm)	[efn.e/i]	0.000 / 0.000	0.000 / 0.000
Max. sliding velocity at tip (m/s)	[vga]	0.524	0.406
Specific sliding at the tip	[zetaa]	0.589	0.512
Specific sliding at the root	[zetaf]	-1.047	-1.431
Sliding factor on tip	[Kga]	0.350	0.272
Sliding factor on root	[Kgf]	-0.272	-0.350
Pitch on reference circle (mm)	[pt]		11.701
Base pitch (mm)	[pbt]		10.911
Transverse pitch on contact-path (mm)	[pet]		10.911
Lead height (mm)	[pz]	739.425	868.020
Axial pitch (mm)	[px]		32.149
Length of path of contact (mm)	[ga, e/i]	14.678	(14.765 / 14.659)
Length T1-A, T2-A (mm)	[T1A, T2A]	26.011(26.011/26.002)	12.558(12.472/12.568)
Length T1-B (mm)	[T1B, T2B]	22.244(22.158/22.254)	16.326(16.326/16.316)
Length T1-C (mm)	[T1C, T2C]	17.742(17.702/17.742)	20.828(20.781/20.828)
Length T1-D (mm)	[T1D, T2D]	15.100(15.100/15.091)	23.470(23.384/23.479)
Length T1-E (mm)	[T1E, T2E]	11.333(11.246/11.343)	27.237(27.237/27.227)
Length T1-T2 (mm)	[T1T2]	38.570	(38.483 / 38.570)
Diameter of single contact point B (mm)	[d-B]	85.401(85.401/85.395)	104.868(104.791/104.876)
Diameter of single contact point D (mm)	[d-D]	91.436(91.352/91.446)	99.298(99.298/99.291)
Addendum contact ratio	[eps]	0.758(0.761/ 0.757)	0.587(0.592/ 0.586)
Minimal length of contact line (mm)	[Lmin]		48.682
Transverse contact ratio	[eps_a]		1.345
Transverse contact ratio with allowances	[eps_a.e/m/i]	1.353 / 1.348 / 1.343	
Overlap ratio	[eps_b]		1.089
Total contact ratio	[eps_g]		2.434
Total contact ratio with allowances	[eps_g.e/m/i]	2.442 / 2.437 / 2.432	

2. FACTORS OF GENERAL INFLUENCE

	----- GEAR 1 -----	GEAR 2 --
Nominal circum. force at pitch circle (N)	[Ft]	0.0
Axial force (N)	[Fa]	0.0
Radial force (N)	[Fr]	0.0
Normal force (N)	[Fnorm]	0.0
Tangent.load at p.c.d.per mm (N/mm) (N/mm)	[w]	0.00
Only as information: Forces at pitch circle:		
Nominal circumferential force (N)	[Ftw]	0.0
Axial force (N)	[Faw]	0.0
Radial force (N)	[Frw]	0.0
Circumferential speed pitch d.. (m/sec)	[v]	1.47
Running-in value (µm)	[yp]	0.6
Running-in value (µm)	[yf]	0.6

Correction coefficient	[CM]	0.800	
Gear body coefficient	[CR]	1.000	
Reference profile coefficient	[CBS]	0.975	
Material coefficient	[E/Est]	1.000	
Singular tooth stiffness (N/mm/μm)	[c']	0.262	
Meshing stiffness (N/mm/μm)	[cg]	0.330	
The formula for c' and cg at w*KA < 25 is imprecise! Therefore the factors KV, KHb or KHa are to high.			
Reduced mass (kg/mm)	[mRed]	0.01585	
Resonance speed (min-1)	[nE1]	1893	
Nominal speed (-)	[N]	0.173	
Subcritical range			
Running-in value (μm)	[ya]	0.6	
Bearing distance l of pinion shaft (mm)	[l]	70.000	
Distance s of pinion shaft (mm)	[s]	7.000	
Outside diameter of pinion shaft (mm)	[dsh]	35.000	
Load according DIN 3990/1 Figure 6.8 (0:6.8a, 1:6.8b, 2:6.8c, 3:6.8d, 4:6.8e)	[-]	4	
coefficient K' according to DIN 3990/1 diagram 6.8	[K']	-1.00	
Without support effect			
Tooth trace deviation (active) (μm)	[Fby]	5.82	
from deformation of shaft (μm)	[fsh*B1]	0.00	
Tooth without tooth trace correction			
Position of Contact pattern: favorable			
from production tolerances (μm)	[fma*B2]	8.50	
Tooth trace deviation, theoretical (μm)	[Fbx]	6.84	
Running-in value (μm)	[yb]	1.0	
Dynamic factor	[KV]	195294.267	
Width factor - flank			
- Tooth root	[KHb]	4.430	
- Scuffing	[KFb]	3.212	
	[KBb]	4.430	
Transverse coefficient - flank			
- Tooth root	[KHa]	2.200	
- Scuffing	[KFa]	2.200	
	[KBa]	2.200	
Helix angle coefficient scuffing	[Kbg]	1.211	
Number of load changes (in mio.)	[NL]	1961739.111	1671111.094

3. TOOTH ROOT STRENGTH

----- GEAR 1 ----- GEAR 2 --			
Calculation of Tooth form coefficients according method: B (Calculate tooth shape coefficient YF with addendum mod. x)			
Application factor	[KAF]	1.00	
Tooth form factor	[YF]	1.27	1.45
Stress correction factor	[YS]	2.20	1.99
Working angle (°)	[alfen]	23.62	21.75
Bending lever arm (mm)	[hF]	3.71	3.94
Tooth thickness at root (mm)	[sFn]	7.75	7.51
Tooth root radius (mm)	[roF]	1.53	1.74
(hF* = 1.060/1.125 sFn* = 2.214/2.145 roF* = 0.437/0.496 dsFn = 81.06/94.30 alfsFn = 30.00/30.00)			
Contact ratio factor	[Yeps]	1.000	
Helix angle factor	[Ybet]	0.833	
Effective facewidth (mm)	[beff]	35.00	35.00
Nominal shear stress at tooth root (N/mm²)			
	[sigF0]	0.00	0.00
	[sigF]	0.00	0.00
Permissible bending stress at root of Test-gear			
Support factor	[YdrelT]	1.000	0.997
Surface factor	[YRrelT]	0.957	0.957
Size coefficient (Tooth root)	[YX]	1.000	1.000
Finite life factor	[YNT]	1.000	1.000
	[YdrelT*YRrelT*YX*YNT]	0.957	0.954
Alternating bending coefficient	[YM]	1.000	1.000
Stress correction factor	[Yst]	2.00	
Limit strength tooth root (N/mm²)	[sigFG]	823.05	820.09
Permissible tooth root stress (N/mm²)	[sigFP=sigFG/SFmin]	587.89	585.78
Required safety	[SFmin]	1.40	1.40
Safety for Tooth root stress	[SF=sigFG/sigF]	9999.00	9999.00
Transmittable power (W)	[kWRating]	0.00	0.00

4. SAFETY AGAINST PITTING (TOOTH FLANK)

		----- GEAR 1 -----	----- GEAR 2 -----
Application factor	[KAH]	1.00	
Zone factor	[ZH]	2.214	
Elasticity coefficient (N ^{0.5} /mm)	[ZE]	189.812	
Contact ratio factor	[Zeps]	0.862	
Helix angle factor	[Zbet]	0.969	
Effective facewidth (mm)	[beff]	35.00	
Nominal flank pressure (N/mm ²)	[sigH0]	0.05	
Surface pressure at Operating pitch circle (N/mm ²)	[sigHw]	71.26	
Single tooth contact factor	[ZB,ZD]	1.00	1.00
Flank pressure (N/mm ²)	[sigH]	71.26	71.26
Lubrication factor	[ZL]	1.047	1.047
Speed factor	[ZV]	0.959	0.959
Roughness factor	[ZR]	0.962	0.962
Material mating factor	[ZW]	1.000	1.000
Finite life factor	[ZNT]	1.000	1.000
	[ZL*ZV*ZR*ZNT]	0.966	0.966
Small amount of pitting permissible (0=no, 1=yes)		0	0
Size coefficient (flank)	[ZX]	1.000	1.000
Limit strength pitting (N/mm ²)	[sigHG]	1449.74	1449.74
Permissible surface pressure (N/mm ²) [sigHP=sigHG/SHmin]		1449.74	1449.74
Safety for surface pressure at pitch circle			
	[SHw]	20.34	20.34
Required safety	[SHmin]	1.00	1.00
Transmittable power (W)	[kWRating]	0.00	0.00
Safety for stress at single tooth contact			
	[SHBD=sigHG/sigH]	20.34	20.34
(Safety regarding nominal torque)	[(SHBD)^2]	413.89	413.89

5. STRENGTH AGAINST SCUFFING

Calculation method according DIN3990

Application factor	[KA]	1.25	
Lubrication coefficient (for lubrication type)	[XS]	1.000	
Relative structure coefficient (Scoring)	[XWrelT]	1.000	
Thermal contact factor (N/mm/s ^{0.5} /K)	[BM]	13.795	13.795
Relevant tip relief (µm)	[Ca]	2.00	2.00
Optimal tip relief (µm)	[Ceff]	0.00	
Effective facewidth (mm)	[beff]	35.000	
Applicable circumferential force/tooth width (N/mm)	[wBt]	2.305	
Flash factor (°K*N ^{-0.75} *s ^{0.5} *m ^{-0.5})	[XM]	50.002	
Pressure angle factor (eps1: 1.023, eps2: 0.758)	[Xalfbet]	0.587	
Flash temperature-criteria			
Tooth mass temperature (°C)	[theM-B]	102.10	
theM-B = theoil + XS*0.47*theflamax	[theflamax]	0.21	
Scuffing temperature (°C)	[theS]	403.59	
Coordinate gamma (point of highest temp.)	[Gamma]	0.254	
[Gamma.A]= 0.466 [Gamma.E]= -0.361			
Highest contact temp. (°C)	[theB]	102.32	
Geometry factor	[XB]	0.170	
Load sharing factor	[XGam]	1.000	
Dynamic viscosity (mPa*s)	[etaM]	17.71	
Coefficient of friction	[mym]	0.034	
Required safety	[SBmin]	2.000	
Safety factor for scuffing (flash-temp)	[SB]	925.818	
Integral temperature-criteria			
Tooth mass temperature (°C)	[theM-C]	102.08	
theM-C = theoil + XS*0.70*theflaint	[theflaint]	0.12	
Integral scuffing temperature (°C)	[theSint]	403.59	
Contact ratio factor	[Xeps]	0.295	
Dynamic viscosity (mPa*s)	[etaOil]	17.71	
Averaged coefficient of friction	[mym]	0.034	
Geometry factor	[XBE]	0.324	
Meshing factor	[XQ]	1.000	
Tip relief factor	[XCa]	1.000	
Integral tooth flank temperature (°C)	[theint]	102.26	
Required safety	[SSmin]	1.800	
Safety factor for scuffing (intg.-temp.)	[SSint]	3.946	
Safety referring to transferred torque	[SSL]	1138.468	

6. MEASUREMENTS FOR TOOTH THICKNESS

	----- GEAR 1 -----	----- GEAR 2 --
Information on preliminary treatments		
Tooth thickness allowance (final treatment) (mm)		
	[As.e/i]	-0.060 / -0.120
Grinding allowance (per flank) (mm)	[q]	0.000
Additional measure for preliminary treatment (mm)		
	[+Asp.e/i]	0.000 / 0.000
Actual base tangent length ('span') (mm)	[Wk.e/i]	38.447 / 38.390
Actual dimension over balls (mm)	[MdK.e/i]	111.202 / 111.069
Actual dimensions over 3 rolls (mm)	[Md3R.e/i]	111.380 / 111.247
Information on final treatment		
Tooth thickness deviation	DIN3967 d26	DIN3967 d26
Tooth thickness allowance (normal section) (mm)		
	[As.e/i]	-0.060 / -0.120
Number of teeth spanned	[k]	4.000
Base tangent length (no backlash) (mm)	[Wk]	38.503
Actual base tangent length ('span') (mm)	[Wk.e/i]	38.447 / 38.390
Diameter of contact point (mm)	[dMWk.m]	87.777
Theoretical diameter of ball/pin (mm)	[DM]	6.492
Eff. Diameter of ball/pin (mm)	[DMeff]	6.500
Theor. dim. centre to ball (mm)	[MrK]	48.950
Actual dimension centre to ball (mm)	[MrK.e/i]	48.889 / 48.827
Diameter of contact point (mm)	[dMMr.m]	88.409
Diametral measurement over two balls without clearance (mm)		
	[MdK]	97.687
Actual dimension over balls (mm)	[MdK.e/i]	111.335
Theor. dimension over two pins (mm)	[MdR]	97.900
Actual dimension over rolls (mm)	[MdR.e/i]	97.777 / 97.654
Dimensions over 3 pins without clearance (mm)		
	[Md3R]	97.900
Actual dimensions over 3 rolls (mm)	[Md3R.e/i]	111.512
Chordal tooth thickness (no backlash) (mm)		
	['sn]	6.550
Actual chordal tooth thickness (mm)	['sn.e/i]	6.490 / 6.430
Reference chordal height from da.m (mm)	[ha]	4.940
Tooth thickness (Arc) (mm)	[sn]	6.555
	[sn.e/i]	6.495 / 6.435
Backlash free center distance (mm)	[aControl.e/i]	94.867 / 94.723
Backlash free center distance, allowances (mm)		
	[jta]	-0.144 / -0.287
Centre distance allowances (mm)	[Aa.e/i]	0.000 / -0.035
Circumferential backlash from Aa (mm)	[jt_Aa.e/i]	0.000 / -0.031
Radial clearance (mm)	[jr]	0.287 / 0.109
Circumferential backlash (transverse section) (mm)		
	[jt]	0.261 / 0.099
Torsional angle using fixed values gear 1 (°)		0.2969 / 0.1130
Normal backlash (mm)	[jn]	0.230 / 0.088

7. TOLERANCES

	----- GEAR 1 -----	----- GEAR 2 --
According ISO 1328:		
Accuracy grade	[Q-ISO1328]	6
Single normal pitch deviation (µm)	[fpt]	8.50
Base circle pitch deviation (µm)	[fpb]	7.50
Cumulative circular pitch deviation over z/8 pitches (µm)		
	[Fpz/8]	12.00
Profile deviation (µm)	[ffa]	8.50
Profile angular deviation (µm)	[fHa]	7.00
Profile total deviation (µm)	[Fa]	11.00
Helix form deviation (µm)	[ffb]	8.50
Helix slope deviation (µm)	[fHb]	8.50
Tooth helix deviation (µm)	[Fb]	12.00
Total cumulative pitch deviation (µm)	[Fp]	27.00
Runout tolerance (µm)	[Fr]	21.00
Total radial composite tolerance (µm)	[Fi"]	36.00
Tooth-to-tooth radial composite tolerance (µm)		
	[fi"]	14.00
Total tangential composite deviation (µm)		
	[Fi']	40.00
Tooth-to-tooth tangential composite deviation (µm)		
	[fi']	13.00

Tolerance for alignment of axes (recommendation acc. ISO/TR 10064, Quality

Maximum value for deviation error of axis (μm) 6)
 [fSigbet] 12.63
 Maximum value for inclination error of axes (μm)
 [fSigdel] 25.26

8. ADDITIONAL DATA

Torsional stiffness (MNm/rad)	[cr]	0.0		0.0
Mean coeff. of friction (acc. Niemann)	[mum]		0.071	
Wear sliding coef. by Niemann	[zetw]		0.733	
Power loss from gear load (W)	[PVZ]		0.000	
Weight - calculated with d_a (g)	[Mass]	1956.02		2531.50
Moment of inertia (System referenced to wheel 1): calculation without consideration of the exact tooth shape				
single gears $((d_a+df)/2...d_i)$ (kgm^2)	[TraeghMom]	0.00157		0.00275
System $((d_a+df)/2...d_i)$ (kgm^2)	[TraeghMom]		0.00357	

9. DETERMINATION OF TOOTHFORM

Data not available.

REMARKS:

- Specifications with [e/i] imply: Maximum [e] and Minimal value [i] with consideration of all tolerances
- Specifications with [m] imply: Mean value within tolerance
- For the backlash tolerance, the center distance tolerances and the tooth thickness deviation are taken into account. Shown is the maximal and the minimal backlash corresponding the largest resp. the smallest allowances
- The calculation is done for the Operating pitch circle..
- Details of calculation method:
 - cg according to method B
 - KV according to method B
 - KHb, KFb according method C
 - KHa, KFa according to method B

End report lines: 494

_O.System.TGB.gp3.GP3

KISSsoft - Release 04-2010E

KISSsoft evaluation

File

Name: 1st.gear_235rpm_1000Nm

Important hint: At least one warning has occurred during the calculation:

1-> Calculation according to DIN 3990, Part 41, for motor gear boxes requires a sensible tooth trace correction

Annotation:

Adjust tooth trace correction accordingly.

CALCULATION OF A HELICAL GEAR PAIR

Drawing or article number:

Gear 1: 0.000.0

Gear 2: 0.000.0

Calculation method DIN 3990 Part 41 (Vehicle gear box) Method B
Calculating according to DIN 3990, part 41

		----- GEAR 1 -----	----- GEAR 2 --
Power (kW)	[P]	24.609	
Speed (1/min)	[n]	327.0	538.5
Torque (Nm)	[T]	718.7	436.4
Application factor	[KAF, KAH]	1.00	1.00
Required service life	[H]	99999999.00	
Gear driving (+) / driven (-)		+	-

1. TOOTH GEOMETRY AND MATERIAL

(Geometry calculation according to ISO 21771)

		----- GEAR 1 -----	----- GEAR 2 --
Center distance (mm)	[a]	94.998	
Centre distance tolerance		ISO 286 Measure h7	
Normal module (mm)	[mn]	4.0000	
Pressure angle at normal section (°)	[alfn]	20.0000	
Helix angle at reference circle (°)	[beta]	20.0000	
Number of teeth	[z]	28	17
Facewidth (mm)	[b]	33.50	35.00
Hand of gear		left	right
Accuracy grade	[Q-ISO1328]	6	6
Inner diameter (mm)	[di]	0.00	0.00
Inside diameter of rim (mm)	[dbi]	0.00	0.00

Material

Gear 1: 15 CrNi 6, Case-carburized steel, case-hardened
ISO 6336-5 Figure 9/10 (MQ), core strength >=25HRC Jominy J=12mm<HRC28

Gear 2: 15 CrNi 6, Case-carburized steel, case-hardened
ISO 6336-5 Figure 9/10 (MQ), core strength >=25HRC Jominy J=12mm<HRC28

		----- GEAR 1 -----	----- GEAR 2 --
Surface hardness		HRC 60	HRC 60
Fatigue strength. tooth root stress (N/mm ²)			
	[sigFlim]	430.00	430.00
Fatigue strength for Hertzian pressure (N/mm ²)			
	[sigHlim]	1500.00	1500.00
Tensile strength (N/mm ²)	[Rm]	1000.00	1000.00
Yield point (N/mm ²)	[Rp]	685.00	685.00
Young's modulus (N/mm ²)	[E]	206000	206000
Poisson's ratio	[ny]	0.300	0.300
Average roughness, Ra, tooth flank (µm)	[RAH]	0.60	0.60
Mean roughness height, Rz, flank (µm)	[RZH]	4.80	4.80
Mean roughness height, Rz, root (µm)	[RZF]	20.00	20.00

Information on preliminary treatments

Tool or reference profile of gear 1 :

Reference profile 1.25 / 0.38 / 1.0 ISO 53.2 Profil A

Grinding allowance (mm)	[g]	0.000
Addendum coefficient	[haP*]	1.000
Dedendum coefficient	[hfP*]	1.250
Tip radius factor	[rhoaP*]	0.000
Root radius factor	[rhofP*]	0.380

Tip form height coefficient	[hFaP*]	0.000
Protuberance height factor	[hprP*]	0.000
Protuberance angle	[alfprP]	0.000
Ramp angle	[alfKP]	0.000

not topping

Tool or reference profile of gear 2 :

Reference profile 1.25 / 0.38 / 1.0 ISO 53.2 Profil A		
Grinding allowance (mm)	[g]	0.000
Addendum coefficient	[haP*]	1.000
Dedendum coefficient	[hfP*]	1.250
Tip radius factor	[rhoaP*]	0.000
Root radius factor	[rhoFP*]	0.380
Tip form height coefficient	[hFaP*]	0.000
Protuberance height factor	[hprP*]	0.000
Protuberance angle	[alfprP]	0.000
Ramp angle	[alfKP]	0.000

not topping

Information on final treatment

Dedendum reference profile (module)	[hfP*]	1.250	1.250
Tooth root radius Refer. profile (module)			
	[rofP*]	0.380	0.380
Addendum Reference profile (module)	[haP*]	1.000	1.000
Protuberance height (module)	[hprP*]	0.000	0.000
Protuberance angle (°)	[alfprP]	0.000	0.000
Buckling root flank height (module)	[hFaP*]	0.000	0.000
Buckling root flank angle (°)	[alfKP]	0.000	0.000

Type of profile modification:

Tip relief (µm)	[Ca]	No	2.00	2.00
-----------------	------	----	------	------

Lubrication type		oil bath lubrication
Type of oil (Own input)		Oil: ISO-VG 320
Lubricant base		Mineral-oil base
Kinem. viscosity oil at 40 °C (mm ² /s)	[nu40]	320.00
Kinem. viscosity oil at 100 °C (mm ² /s)	[nu100]	22.51
FZG-Test A/8.3/90 (ISO 14635-1)	[FZGtestA]	12
Specific density at 15 °C (kg/dm ³)	[roOil]	0.902
Oil temperature (°C)	[TS]	102.000

		----- GEAR 1 -----	----- GEAR 2 -----
Overall transmission ratio	[itot]	-0.607	
Gear ratio	[u]	1.647	
Transverse module (mm)	[mt]	4.257	
Pressure angle at Pitch circle (°)	[alfT]	21.173	
Working transverse pressure angle (°)	[alfwt]	19.927	
	[alfwt.e/i]	19.927 / 19.869	
Working pressure angle at normal section (°)	[alfwn]	18.829	
Helix angle at operating pitch circle (°)			
	[betaw]	19.850	
Base helix angle (°)	[betab]	18.747	
Reference centre distance (mm)	[ad]	95.776	
Sum of profile shift coefficients	[Summexi]	-0.1890	
Profile shift coefficient	[x]	-0.2400	0.0510
Tooth thickness (Arc) (module)	[sn*]	1.3961	1.6079
Tip alteration (mm)	[k]	-0.022	-0.022
Reference diameter (mm)	[d]	119.188	72.364
Base diameter (mm)	[dB]	111.142	67.479
Tip diameter (mm)	[da]	125.224	80.728
	[da.e/i]	125.224 / 125.214	80.728 / 80.718
Tip diameter allowances (mm)	[Ada.e/i]	0.000 / -0.010	0.000 / -0.010
Tip chamfer / tip rounding (mm)	[hK]	0.000	0.000
Tip form diameter (mm)	[dFa]	125.224	80.728
	[dFa.e/i]	125.224 / 125.214	80.728 / 80.718
Operating pitch diameter (mm)	[dw]	118.220	71.777
	[dw.e/i]	118.220 / 118.177	71.777 / 71.750
Root diameter (mm)	[df]	107.268	62.772
Generating Profile shift coefficient			
Information on preliminary treatments	[xE.e/i]	-0.2606 / -0.2812	0.0304 / 0.0098
Information on final treatment	[xE.e/i]	-0.2606 / -0.2812	0.0304 / 0.0098
Manufactured root diameter with xE (mm)	[df.e/i]	107.103 / 106.938	62.607 / 62.442
(calculated with preliminary treatment tool)			
Theoretical tip clearance (mm)	[c]	1.000	1.000
Effective tip clearance (mm)	[c.e/i]	1.170 / 1.048	1.170 / 1.048
Active root diameter (mm)	[dNf]	113.007	67.848
	[dNf.e/i]	113.010 / 112.970	67.850 / 67.827
Root form diameter (mm)	[dFf]	112.229	67.673

		[dFf.e/i]	112.167 / 112.106	67.640 / 67.610
(calculated with final machining tool)				
Reserve (dNf-dFf)/2 (mm)	[cF.e/i]		0.452 / 0.401	0.120 / 0.093
Addendum (mm)	[ha]		3.018	4.182
(mm)	[ha.e/i]		3.018 / 3.013	4.182 / 4.177
Deaddendum (mm)	[hf]		5.960	4.796
(mm)	[hf.e/i]		6.042 / 6.125	4.878 / 4.961
Roll angle at dFa (°)	[xsi_dFa.e/i]		29.742 / 29.730	37.625 / 37.610
Roll angle to dNa (°)	[xsi_dNa.e/i]		29.742 / 29.730	37.625 / 37.610
Roll angle to dNf (°)	[xsi_dNf.e/i]		10.548 / 10.433	6.015 / 5.822
Roll angle at dFf (°)	[xsi_dFf.e/i]		7.799 / 7.563	3.958 / 3.570
Tooth height (mm)	[H]		8.978	8.978
Virtual gear no. of teeth	[zn]		33.229	20.175
Normal Tooth thickness at Tip cyl. (mm)	[san]		3.201	2.749
(mm)	[san.e/i]		3.143 / 3.076	2.689 / 2.617
Normal space width at tip cylinder (mm)	[efn]		0.000	0.000
(mm)	[efn.e/i]		0.000 / 0.000	0.000 / 0.000
Max. sliding velocity at tip (m/s)	[vga]		0.789	0.899
Specific sliding at the tip	[zetaa]		0.798	0.720
Specific sliding at the root	[zetaf]		-2.570	-3.960
Sliding factor on tip	[Kga]		0.390	0.444
Sliding factor on root	[Kgf]		-0.444	-0.390
Pitch on reference circle (mm)	[pt]		13.373	
Base pitch (mm)	[pbt]		12.470	
Transverse pitch on contact-path (mm)	[pet]		12.470	
Lead height (mm)	[pz]		1028.765	624.607
Axial pitch (mm)	[px]		36.742	
Length of path of contact (mm)	[ga, e/i]		18.625 (18.728 / 18.605)	
Length T1-A, T2-A (mm)	[T1A, T2A]		10.221 (10.119/10.231)	22.156 (22.156/22.147)
Length T1-B (mm)	[T1B, T2B]		16.376 (16.376/16.365)	16.001 (15.899/16.012)
Length T1-C (mm)	[T1C, T2C]		20.146 (20.082/20.146)	12.232 (12.193/12.232)
Length T1-D (mm)	[T1D, T2D]		22.692 (22.589/22.701)	9.686 (9.686 / 9.677)
Length T1-E (mm)	[T1E, T2E]		28.846 (28.846/28.836)	3.531 (3.428 / 3.542)
Length T1-T2 (mm)	[T1T2]		32.378 (32.275 / 32.378)	
Diameter of single contact point B (mm)	[d-B]		115.868 (115.868/115.861)	74.683 (74.595/74.693)
Diameter of single contact point D (mm)	[d-D]		120.051 (119.973/120.058)	70.205 (70.205/70.200)
Addendum contact ratio	[eps]		0.698 (0.703 / 0.697)	0.796 (0.799 / 0.795)
Minimal length of contact line (mm)	[Lmin]		51.104	
Transverse contact ratio	[eps_a]		1.494	
Transverse contact ratio with allowances	[eps_a.e/m/i]		1.502 / 1.497 / 1.492	
Overlap ratio	[eps_b]		0.912	
Total contact ratio	[eps_g]		2.405	
Total contact ratio with allowances	[eps_g.e/m/i]		2.414 / 2.409 / 2.404	

2. FACTORS OF GENERAL INFLUENCE

	----- GEAR 1 -----	GEAR 2 --
Nominal circum. force at pitch circle (N)	[Ft]	12060.8
Axial force (N)	[Fa]	4389.8
Radial force (N)	[Fr]	4671.5
Normal force (N)	[Fnorm]	13658.5
Tangent.load at p.c.d.per mm (N/mm) (N/mm)	[w]	360.02
Only as information: Forces at pitch circle:		
Nominal circumferential force (N)	[Ftw]	12159.5
Axial force (N)	[Faw]	4389.8
Radial force (N)	[Frw]	4408.2
Circumferential speed pitch d.. (m/sec)	[v]	2.04
Running-in value (µm)	[yp]	0.6
Running-in value (µm)	[yf]	0.8
Correction coefficient	[CM]	0.800
Gear body coefficient	[CR]	1.000
Reference profile coefficient	[CBS]	0.975
Material coefficient	[E/Est]	1.000
Singular tooth stiffness (N/mm/µm)	[c']	11.380
Meshing stiffness (N/mm/µm)	[cg]	15.592
Reduced mass (kg/mm)	[mRed]	0.01284
Resonance speed (min-1)	[nE1]	11884
Nominal speed (-)	[N]	0.028
Subcritical range		
Running-in value (µm)	[ya]	0.8
Bearing distance l of pinion shaft (mm)	[l]	70.000
Distance s of pinion shaft (mm)	[s]	7.000
Outside diameter of pinion shaft (mm)	[dsh]	35.000
Load according DIN 3990/1 Figure 6.8 (0:6.8a, 1:6.8b, 2:6.8c, 3:6.8d, 4:6.8e)	[-]	4

coefficient K' according to DIN 3990/1 diagram 6.8	[K']		-1.00
Without support effect			
Tooth trace deviation (active) (μm)	[Fby]		3.61
from deformation of shaft (μm)	[fsh*B1]		2.34
Tooth without tooth trace correction			
Position of Contact pattern: favorable			
from production tolerances (μm)	[fma*B2]		8.50
Tooth trace deviation, theoretical (μm)	[Fbx]		4.25
Running-in value (μm)	[yb]		0.6
Dynamic factor	[KV]		1.007
Width factor - flank	[KHb]		1.078
- Tooth root	[KFb]		1.057
- Scuffing	[KBb]		1.078
Transverse coefficient - flank	[KH α]		1.060
- Tooth root	[KF α]		1.060
- Scuffing	[KB α]		1.060
Helix angle coefficient scuffing	[Kbg]		1.205
Number of load changes (in mio.)	[NL]	1961739.111	3231099.712

3. TOOTH ROOT STRENGTH

		----- GEAR 1 -----	GEAR 2 --
Calculation of Tooth form coefficients according method: B			
(Calculate tooth shape coefficient YF with addendum mod. x)			
Application factor	[KAF]	1.00	
Tooth form factor	[YF]	1.62	1.46
Stress correction factor	[YS]	1.75	1.89
Working angle ($^{\circ}$)	[alfen]	17.46	17.99
Bending lever arm (mm)	[hF]	4.21	3.77
Tooth thickness at root (mm)	[sFn]	7.95	7.91
Tooth root radius (mm)	[roF]	2.49	2.22
(hF* = 1.051/0.942 sFn* = 1.988/1.977 roF* = 0.623/0.554 dsFn = 109.08/64.35 alfsFn = 30.00/30.00)			
Contact ratio factor	[Yeps]	1.000	
Helix angle factor	[Ybet]	0.848	
Effective facewidth (mm)	[beff]	33.50	35.00
Nominal shear stress at tooth root (N/mm 2)			
	[sigF0]	216.68	202.30
Tooth root stress (N/mm 2)	[sigF]	244.52	228.29
Permissible bending stress at root of Test-gear			
Support factor	[YdrelT]	0.991	0.993
Surface factor	[YRrelT]	0.957	0.957
Size coefficient (Tooth root)	[YX]	1.000	1.000
Finite life factor	[YNT]	1.000	1.000
	[YdrelT*YRrelT*YX*YNT]	0.948	0.950
Alternating bending coefficient	[YM]	1.000	1.000
Stress correction factor	[Yst]	2.00	
Limit strength tooth root (N/mm 2)	[sigFG]	815.14	816.85
Permissible tooth root stress (N/mm 2)			
	[sigFP=sigFG/SFmin]	582.25	583.47
Required safety	[SFmin]	1.40	1.40
Safety for Tooth root stress	[SF=sigFG/sigF]	3.33	3.58
Transmittable power (kW)	[kWRating]	58.60	62.90

4. SAFETY AGAINST PITTING (TOOTH FLANK)

		----- GEAR 1 -----	GEAR 2 --
Application factor	[KAH]	1.00	
Zone factor	[ZH]	2.451	
Elasticity coefficient (N $^{.5}$ /mm)	[ZE]	189.812	
Contact ratio factor	[Zeps]	0.827	
Helix angle factor	[Zbet]	0.969	
Effective facewidth (mm)	[beff]	33.50	
Nominal flank pressure (N/mm 2)	[sigH0]	1054.85	
Surface pressure at Operating pitch circle (N/mm 2)			
	[sigHw]	1131.38	
Single tooth contact factor	[ZB, ZD]	1.00	1.01
Flank pressure (N/mm 2)	[sigH]	1131.38	1137.25
Lubrication factor	[ZL]	1.047	1.047
Speed factor	[ZV]	0.964	0.964
Roughness factor	[ZR]	0.962	0.962

Material mating factor	[ZW]	1.000	1.000
Finite life factor	[ZNT]	1.000	1.000
	[ZL*ZV*ZR*ZNT]	0.972	0.972
Small amount of pitting permissible (0=no, 1=yes)		0	0
Size coefficient (flank)	[ZX]	1.000	1.000
Limit strength pitting (N/mm ²)	[sigHG]	1457.37	1457.37
Permissible surface pressure (N/mm ²) [sigHP=sigHG/SHmin]		1457.37	1457.37
Safety for surface pressure at pitch circle			
Required safety	[SHw]	1.29	1.29
Transmittable power (kW)	[SHmin]	1.00	1.00
Safety for stress at single tooth contact	[kWRating]	40.83	40.41
	[SHBD=sigHG/sigH]	1.29	1.28
(Safety regarding nominal torque)	[(SHBD)^2]	1.66	1.64

5. STRENGTH AGAINST SCUFFING

Calculation method according DIN3990

Application factor	[KA]	1.25	
Lubrication coefficient (for lubrication type)	[XS]	1.000	
Relative structure coefficient (Scoring)	[XWrelT]	1.000	
Thermal contact factor (N/mm/s ^{0.5} /K)	[BM]	13.795	13.795
Relevant tip relief (µm)	[Ca]	2.00	2.00
Optimal tip relief (µm)	[Ceff]	23.09	
Effective facewidth (mm)	[beff]	33.500	
Applicable circumferential force/tooth width (N/mm)	[wBt]	499.104	
Flash factor (°K*N ^{-0.75} *s ^{0.5} *m ^{-0.5} mm)	[XM]	50.002	
Pressure angle factor (eps1: 0.965, eps2: 0.698)	[Xalfbet]	0.796	
Flash temperature-criteria			
Tooth mass temperature (°C)	[theM-B]	152.86	
theM-B = theoil + XS*0.47*theflamax	[theflamax]	108.21	
Scuffing temperature (°C)	[theS]	403.59	
Coordinate gamma (point of highest temp.)	[Gamma]	-0.711	
[Gamma.A]= -0.493 [Gamma.E]= 0.432			
Highest contact temp. (°C)	[theB]	261.07	
Geometry factor	[XB]	0.602	
Load sharing factor	[XGam]	0.333	
Dynamic viscosity (mPa*s)	[etaM]	5.47	
Coefficient of friction	[mym]	0.231	
Required safety	[SBmin]	2.000	
Safety factor for scuffing (flash-temp)	[SB]	1.896	
Integral temperature-criteria			
Tooth mass temperature (°C)	[theM-C]	129.47	
theM-C = theoil + XS*0.70*theflaint	[theflaint]	39.25	
Integral scuffing temperature (°C)	[theSint]	403.59	
Contact ratio factor	[Xeps]	0.270	
Dynamic viscosity (mPa*s)	[etaOil]	17.71	
Averaged coefficient of friction	[mym]	0.133	
Geometry factor	[XBE]	0.474	
Meshing factor	[XQ]	1.000	
Tip relief factor	[XCa]	1.012	
Integral tooth flank temperature (°C)	[theint]	188.35	
Required safety	[SSmin]	1.800	
Safety factor for scuffing (intg.-temp.)	[SSint]	2.143	
Safety referring to transferred torque	[SSL]	3.493	

6. MEASUREMENTS FOR TOOTH THICKNESS

	----- GEAR 1 -----	----- GEAR 2 --
Information on preliminary treatments		
Tooth thickness allowance (final treatment) (mm)		
	[As.e/i]	-0.060 / -0.120 -0.060 / -0.120
Grinding allowance (per flank) (mm)	[q]	0.000 0.000
Additional measure for preliminary treatment (mm)		
	[+Asp.e/i]	0.000 / 0.000 0.000 / 0.000
Actual base tangent length ('span') (mm)	[Wk.e/i]	42.489 / 42.433 30.741 / 30.685
Actual dimension over balls (mm)	[MdK.e/i]	127.275 / 127.118 82.106 / 81.973
Actual dimensions over 3 rolls (mm)	[Md3R.e/i]	0.000 / 0.000 82.427 / 82.294
Information on final treatment		
Tooth thickness deviation	DIN3967 d26	DIN3967 d26
Tooth thickness allowance (normal section) (mm)		
	[As.e/i]	-0.060 / -0.120 -0.060 / -0.120

Number of teeth spanned	[k]	4.000	3.000
Base tangent length (no backlash) (mm)	[Wk]	42.546	30.798
Actual base tangent length ('span') (mm)	[Wk.e/i]	42.489 / 42.433	30.741 / 30.685
Diameter of contact point (mm)	[dMWk.m]	118.192	73.480
Theoretical diameter of ball/pin (mm)	[DM]	6.643	6.967
Eff. Diameter of ball/pin (mm)	[DMeff]	7.000	7.000
Theor. dim. centre to ball (mm)	[MrK]	63.715	41.280
Actual dimension centre to ball (mm)	[MrK.e/i]	63.637 / 63.559	41.214 / 41.147
Diameter of contact point (mm)	[dMMr.m]	117.832	72.652
Diametral measurement over two balls without clearance (mm)	[MdK]	127.430	82.238
Actual dimension over balls (mm)	[MdK.e/i]	127.275 / 127.118	82.106 / 81.973
Theor. dimension over two pins (mm)	[MdR]	127.430	82.560
Actual dimension over rolls (mm)	[MdR.e/i]	127.275 / 127.118	82.427 / 82.294
Dimensions over 3 pins without clearance (mm)	[Md3R]	0.000	82.560
Actual dimensions over 3 rolls (mm)	[Md3R.e/i]	0.000 / 0.000	82.427 / 82.294
Chordal tooth thickness (no backlash) (mm)	['sn]	5.583	6.425
Actual chordal tooth thickness (mm)	['sn.e/i]	5.523 / 5.463	6.365 / 6.305
Reference chordal height from da.m (mm)	[ha]	3.073	4.306
Tooth thickness (Arc) (mm)	[sn]	5.584	6.432
(mm)	[sn.e/i]	5.524 / 5.464	6.372 / 6.312
Backlash free center distance (mm)	[aControl.e/i]	94.822	94.646
Backlash free center distance, allowances (mm)	[jta]	-0.176 / -0.352	
Centre distance allowances (mm)	[Aa.e/i]	0.000 / -0.035	
Circumferential backlash from Aa (mm)	[jt_Aa.e/i]	0.000 / -0.025	
Radial clearance (mm)	[jx]	0.352 / 0.141	
Circumferential backlash (transverse section) (mm)	[jt]	0.253 / 0.101	
Torsional angle using fixed values gear 1 (°)		0.4012 / 0.1604	
Normal backlash (mm)	[jn]	0.224 / 0.089	

7. TOLERANCES

		----- GEAR 1 -----	GEAR 2 ---
According ISO 1328:			
Accuracy grade	[Q-ISO1328]	6	6
Single normal pitch deviation (µm)	[fpt]	9.00	9.00
Base circle pitch deviation (µm)	[fpb]	8.50	8.50
Cumulative circular pitch deviation over z/8 pitches (µm)	[Fpz/8]	16.00	14.00
Profile deviation (µm)	[ffa]	10.00	10.00
Profile angular deviation (µm)	[fHa]	8.50	8.50
Profile total deviation (µm)	[Fa]	13.00	13.00
Helix form deviation (µm)	[fFb]	8.50	8.50
Helix slope deviation (µm)	[fHb]	8.50	8.50
Tooth helix deviation (µm)	[Fb]	12.00	12.00
Total cumulative pitch deviation (µm)	[Fp]	28.00	28.00
Runout tolerance (µm)	[Fr]	22.00	22.00
Total radial composite tolerance (µm)	[Fi"]	36.00	36.00
Tooth-to-tooth radial composite tolerance (µm)	[fi"]	14.00	14.00
Total tangential composite deviation (µm)	[Fi']	43.00	43.00
Tooth-to-tooth tangential composite deviation (µm)	[fi']	15.00	15.00
Tolerance for alignment of axes (recommendation acc. ISO/TR 10064, Quality 6)			
Maximum value for deviation error of axis (µm)	[fSigbet]	13.21	
Maximum value for inclination error of axes (µm)	[fSigdel]	26.41	

8. ADDITIONAL DATA

Torsional stiffness (MNm/rad)	[cr]	1.6	0.6
Mean coeff. of friction (acc. Niemann)	[mum]	0.091	
Wear sliding coef. by Niemann	[zetw]	1.138	
Power loss from gear load (kW)	[PVZ]	0.439	
(Meshing efficiency (%))	[etaz]	98.216)	
Weight - calculated with da (g)	[Mass]	3230.51	1402.71
Moment of inertia (System referenced to wheel 1):			
calculation without consideration of the exact tooth shape			
single gears ((da+df)/2...di) (kgm ²)	[TraeghMom]	0.00468	0.00071
System ((da+df)/2...di) (kgm ²)	[TraeghMom]	0.00660	

_O.System.TGB.s1.B56

KISSsoft - Release 04-2010E

KISSsoft evaluation

File

Name: 1st.gear_235rpm_1000Nm

Important hint: At least one warning has occurred during the calculation:

1-> Bearing1:

Cylindrical roller bearings:

The axial force should be at most 1405.6 N (at full complement roller bearings 1584.5 N), in order that a hydro-dynamical lubricant film may be formed.

More detailed input about the lubricant may be entered in the tab 'Basic Data', under 'Additional Data' and 'Enhanced bearing service life'.

2-> For one or more bearings:

The required service life is not achieved!

ROLLER BEARING ANALYSIS

Calculation method: ISO 281 and manufacturer information

- With enhanced service life calculation (Annex 1 to DIN ISO 281)

General data:

Speed (1/min)	235.000
Axial force (N)	-6107.497
Required service life (h)	20000.000

Operating temperature (°C)	102
Type of oil	Oil: ISO-VG 320
Lubricant base	Mineral-oil base
Kinematic viscosity oil at 40 °C (mm ² /s)	320.00
Specific density oil at 15 °C (kg/dm ³)	0.902
Oil lubrication with filtration, ISO 4406 -/19/16, beta40=75	
Lubricant with additive	

Roller bearing No. 1:

Bearing type	SKF *NJ 309 ECP	
Type	Cylindrical roller bearing (single row)	
Radial and axial load		
Radial force (N)	[Fr]	24667.509
Axial force (N)	[Fa]	-6107.497
Inner diameter (mm)	[d]	45.000
External diameter (mm)	[D]	100.000
Width (mm)	[B]	25.000
Dynamic load number (kN)	[C]	112.000
Static load number (kN)	[C0]	100.000
Speed limit (oil) (1/min)	[n.max]	8500
Dynamic equivalent load (N)	[P]	26358.606
Static equivalent load (N)	[P0]	24667.509
Operating viscosity (mm ² /s)	[nu]	21.205
Reference viscosity (mm ² /s)	[nul]	56.893
Fatigue load limit (kN)	[Cu]	12.900
Impurity characteristic quantity	[ec]	0.052
Service life coefficient	[aISO]	0.127
Torque of friction (Nmm)	[M]	138.404
Service life (h)	[Lh]	1115.590
Static safety factor	[S0]	4.054

Roller bearing No. 2:

Bearing type	SKF *6307
Type	Deep groove ball bearing (single row)
Bearing clearance:	normal

20/47

Radial and axial load		
Radial force (N)	[Fr]	7133.322
Axial force (N)	[Fa]	0.000
Inner diameter (mm)	[d]	35.000
External diameter (mm)	[D]	80.000
Width (mm)	[B]	21.000
Dynamic load number (kN)	[C]	35.100
Static load number (kN)	[C0]	19.000
Speed limit (oil) (l/min)	[n.max]	12000
Dynamic equivalent load (N)	[P]	7133.322
Static equivalent load (N)	[P0]	7133.322
Operating viscosity (mm ² /s)	[nu]	21.205
Reference viscosity (mm ² /s)	[nul]	63.884
Fatigue load limit (kN)	[Cu]	0.820
Impurity characteristic quantity	[ec]	0.038
Service life coefficient	[aISO]	0.141
Torque of friction (Nmm)	[M]	46.908
Service life (h)	[Lh]	1191.452
Static safety factor	[S0]	2.664

Notice:

The extended service life calculation according to DIN ISO 281 add. page 1 contains only approximate formulae for the calculation of the fatigue load boundary and the resulting values for a23 are sometimes very high..
 Torque of friction M is calculated according to the indications in the SKF catalog 2004..

End report lines: 90

O.System.TGB.s1.S1

KISSsoft - Release 04-2010E

KISSsoft evaluation

File

Name: 1st.gear_235rpm_1000Nm

Important hint: At least one warning has occurred during the calculation:

1-> Shaft 'Shaft 1':
the sum of torques is not zero.
DeltaT = -1000.000 Nm

2-> Shaft 'Shaft 1', Roller bearing 'b5':
Cylindrical roller bearings:

The axial force should be at most 1405.6 N (at full complement roller bearings 1584.5 N), in order that a hydro-dynamical lubricant film may be formed.

More detailed input about the lubricant may be entered in the tab 'Basic Data', under 'Additional Data' and 'Enhanced bearing service life'.

Analysis of shafts, axle and beams

Input data

Coordinate system shaft: see picture W-002

Label	Shaft 1
Drawing	
Initial position (mm)	0.000
Length (mm)	226.500
Speed (1/min)	235.00
Sense of rotation: clockwise	
Material	C45 (1)
Young's modulus (N/mm ²)	206000.000
Poisson's ratio nu	0.300
Specific weight (kg/m ³)	7830.000
Warmth elongation coefficient (10 ⁻⁶ /K)	11.500
Temperature (°C)	20.000
Weight of shaft (kg)	2.848
Mass moment of inertia (kgm ²)	0.007
Momentum of mass GD2 (Nm ²)	0.258
(Notice: Weight, moment of inertia and GD2 are valid for the shaft without considering gears)	
Weight towards	(0.000, 0.000,-1.000)
Regard gears as masses	
Consider deformations due to shearing	
Shear correction coefficient	1.100
Contact angle of roller bearings is considered	
Reference temperature (°C)	50.000

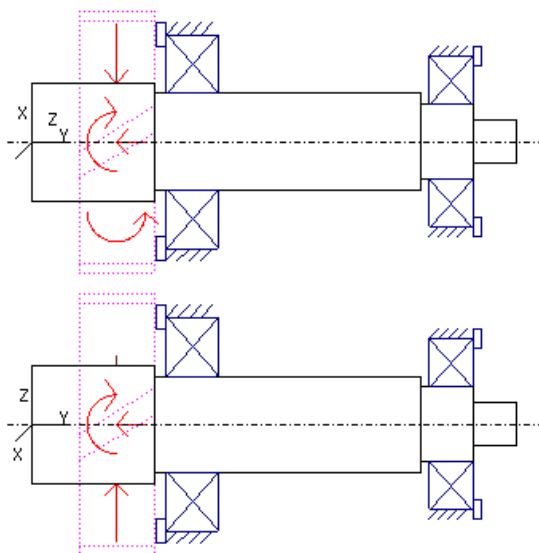


Figure: Load applications

SHAFT GEOMETRY, BEARING AND FORCES

Shaft 'Shaft 1':

Cylinder outside ('Cylinder')		y= 0.00...57.00 (mm)
d=55.00 (mm), l=57.00 (mm), Rz= 8.0		
Cylinder outside ('Cylinder')		y= 57.00...181.50 (mm)
d=45.00 (mm), l=124.50 (mm), Rz= 8.0		
Cylinder outside ('Cylinder')		y= 181.50...206.50 (mm)
d=35.00 (mm), l=25.00 (mm), Rz= 8.0		
Cylinder outside ('Cylinder')		y= 206.50...226.50 (mm)
d=20.00 (mm), l=20.00 (mm), Rz= 8.0		
Splined shaft: da=31.50 mm df=29.00 mm z=16.00		y= 179.50...233.50 (mm)
Form=A l=54.00 mm Rz= 8.0		
Coupling ('cInput(Input)')		y= 234.00 (mm)
Eff. Diameter	(mm)	31.5000
Radial force coefficient	(-)	0.0000
Direction of radial force	(°)	0.0000
Axial force coefficient	(-)	0.0000
Width of force input	(mm)	54.0000
Power	(kW)	24.6091
Torque	(Nm)	1000.0000
Mass	(kg)	0.0000
		driven (Input)
Cylindrical gear ('z1(gp1)')		y= 39.50 (mm)
Reference diameter	(mm)	122.1950
Helix angle	(°)	20.4632
Pressure angle	(°)	23.1758
Position of contact point	(°)	0.0000
Width of force input	(mm)	35.0000
Power	(kW)	24.6091
Torque	(Nm)	-1000.0000
		driving (Output)

Axial force	(N)	-6107.4969
Shear force X	(N)	-7478.7784
Shear force Z	(N)	16367.2818
Bending moment X	(Nm)	0.0000
Bending moment Z	(Nm)	-373.1528

Coupling ('f 2')			y= 234.00 (mm)
Eff. Diameter	(mm)	29.0000	
Radial force coefficient	(-)	0.0000	
Direction of radial force	(°)	0.0000	
Axial force coefficient	(-)	0.0000	
Width of force input	(mm)	54.0000	
Power	(kW)	24.6091	driven (Input)
Torque	(Nm)	1000.0000	
Mass	(kg)	0.0000	

Set fixed bearing left

Cylindrical roller bearing (single row) (SKF *NJ 309 ECP)	y= 75.00 (mm)
d=45.00 (mm), D=100.00 (mm), B=25.00 (mm), r=1.50 (mm)	
C=112.000 kN, C0=100.000 kN, Cu=12.900 kN	

Set fixed bearing right

Deep groove ball bearing (single row) (SKF *6307)	y= 196.00 (mm)
d=35.00 (mm), D=80.00 (mm), B=21.00 (mm), r=1.50 (mm)	
C=35.100 kN, C0=19.000 kN, Cu=0.820 kN	

Shaft 'Shaft 1': The mass of the following element is taken into account (y= 39.5000 (mm)):

Cylindrical gear 'z1(gp1)'
m (yS= 39.5000 (mm)): 2.5628 (kg)
Jp: 0.0058 (kg*m2), Jxx: 0.0031 (kg*m2), Jzz: 0.0031 (kg*m2)

Probability of failure	[n]	10.00	%
------------------------	-----	-------	---

Shaft 'Shaft 1' Roller bearing 'b5'

Position (Y-co-ordinate)	[y]	75.00	mm
Equivalent load	[P]	26.36	kN
Equivalent load	[P0]	24.67	kN
Life modification factor for reliability[a1]		1.000	
Service life	[Lnh]	8812.51	h
static safety factor	[S0]	4.05	
Bearing reaction force	[Fx]	12.757	kN
Bearing reaction force	[Fy]	6.107	kN
Bearing reaction force	[Fz]	-21.113	kN
Bearing reaction force	[Fr]	24.668	kN
Torque of friction	[Mloss]	3.30	Nm
Displacement of bearing	[ux]	-0.000	mm
Displacement of bearing	[uy]	-0.010	mm
Displacement of bearing	[uz]	0.000	mm
Displacement of bearing	[ur]	0.000	mm
Misalignment of bearing	[rx]	-0.611	mrاد (-2.1')
Misalignment of bearing	[ry]	2.175	mrاد (7.48')
Misalignment of bearing	[rz]	-0.673	mrاد (-2.31')
Misalignment of bearing	[rr]	0.909	mrاد (3.12')

Shaft 'Shaft 1' Roller bearing 'b6'

Position (Y-co-ordinate)	[y]	196.00	mm
Equivalent load	[P]	7.13	kN
Equivalent load	[P0]	7.13	kN
Life modification factor for reliability[a1]		1.000	
Service life	[Lnh]	8449.42	h
static safety factor	[S0]	2.66	
Bearing reaction force	[Fx]	-5.278	kN
Bearing reaction force	[Fy]	0.000	kN
Bearing reaction force	[Fz]	4.799	kN
Bearing reaction force	[Fr]	7.133	kN
Torque of friction	[Mloss]	0.23	Nm
Displacement of bearing	[ux]	0.000	mm
Displacement of bearing	[uy]	-0.052	mm
Displacement of bearing	[uz]	-0.000	mm
Displacement of bearing	[ur]	0.000	mm
Misalignment of bearing	[rx]	0.256	mrاد (0.88')
Misalignment of bearing	[ry]	11.338	mrاد (38.98')

Misalignment of bearing	[rz]	0.282	mrad	(0.97')
Misalignment of bearing	[rr]	0.381	mrad	(1.31')

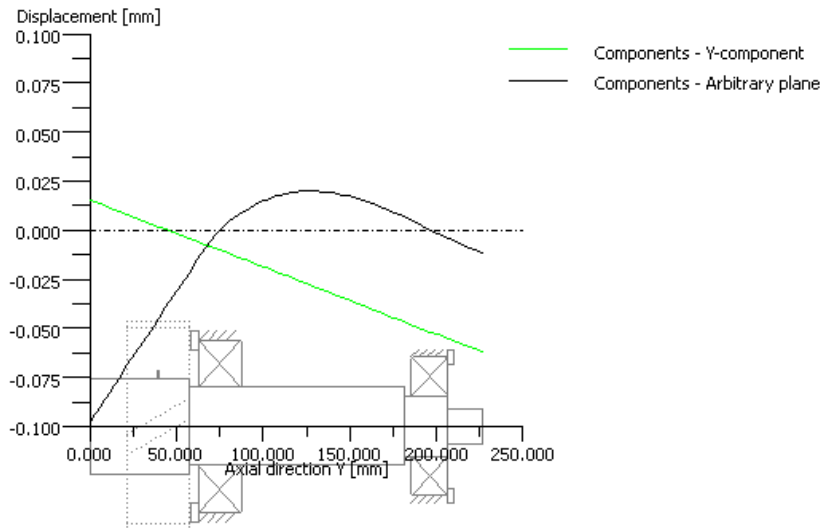


Figure: Displacement (bending etc.) (Arbitrary plane -41.46746 °)

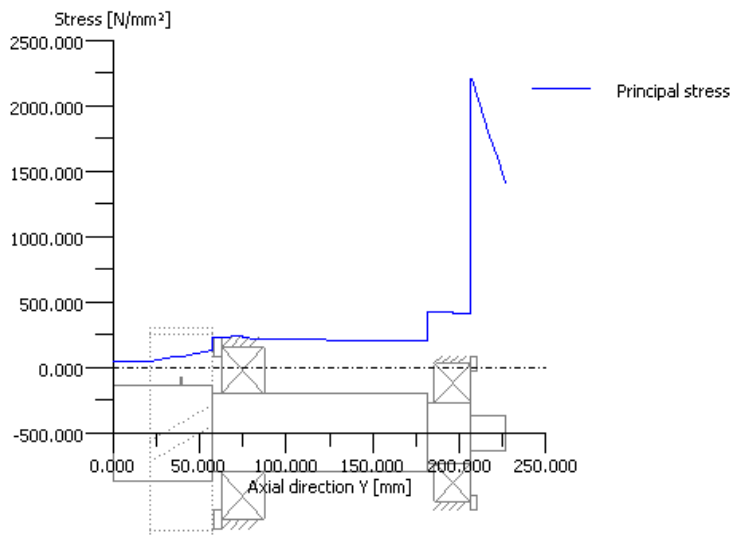


Figure: Principal stress

_O.System.TGB.s2.B34

KISSsoft - Release 04-2010E

KISSsoft evaluation

File

Name: 1st.gear_235rpm_1000Nm

Important hint: At least one warning has occurred during the calculation:

1-> For one or more bearings:
The required service life is not achieved!

ROLLER BEARING ANALYSIS

Calculation method: ISO 281 and manufacturer information

- With enhanced service life calculation (Annex 1 to DIN ISO 281)

General data:
Speed (1/min) 326.957
Axial force (N) 10497.274
Pretension force (N) 3477.709
Required service life (h) 20000.000

Operating temperature (°C) 102
Type of oil Oil: ISO-VG 320
Lubricant base Mineral-oil base
Kinematic viscosity oil at 40 °C (mm²/s) 320.00
Specific density oil at 15 °C (kg/dm³) 0.902
Oil lubrication with filtration, ISO 4406 -/19/16, beta40=75
Lubricant with additive

Roller bearing No. 1:

Bearing type SKF 32306 J2/Q
Type Taper roller bearing (single row)
Bearings in face-to-face arrangement
Radial force (N) [Fr] 13215.292
Axial force (N) [Fa] -3477.709

Inner diameter (mm) [d] 30.000
External diameter (mm) [D] 72.000
Width (mm) [T] 28.750
Dynamic load number (kN) [C] 76.500
Static load number (kN) [C0] 85.000
Speed limit (oil) (1/min) [n.max] 10000
Dynamic equivalent load (N) [P] 13215.292
Static equivalent load (N) [P0] 13215.292
Operating viscosity (mm²/s) [nu] 21.205
Reference viscosity (mm²/s) [nu1] 51.570
Fatigue load limit (kN) [Cu] 9.650
Impurity characteristic quantity [ec] 0.038
Service life coefficient [aISO] 0.132
Torque of friction (Nmm) [M] 192.943

Service life (h) [Lh] 2351.118
Static safety factor [S0] 6.432

Roller bearing No. 2:

Bearing type SKF 32306 J2/Q
Type Taper roller bearing (single row)
Bearings in face-to-face arrangement
Radial force (N) [Fr] 16415.060
Axial force (N) [Fa] 13974.983

Inner diameter (mm) [d] 30.000
External diameter (mm) [D] 72.000
Width (mm) [T] 28.750
Dynamic load number (kN) [C] 76.500
Static load number (kN) [C0] 85.000
Speed limit (oil) (1/min) [n.max] 10000

Dynamic equivalent load (N)	[P]	33118.492
Static equivalent load (N)	[P0]	23580.012
Operating viscosity (mm ² /s)	[nu]	21.205
Reference viscosity (mm ² /s)	[nul]	51.570
Fatigue load limit (kN)	[Cu]	9.650
Impurity characteristic quantity	[ec]	0.038
Service life coefficient	[aISO]	0.121
Torque of friction (Nmm)	[M]	294.532
Service life (h)	[Lh]	100.783
Static safety factor	[S0]	3.605

Notice:

The extended service life calculation according to DIN ISO 281 add. page 1 contains only approximate formulae

for the calculation of the fatigue load boundary and the resulting values for a23 are sometimes very high..

Torque of friction M is calculated according to the indications in the SKF catalog 2004..

End report lines: 90

_O.System.TGB.s2.S2

KISSsoft - Release 04-2010E

KISSsoft evaluation

File

Name: 1st.gear_235rpm_1000Nm

Analysis of shafts, axle and beams

Input data

Coordinate system shaft: see picture W-002

Label	Shaft 1
Drawing	
Initial position (mm)	0.000
Length (mm)	185.000
Speed (1/min)	326.96
Sense of rotation: counterclockwise	
Material	C45 (1)
Young's modulus (N/mm ²)	206000.000
Poisson's ratio nu	0.300
Specific weight (kg/m ³)	7830.000
Warmth elongation coefficient (10 ⁻⁶ /K)	11.500
Temperature (°C)	20.000
Weight of shaft (kg)	2.369
Mass moment of inertia (kgm ²)	0.001
Momentum of mass GD ² (Nm ²)	0.030
Weight towards	(0.000, 0.000,-1.000)
Consider deformations due to shearing	
Shear correction coefficient	1.100
Contact angle of roller bearings is considered	
Reference temperature (°C)	50.000

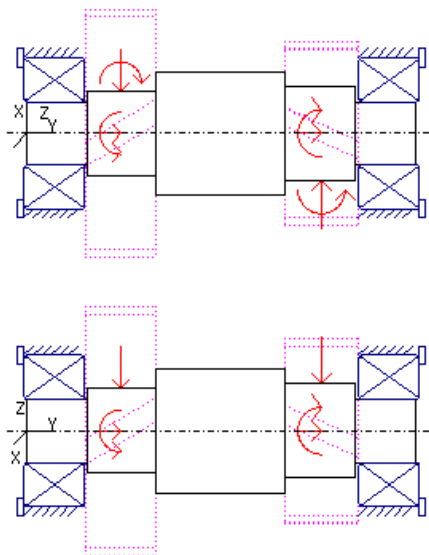


Figure: Load applications

SHAFT GEOMETRY, BEARING AND FORCES

Shaft 'Shaft 1':

<u>Cylinder outside ('Cylinder')</u>		y= 0.00...28.50 (mm)
d=30.00 (mm), l=28.50 (mm), Rz= 8.0		
<u>Cylinder outside ('Cylinder')</u>		y= 28.50...61.50 (mm)
d=40.00 (mm), l=33.00 (mm), Rz= 8.0		
Groove (e): l=30.00 mm Rz= 8.0		y= 30.00...60.00 (mm)
<u>Cylinder outside ('Cylinder')</u>		y= 61.50...122.50 (mm)
d=59.00 (mm), l=61.00 (mm), Rz= 8.0		
<u>Cylinder outside ('Cylinder')</u>		y= 122.50...156.50 (mm)
d=45.00 (mm), l=34.00 (mm), Rz= 8.0		
Groove (e): l=31.00 mm Rz= 8.0		y= 124.00...155.00 (mm)
<u>Cylinder outside ('Cylinder')</u>		y= 156.50...185.00 (mm)
d=30.00 (mm), l=28.50 (mm), Rz= 8.0		
<u>Cylindrical gear ('z2(gp1)')</u>		y= 140.25 (mm)
Reference diameter	(mm)	87.8278
Helix angle	(°)	20.4632 right
Pressure angle	(°)	23.1758
Position of contact point	(°)	180.0000
Width of force input	(mm)	35.0000
Power	(kW)	24.6091 driven (Input)
Torque	(Nm)	-718.7500
Axial force	(N)	6107.4869
Shear force X	(N)	7478.7661
Shear force Z	(N)	-16367.2550
Bending moment X	(Nm)	-0.0000
Bending moment Z	(Nm)	-268.2036
<u>Cylindrical gear ('z2(gp2)')</u>		y= 140.25 (mm)
Reference diameter	(mm)	87.4098
Helix angle	(°)	20.3739 right
Pressure angle	(°)	22.6073
Position of contact point	(°)	0.0000
Width of force input	(mm)	35.0000
Torque	(Nm)	0.0000
<u>Cylindrical gear ('z3(gp3)')</u>		y= 44.50 (mm)
Reference diameter	(mm)	118.2200
Helix angle	(°)	19.8504 left
Pressure angle	(°)	18.8287
Position of contact point	(°)	0.0000
Width of force input	(mm)	33.5000
Power	(kW)	24.6091 driving (Output)
Torque	(Nm)	718.7500
Axial force	(N)	4389.7876
Shear force X	(N)	-4408.1629
Shear force Z	(N)	-12159.5331
Bending moment X	(Nm)	-0.0000
Bending moment Z	(Nm)	259.4803
Set fixed bearing left		
<u>Taper roller bearing (single row) (SKF 32306 J2/Q)</u>		y= 13.00 (mm)
d=30.00 (mm), D=72.00 (mm), B=28.75 (mm), r=1.50 (mm)		
C=76.500 kN, C0=85.000 kN, Cu=9.650 kN		
The bearing pressure angle will be considered in the calculation		
Position (center of pressure)	(mm)	16.6250
Set fixed bearing right		
<u>Taper roller bearing (single row) (SKF 32306 J2/Q)</u>		y= 172.50 (mm)
d=30.00 (mm), D=72.00 (mm), B=28.75 (mm), r=1.50 (mm)		
C=76.500 kN, C0=85.000 kN, Cu=9.650 kN		

The bearing pressure angle will be considered in the calculation
 Position (center of pressure) (mm) 168.8750

Probability of failure	[n]	10.00	%	
Shaft 'Shaft 1' Roller bearing 'b3'				
Position (Y-co-ordinate)	[y]	13.00	mm	
Equivalent load	[P]	13.22	kN	
Equivalent load	[P0]	13.22	kN	
Life modification factor for reliability[a1]		1.000		
Service life	[Lnh]	17754.47	h	
static safety factor	[S0]	6.43		
Bearing reaction force	[Fx]	2.252	kN	
Bearing reaction force	[Fy]	3.478	kN	
Bearing reaction force	[Fz]	13.022	kN	
Bearing reaction force	[Fr]	13.215	kN	
Bearing reaction moment	[Mx]	47.20	Nm	
Bearing reaction moment	[My]	0.00	Nm	
Bearing reaction moment	[Mz]	-8.16	Nm	
Bearing reaction moment	[Mr]	47.91	Nm	
Torque of friction	[Mloss]	0.31	Nm	
Displacement of bearing	[ux]	0.001	mm	
Displacement of bearing	[uy]	0.070	mm	
Displacement of bearing	[uz]	0.002	mm	
Displacement of bearing	[ur]	0.002	mm	
Misalignment of bearing	[rx]	-0.571	mrاد	(-1.96')
Misalignment of bearing	[ry]	0.000	mrاد	(0')
Misalignment of bearing	[rz]	0.238	mrاد	(0.82')
Misalignment of bearing	[rr]	0.618	mrاد	(2.13')
Shaft 'Shaft 1' Roller bearing 'b4'				
Position (Y-co-ordinate)	[y]	172.50	mm	
Equivalent load	[P]	33.12	kN	
Equivalent load	[P0]	23.58	kN	
Life modification factor for reliability[a1]		1.000		
Service life	[Lnh]	830.48	h	
static safety factor	[S0]	3.60		
Bearing reaction force	[Fx]	-5.323	kN	
Bearing reaction force	[Fy]	-13.975	kN	
Bearing reaction force	[Fz]	15.528	kN	
Bearing reaction force	[Fr]	16.415	kN	
Bearing reaction moment	[Mx]	-56.29	Nm	
Bearing reaction moment	[My]	0.00	Nm	
Bearing reaction moment	[Mz]	-19.30	Nm	
Bearing reaction moment	[Mr]	59.50	Nm	
Torque of friction	[Mloss]	1.16	Nm	
Displacement of bearing	[ux]	0.000	mm	
Displacement of bearing	[uy]	0.010	mm	
Displacement of bearing	[uz]	0.002	mm	
Displacement of bearing	[ur]	0.002	mm	
Misalignment of bearing	[rx]	0.537	mrاد	(1.85')
Misalignment of bearing	[ry]	-1.481	mrاد	(-5.09')
Misalignment of bearing	[rz]	-0.088	mrاد	(-0.3')
Misalignment of bearing	[rr]	0.544	mrاد	(1.87')

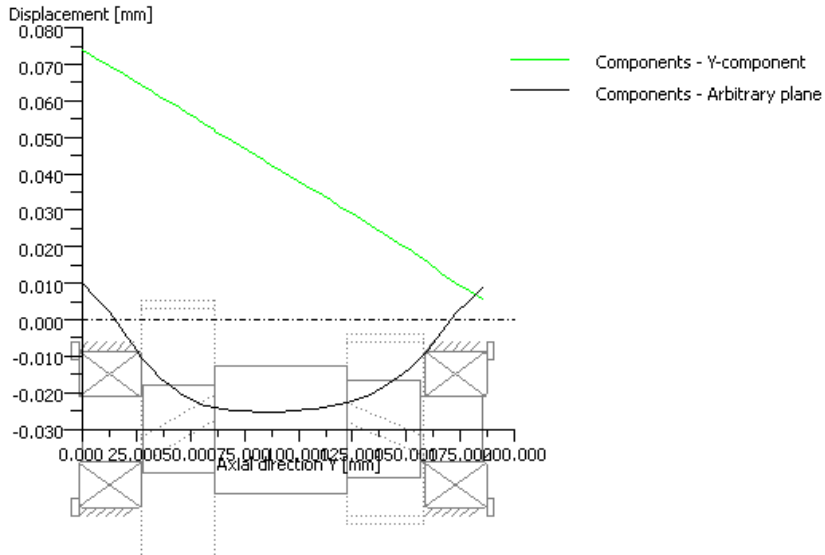


Figure: Displacement (bending etc.) (Arbitrary plane 73.447604 °)

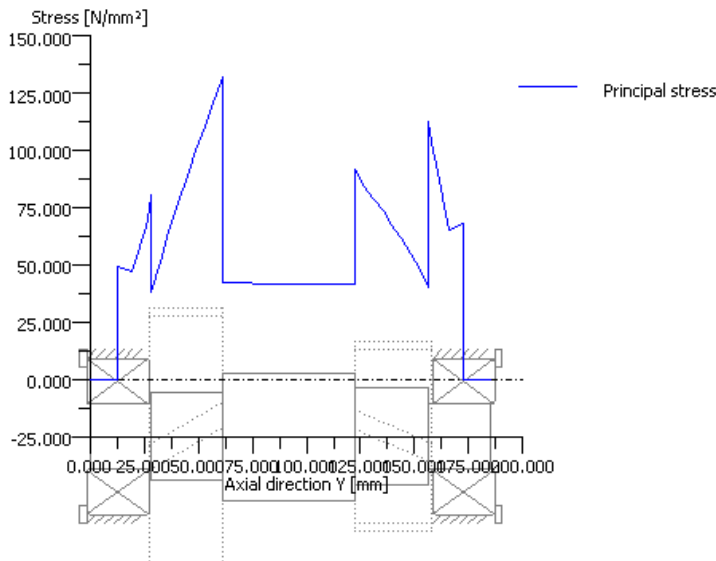


Figure: Principal stress

_O.System.TGB.s3.B12

KISSsoft - Release 04-2010E

KISSsoft evaluation

File

Name: 1st.gear_235rpm_1000Nm

Important hint: At least one warning has occurred during the calculation:

1-> Bearing2:

The fatigue load limit is not specified in the database.
An approximation equation according to ISO 281 (2007) B3.3 will be used.

2-> For one or more bearings:

The required service life is not achieved!
The static margin of safety is low (in range 0.5 - 2.0).
Please check whether these values are acceptable or not.

ROLLER BEARING ANALYSIS

Calculation method: ISO 281 and manufacturer information

- With enhanced service life calculation (Annex 1 to DIN ISO 281)

General data:

Speed (1/min) 538.517
Axial force (N) -4389.780
Required service life (h) 20000.000

Operating temperature (°C) 102

Type of oil Oil: ISO-VG 320
Lubricant base Mineral-oil base
Kinematic viscosity oil at 40 °C (mm²/s) 320.00
Specific density oil at 15 °C (kg/dm³) 0.902
Oil lubrication with filtration, ISO 4406 -/19/16, beta40=75
Lubricant with additive

Roller bearing No. 1:

Bearing type SKF *6307
Type Deep groove ball bearing (single row)
Bearing clearance: normal
Radial and axial load
Radial force (N) [Fr] 10008.625
Axial force (N) [Fa] -4389.780

Inner diameter (mm) [d] 35.000
External diameter (mm) [D] 80.000
Width (mm) [B] 21.000
Dynamic load number (kN) [C] 35.100
Static load number (kN) [C0] 19.000
Speed limit (oil) (1/min) [n.max] 12000
Dynamic equivalent load (N) [P] 10871.532
Static equivalent load (N) [P0] 10008.625
Operating viscosity (mm²/s) [nu] 21.205
Reference viscosity (mm²/s) [nu1] 32.098
Fatigue load limit (kN) [Cu] 0.820
Impurity characteristic quantity [ec] 0.060
Service life coefficient [aISO] 0.214
Torque of friction (Nmm) [M] 197.008

Service life (h) [Lh] 223.318
Static safety factor [S0] 1.898

Roller bearing No. 2:

Bearing type Koyo 63/32
Type Deep groove ball bearing (single row)
Bearing clearance: normal
Radial and axial load
Radial force (N) [Fr] 3041.641
Axial force (N) [Fa] 0.000

32/47

Inner diameter (mm)	[d]	32.000
External diameter (mm)	[D]	75.000
Width (mm)	[B]	20.000
Dynamic load number (kN)	[C]	30.100
Static load number (kN)	[C0]	16.200
Speed limit (oil) (1/min)	[n.max]	11000
Dynamic equivalent load (N)	[P]	3041.641
Static equivalent load (N)	[P0]	3041.641
Operating viscosity (mm ² /s)	[nu]	21.205
Reference viscosity (mm ² /s)	[nu1]	33.277
Fatigue load limit (kN)	[Cu]	0.736
Impurity characteristic quantity	[ec]	0.054
Service life coefficient	[aISO]	0.292
Torque of friction (Nmm)	[M]	34.077
Service life (h)	[Lh]	8758.825
Static safety factor	[S0]	5.326

Notice:

The extended service life calculation according to DIN ISO 281 add. page 1 contains only approximate formulae for the calculation of the fatigue load boundary and the resulting values for a23 are sometimes very high..
 Torque of friction M is calculated according to the indications in the SKF catalog 2004..

End report lines: 91

_O.System.TGB.s3.S3

KISSsoft - Release 04-2010E

KISSsoft evaluation

File

Name: 1st.gear_235rpm_1000Nm

Important hint: At least one warning has occurred during the calculation:

1-> For one or more bearings:

The static margin of safety is low (in range 0.5 - 2.0).
Please check whether these values are acceptable or not.

2-> Shaft 'Shaft 1', Roller bearing 'b2':

The fatigue load limit is not specified in the database.
An approximation equation according to ISO 281 (2007) B3.3 will be used.

Analysis of shafts, axle and beams

Input data

Coordinate system shaft: see picture W-002

Label	Shaft 1
Drawing	
Initial position (mm)	0.000
Length (mm)	251.500
Speed (1/min)	538.52
Sense of rotation: clockwise	
Material	C45 (1)
Young's modulus (N/mm ²)	206000.000
Poisson's ratio nu	0.300
Specific weight (kg/m ³)	7830.000
Warmth elongation coefficient (10 ⁻⁶ /K)	11.500
Temperature (°C)	20.000
Weight of shaft (kg)	2.604
Mass moment of inertia (kgm ²)	0.001
Momentum of mass GD2 (Nm ²)	0.044
(Notice: Weight, moment of inertia and GD2 are valid for the shaft without considering gears)	
Weight towards	(0.000, 0.000,-1.000)
Regard gears as masses	
Consider deformations due to shearing	
Shear correction coefficient	1.100
Contact angle of roller bearings is considered	
Reference temperature (°C)	50.000

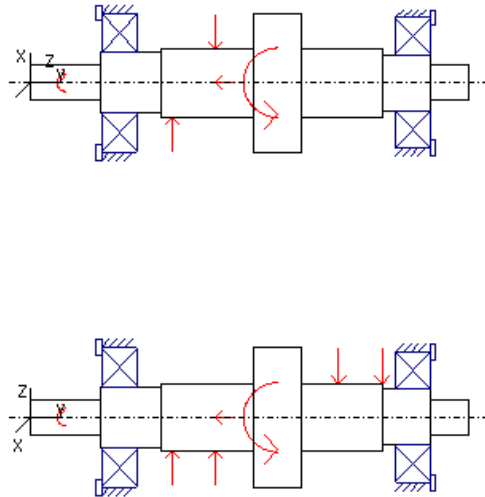


Figure: Load applications

SHAFT GEOMETRY, BEARING AND FORCES

Shaft 'Shaft 1':

Cylinder outside ('Cylinder')	y= 0.00...40.00 (mm)
d=20.00 (mm), l=40.00 (mm), Rz= 8.0	
Splined shaft: da=31.50 mm df=29.00 mm z= 6.00	y= -20.00...20.00 (mm)
Form=A l=40.00 mm Rz= 8.0	
Cylinder outside ('Cylinder')	y= 40.00...75.00 (mm)
d=35.00 (mm), l=35.00 (mm), Rz= 8.0	
Cylinder outside ('Cylinder')	y= 75.00...128.00 (mm)
d=39.00 (mm), l=53.00 (mm), Rz= 8.0	
Cylinder outside ('Cylinder')	y= 128.00...155.50 (mm)
d=80.00 (mm), l=27.50 (mm), Rz= 8.0	
Cylinder outside ('Cylinder')	y= 155.50...202.50 (mm)
d=39.00 (mm), l=47.00 (mm), Rz= 8.0	
Cylinder outside ('Cylinder')	y= 202.50...229.50 (mm)
d=32.00 (mm), l=27.00 (mm), Rz= 8.0	
Cylinder outside ('Cylinder')	y= 229.50...251.50 (mm)
d=20.00 (mm), l=22.00 (mm), Rz= 8.0	
Splined shaft: da=31.50 mm df=29.00 mm z= 6.00	y= 218.50...240.50 (mm)
Form=A l=22.00 mm Rz= 8.0	
Coupling ('cOutput(cOutput)')	y= 20.00 (mm)
Eff. Diameter (mm)	31.5000
Radial force coefficient (-)	0.0000
Direction of radial force (°)	0.0000
Axial force coefficient (-)	0.0000

Width of force input	(mm)	40.0000	
Power	(kW)	24.6091	driving (Output)
Torque	(Nm)	-436.3840	
Mass	(kg)	0.0000	
<hr/>			
Coupling ('cShift(c24)')			y= 142.00 (mm)
Eff. Diameter	(mm)	90.0000	
Radial force coefficient	(-)	0.0000	
Direction of radial force	(°)	0.0000	
Axial force coefficient	(-)	0.0000	
Width of force input	(mm)	10.0000	
<hr/>			
Torque	(Nm)	-0.0000	
Mass	(kg)	0.0000	
<hr/>			
Coupling ('cShift(c35)')			y= 142.00 (mm)
Eff. Diameter	(mm)	90.0000	
Radial force coefficient	(-)	0.0000	
Direction of radial force	(°)	0.0000	
Axial force coefficient	(-)	0.0000	
Width of force input	(mm)	10.0000	
Power	(kW)	24.6091	driven (Input)
Torque	(Nm)	436.3840	
Mass	(kg)	0.0000	
<hr/>			
Centric force ('f10')			y= 176.75 (mm)
Width of force input	(mm)	0.0000	
<hr/>			
Torque	(Nm)	-0.0000	
Axial force	(N)	0.0000	
Shear force X	(N)	-0.0000	
Shear force Z	(N)	-9.7490	
Bending moment X	(Nm)	-0.0000	
Bending moment Z	(Nm)	-0.0000	
<hr/>			
Centric force ('f11')			y= 201.75 (mm)
Width of force input	(mm)	0.0000	
<hr/>			
Torque	(Nm)	-0.0000	
Axial force	(N)	-0.0000	
Shear force X	(N)	-0.0000	
Shear force Z	(N)	-9.5536	
Bending moment X	(Nm)	-0.0000	
Bending moment Z	(Nm)	-0.0000	
<hr/>			
Centric force ('f8')			y= 81.00 (mm)
Width of force input	(mm)	0.0000	
<hr/>			
Torque	(Nm)	-0.0000	
Axial force	(N)	-0.0000	
Shear force X	(N)	8505.7400	
Shear force Z	(N)	6075.8800	
Bending moment X	(Nm)	-0.0000	
Bending moment Z	(Nm)	-0.0000	
<hr/>			
Centric force ('f9')			y= 106.00 (mm)
Width of force input	(mm)	0.0000	
<hr/>			
Torque	(Nm)	-0.0000	
Axial force	(N)	-4389.7800	
Shear force X	(N)	-4097.5900	
Shear force Z	(N)	6075.6800	
Bending moment X	(Nm)	-0.0000	
Bending moment Z	(Nm)	-0.0000	
<hr/>			
Coupling ('f 7')			y= 20.00 (mm)
Eff. Diameter	(mm)	29.0000	
Radial force coefficient	(-)	0.0000	
Direction of radial force	(°)	0.0000	
Axial force coefficient	(-)	0.0000	
Width of force input	(mm)	40.0000	
Power	(kW)	24.6091	driving (Output)
Torque	(Nm)	-436.3840	
Mass	(kg)	0.0000	

Coupling ('f 8')			y= 142.00 (mm)
Eff. Diameter	(mm)	0.0000	
Radial force coefficient	(-)	0.0000	
Direction of radial force	(°)	0.0000	
Axial force coefficient	(-)	0.0000	
Width of force input	(mm)	27.5000	
Torque	(Nm)	-0.0000	
Mass	(kg)	0.0000	

Coupling ('f 9')			y= 142.00 (mm)
Eff. Diameter	(mm)	0.0000	
Radial force coefficient	(-)	0.0000	
Direction of radial force	(°)	0.0000	
Axial force coefficient	(-)	0.0000	
Width of force input	(mm)	27.5000	
Power	(kW)	24.6091	driven (Input)
Torque	(Nm)	436.3840	
Mass	(kg)	0.0000	

Set fixed bearing left
Deep groove ball bearing (single row) (SKF *6307) y= 51.00 (mm)
 d=35.00 (mm), D=80.00 (mm), B=21.00 (mm), r=1.50 (mm)
 C=35.100 kN, C0=19.000 kN, Cu=0.820 kN

Set fixed bearing right
Deep groove ball bearing (single row) (Koyo 63/32) y= 219.50 (mm)
 d=32.00 (mm), D=75.00 (mm), B=20.00 (mm), r=1.10 (mm)
 C=30.100 kN, C0=16.200 kN, Cu=0.000 kN

Probability of failure	[n]	10.00	%
Lubricant	Oil: ISO-VG 320		
Lubricant with additive, effect on bearing lifetime confirmed in tests			
Oil lubrication with filtration, ISO4406 -/19/16			
Lubricant - service temperature[TB]		102.00	°C
Limit for factor aISO	[aISOmax]	50.00	

Shaft 'Shaft 1' Roller bearing 'b1'

Position (Y-co-ordinate)	[y]	51.00	mm
Equivalent load	[P]	10.87	kN
Equivalent load	[P0]	10.01	kN
Life modification factor for reliability[a1]		1.000	
Service life modification factor[aISO]		0.214	
Service life	[Lnh]	1041.59	h
Service life	[Lnmh]	223.32	h
static safety factor	[S0]	1.90	
Bearing reaction force	[Fx]	-4.231	kN
Bearing reaction force	[Fy]	4.390	kN
Bearing reaction force	[Fz]	-9.070	kN
Bearing reaction force	[Fr]	10.009	kN
Torque of friction	[Mloss]	0.20	Nm
Displacement of bearing	[ux]	0.000	mm
Displacement of bearing	[uy]	-0.010	mm
Displacement of bearing	[uz]	0.000	mm
Displacement of bearing	[ur]	0.000	mm
Misalignment of bearing	[rx]	0.705	mrاد (2.42')
Misalignment of bearing	[ry]	14.848	mrاد (51.04')
Misalignment of bearing	[rz]	-0.170	mrاد (-0.59')
Misalignment of bearing	[rr]	0.725	mrاد (2.49')

Shaft 'Shaft 1' Roller bearing 'b2'

Position (Y-co-ordinate)	[y]	219.50	mm
Equivalent load	[P]	3.04	kN
Equivalent load	[P0]	3.04	kN
Life modification factor for reliability[a1]		1.000	
Service life modification factor[aISO]		0.292	
Service life	[Lnh]	29993.38	h
Service life	[Lnmh]	8758.83	h
static safety factor	[S0]	5.33	
Bearing reaction force	[Fx]	-0.177	kN
Bearing reaction force	[Fy]	0.000	kN
Bearing reaction force	[Fz]	-3.036	kN
Bearing reaction force	[Fr]	3.042	kN

Torque of friction	[Mloss]	0.03	Nm
Displacement of bearing	[ux]	0.000	mm
Displacement of bearing	[uy]	-0.069	mm
Displacement of bearing	[uz]	0.000	mm
Displacement of bearing	[ur]	0.000	mm
Misalignment of bearing	[rx]	-0.461	mrاد (-1.58')
Misalignment of bearing	[ry]	19.251	mrاد (66.18')
Misalignment of bearing	[rz]	0.053	mrاد (0.18')
Misalignment of bearing	[rr]	0.464	mrاد (1.59')

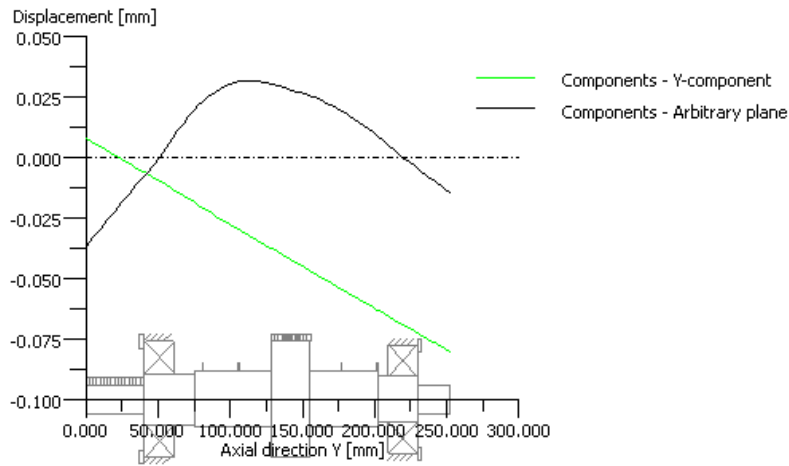


Figure: Displacement (bending etc.) (Arbitrary plane 76.416552 °)

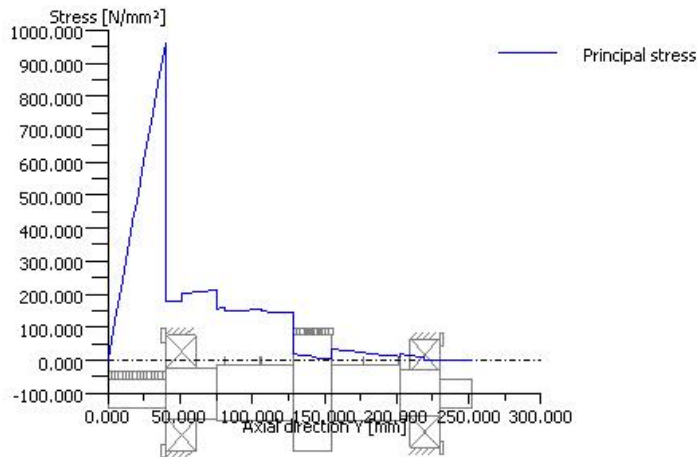


Figure: Principal stress

End report

lines: 273

_O.System.TGB.s3.sz4.SZ4

KISSsoft - Release 04-2010E

KISSsoft evaluation

File

Name: 1st.gear_235rpm_1000Nm

Analysis of shafts, axle and beams

Input data

Coordinate system shaft: see picture W-002

Label	Shaft 1
Drawing	
Initial position (mm)	0.000
Length (mm)	40.000
Speed (1/min)	278.52
Sense of rotation: clockwise	
Material	C45 (1)
Young's modulus (N/mm ²)	206000.000
Poisson's ratio nu	0.300
Specific weight (kg/m ³)	7830.000
Warmth elongation coefficient (10 ⁻⁶ /K)	11.500
Temperature (°C)	20.000
Weight of shaft (kg)	0.100
Mass moment of inertia (kgm ²)	0.003
Momentum of mass GD2 (Nm ²)	0.115
(Notice: Weight, moment of inertia and GD2 are valid for the shaft without considering gears)	
Weight towards	(0.000, 0.000,-1.000)
Regard gears as masses	
Consider deformations due to shearing	
Shear correction coefficient	1.100
Contact angle of roller bearings is considered	
Reference temperature (°C)	50.000

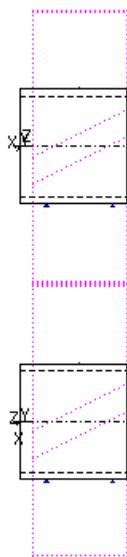


Figure: Load applications

SHAFT GEOMETRY, BEARING AND FORCES

Shaft 'Shaft 1':

Cylinder outside ('Cylinder') y= 0.00...40.00 (mm)
d=43.00 (mm), l=40.00 (mm), Rz= 8.0

Cylinder inside ('Cylindrical bore') y= 0.00...40.00 (mm)
d=38.00 (mm), l=40.00 (mm)

Coupling ('c24(c24)') y= 2.00 (mm)

Eff. Diameter	(mm)	80.0000	
Radial force coefficient	(-)	0.0000	
Direction of radial force	(°)	0.0000	
Axial force coefficient	(-)	0.0000	
Width of force input	(mm)	4.0000	
Torque	(Nm)	-0.0000	
Mass	(kg)	0.0000	

Cylindrical gear ('z4(gp2)') y= 22.50 (mm)

Reference diameter	(mm)	102.6120	
Helix angle	(°)	20.3739	left
Pressure angle	(°)	22.6073	
Position of contact point	(°)	180.0000	
Width of force input	(mm)	35.0000	
Torque	(Nm)	-0.0000	

Fixed bearing adjusted on both sides ('b10') y= 10.00 (mm)

Degrees of freedom

X: fixed
Y: fixed
Z: fixed
Rx: free
Ry: free
Rz: free

Free bearing ('b11') y= 35.00 (mm)

Degrees of freedom

X: fixed
Y: free
Z: fixed
Rx: free
Ry: free
Rz: free

Shaft 'Shaft 1': The mass of the following element is taken into account (y= 22.5000 (mm)):
Cylindrical gear 'z4(gp2)'
m (yS= 22.5000 (mm)): 1.8683 (kg)
Jp: 0.0029 (kg*m2), Jxx: 0.0016 (kg*m2), Jzz: 0.0016 (kg*m2)

Shaft 'Shaft 1' Bearing 'b10'

Position (Y-co-ordinate)	[y]	10.00	mm	
Bearing reaction force	[Fx]	0.000	kN	
Bearing reaction force	[Fy]	-0.000	kN	
Bearing reaction force	[Fz]	0.010	kN	
Bearing reaction force	[Fr]	0.010	kN	
Displacement of bearing	[ux]	0.000	mm	
Displacement of bearing	[uy]	0.000	mm	
Displacement of bearing	[uz]	-0.000	mm	
Displacement of bearing	[ur]	0.000	mm	
Misalignment of bearing	[rx]	-0.000	mrاد (0')	
Misalignment of bearing	[ry]	0.000	mrاد (0')	
Misalignment of bearing	[rz]	0.000	mrاد (0')	
Misalignment of bearing	[rr]	0.000	mrاد (0')	

Shaft 'Shaft 1' Bearing 'b11'

Position (Y-co-ordinate)	[y]	35.00	mm
Bearing reaction force	[Fx]	0.000	kN
Bearing reaction force	[Fy]	0.000	kN
Bearing reaction force	[Fz]	0.010	kN
Bearing reaction force	[Fr]	0.010	kN
Displacement of bearing	[ux]	0.000	mm
Displacement of bearing	[uy]	-0.009	mm
Displacement of bearing	[uz]	-0.000	mm
Displacement of bearing	[ur]	0.000	mm
Misalignment of bearing	[rx]	0.000	mrad (0')
Misalignment of bearing	[ry]	0.000	mrad (0')
Misalignment of bearing	[rz]	0.000	mrad (0')
Misalignment of bearing	[rr]	0.000	mrad (0')

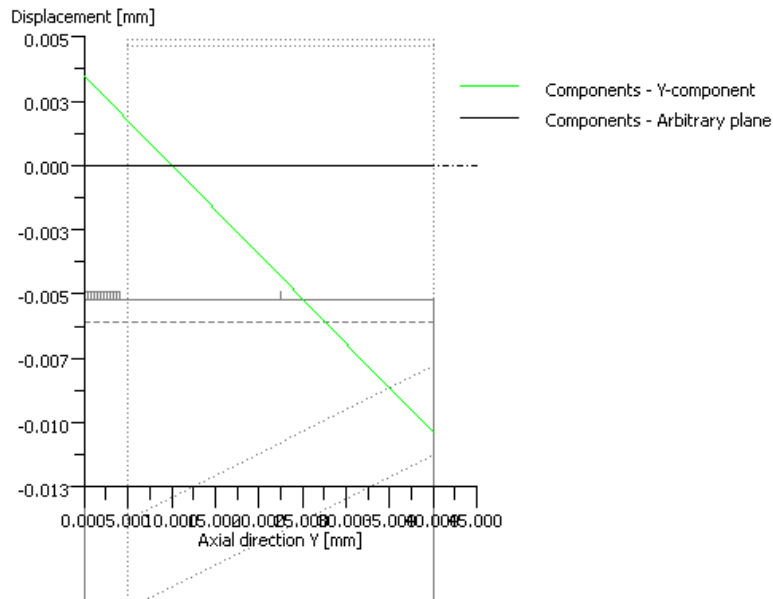


Figure: Displacement (bending etc.) (Arbitrary plane 90 °)

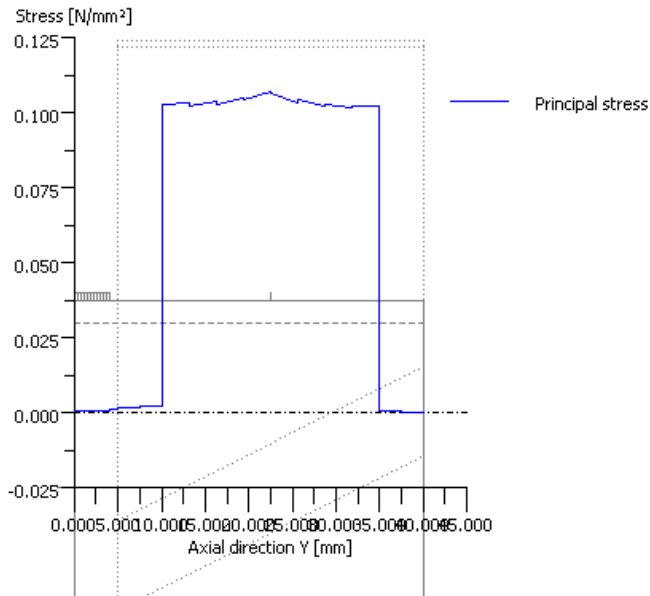


Figure: Principal stress

_O.System.TGB.s3.sz5.SZ5

KISSsoft - Release 04-2010E

KISSsoft evaluation

File
Name: 1st.gear_235rpm_1000Nm

Analysis of shafts, axle and beams

Input data

Coordinate system shaft: see picture W-002

Label	Shaft 1
Drawing	
Initial position (mm)	0.000
Length (mm)	40.000
Speed (1/min)	538.52
Sense of rotation: clockwise	
Material	C45 (1)
Young's modulus (N/mm ²)	206000.000
Poisson's ratio nu	0.300
Specific weight (kg/m ³)	7830.000
Warmth elongation coefficient (10 ⁻⁶ /K)	11.500
Temperature (°C)	20.000
Weight of shaft (kg)	0.100
Mass moment of inertia (kgm ²)	0.001
Momentum of mass GD2 (Nm ²)	0.026
(Notice: Weight, moment of inertia and GD2 are valid for the shaft without considering gears)	
Weight towards	(0.000, 0.000,-1.000)
Regard gears as masses	
Consider deformations due to shearing	
Shear correction coefficient	1.100
Contact angle of roller bearings is considered	
Reference temperature (°C)	50.000

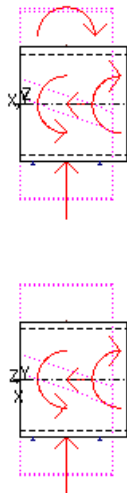


Figure: Load applications

SHAFT GEOMETRY, BEARING AND FORCES

Shaft 'Shaft 1':

Cylinder outside ('Cylinder') y= 0.00...40.00 (mm)
d=43.00 (mm), l=40.00 (mm), Rz= 8.0

Cylinder inside ('Cylindrical bore') y= 0.00...40.00 (mm)
d=38.00 (mm), l=40.00 (mm)

Coupling ('c35(c35)') y= 38.00 (mm)

Eff. Diameter	(mm)	80.0000	
Radial force coefficient	(-)	0.0000	
Direction of radial force	(°)	0.0000	
Axial force coefficient	(-)	0.0000	
Width of force input	(mm)	4.0000	
Power	(kW)	24.6091	driving (Output)
Torque	(Nm)	-436.3840	
Mass	(kg)	0.0000	

Cylindrical gear ('z5(gp3)') y= 17.50 (mm)

Reference diameter	(mm)	71.7766	
Helix angle	(°)	19.8504	right
Pressure angle	(°)	18.8287	
Position of contact point	(°)	180.0000	
Width of force input	(mm)	35.0000	
Power	(kW)	24.6091	driven (Input)
Torque	(Nm)	436.3840	
Axial force	(N)	-4389.7778	
Shear force X	(N)	4408.1531	
Shear force Z	(N)	12159.5060	
Bending moment X	(Nm)	0.0000	
Bending moment Z	(Nm)	157.5417	

Free bearing ('b8') y= 5.00 (mm)
Degrees of freedom

X: fixed
Y: free
Z: fixed
Rx: free
Ry: free
Rz: free

Fixed bearing adjusted on both sides ('b9') y= 30.00 (mm)
Degrees of freedom

X: fixed
Y: fixed
Z: fixed
Rx: free
Ry: free
Rz: free

Shaft 'Shaft 1': The mass of the following element is taken into account (y= 17.5000 (mm)):

Cylindrical gear 'z5(gp3)'
m (yS= 17.5000 (mm)): 0.7109 (kg)
Jp: 0.0006 (kg*m2), Jxx: 0.0004 (kg*m2), Jzz: 0.0004 (kg*m2)

Shaft 'Shaft 1' Bearing 'b8'

Position (Y-co-ordinate)	[y]	5.00	mm
Bearing reaction force	[Fx]	-8.506	kN
Bearing reaction force	[Fy]	0.000	kN
Bearing reaction force	[Fz]	-6.076	kN
Bearing reaction force	[Fr]	10.453	kN
Displacement of bearing	[ux]	0.000	mm
Displacement of bearing	[uy]	0.008	mm
Displacement of bearing	[uz]	0.000	mm
Displacement of bearing	[ur]	0.000	mm

Misalignment of bearing	[rx]	0.013	mrاد	(0.04')
Misalignment of bearing	[ry]	-0.015	mrاد	(-0.05')
Misalignment of bearing	[rz]	0.278	mrاد	(0.95')
Misalignment of bearing	[rr]	0.278	mrاد	(0.96')

Shaft 'Shaft 1' Bearing 'b9'

Position (Y-co-ordinate)	[y]	30.00	mm	
Bearing reaction force	[Fx]	4.098	kN	
Bearing reaction force	[Fy]	4.390	kN	
Bearing reaction force	[Fz]	-6.076	kN	
Bearing reaction force	[Fr]	7.328	kN	
Displacement of bearing	[ux]	-0.000	mm	
Displacement of bearing	[uy]	-0.000	mm	
Displacement of bearing	[uz]	0.000	mm	
Displacement of bearing	[ur]	0.000	mm	
Misalignment of bearing	[rx]	-0.013	mrاد	(-0.04')
Misalignment of bearing	[ry]	-0.541	mrاد	(-1.86')
Misalignment of bearing	[rz]	0.287	mrاد	(0.99')
Misalignment of bearing	[rr]	0.287	mrاد	(0.99')

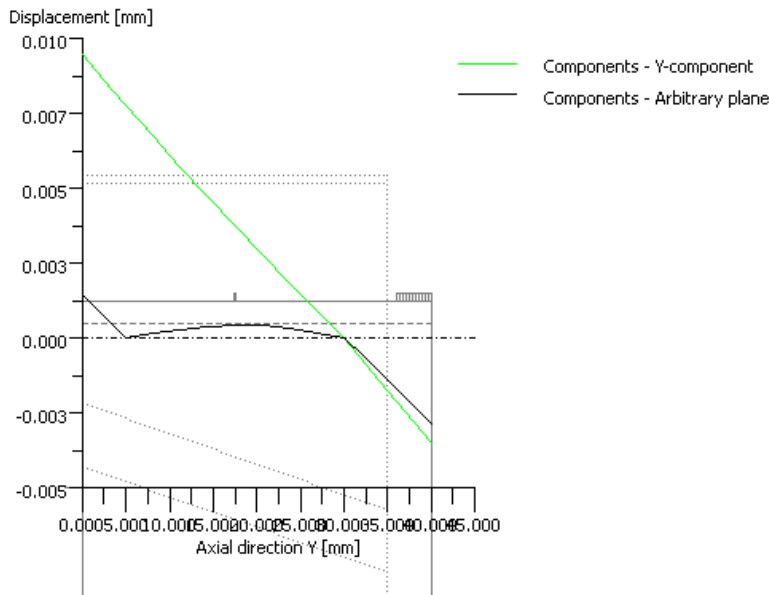


Figure: Displacement (bending etc.) (Arbitrary plane -1.355088 °)

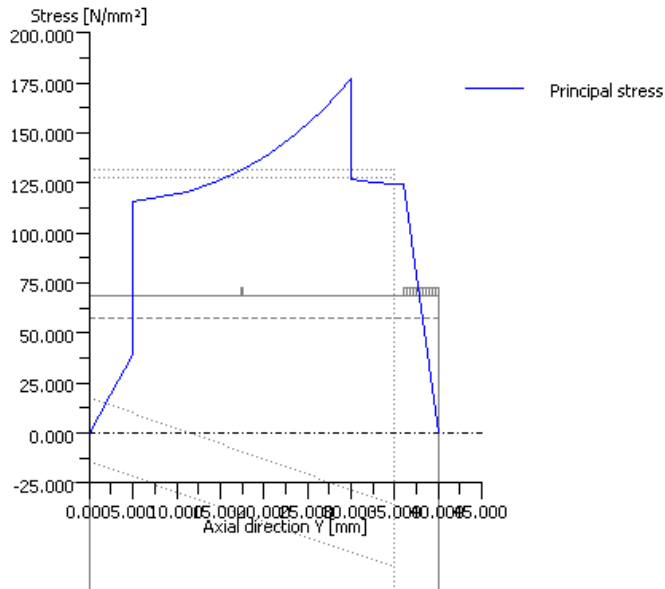


Figure: Principal stress